

Structure-Function Study of Human Spindly

by

Devinderjit Kaur Moudgil

A thesis submitted in partial fulfillment of the requirements for the degree of

Doctor of Philosophy

in

EXPERIMENTAL ONCOLOGY

Department of Experimental Oncology
University of Alberta

© Devinderjit Kaur Moudgil, 2015

Abstract

Mitosis is the last and the shortest stage of the cell cycle with the ultimate goal of equal distribution of replicated genetic material into two daughter cells. Proper execution of mitosis is very important for the maintenance of genomic integrity. Failure of the accurate segregation of genetic material can lead to aneuploidy as well as cell death. Aneuploidy is a common occurrence in cancer cells and it can also lead to severe birth defects. The mitotic checkpoint is a surveillance mechanism that regulates metaphase to anaphase transition and ensures precise chromosome segregation during mitosis. The mitotic checkpoint-signaling pathway is a biochemical system that involves multi-protein networks present on kinetochores during mitosis. Therefore, understanding how these mitotic checkpoint proteins regulate the function of this checkpoint has been the focus of extensive research.

How the mitotic checkpoint signal is generated is widely studied however far less is known about how the checkpoint is silenced. Here, we investigated the mitotic checkpoint function of the human Spindly protein, which recruits the dynein/dynactin complex to kinetochores, both of which are involved in checkpoint silencing. I have characterized the kinetochore localization domain of Spindly to its 294-605 C-terminal amino acids. Furthermore, I examined the underlying molecular mechanism of Spindly kinetochore localization and discovered that Spindly undergoes a posttranslational lipid modification known as farnesylation on its C-terminal cysteine residue. Inhibition of farnesyl transferase

enzyme with farnesyl transferase inhibitors prevented kinetochore localization of Spindly. A key upstream regulator of Spindly kinetochore localization is an essential checkpoint component, the RZZ complex. We showed that Spindly farnesylation is essential for its interaction with the RZZ complex and hence its kinetochore localization. Farnesylation transferase inhibitor was reported to cause aberrant mitotic progression in cells over a decade ago and now my work has reinforced the importance of farnesylation for the proper execution of mitosis through Spindly kinetochore localization. I postulated that Spindly is likely the primary mitotic target of farnesyl transferase.

Spindly is phosphorylated during mitosis and its phosphorylation sites are located within the kinetochore localization domain. Here I show that Spindly phosphorylation affects its kinetochore binding affinity and leads to premature transport to spindle poles. I also demonstrate that Spindly becomes a dynamic kinetochore component at metaphase kinetochores compared to prometaphase. These results indicate that Spindly phosphorylation is perhaps the regulatory mechanism for its release from kinetochores. Furthermore, I also identified p50/dynamitin as a novel interaction partner of Spindly, potentially explaining the dynein/dynactin kinetochore recruitment through Spindly. Together, these results support a model where farnesylation regulates physical association of Spindly/RZZ complex and Spindly acts as a direct linker between RZZ and the dynein/dynactin complex.

Preface

This thesis is an original work by Devinderjit K. Moudgil. Portions of this thesis have been previously published as well as accepted for publication.

Chapter 3 of this thesis has been published as D.K. Moudgil, N. Westcott, J.K. Famulski, K. Patel, D. Macdonald, H. Hang, and G.K.T. Chan, “A novel role of farnesylation in targeting a mitotic checkpoint protein, human Spindly, to kinetochores,” *Journal of Cell Biology*, vol. 208, issue 7, 881-96. I was responsible for the experimental design, data collection and analysis as well as the manuscript writing. N. Westcott performed click chemistry experiments on the cell lysates metabolically labeled by me. J.K. Famulski constructed the random insertion mutant library of hSpindly. K. Patel constructed hSpindly’s E, F and GG mutants. D. MacDonald assisted with manuscript edits. G.K.T. Chan was the supervisory author and was involved with experimental design and manuscript writing.

Portions of Chapter 5 have been published in a brief Feature Editorial as D.K. Moudgil and G.K.T. Chan, “Lipids beyond membranes; Farnesylation targets Spindly to kinetochores,” *Cell Cycle*, vol 14, issue 14, 2185-2186. I wrote the review and G.K.T Chan helped with editing the review.

Copyright permissions have been obtained for chapter 1 figures used from other articles.

Dedication

To my incredible parents & grandparents,

for their unwavering love and support

And also to the memory of my dear aunt 'Amarjit Kaur Rakkar'

Acknowledgements

It has been an absolute privilege and honor to work in the Chan Lab. With immense gratitude, I would like to express sincere appreciation for my supervisor Dr. Gordon Chan. His expertise, enthusiasm, determination, and dedication to science are truly inspiring. I am grateful to him for providing me freedom in my research projects. I am also extremely thankful and grateful to my committee members Dr. Roseline Godbout and Dr. Martin Srayko for all their assistance and guidance over the years. Dr. Roseline Godbout has always been available for an excellent advice and suggestions even at the most random h of the day throughout the week. I would also like to thank Dr. Michael Weinfeld and my external examiner Dr. Paul Maddox for taking the time to review my thesis and be a part of my thesis defence committee. My gratitude also goes to our collaborators, Dr. Howard Hang and Dr. Nathan Westcott at Rockefeller University. Also, a special thank you to Dr. Luc Berthiaume for his assistance and suggestions regarding farnesylation work.

This work would not have been possible without the immense support from CCI Imaging facility and I am indebted to Dr. Xuejun Sun and Gerry Baron. I also consider myself blessed for an opportunity to work with a number of talented and interesting people at Cross Cancer institutes over the years. In particular, I would like to thank Dr. Larissa Vos for her valuable research insights and assistance throughout my Ph.D. career especially during the last two years.

Nothing of this would have possible without the continuous support and encouragement of my husband, Navodit Moudgil, and my parents. I fall short of words to express how much love and support I have received from my parents throughout this journey. I would like to acknowledge my two little siblings, my sister Rumi and my brother Raman for always being there for me for everything.

Table of Contents

Chapter 1 Introduction	1
1.1 Cell Cycle and Checkpoints	2
1.2 Mitosis	6
1.3 The Mitotic Spindle.....	9
1.3.1 Centrosomes.....	9
1.3.2 Microtubules	11
1.3.3 Chromosomes.....	12
1.4 The Centromere.....	14
1.4.1 Centromeric DNA sequence.....	14
1.4.2 Epigenetic control of centromere formation.....	15
1.5 The Kinetochore: Dynamic and Hierarchical Assembly.....	18
1.5.1 The constitutive centromere-associated network.....	22
1.5.2 KMN network.....	25
1.5.3 Mitotic kinases.....	26
1.6 Kinetochore-Microtubule Attachment	31
1.6.1 Classic search and capture model	31
1.6.2 Self-assembly of spindles or chromatin pathway.....	32
1.6.3 Lateral attachments	35
1.6.4 End-on attachments.....	35
1.6.5 Error-correction mechanism by Aurora B kinase	36
1.7 The Mitotic Checkpoint and Mitotic Checkpoint Proteins.....	39
1.7.1 Anaphase promoting complex/cyclosome	42
1.7.2 Mitotic checkpoint complex.....	43
1.7.3 The RZZ complex and Spindly.....	46
1.7.4 Mitotic checkpoint and cancer.....	53
1.8 Mitotic Checkpoint Silencing.....	55
1.8.1 Dynein/Dynactin stripping.....	55
1.8.2 p31 ^{comet} mediated MCC disassembly	58
1.9 Protein Prenylation.....	60
1.9.1 Farnesylation	60
1.9.2 Farnesyl transferase inhibitors.....	64
1.9.3 Farnesylated mitotic proteins: CENP-E and CENP-F.....	65

1.10 Thesis Focus.....	67
Chapter 2 Experimental Procedures.....	68
2.1 Cloning.....	69
2.2 Mutagenesis and siRNA	69
2.3 Cell culture and Synchronization	70
2.4 Transient Transfections	70
2.5 Western Blotting.....	71
2.6 Fluorescence Microscopy	71
2.7 Fluorescence Quantification	73
2.8 MBP Spindly and Rat anti hSpindly Antibody Production.....	73
2.9 Metabolic Labeling, Click Chemistry Reactions and In-gel Fluorescence Imaging.....	74
2.10 Immunoprecipitation and GFP Trap.....	76
2.11 Live-Cell Imaging.....	77
2.12 Fluorescent Recovery After Photobleaching (FRAP)	77
2.13 Yeast Two-Hybrid	78
2.13 Statistical Analysis.....	79
2.14 Reagent and Buffer Recipes	80
Chapter 3 A novel role of farnesylation in targeting a mitotic checkpoint protein, human Spindly, to kinetochores.....	88
3.1 Abstract.....	89
3.2 Introduction:	90
3.3 Results	93
3.3.1 hSpindly kinetochore localization is dependent on its C-terminus	93
3.3.2 FTI treatment abrogated hSpindly kinetochore localization without affecting the RZZ complex, CENP-E and CENP-F kinetochore localization	106
3.3.3 hSpindly CPQQ motif can be substituted with other farnesylation motifs	114
3.3.4 hSpindly is farnesylated on its C-terminal cysteine residue and farnesylation is essential for its interaction with the RZZ complex.....	119
3.3.5 hSpindly depletion and FTI treatment have similar mitotic phenotype	126
3.4 Discussion	132

Chapter 4 Phospho Regulation of hSpindly and dynein/dynactin complex recruitment through hp50 subunit.....	142
4.1 Abstract.....	143
4.2 Introduction:	144
4.4 Results	147
4.4.1 hSpindly has numerous phosphorylation sites within the kinetochore localization domain.....	147
4.4.2 Mutation of hSpindly phosphorylation sites leads to altered kinetochore localization.....	153
4.4.3 Kinetochore dynamics of WT-hSpindly and phospho mutants	162
4.4.4 Inhibition of Plk1 and Mps1 kinase affects hSpindly kinetochore localization.....	167
4.4.5 hSpindly interacts with human p50/dynamitin (hp50), a subunit of the dynactin complex in the yeast 2-hybrid system.....	170
4.5 Discussion	175
Chapter 5 Discussion	179
5.1 Synopsis	180
5.2 hSpindly Kinetochore Localization.....	182
5.3 hSpindly and the RZZ Complex Connections	183
5.3 hSpindly Kinetochore Residency Patterns.....	185
5.4 Role of hSpindly in Checkpoint Silencing	187
5.5 hSpindly Cytoplasmic Function.....	188
5.6 Farnesylation and mitotic checkpoint inhibition through Spindly for cancer treatment	189
References.....	192
Appendix.....	229

List of Tables

Table 1.1: Comparison of Spindly function in different organisms shows conserved function in dynein recruitment but differences in terms of checkpoint activation through Mad1/Mad2 recruitment.....	50
Table 2.1 Composition of buffers and solutions.....	81
Table 2.2 Primary antibodies	82
Table 2.3: hSpindly and hCENP-F cloning and truncation mutant primers.....	83
Table 2.4: hSpindly deletion mutant primers.....	84
Table 2.5: hSpindly and hCENP-F mutant substitution primers	85
Table 3.1: hSpindly random insertion mutants show that the far C-terminus is required for kinetochore localization.....	99
Table 4.1: Predicted serine (S) and threonine (T) phosphorylation sites in hSpindly using GPS 3.0.....	149
Table 4.2: Kinases predicted by GPS3.0 to phosphorylate sites reported by PhosphoSite Plus.....	151
Table 4.3: hSpindly phospho-mimics and their kinetochore localization.....	158

List of Figures

Figure 1.1: Cell cycle is divided into interphase and mitosis.	4
Figure 1.2: Cell cycle progression is controlled by three major checkpoints G/S, G2/M and mitotic checkpoint.	5
Figure 1.3: Different phases of mitosis results in chromosome segregation into two daughter cells.	8
Figure 1.4: Components of the mitotic spindle.....	10
Figure 1.5: Schematic representation of genomic centromere organization of eukaryotic organisms shows diversity.	17
Figure 1.6: Comparison of kinetochore structure using conventional fixation (left) and high-pressure freezing/freeze substitution (right) using electron microscopy.....	20
Figure 1.7: Relative positions of the kinetochore proteins to CENP-I (set to 0) based on distance measurements (delta measurements).	21
Figure 1.8: Kinetochore architecture showing its components in interphase and mitosis.....	24
Figure 1.9: Mitotic kinases regulating cell cycle progression at different stages.	30
Figure 1.10: Mitotic spindle assembly models: (A) Random search and capture & (B) Self-assembly/chromatin pathway/acentrosomal.	34
Figure 1.11: Kinetochore-MT attachment errors and correction mechanism.....	37
Figure 1.12: Schematic diagram representing Aurora B error correction mechanism during mitosis.	38
Figure 1.13: MCC complex inhibits APC/C complex.....	45
Figure 1.14: A schematic representation of selective proteins in the inner, outer and fibrous corona of the kinetochore.	51
Figure 1.15: A schematic representation of the dynein/dynactin complex subunits and ternary complex between dynein, dynactin and Spindly.	52
Figure 1.16: Mitotic checkpoint silencing through dynein/dynactin mediated stripping and p31 ^{comet}	59
Figure 1.17: Schematic representation of protein prenylation.....	62

Figure 1.18: Schematic representation of the steps involved in the farnesylation process mediated by FTase.	63
Figure 3.1: Endogenous hSpindly kinetochore localization during mitosis.	94
Figure 3.2: hSpindly C-terminal is required for kinetochore localization.	96
Figure 3.3: Expression of hSpindly mutant library using western blot analysis. .	97
Figure 3.4: hSpindly far C-terminal residues are required for kinetochore localization.	100
Figure 3.5: Far C-terminal residues of hSpindly are essential for kinetochore localization.	102
Figure 3.6: Kinetochore localization of GFP-hSpindly insertion mutants.	104
Figure 3.7: Kinetochore localization of EGFP-hSpindly deletion and substitution mutants.	105
Figure 3.8: Spindly C-terminal residues are highly conserved in different species.	107
Figure 3.9: Inhibition of farnesylation abrogates kinetochore localization of hSpindly but not the RZZ complex.	108
Figure 3.10: hSpindly kinetochore localization is abrogated with FTI treatment in breast cancer and melanoma cell lines without affecting Rod kinetochore localization.	109
Figure 3.11: Inhibition of farnesylation does not affect CENP-E and CENP-F kinetochore localization.	111
Figure 3.12: Farnesylation motif of CENP-F is not required for kinetochore localization.	113
Figure 3.13: hSpindly farnesylation motif can be substituted with CENP-E or CENP-F farnesylation motif but not a geranylgeranylation motif.	116
Figure 3.14: Expression of hSpindly mutants and hCENP-F mutant using western blot analysis.	118
Figure 3.15: hSpindly is farnesylated <i>in vivo</i>	120
Figure 3.16: Inhibition of farnesylation abrogates hSpindly interaction with the RZZ complex.	122
Figure 3.17: Knockdown of hSpindly protein in HeLa cells using siRNA.	124

Figure 3.18: Inhibition of hSpindly farnesylation abrogates its interaction with the RZZ complex.	125
Figure 3.19: FTI treatment leads to mitotic accumulation in HeLa cells.	128
Figure 3.20: Phenocopying of farnesylation inhibition with hSpindly knockdown by siRNA.	129
Figure 3.21: Comparison of mitotic duration of FTI-treated and Spindly knockdown cells show enhanced prometaphase-metaphase delay in Spindly knockdown cells.....	131
Figure 3.22: A schematic representation of hSpindly domains.	133
Figure 3.23: A proposed model of hSpindly kinetochore localization.	138
Figure 4.1: Schematic of hSpindly C-terminus showing phosphorylation sites.	150
Figure 4.2: hSpindly PSP phospho-sites are not conserved in different species.	152
Figure 4.3: Enhanced localization of hSpindly non-phosphorylatable mutants at spindle poles during prometaphase and metaphase.	154
Figure 4.4: Enhanced localization of hSpindly double non-phosphorylatable mutants at spindle poles.	155
Figure 4.5: hSpindly non-phosphorylatable mutants localized to kinetochores under vinblastine treatment showing polar localization is MT dependent.	156
Figure 4.6: hSpindly single phospho-mimics localized to kinetochores in untreated and vinblastine treated HeLa cells similar to WT-hSpindly.	159
Figure 4.7: hSpindly double phospho-mimics showing enhanced streaming on the mitotic spindle, transport to spindle poles at prometaphase but not accumulation at poles.....	160
Figure 4.8: hSpindly double phospho-mimics showing normal kinetochore localization.....	161
Figure 4.9: hSpindly shows rapid turnover at metaphase but not at prometaphase.	164
Figure 4.10: Correct expression of siRNA resistant WT-hSpindly and hSpindly phospho mutants using western blot analysis.	165
Figure 4.11: Kinetochore localization of siRNA resistant hSpindly phospho mutants.....	166

Figure 4.12: Mps1 inhibitor treatment leads to loss of hSpindly kinetochore localization.....	168
Figure 4.13: Plk1 kinase regulates the RZZ complex and hSpindly kinetochore localization.....	169
Figure 4.14: hSpindly interacts with the hp50 subunit of dynactin through the Spindly motif and its C-terminus.....	171
Figure 4.15: hSpindly interacts with hp50 subunit of dynactin complex.	173
Figure 4.16: Immunoblots showing correct size expression of hSpindly mutants (prey) and p50 (bait).	174
Figure 4.17: Model of hSpindly phosphorylation regulating its kinetochore localization pattern.....	178
Figure 5.1: Farnesylation targets hSpindly to kinetochores and hSpindly regulates the checkpoint silencing pathways.....	181
Figure A.1: hSpindly has reduced kinetochore occupancy in a subset of breast cancer cell lines similar to Zw10.	233
Figure A.2: hSpindly robustly localizes to kinetochores devoid of MT attachments.	235
Figure A.3: hSpindly protein expression is variable in breast cancer cell lines and does not correlate with their localization pattern.	237
Figure A.4: WT-GFP-Zw10 expressing cells rescue normal Zw10 kinetochore localization in MDA-MB-231 cells.	239
Figure A.5: WT-GFP-Zw10 expressing T47-D cells display a heterogeneous population with normal as well as absence of kinetochore localization of GFP-Zw10.....	241

List of Symbols, Abbreviations and Nomenclature

Symbols

~	approximately
+/-	plus/minus or positive/negative
%	percentage
°C	degree Celsius
α	alpha
β	beta
γ	gamma
Δ	delta

Abbreviations

aa	amino acid
ACA	anti centromere antigen
Alk-FOH	Alkynyl-Farnesol
APC/C	Anaphase Promoting Complex/Cyclosome
APC ^{Cdh1}	Cdh1 activated Anaphase Promoting Complex/Cyclosome
APC ^{Cdc20}	Cdc20 activated Anaphase Promoting Complex/Cyclosome
ATP	adenine triphosphate
bp	base pair
BSA	bovine serum albumin
BUB	budding uninhibited by benzimidazole
CCAN	constitutive centromere associated network
CCD	charge coupled device
Cdk	cyclin dependent kinase
cDNA	complementary DNA
CENP	centromere protein
co-IP	co-immunoprecipitation
CPC	chromosome passenger complex
CREST	autoimmune disease (calcinosis, Raynaud's phenomenon, esophageal dysmotility, sclerodactyly and telangiectasia)

C-terminus	carboxy terminus
Da	Dalton
DAPI	4',6-diamino-2-phenylindole
DMEM	Dulbecco's Modified Eagle's Medium
DNA	deoxyribonucleic acid
EGFP	enhanced green fluorescent protein
FRAP	fluorescence recovery after photobleaching
FTase	farnesyl transferase
FTI	farnesyl transferase inhibitor
g	gram
g (x g)	gravity (measure of relative centrifugal force)
G1	gap phase 1
G2	gap phase 2
gal	galactose
GAVE	autoimmune disease (gastric antral vascular syndrome)
GDP	guanosine diphosphate
GFP	green fluorescent protein
GST	glutathione -S-transferase
GTP	guanosine triphosphate
H	hour
H2A	histone H2A
H2B	histone H2B
H3	histone H3
HCl	hydrochloric acid
HIS	histidine
KMN	KNL-1, Mis12 and Ndc80 network
kD	kilodalton
l/ml/ μ l	liter/ milliliter/ microliter
m/mm/ μ m	meter/millimeter/micrometer
M/mM/ μ M	molar/ millimolar/ micromolar
M	mitosis

MBP	Maltose binding protein
MAD	mitotic arrest deficient
Mad2-O	open confirmation of Mad2
Mad2-C	closed confirmation of Mad2
MAPs	microtubule associated proteins
MCAK	mitotic centromere-associated kinesin
MCC	mitotic checkpoint complex
mCherry	monomeric Cherry fluorescent protein
min	minutes
MT(s)	microtubules(s)
MTOC	microtubule organizing center
n	number of samples
NA	numerical aperture
NDGA	Nordihydroguaiaretic acid
NEB	nuclear envelope breakdown
N-terminus	amino terminus
OD	optical density
p50	dynamitin
PAGE	polyacrylamide gel electrophoresis
PBS	phosphate buffered saline
PCR	polymerase chain reaction
PEI	polyethylenimine
pH	$\log[H^+]$
Plk1	polo-like kinase 1
PP1	protein phosphatase 1
raff	raffinose
Rod	Roughdeal
RZZ	complex of Zw10, Rod and Zwilch
S	synthesis
SDS	sodium dodecyl sulfate
SD	standard deviation

siRNA	small interfering ribonucleic acid
STLC	S-trytil-L-cystine
T _{1/2}	time to achieve 50% recovery of fluorescence in FRAP
TRP	tryptophan
URA	uracil
WT	wild type
Zw10	Zeste white 10
Zwint-1	Zeste white 10 interacting protein

Chapter 1 Introduction

1.1 Cell Cycle and Checkpoints

The cell cycle is a highly regulated process that is conserved from single cell organisms such as yeast to multicellular organisms such as humans, in which a cell proceeds through a tightly ordered series of events and divides into two genetically identical daughter cells. The cell cycle is broadly divided into interphase and mitosis. Interphase is further composed of three stages: Gap1 (G1), Synthesis/ DNA replication (S), and Gap2 (G2) (Figure 1.1). In G1, the cell enlarges and synthesizes materials for DNA replication in S phase. Cells can enter a quiescent stage called G0 during G1 and stop dividing. Progression through the cell cycle accompanied by screening for errors by surveillance mechanisms called checkpoints, which halt cell cycle progression in the presence of an anomaly. The cell cycle is controlled by 3 checkpoints. The G1/S checkpoint ensures the cell is large enough and ready to undergo genome duplication. The G2/M checkpoint ensures complete DNA replication and error correction. The mitotic checkpoint also known as the spindle assembly checkpoint ensures bi-polar alignment of duplicated chromosomes on the metaphase plate (Figure 1.2). Five cyclin dependent kinases (CDKs) function along with their activating protein partner, cyclin, to promote cell cycle progression as shown in Figure 1.1 {reviewed in (Vermeulen et al., 2003)}. CDK-cyclin complexes phosphorylate their specific substrates and regulate the transition into the next cell cycle phase. G0 quiescent stage is achieved by hypophosphorylated retinoblastoma (RB) protein that binds to and sequesters the transcription factor E2F required for transcription of genes for entry into S phase (Henley and Dick, 2012). Growth factors stimulate the activation of Cdk, which phosphorylate RB protein leading to S phase entry. Upon faithful completion of DNA replication in S phase, the cell enters G2 phase during which the cell continues to grow and prepare for entry into mitosis. Mitotic entry is delayed in the presence of DNA damage to allow time for DNA repair. The G2 arrest is achieved through phosphorylation of CHK1/2 protein kinases by ATM and ATR, which further phosphorylate and inactivate the Cdc25 phosphatase (Sanchez et al., 1997). Cdc25 activity is required for Cdk1

dephosphorylation, which allows entry into mitosis. Alternatively, in the presence of microtubule (MT) poisons, p38 kinase suppresses Cdk activity and prevents entry into mitosis through CHFR (checkpoint with forkhead and ring finger domains) protein regulation (Matsusaka and Pines, 2004; Sanchez et al., 1997).

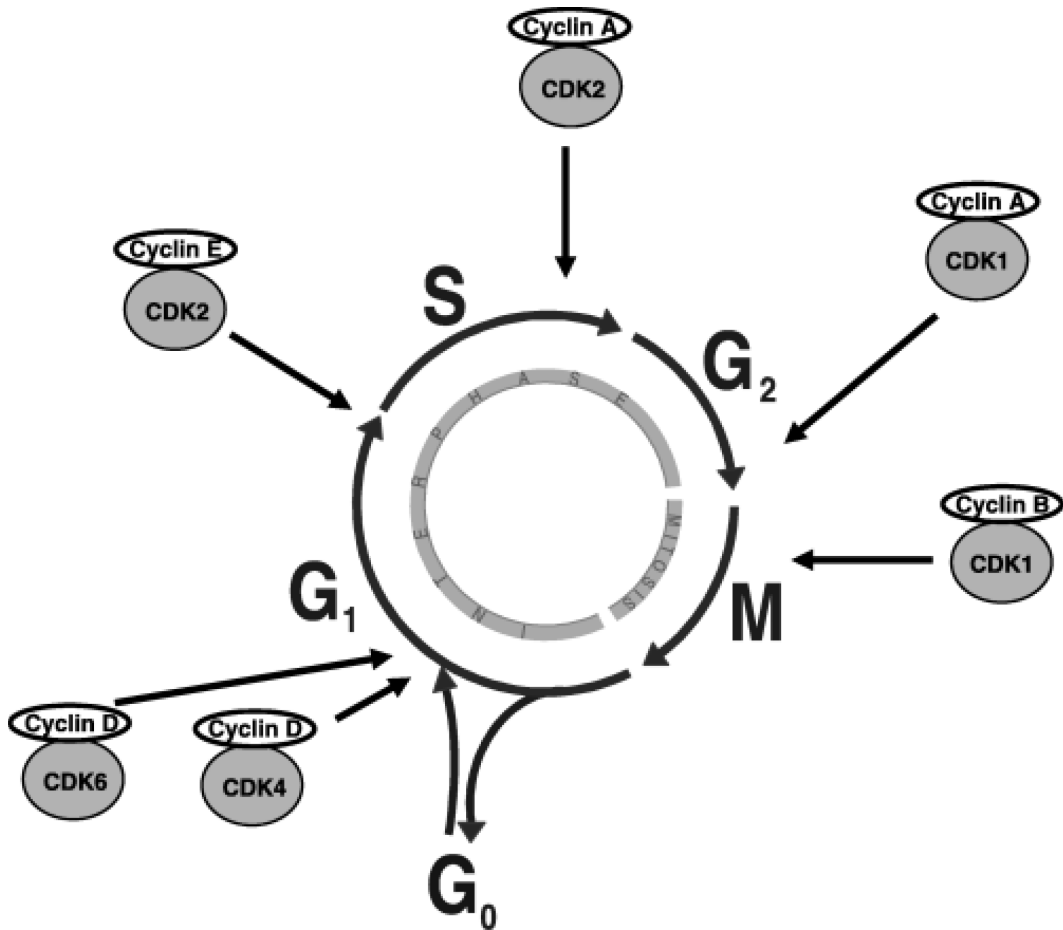


Figure 1.1: Cell cycle is divided into interphase and mitosis.

Interphase is composed of G₁ phase, S phase and G₂ phases. Association of D type cyclins with CDK4 and 6 promotes G₁ entry. The cyclin E-Cdk2 complex facilitates transition from G₁ to S phase. In S-phase, the cyclin A-Cdk1 complex is required and at the end of G₂, this complex promotes entry into mitosis. The cyclin B-Cdk1 complex is required during mitosis. Cyclin levels increase or decrease during different phases of cell cycle. Mitosis is further comprised of different phases explained in Figure 1.3. Adapted from (Vermeulen et al., 2003).

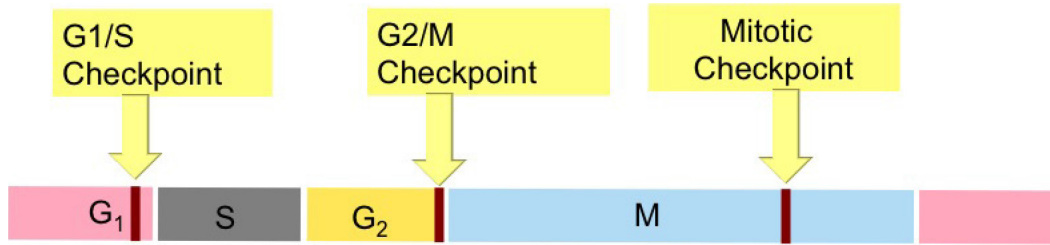


Figure 1.2: Cell cycle progression is controlled by three major checkpoints G₁/S, G₂/M and mitotic checkpoint.

G₁/S checkpoint ensures that the cell is ready to undergo DNA replication. G₂/M checkpoint regulates entry into mitosis by ensuring complete DNA replication, allowing time for DNA repair if required. Mitotic checkpoint is active from entry into mitosis and governs metaphase to anaphase transition and ensures that two daughter cells receive equal genetic material.

1.2 Mitosis

Mitosis is a highly controlled and dynamic cell cycle process in which a cell divides into two daughter cells. Despite being the shortest phase of the cell cycle (1 hour out of 24 hour for a typical human cell), mitosis is a very complex, ordered and well-defined process that ensures the genomic integrity of the two daughter cells. Scientists have been studying mitosis since the 1880s and the term mitosis (mitos means thread in Greek) was coined by German anatomist Walther Flemming due to the thread like appearance of chromosomes. Significant progress has been made in the understanding of mitosis since then, however, the detailed molecular mechanisms are still incomplete. Mitosis is composed of 5 stages: prophase, prometaphase, metaphase, anaphase and telophase followed by cytokinesis (Figure 1.3). Entry into prophase begins with DNA condensation and nuclear envelope breakdown (NEBD). DNA condenses into compact chromosomes with sister chromatids attached to each other at their centromeres through cohesins from S-phase up to metaphase (Guacci et al., 1997; Michaelis et al., 1997). Replicated centrosomes segregate and migrate to opposite poles of the cell to generate a bi-polar mitotic spindle. In prometaphase, centrosomes nucleate MTs from centrosomes and emanating spindle MTs form contacts with chromosomes through kinetochores, specialized mitosis-specific proteinaceous structures positioned at centromeres. Chromosomes are often observed to form a ring like pattern during prometaphase referred to as a rosette arrangement. Within a rosette, maternal and paternal chromosomes are arranged on opposite sides, establishing chromosome topology throughout the cell cycle (Nagele et al., 1995), however, a later study has argued against such a spatial arrangement (Bolzer et al., 2005). A cell is defined to be in metaphase when all the chromosomes are bi-polarly attached to spindle poles and are under equal tension leading to alignment of chromosomes at the center of the cell called the metaphase plate. Sister chromatids aligned on the metaphase plate physically separate from each other (degradation of cohesins) during anaphase. Anaphase is further sub-divided into anaphase A and anaphase B. The initial physical separation of sister chromatids is

defined as anaphase A. During anaphase B, spindle poles move further apart and the sister chromatids rapidly move towards the opposite spindle poles. In telophase, the chromatids reach the spindle poles, the nuclear envelope reforms and cleavage furrow formation starts at the site of the metaphase plate also known as the spindle midzone. Finally, during cytokinesis nuclear envelope formation is complete and the two daughter cells physically separate from each other at the cleavage furrow dividing the cytoplasm. Many machines are required for mitosis including centrosomes, centromeres, mitotic spindles and kinetochores as discussed in detail in later sections.

To ensure two daughter cells receive equal genetic material, cells have evolved a surveillance mechanism called the mitotic checkpoint that prevents transition from metaphase to anaphase in the presence of unaligned chromosomes. I will be focusing on the mitotic checkpoint regulation machinery in this thesis. Failure of the mitotic checkpoint has been closely linked to aneuploidy, which is a hallmark of most solid tumors, and mutations in mitotic checkpoint proteins have been linked to mitotic checkpoint dysfunction and cancer (Cahill et al., 1998; Dai et al., 2004; Michel et al., 2001; Wang et al., 2004b). Detailed mitotic checkpoint mechanism at the molecular level is discussed later in this chapter.

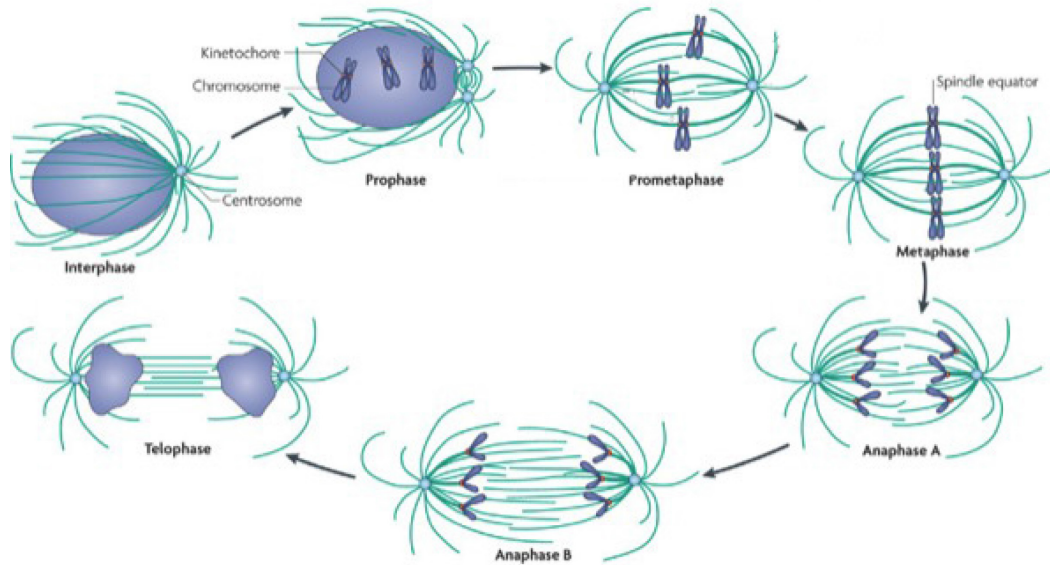


Figure 1.3: Different phases of mitosis results in chromosome segregation into two daughter cells.

Visualization of individual chromosomes due to chromatin condensation at the beginning of prophase. Kinetochores formed on the chromosomes form links with the microtubules arising from centrosomes during prometaphase. All the chromosomes align at the spindle equator called the metaphase plate during metaphase. Sister chromatids are separated from each other and pulled towards spindle poles at anaphase. At telophase, nuclear envelope reformation begins along with DNA decondensation initiation. Adapted from (Walczak et al., 2010).

1.3 The Mitotic Spindle

Accurate division of the replicated genetic material into two daughter cells is dependent on a MT-based mitotic spindle. The interphase MT network of the cell disassembles to form the more organized anti-parallel arrays of the mitotic spindle during mitosis. The mitotic spindle is composed of centrosomes (spindle poles), MTs and chromosomes (Figure 1.4).

1.3.1 Centrosomes

In mammalian cells, the centrosome is a complex organelle consisting of a pair of centrioles surrounded by pericentriolar material also known as centrosome matrix and it nucleates and spatially organizes MTs of the spindle (Figure 1.4) (Doxsey, 2001; Urbani and Stearns, 1999). Centrosomes contain more than 100 proteins and are also called MT organizing centers (MTOC) (Bettencourt-Dias and Glover, 2007). The mother centrosome is duplicated during S phase of the cell cycle and the two daughter centrosomes separate during prophase. MT nucleation is initiated in the centrosome matrix and requires the multi-subunit γ -tubulin ring complex (γ -TURC). γ -TURC consists of 13 γ -TURC tubulins along with pericentrin and acts as a base layer for α -tubulin and β -tubulin dimers for MT nucleation (Gunawardane et al., 2000; Zheng et al., 1995). The two centrosomes are held at their locations by the forces generated by MTs as discussed in the next section. Oocytes of some animal species and mitotic cells of higher plants assemble their spindles in the absence of centrosomes (Compton, 2000). Furthermore, absence of centrosomes (by micro-surgical removal, laser ablation or mutations) in *Drosophila* and human cells does not interfere with the spindle assembly and chromosome segregation indicating that centrosomes are dispensable for chromosome segregation (Basto et al., 2006; Khodjakov et al., 2000; Nahaboo et al., 2015). Despite the presence of centrosome-redundant mechanisms during mitosis, the centrosome is essential for cell cycle progression during G1 phase and centrosomal abnormalities are frequently observed in cancer cells (Chan, 2011; Khodjakov and Rieder, 2001; Rieder et al., 2001).

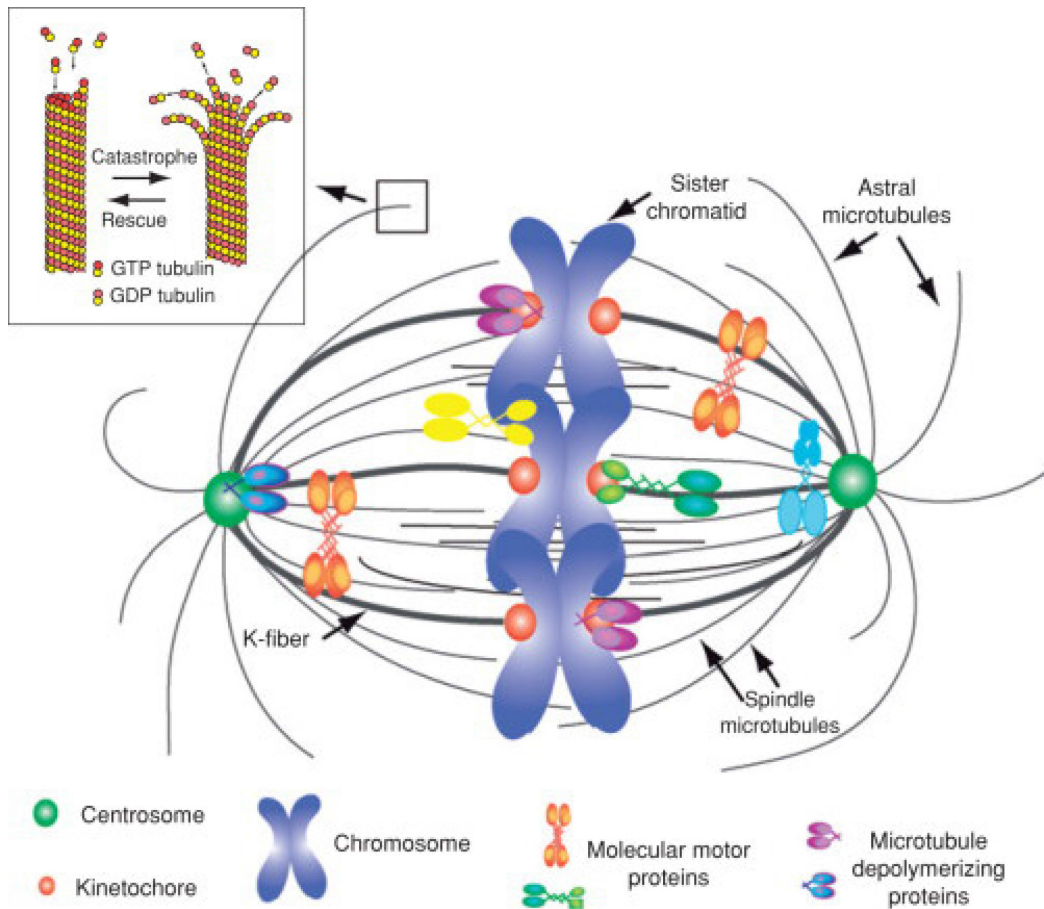


Figure 1.4: Components of the mitotic spindle.

Duplicated centrosomes migrate to the two opposite ends and generate astral MTs shown in light gray. MTs that form links with the kinetochores are shown in dark gray and referred as K-fibers. Microtubules continuously switch between growth (rescue) and shrinkage (catastrophe) phase as shown in the inset. Motor proteins cross-link microtubule bundles, regulate microtubule dynamics and function in chromosome movement. Adapted from (Walczak and Heald, 2008).

1.3.2 Microtubules

MTs are dynamic polarized filaments composed of α -tubulin and β -tubulin dimers with a fast-growing plus end exposing β -tubulin and a slow-growing minus end exposing α -tubulin (Desai and Mitchison, 1997; Mitchison and Kirschner, 1984). Typically 13 protofilaments are associated laterally head to tail to generate a hollow MT filament of 25nm diameter (Nogales et al., 1999). As mentioned earlier, MTs are dynamic structures with minus ends embedded at centrosomes/MTOC and plus ends extending away from centrosomes (Figure 1.4). MTs switch between growth (polymerization) and shrinkage (depolymerization), a property termed as dynamic instability (Desai and Mitchison, 1997; Mitchison and Kirschner, 1984). MTs grow through the addition of α - β -tubulin heterodimer subunits at the plus ends. A GTP molecule is hydrolyzed to GDP upon incorporation into the protofilament and the GDP bound form of tubulin is unstable (Mitchison and Kirschner, 1984). Dynamic instability of MTs is facilitated by MT-associated proteins (MAPs) (Olmsted, 1986). MAPs can promote MT growth (e.g. CLIP170, EB1, CLASP1 and MAP4) or MT shrinkage (e.g. Kin1, Stathmin and MCAK), and some MAPs can promote both MT polymerization and depolymerization (e.g. ch-TOG) (Maiato et al., 2004b). Furthermore, structural polarity (minus and plus ends) of MTs due to asymmetric tubulin subunits allows motor proteins such as dynein (minus end directed) and kinesin (plus end directed) to move the cargo along MTs according to the polarity. MT motor proteins such as dynein and NuMA also anchor MTs at the MTOC (Compton, 1998; Silk et al., 2009). In chapter four, I will address the mechanism of kinetochore localization of dynein during mitosis in detail. Spindle MTs can be differentiated into astral and kinetochore-fibers (K-fibers) as shown in Figure 1.4. Astral MTs grow out of centrosomes with plus ends facing away from centrosomes and anchor the mitotic spindle. K-fibers are spindle MTs that make end-on attachment with the chromosomes. Astral MTs that do not form contact with chromosomes, but instead interact at the spindle midzone, are referred to as interpolar MTs.

In addition to their kinetochore-MT attachment function, forces generated by MTs also help in sister chromatid separation during anaphase, spindle positioning and spindle shape. K-fiber depolymerization (Desai et al., 1998; Mitchison and Salmon, 1992; Skibbens et al., 1993; Zhai et al., 1995) and sliding of K-fibers on adjacent MTs (Elting et al., 2014; Sikirzhytski et al., 2014) are shown to contribute to sister chromatid separation during anaphase A. The interpolar MTs from two opposite poles slide against each other in the center of the spindle and exert repulsive forces on the centrosomes, maintaining their separation and also contributing to centrosome movement during anaphase B (Brust-Mascher et al., 2004; Dumont and Mitchison, 2009; Khodjakov et al., 2004; Mogilner and Craig, 2010; Tolic-Norrelykke et al., 2004). In addition, tension generated by the bipolar K-fiber attachment also helps in positioning of the mitotic spindle (Dumont and Mitchison, 2009; Mogilner and Craig, 2010). MT-associated motor proteins play a major role in the above functions of the mitotic spindle (Brust-Mascher et al., 2004; Khodjakov et al., 2004; Rogers et al., 2004; Tolic-Norrelykke et al., 2004).

1.3.3 Chromosomes

The mitotic spindle is ultimately responsible for chromosome alignment at metaphase and separation of sister chromatids at anaphase. Hence chromosomes serve as a substrates for the mitotic spindle rather than a corpse at a funeral as stated in the past (Earnshaw and Carmena, 2003; Mazia, 1961). However on the flip side Bucciarelli *et al.*, showed that two *Drosophila* mutants lacking chromosomes could assemble mitotic spindles and undergo cytokinesis (Bucciarelli et al., 2003). This observation clouds the area further regarding whether chromosomes are active participants of the mitotic spindle or not.

Chromosomes play an important role in acentrosomal spindle formation discussed in detail later (Section 1.6.2). In addition, sister chromatids undergo cohesive and repulsive forces leading to structural chromatin changes to aid their own separation during anaphase. These opposing forces are due to the presence of

cohesins and condensin protein complexes (which counteract cohesin forces) on chromosomes (Hirano, 2015). Furthermore, chromatin size and geometry is an important determinant factor of spindle size during mitosis (Dinarina et al., 2009). Chromosomes have also been shown to stabilize spindle MTs through their attachment to kinetochores. A kinetochore is a large proteinaceous complex assembled on the centromeres of chromosomes during late G2-M phase. It links chromosomes to spindle MTs, and is the site for mitotic checkpoint activity.

1.4 The Centromere

The centromere is the primary constriction of condensed chromosomes and is a site for cohesin binding of sister chromatids. The multi-protein kinetochore structure assembles on the centromere during late G₂/M and serves as a site for MT attachment and mitotic checkpoint activity. Budding yeast, which are the simplest eukaryotic organisms, have point centromeres defined by a specific DNA sequence. Yeast centromeres are not as complex as human centromeres and only have one MT attachment for each chromosome. However, *C. elegans* assemble holocentric centromeres, which are formed along the length of the chromosomes (Albertson and Thomson, 1993; Buchwitz et al., 1999; Maddox et al., 2004). Human centromeres have multiple subunits leading to multiple kinetochore-MT attachments. Centromere site specification and number of subunits is highly regulated for error free mitosis.

1.4.1 Centromeric DNA sequence

The centromere site was initially thought to be defined by a specific DNA sequence on the chromosomes. Surprisingly, the DNA sequence at the centromere locus is not conserved among different organisms, however, protein components of the centromere are conserved in these organisms. *Saccharomyces cerevisiae* is the only organism that shares three conserved centromeric DNA sequences for all chromosomes and forms a 116–125 base pair sequence sufficient for centromere formation (Clarke and Carbon, 1983). In *Schizosaccharomyces pombe*, the repetitive centromeric DNA sequences are variable in different species as well as in chromosomes of the same cell (Willard, 1991).

Human centromeric DNA is composed of AT-rich alpha (α) satellite DNA repeats (Manuelidis, 1976) and ranges in size from 250 to 5,000 kb (Figure 1.5). α -satellite DNA is composed of 171-bp repeat units termed α -I satellite arranged in a head to tail fashion (Gray et al., 1985; Manuelidis, 1976). A sequence comparison of these individual repeat units reveals a ~60–80% sequence identity (Rudd and Willard, 2004). *De novo* centromere assembly was shown to be

dependent on centromeric DNA in yeast and human cells (Harrington et al., 1997; Takahashi et al., 1992). The topic of sequence basis of centromere specification has been debated since centromeres were shown to form on DNA lacking α satellite repeats (du Sart et al., 1997; Voullaire et al., 1993). However, these unusual centromeric DNA sites tend to be AT-rich similar to normal centromeric sites (du Sart et al., 1997). In addition, evidence showing that α satellite repeats are not sufficient for centromere formation comes from dicentric human chromosomes formed by Robertsonian translocation. Such chromosomes form only one functional kinetochore despite the presence of two centromeric regions (Warburton et al., 1997). These two lines of evidence indicate that α satellite repeats are neither necessary nor sufficient for centromere function. A few studies suggested proximity to heterochromatin plays a role in the formation of neo-centromere (Ishii et al., 2008; Olszak et al., 2011) but exceptions have been reported (Alonso et al., 2003). As compared to the role of centromeric DNA in centromere specification, conserved protein components of the centromere suggest an epigenetic regulation of centromere formation rather than DNA sequence.

1.4.2 Epigenetic control of centromere formation

Centromere protein components were first identified using sera from patients with the auto-immune disease CREST (calcinosis, Raynaud phenomenon, esophageal dysmotility, sclerodactyly, and telangiectasia), which recognized these centromere antigens (Earnshaw and Rothfield, 1985). The chromatin consisting of CENP-A instead of a canonical histone H3 marks the kinetochore formation site of the centromere (Blower et al., 2002; Palmer et al., 1991). Human centromeres contain both CENP-A and histone H3 containing nucleosomes as shown in Figure 1.5. CENP-A serves as a key component of centromere formation and is well conserved in eukaryotes.

CENP-A is the most extensively studied centromere protein and is crucial for the formation of the centromere and kinetochore. CENP-A knockdown leads to a kinetochore null phenotype and is lethal in all organisms studied to date

(Blower and Karpen, 2001; Howman et al., 2000; Liu et al., 2006; Regnier et al., 2005). Contrary to histone loading during S-phase, CENP-A loading occurs in early G1 phase of the cell cycle (Hemmerich et al., 2008; Schuh et al., 2007). CENP-A loading to centromeres is dependent on a complex consisting of hMis18 α (missegregation 18 α), hMis18 β , and M18BP1 (Mis18 binding protein) and this complex is accumulated at the centromere site in late mitosis and G1 phase of the cell cycle (Fujita et al., 2007; Maddox et al., 2007). Mis18 is also required for the recruitment of HJURP (Holliday junction recognition protein) to centromeres in late telophase and early G1, and HJURP promotes CENP-A centromere loading. In addition to Mis18 and HJURP, other factors such as ligase for ubiquitylation (Niikura et al., 2015), GTPase activating protein (MgcRacGAP) (Lagana et al., 2010; Perpelescu et al., 2009) and chromatin-remodeling factor (Rsf-1 & Suv39h) also play a role in CENP-A assembly (Perpelescu et al., 2009; Peters et al., 2001). Centromere assembly and specification has been a topic of extensive research and future discoveries will hopefully shed more light on this complex process.

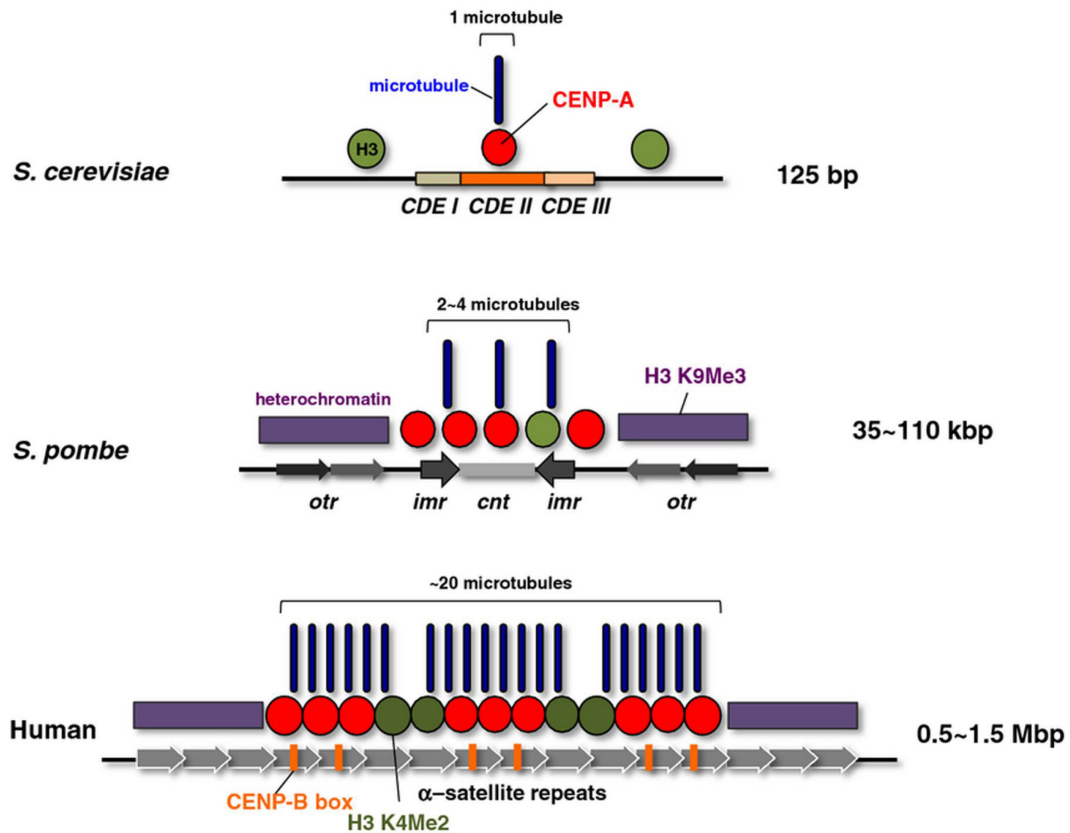


Figure 1.5: Schematic representation of genomic centromere organization of eukaryotic organisms shows diversity.

Budding yeast (*Saccharomyces cerevisiae*) centromere consists of a single CENP-A containing nucleosomes specified by 125 base pair sequence. DNA sequences specifying centromere are named CDEI (centromere DNA element I), CDEII and CDEIII. Fission yeast (*Schizosaccharomyces pombe*) regional centromeric DNA consists of a unique central core region (cnt) surrounded by inverted repeat sequences (imr) and flanking repetitive outer repeat sequences (otr) forming heterochromatin, which extends from 35-110 kilo base pair. Human centromeric DNA consists of 171 bp alpha satellite DNA repeats tandemly organized in higher order repeats. Centromeric DNA consists of CENP-A nucleosomes interspersed with histone H3 flanked by pericentromeric heterochromatin. CENP-B, a highly conserved centromere protein binds to a 17 base pair motif called the CENP-B box in centromeric DNA. The number of MTs to which centromere binds also varies in different organisms. Adapted from (Yamagishi et al., 2014)

1.5 The Kinetochores: Dynamic and Hierarchical Assembly

The kinetochore is a transient macromolecular proteinaceous structure assembled on centromeric chromatin during late G2-M phase of the cell cycle. It links chromosomes to spindle MTs, and is the site for mitotic checkpoint activity. Kinetochores were first identified by electron microscopy as a trilaminar plate like structure on centromeric chromatin of each sister chromatid (Brenner et al., 1981; Brinkley and Stubblefield, 1966; He and Brinkley, 1996; Jokelainen, 1967). The innermost electron dense centromere layer consists of structural proteins that are constitutively associated with centromeres during the cell cycle. The middle translucent layer links the inner kinetochore components with the outer kinetochore proteins. The outer electron dense layer consists of proteins that are responsible for MT attachment. The outermost fibrillar-like region is electron opaque and is termed the fibrous corona (Figure 1.6). The fibrous corona disappears upon MT attachment indicating the dynamic nature of kinetochores during mitosis (Cheeseman and Desai, 2008; Dong et al., 2007). The McEwen group later performed a sophisticated study using high pressure freezing and freeze substitution instead of conventional fixation methods that extract cytoplasmic components and can lead to subtle or more pronounced structural changes in kinetochore structure in a quest to uncover kinetochore structure (McEwen et al., 1998). In their study, they discovered a refined kinetochore structure with a distinct thick mat of light-staining fine fibers corresponding to the outer plate, establishing contacts with centromeric heterochromatin and a zone analogous to the fibrous corona suggesting that the middle layer seen with conventional fixation protocols is an artifact (Figure 1.6) (McEwen et al., 1998). Kinetochore assembly occurs in a step-wise process with ~100 proteins building the kinetochore in a hierarchical and interdependent manner (Ohta et al., 2010). The Salmon lab performed nanometer scale measurements of the outer kinetochore components using super resolution microscopy revealing similar stoichiometry and position of subcomplexes across species (Joglekar et al., 2009; Joglekar et al., 2008; Joglekar et al., 2006; Wan et al., 2009). The relative

locations of various proteins in the fibrous corona (RZZ complex, Spindly, and Mad1-Mad2- discussed in detail in section 1.7.3) were recently mapped providing insight into spatial relationships of these kinetochore components (Varma et al., 2013). Relative locations of different checkpoint proteins are very informative to better understand kinetochore organization as well as provide an idea regarding proteins that interact with each other. Functions of all the kinetochore proteins, as shown in Figure 1.7, are discussed in later sections. Researchers dissecting the kinetochore composition and assembly face major challenges such as transient formation of insoluble kinetochore protein complexes and mounting increase in the number of kinetochore proteins forming many intermediate complexes.

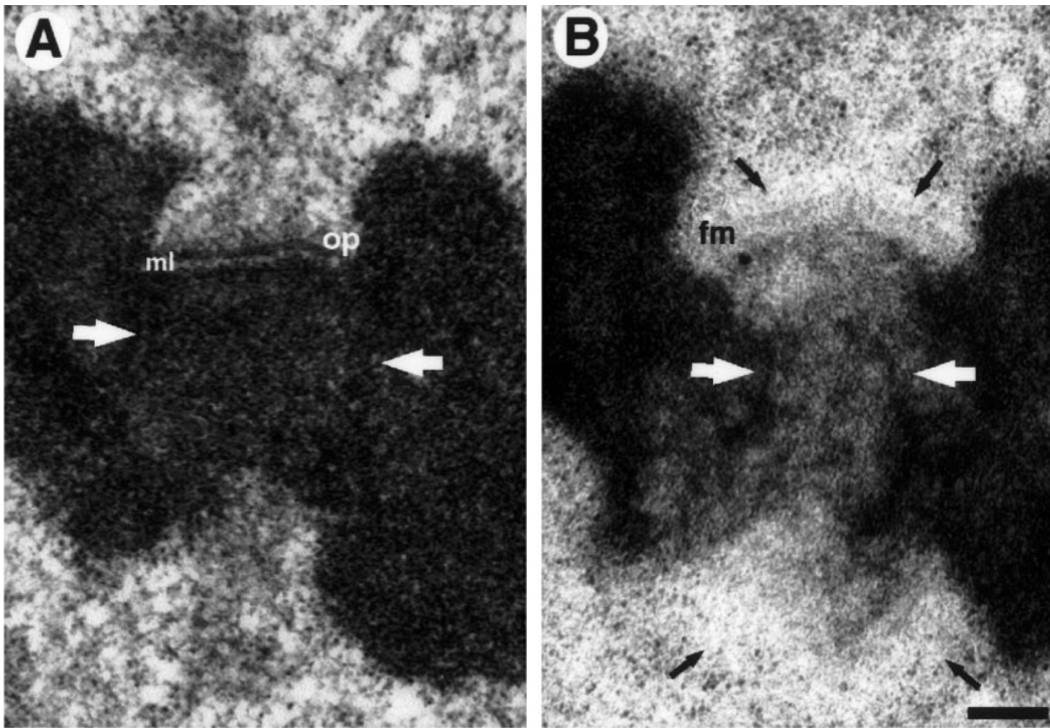


Figure 1.6: Comparison of kinetochore structure using conventional fixation (left) and high-pressure freezing/freeze substitution (right) using electron microscopy.

The outer plate (op) of the trilaminar kinetochore structure is separated from centromeric heterochromatin by a translucent middle layer (ml). The fibrous corona extends from the exterior of outer plate. The kinetochore on the right shows the outer plate as a fibrous mat-like structure (fm) lacking the middle translucent layer seen on the left and the corona appears as a cytoplasmic exclusion zone (black arrows). White arrows indicate heterochromatin. Adapted from (McEwen et al., 1998).

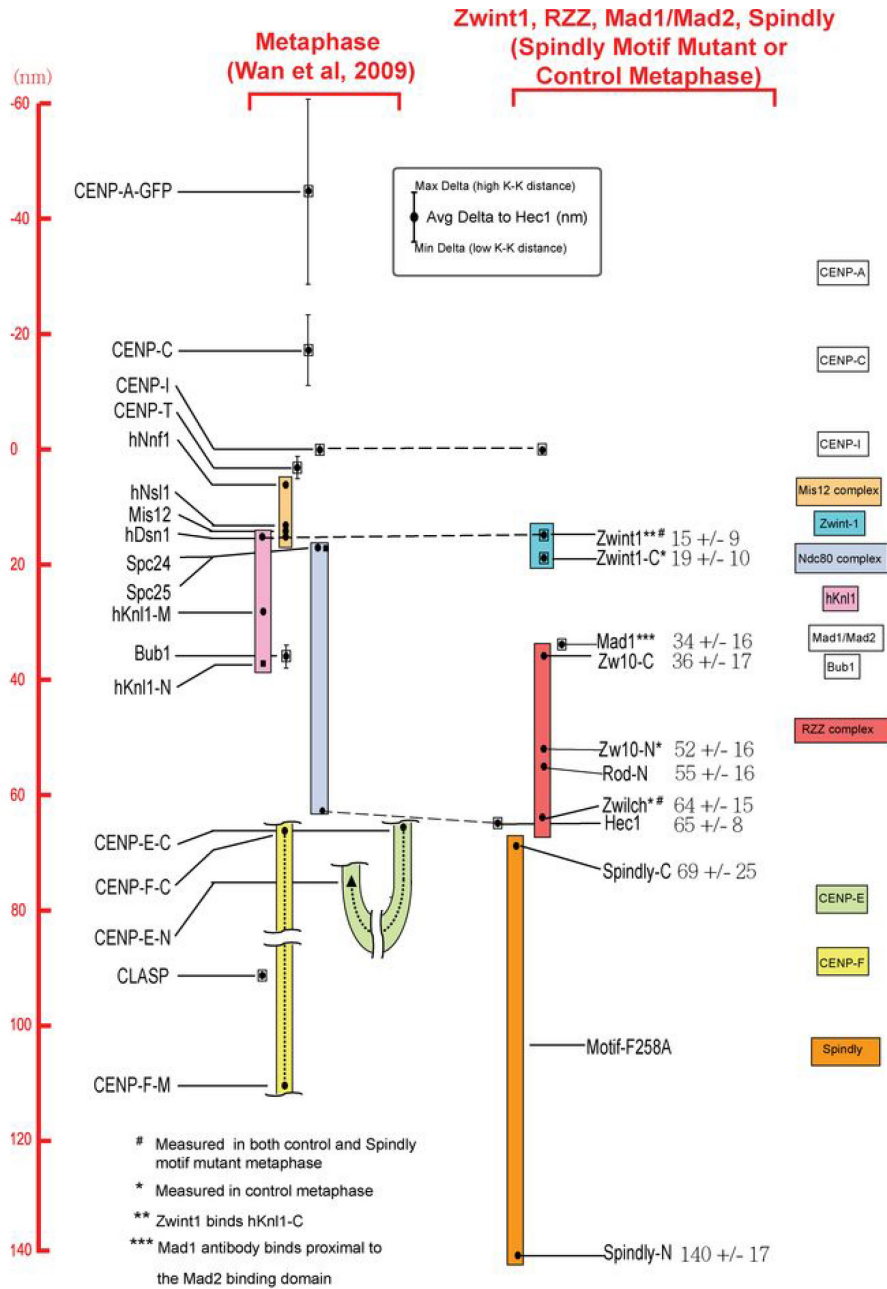


Figure 1.7: Relative positions of the kinetochore proteins to CENP-I (set to 0) based on distance measurements (delta measurements).

Relative positions of various kinetochore proteins are shown. Positive value distance proteins are located towards the spindle MTs and negative value proteins are positioned towards the centromeric DNA. The vertical lines indicate the minimum and maximum Delta values measured across the variation in centromere stretch. Functions of all these proteins are discussed in detail in the next sections. Adapted from (Varma et al., 2013). (©Varma et al., 2013. Originally published in *Journal of Cell Biology*. doi: 10.1083/jcb.201304197)

1.5.1 The constitutive centromere-associated network

Kinetochore assembly is transient and cell cycle regulated, which makes it challenging to define its precise mechanism at the molecular level (Cheeseman and Desai, 2008; Liu et al., 2006; Vos et al., 2006). Nevertheless, extensive research has characterized temporal order and interdependency of many inner and outer kinetochore proteins. The constitutive centromere-associated network (CCAN) consists of seventeen proteins that reside at the centromeric DNA throughout the cell cycle (Figure 1.8) (Cheeseman and Desai, 2008). These proteins were copurified with either CENP-A nucleosomes or other subunits of CCAN in human cells (Foltz et al., 2006; Izuta et al., 2006; Obuse et al., 2004b; Okada et al., 2006). A novel CENP-X protein copurified with CENP-S and was added to the list of CCAN proteins (Amano et al., 2009). The detailed function of each component of the CCAN is not known but each one is essential for kinetochore assembly and function (Amano et al., 2009; McClelland et al., 2007; Okada et al., 2006; Regnier et al., 2005). The CCAN proteins interact with CENP-A-containing histones and establish a links with chromosomes (Nishino et al., 2012). Furthermore, the CCAN recruits the KMN complex (described in detail next), which is required for kinetochore-MT attachment and checkpoint signaling.

The kinetochore localization of CENP-C (of CCAN) is dependent on CENP-A nucleosomes (Carroll et al., 2010; Kato et al., 2013) and it interacts with the outer kinetochore components (Przewloka et al., 2011; Screpanti et al., 2011). CENP-A overexpression leads to localization of CENP-A and CENP-C at ectopic sites, along with Zwint-1 (Zw10-interacting protein 1), indicating that CENP-A and/or CENP-C might be interacting with Zwint-1 (Saunders et al., 1993). Zwint-1 is involved in the kinetochore localization of the RZZ complex and my studies in this thesis are focused on the RZZ complex mediated checkpoint function through Spindly (discussed in detail in section 1.7.3). CENP-H and CENP-I kinetochore localization is interdependent as well as dependent on CENP-A (Figure 1.8) (Nishihashi et al., 2002). The kinetochore-localization of CENP-C and CENP-U is dependent on CENP-H and CENP-I (Minoshima et al., 2005;

Nishihashi et al., 2002) and CENP-C binds to Mis12 complex. The second DNA binding complex consists of CENP-T, W, S and X proteins and CENP-T binds Ndc80 complex of the KMN network (described in detail next) (Schleiffer et al., 2012). The assembly of both the CENP-C and CENP-T complexes is regulated by mitotic phosphorylation downstream of CDK (Gascoigne and Cheeseman, 2013). CENP-C directly binds to Mis12 and CENP-T to Ndc80 and thus the CCAN acts as a scaffold for the assembly of outer kinetochore complexes (Gascoigne et al., 2011; Kim and Yu, 2015; Schleiffer et al., 2012; Screpanti et al., 2011).

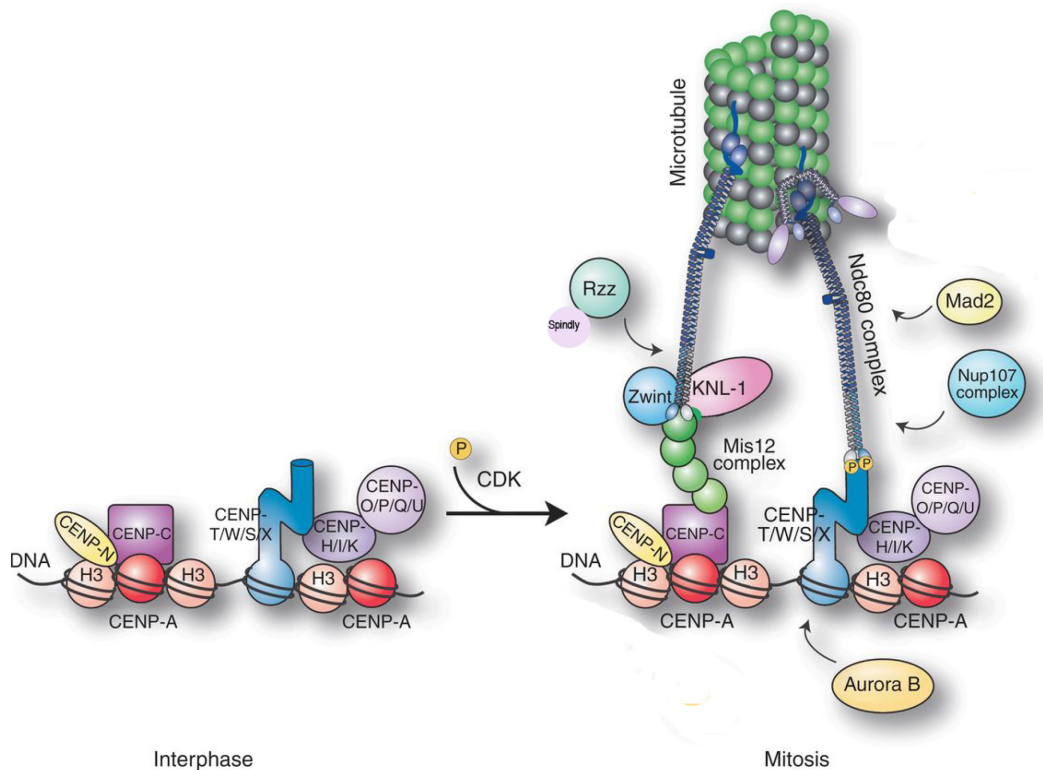


Figure 1.8: Kinetochore architecture showing its components in interphase and mitosis.

A schematic representation of the general organization of the kinetochore. The assembly of kinetochore components is complex, hierarchical and interdependent. The CCAN directly interacts with DNA and consists of 17 proteins (all protein components not shown here). The CCAN proteins bind to the KMN (KNL1/Blinkin, Mis12, Ndc80/Hec1) protein subunits in mitosis. The CCAN and KMN together form the inner and outer kinetochore. The KMN further recruits the regulatory kinetochore proteins present in the fibrous corona such as the RZZ complex and Mad2. All the protein complexes are discussed in detail in the text. Adapted from (Cheeseman, 2014). Cold Spring Harb Perspect Biol 2014;6:a015826. Copyright © 2014 Cold Spring Harbor Laboratory Press; all rights reserved; doi: 10.1101/cshperspect.a015826

1.5.2 KMN network

The outer kinetochore consists of the conserved KMN network (Figure 1.8) named after its protein subcomplexes: KNL1/Blinkin (kinetochore null protein 1), Mis12 (missegregation 12), Ndc80/Hec1 (nuclear division cycle 80/highly expressed in cancer 1). The KMN network members localize to kinetochores from late G2 to telophase. The KMN network forms a specialized binding site for spindle MTs (Cheeseman et al., 2006; Cheeseman et al., 2004; Obuse et al., 2004a; Przewloka et al., 2011) and helps in anaphase chromosome movements by coupling chromosome movement to MT depolymerization (Tooley et al., 2011). The KMN network binds MTs as well as centromeric DNA and is conserved across eukaryotes. I discuss the hypothetical idea of KMN function regulation by Spindly through the RZZ complex in this thesis.

The Mis12 complex (composed of Mis12, Dsn1, Nsl1 and Nnf1 proteins) interacts directly with CENP-C of the CCAN (Przewloka et al., 2011; Screpanti et al., 2011). The Mis12 complex also interacts with KNL1 (Maskell et al., 2010), the Ndc80 complex and Zwint-1 (Cheeseman et al., 2004; Obuse et al., 2004a; Petrovic et al., 2010). Furthermore, the Mis12 complex also interacts with heterochromatin proteins HP1 α and HP1 γ (Saunders et al., 1993), which are essential for Mis12 kinetochore recruitment (Obuse et al., 2004a). This finding explains the importance of heterochromatin in kinetochore assembly. The Mis12 complex is localized to centromeres throughout the cell cycle and its depletion leads to kinetochore structural defects due to mislocalization of kinetochore proteins and chromosome segregation errors (Goshima et al., 2003; Kline et al., 2006). Mis12 proteins bind to both KNL1 and Ndc80 and hence Mis12 complex serves as a link between the two complexes (Gascoigne and Cheeseman, 2013; Petrovic et al., 2014).

KNL1/Blinkin interacts directly with Bub1, Bub3 and Zwint-1 and recruits these proteins to kinetochores (Kops et al., 2005). KNL1 phosphorylation by Mps1 kinase is a pre-requisite for the recruitment of Bub1 and Bub3 proteins (London et al., 2012; Shepperd et al., 2012; Yamagishi et al., 2012) and hence

mitotic checkpoint activation (Krenn et al., 2014; Primorac et al., 2013; Vleugel et al., 2013). KNL1 interacts with the Nsl1 and Dsn1 subunits of the Mis12 complex as mentioned above. Hence, KNL1 acts as a linker between outer kinetochore components and fibrous corona protein components. KNL1 is also believed to have a role in MT attachment (Cheeseman et al., 2006; Kiyomitsu et al., 2007).

The Ndc80 complex is a heterotetramer consisting of heterodimers of Spc24-Spc25 (spindle pole component) and Ndc80/Hec1-Nuf2 (nuclear filamentous 2) (Ciferri et al., 2005; Wei et al., 2005). The Spc24-Spc25 globular domain, pointing towards the centromere, binds to Mis12 (Petrovic et al., 2010) and CCAN components (Bock et al., 2012). The Ndc80-Nuf2 globular domain pointing away from the centromere mediates interactions with MTs of the spindle (Cheeseman et al., 2006; Ciferri et al., 2008; Guimaraes et al., 2008; Wei et al., 2007). Disruption of Ndc80 function leads to gross kinetochore-MT attachment defects along with chromosome mis-segregation (DeLuca et al., 2002). Additionally, the Ska (spindle and kinetochore associated) complex (Ska1, Ska2 and Ska3) assists in kinetochore-MT interactions by associating with the depolymerizing end of MTs (Daum et al., 2009; Hanisch et al., 2006; Welburn et al., 2009). Although challenging, future research will explain the complete molecular architecture of the kinetochore in detail.

To conclude, the KMN network acts as a landing pad for kinetochore checkpoint proteins of the fibrous corona and is the core site for MT attachment on kinetochores.

1.5.3 Mitotic kinases

Phosphorylation is a robust and reversible protein post-translational modification that is extensively used in cell growth, differentiation, apoptosis and cell cycle progression. In Chapter 4, I have addressed how Spindly phosphorylation affects its kinetochore localization and function. To date, numerous mitotic kinases have been identified with functions such as centrosome duplication/maturation, mitotic spindle formation, kinetochore assembly and

checkpoint regulation. Mitotic kinases include but are not limited to Cdk1, Aurora A-C, Bub1, Bub3, BubR1, Plk1, Mps1 and NEK kinases as shown in Figure 1.9 reviewed in (Ma and Poon, 2011). Here I discuss checkpoint regulation by kinases present at kinetochores that are relevant to this thesis.

Activity of Cdk1 in complex with cyclin B is required for entry into mitosis, at which point it phosphorylates BubR1 (Porter and Donoghue, 2003; Wong and Fang, 2007). The Cdk1-cyclin B complex phosphorylates several subunits of APC/C^{Cdc20} and thus generates a negative feedback loop for its own destruction by APC/C (Kraft et al., 2003). Cdk1 phosphorylates Cdc20 and hence controls mitotic checkpoint silencing through its degradation (Miniowitz-Shemtov et al., 2012). Cdk1-cyclin B1 regulates mitotic spindle formation by phosphorylating MAPs, MT motor proteins and tubulin (Blangy et al., 1995; Fourest-Lieuvin et al., 2006).

Aurora A kinase present at centrosomes regulates centrosome maturation and entry into mitosis (Barr and Gergely, 2007; Bayliss et al., 2003; Lioutas and Vernos, 2013). Aurora B function is discussed in detailed under kinetochore-MT error correction mechanism in a later section. Little is known about Aurora C, which is expressed in testis. Aurora C is proposed to have the same function as Aurora B since it rescues the Aurora B multinucleation phenotype (Sasai et al., 2004). Aurora B kinase recruits the RZZ complex and Spindly to kinetochores through Zwint-1 phosphorylation (Ditchfield et al., 2003; Kasuboski et al., 2011). Aurora B kinase also phosphorylates Dsn1 subunit of the Mis12 complex and recruits KMN network to kinetochores (Yang et al., 2008).

Bub1 and BubR1 kinases act sensors of unattached kinetochores and are recruited to kinetochores during prophase. Bub1 is mainly known to protect sister chromatid cohesion on centromeric chromatin by regulating the localization of Shugoshin protein which preserves centromeric cohesion (Kitajima et al., 2005). The role of Bub1 in checkpoint activation is controversial as depletion of Bub1 in human cells results in robust checkpoint activity in response to MT poisons (Johnson et al., 2004; Morrow et al., 2005). However, Bub1 depletion in human

and *Drosophila* cells leads to chromosome segregation errors perhaps through Aurora B mislocalization (Basu et al., 1999; Musio et al., 2003). Bub1 also phosphorylates Cdc20 and inhibits APC/C^{cdc20} activity thus preventing anaphase onset (Tang et al., 2004). In this section, I will briefly discuss the function of the kinases implicated in Spindly phosphorylation as well as kinases that localize to kinetochores during mitosis.

Bub1 phosphorylates histone H2A and recruits the chromosome cohesin regulator Shugosin (Kawashima et al., 2010; Yamagishi et al., 2010). BubR1 is a component of the mitotic checkpoint complex, which recruits Cdc20 to kinetochores (Lischetti et al., 2014) that inhibit the activity of APC/C during mitosis. Interaction between BubR1 and CENP-E is known to enhance its kinase activity, however, once CENP-E is bound to MTs, it suppresses BubR1's kinase activity for reasons that remain to be investigated (Chan et al., 1999; Mao et al., 2003; Mao et al., 2005; Yao et al., 2000). Based on these results, Chan *et al.* (1999), hypothesized that the BubR1 and CENP-E complex acts as a mechanosensor of kinetochore-MT attachments. However, this hypothesis is disputed by the observation that BubR1 kinase activity is not essential for mitotic checkpoint activation and the yeast homologue of BubR1 (Mad3) lacks kinase activity (Chen, 2002; Elowe et al., 2010).

Mps1 is an essential checkpoint kinase and has functions ranging from centrosome duplication to mitotic checkpoint regulation (Liu and Winey, 2012). Mps1 has been shown to phosphorylate itself (Mattison et al., 2007) as well as Dam1 (in yeast) (Jelluma et al., 2008; Shimogawa et al., 2006), Mad1 (in yeast) (Hardwick et al., 1996), CENP-E (in *Xenopus*) (Espeut et al., 2008) and the Borealin subunit of CPC in humans (Jelluma et al., 2008). Studies dissecting the requirement of Mps1 in centrosome duplication yielded contradictory results showing that Mps1 deleted human cell lines underwent centrosome duplication {reviewed in (Liu and Winey, 2012)}. Mps1 kinetochore localization is required for kinetochore recruitment of the RZZ complex (Santaguida et al., 2010), Mad1,

Mad2 (Santaguida et al., 2010), Bub1/Bub3 (Shepperd et al., 2012) and CENP-E (Abrieu et al., 2001) and hence checkpoint activation.

Polo-like kinase 1 (Plk1) kinase is the most extensively studied member of the five Plk family members (Plk1-5). Plk1 kinase localizes to both centrosomes and kinetochores and is implicated in centrosome maturation, kinetochore-MT attachment and chromosome segregation during mitosis {reviewed in (Archambault and Glover, 2009)}. Plk1 homozygous mutations in mice are lethal and mice with heterozygous mutations develop tumors (Lu et al., 2008). Plk1 phosphorylates Cdc25 and thus activates Cdk1 (Roshak et al., 2000). A Phosphoepitope (3F3/2) generated by Plk1 at kinetochores regulates the association of various checkpoint proteins such as Mad2, CENP-E, Hec1/Ndc80, Spc24, and Cdc20 (Ahonen et al., 2005). Plk1 is also required for the removal of most cohesin during prophase and prometaphase (Sumara et al., 2002). In addition, Plk1 along with Cdk1 phosphorylate different sites of APC/C and activate the Cyclosome (Golan et al., 2002).

Overall, mitotic kinases play a major role in mitotic checkpoint signaling during mitosis.

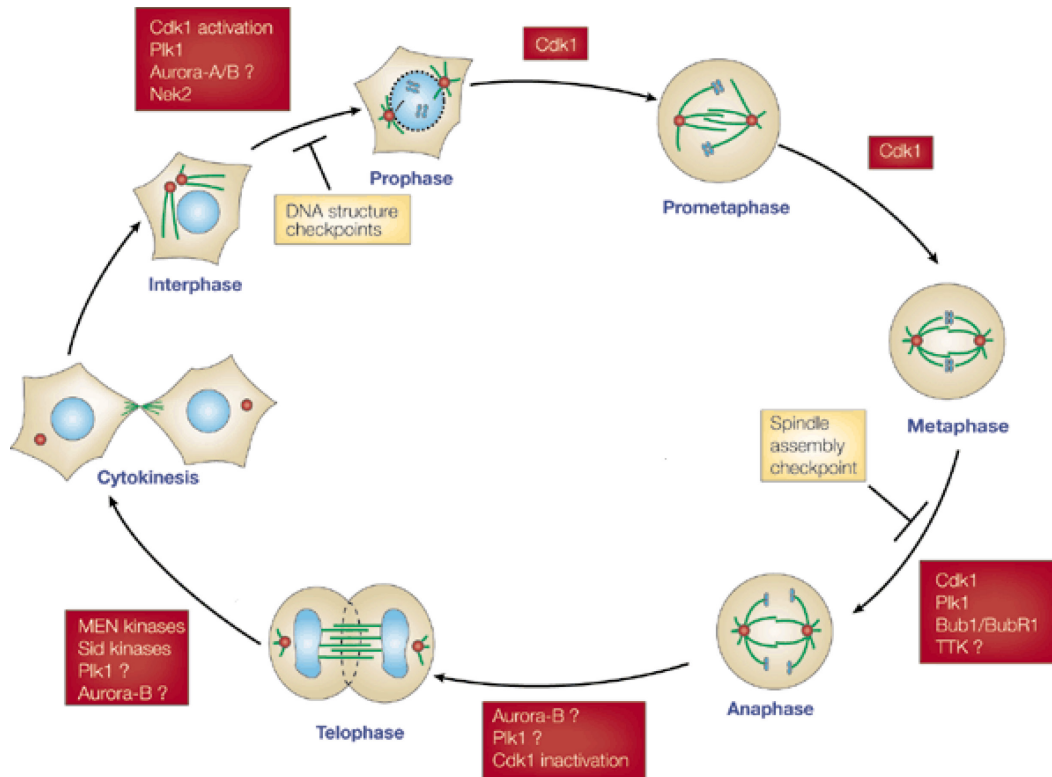


Figure 1.9: Mitotic kinases regulating cell cycle progression at different stages.

A brief description of the function of these mitotic kinases is provided in the section 1.6.4. Adapted from (Nigg, 2001).

1.6 Kinetochores-Microtubule Attachment

Kinetochores must physically link with MTs of the mitotic spindle in a bipolar manner for equal segregation of genetic material into two daughter cells. A human kinetochore can bind 20-30 microtubules (McEwen et al., 1997). The physical attachment between MTs and kinetochore involve both lateral and end-on attachments. Mature kinetochore-MT attachments result in rapid removal of checkpoint proteins from kinetochores leading to checkpoint silencing. I present a possible role for Spindly in kinetochore-MT attachment formation and how kinetochore-MT attachments affect the kinetochore localization pattern of Spindly during mitosis in chapter 4. There are two proposed mechanisms of kinetochore-MT attachment: Classic search and capture model and the self-assembly model. These models are described below.

1.6.1 Classic search and capture model

According to the search and capture model, centrosome nucleated MTs search the cytoplasm and randomly establish contacts with kinetochores resulting in monopolar attachment and stabilization of MTs (Figure 1.10) (Holy and Leibler, 1994; Kirschner and Mitchison, 1986). These mono-oriented chromosomes rapidly move toward the attached spindle pole and wait for MTs from the opposite pole to make contact with the sister chromatid. Upon bi-polar attachment chromosomes rapidly move towards the metaphase plate and oscillate due to opposing forces from the two spindle poles. While this model is supported by increased turnover of mitotic MTs and the dynamic nature of MTs (Desai and Mitchison, 1997), computational studies indicate that this model does not explain the rapid kinetochore-MT attachment in cells (Wollman et al., 2005). Furthermore, mitotic spindle assembly in mutant flies lacking centrosomes (Basto et al., 2006) and meiotic chromosome segregation in the absence of spindle poles brings into question the basis of the search and capture model (Heald et al., 1997; Khodjakov et al., 2000).

1.6.2 Self-assembly of spindles or chromatin pathway

The 'self assembly' model proposes that acentrosomal MTs are nucleated in the vicinity of chromosomes and organized into bi-polar spindles with the help of motor proteins (Figure 1.10) (Albertson and Thomson, 1993; McKim and Hawley, 1995; Szollosi et al., 1972; Theurkauf and Hawley, 1992). Oocytes of most animal species and mitotic cells of higher plants assemble their spindles in the absence of centrosomes (Compton, 2000). Furthermore, depletion of centrosomes (by micro-surgical removal, laser ablation or mutations) in *Drosophila* and human cells and meiotic chromosome segregation in *C. elegans* does not interfere with the spindle assembly and chromosome segregation indicating that centrosomal initiation of the mitotic spindle is dispensable for chromosome segregation (Basto et al., 2006; Khodjakov et al., 2000; Nahaboo et al., 2015). Additionally studies have shown that kinetochores are not essential for the formation of the spindle as prokaryotic DNA lacking centromeric chromatin show proper spindle formation at metaphase (Karsenti et al., 1984), however, kinetochores are essential during anaphase for proper chromosome segregation. Assembly of the mitotic spindle by the addition of magnetic beads coated with plasmid DNA in *Xenopus* egg extracts lacking kinetochores and centrosomes demonstrated that MT nucleation around chromatin is sufficient for mitotic spindle generation (Heald et al., 1996). Acentrosomal spindles were proposed to sort their MTs according to polarity with the help of MT motor proteins (Heald et al., 1996).

MT nucleation independent of centrosomes was observed to arise from regions proximal to kinetochores (Khodjakov et al., 2000; Khodjakov et al., 2003; Maiato et al., 2004a; Tulu et al., 2006). This kinetochore-MT nucleation was induced by the addition of a small GTPase called Ran in *Xenopus* egg extracts (Carazo-Salas et al., 2001; Kalab et al., 2002; Ohba et al., 1999; Wilde and Zheng, 1999). RanGEF (guanine exchange factor), RCC1 (Regulator of chromosome condensation) creates a Ran GTP gradient around chromosomes, which further generates an environment for MT nucleation (Kalab et al., 2002).

MTs generated by Ran GTP gradient orient their minus end towards the spindle poles and their plus ends towards the kinetochores similar to centrosomal MTs and eventually make contacts with kinetochores (Khodjakov et al., 2003). Kinetochores nucleated MTs interact with motor proteins such as dynein and NuMa to crosslink with centrosomal MTs. Cross-linking between kinetochores and centrosomal MTs leads to the attachment of kinetochores-MTs to centrosomes and they form a common spindle {reviewed in (Wadsworth and Khodjakov, 2004)}. Kinetochores-fiber (K-fiber) formation and maturation also aligns the mono-oriented chromosomes at the metaphase plate. The un-attached kinetochores can further form lateral connections with the mature K-fibers of other chromosomes leading to congression on the metaphase plate (Kapoor et al., 2006). In conclusion, a cell may rely on both classic search and capture and self-assembly spindle pathways to generate a mitotic spindle.

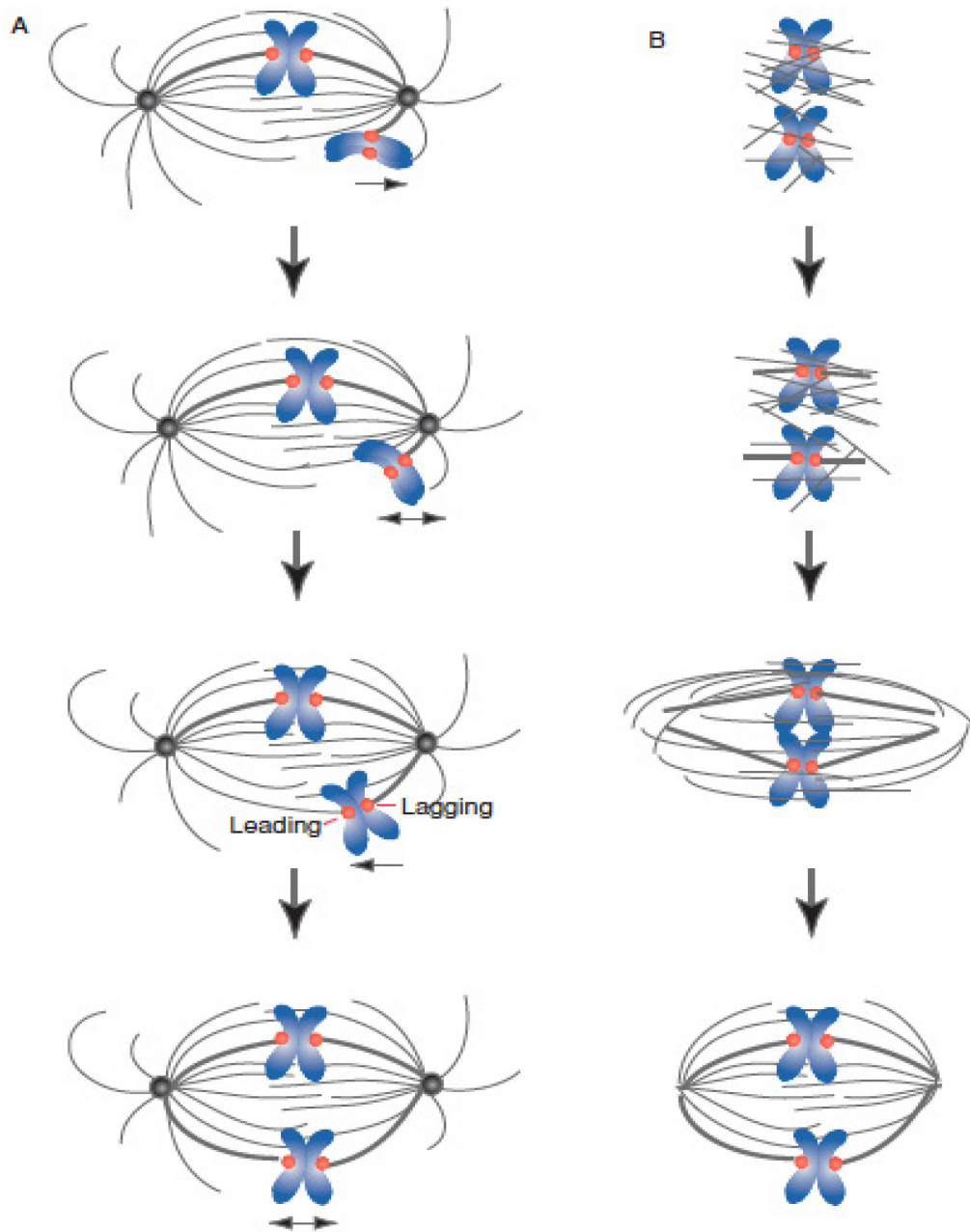


Figure 1.10: Mitotic spindle assembly models: (A) Random search and capture & (B) Self-assembly/chromatin pathway/ acentrosomal.

According to search and capture, centrosomal nucleated MTs probe the cytoplasm randomly and establish kinetochore-MT attachment. According to the self-assembly model, MTs are nucleated in the periphery of chromosomes and these MTs are sorted according to polarity by MT associated motor proteins to assemble a mitotic spindle. The kinetochore pulled towards the centrosome is called leading kinetochore and the opposite sister kinetochore is called the lagging kinetochore. Adapted from (Walczak and Heald, 2008).

1.6.3 Lateral attachments

Initially, MT polymers form lateral attachments with the kinetochores during prometaphase. These lateral interactions require MT motor CENP-E, a plus end directed motor and dynein/dynactin, a minus end directed motor (Sharp et al., 2000b) (Vitre et al., 2014). Dynein/dynactin plays a role in chromosome movement facilitating kinetochore-MT attachments as well as MT capture during prometaphase (Bader and Vaughan, 2010; Howell et al., 2001; Yang et al., 2007b). Monopolar chromosomes move towards the middle of the cell with the help of the CENP-E kinesin motor to make a contact with the MTs from the opposite pole (Kapoor et al., 2006; Yen et al., 1992). CENP-E laterally attaches to k-fibers of aligned chromosomes and ferries unaligned chromosomes to the metaphase plate (Kapoor et al., 2006). MT motors allow initial lateral kinetochore-MT attachments and further enhance the chances of robust end-on bipolar attachments.

1.6.4 End-on attachments

Eventually all the chromosomes establish end-on MT attachments through their kinetochores. End-on attachments are crucial for accurate chromosome segregation during anaphase. However, chromosomes can engage in a number of erroneous kinetochore-MT attachments during prometaphase. Monopolar chromosomes fail to attach one kinetochore to MTs. Syntelic chromosomes attach both kinetochores to the same pole and merotelic chromosomes have one kinetochore attached to both poles (Figure 1.11). All of these kinetochore-MT attachment errors result in severe chromosome segregation defects and ultimately aneuploidy if not corrected. Aneuploidy is a hallmark of most solid tumors and can result in cell death as well (Cimini and Degrossi, 2005). Aurora B kinase plays a key role in the correction of kinetochore-MT attachments.

1.6.5 Error-correction mechanism by Aurora B kinase

Aurora B was first identified in a yeast mutant with a loss of function mutation in the *Ipl1* gene (Aurora B homologue) and this mutant exhibited high rates of improper kinetochore-MT attachments leading to chromosome missegregation (Chan and Botstein, 1993). Aurora B kinase along with Inner Centromere protein (INCENP), Survivin and Borealin form the Chromosomal Passenger complex (CPC) (Earnshaw and Bernat, 1991; Vagnarelli and Earnshaw, 2004). The CPC localizes to the inner centromere during prometaphase and metaphase, and localizes to the spindle midzone at anaphase (Earnshaw and Bernat, 1991; Vagnarelli and Earnshaw, 2004). Aurora B kinase destabilizes the kinetochore-MT attachments by phosphorylating the Ndc80/Hec1 complex (Chan et al., 2012; DeLuca et al., 2006), Skl1 complex (Chan et al., 2012), and deactivating MCAK which depolymerizes MTs (Figure 1.11) (Knowlton et al., 2006; Lan et al., 2004; Ohi et al., 2003). Phosphorylation of Aurora B substrates promotes kinetochore-MT dissociation and hence generates unattached kinetochores. Generation of tension across sister kinetochores upon bi-polar attachment spatially separates Aurora B and its substrates (Figure 1.11) (Liu et al., 2009). Additional studies on Aurora B suggested it functions in the mitotic checkpoint independent of its tension-sensing error correction pathway (Kallio et al., 2002; Petersen and Hagan, 2003). A recent study showed that Aurora B destabilizes only end-on attachment leading to phosphorylation of Ndc80 and destabilizes end-on attachments. The lateral attachments not sensed by the Aurora B pathway lead to the formation of stabilized bi-polar end-on attachments (Kalantzaki et al., 2015).

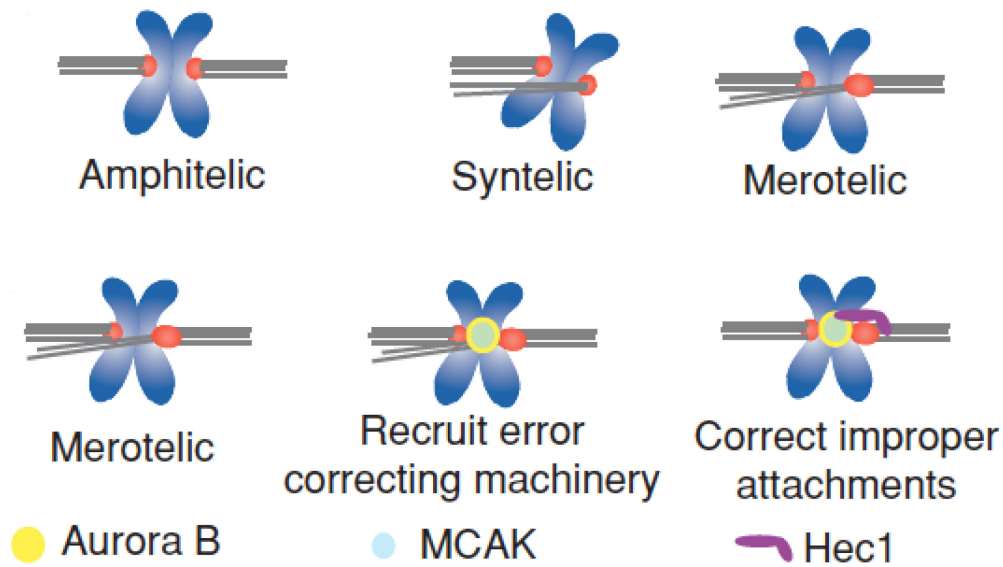


Figure 1.11: Kinetochore-MT attachment errors and correction mechanism. Top panel shows bi-polar kinetochore-MT attachment (amphitelic), sister chromatid kinetochores attached to one pole (syntelic) and one kinetochore attached to both poles (merotelic). Lower panel shows the detection of improper kinetochore attachment (merotelic) by Aurora B kinase and recruitment of kinesin MCAK. The latter destabilizes spindle MTs, generates an unattached kinetochore and subsequently promotes amphitelic attachment. Adapted from (Walczak and Heald, 2008)

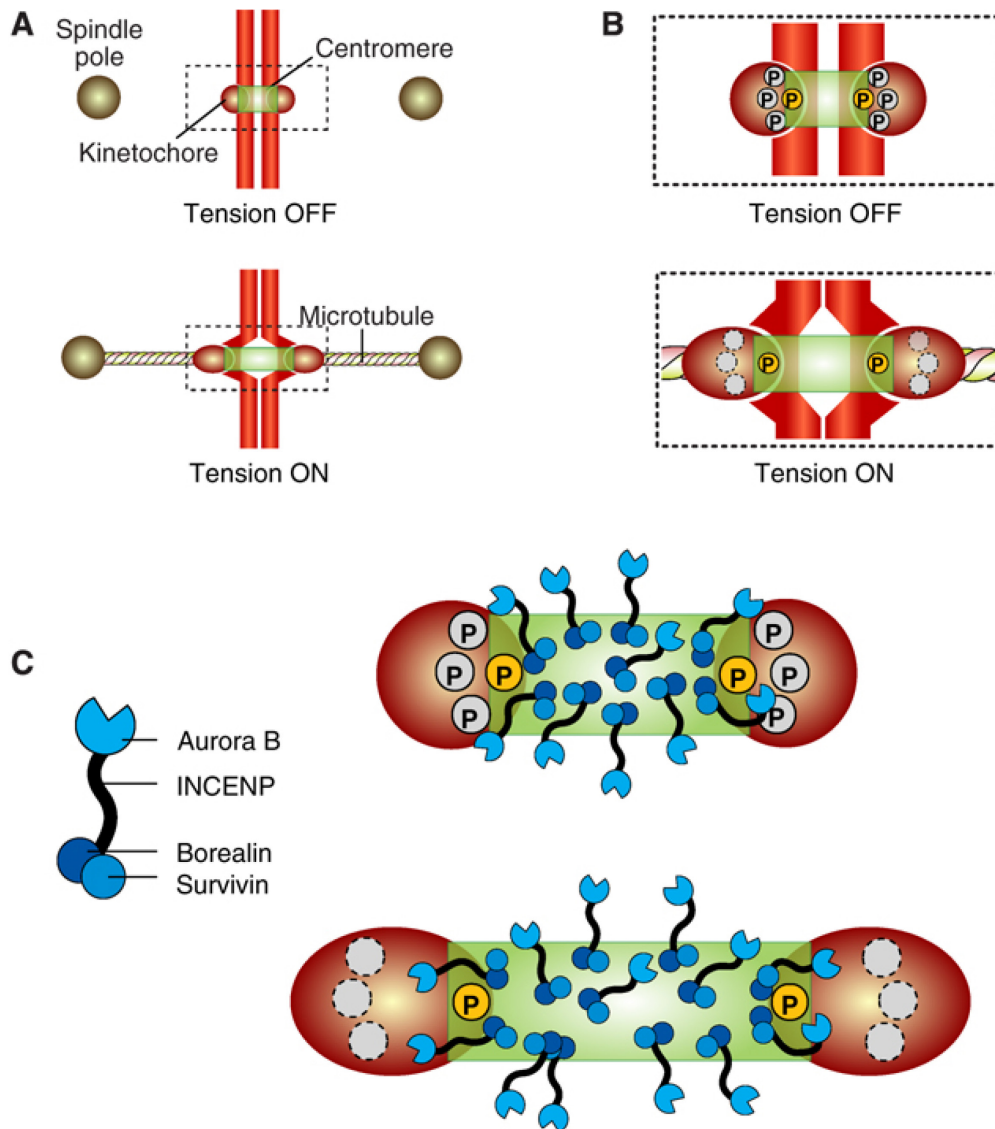


Figure 1.12: Schematic diagram representing Aurora B error correction mechanism during mitosis.

(A) Aurora B phosphorylates kinetochore protein complexes in the absence of tension due to their proximity to the kinase. (B) Bi-polar kinetochore-MT attachments generate tension across sister chromatids as well as within kinetochore components due to opposing forces exerted by MTs from opposite poles and hence physically separates Aurora B from its substrates. Conversely lack of tension due to improper kinetochore-MT attachments leads to Aurora B mediated phosphorylation of its substrates and destabilization of kinetochore-MT attachments. (C) Schematic of CPC and its phosphorylation during lack of tension and in the presence of tension. Adapted from (Santaguida and Musacchio, 2009).

1.7 The Mitotic Checkpoint and Mitotic Checkpoint Proteins

During cell division, the faithful segregation of genetic material into two daughter cells is controlled by the mitotic checkpoint (Musacchio and Salmon, 2007). Failure of the mitotic checkpoint has been closely linked to aneuploidy, which is a hallmark of most solid tumors, and mutations in mitotic checkpoint proteins have been linked to mitotic checkpoint dysfunction and cancer (Cahill et al., 1998; Dai et al., 2004; Michel et al., 2001; Wang et al., 2004b). The mitotic checkpoint prevents cells from entering anaphase until all the chromosomes are bi-polarly attached to spindle microtubules (MTs) through their kinetochores and are under tension (Musacchio and Salmon, 2007). Chemical inhibition of mitotic spindle formation prevents the metaphase-anaphase transition during mitosis (Jordan et al., 1992; Sluder, 1979). Mitotic checkpoint proteins were first identified in two studies, which isolated yeast mutants that failed to halt the cell cycle in the presence of MT poisons such as nocodazole and benomyl. The first group of mutants were named *mad1* (mitotic arrest deficient), *mad2* and *mad3* (BubR1 in higher eukaryotes) (Li and Murray, 1991) and the second group of mutants were named *bub1* (budding uninhibited by benzimidazole, a MT depolymerizing drug), *bub2*, and *bub3* due to impaired microtubule formation (Hoyt et al., 1991). Subsequently, the *Mps1* kinase (Monopolar Spindle) yeast mutant was observed to fail to arrest in mitosis upon disruption of spindle formation (Weiss and Winey, 1996). The function of mitotic checkpoint proteins is also required for cell cycle delay in response to mutation of centromeric DNA and dysfunctional kinetochore indicating the role of the mitotic checkpoint in establishing kinetochore-MT attachments (Hardwick et al., 1996; Spencer and Hieter, 1992; Wang and Burke, 1995). Mad, Bub and Mps1 homologues have been identified in all other eukaryotic organisms indicating an evolutionarily conserved mitotic checkpoint (Elledge, 1996). Since then, many other checkpoint proteins have been identified in addition to these core checkpoint proteins as described next.

Mitotic checkpoint proteins can be divided into three main components: a sensor that detects kinetochore-MT attachment status (Mad1-Mad2), a signal produced by sensor molecules in the presence of faulty kinetochore-MT attachments or unattached kinetochores (MCC complex) and a response element with a biochemical activity mediating the checkpoint induced arrest (Anaphase promoting complex/cyclosome) (Chan and Yen, 2003; Murray, 1992). The signal generated by the sensor molecules is amplified globally to prevent anaphase onset.

The mitotic checkpoint acts as a surveillance mechanism and prevents metaphase to anaphase transition until all the chromosomes are aligned on the metaphase plate with bi-polar attachments. It is still unclear if the mitotic checkpoint senses kinetochore-MT attachment or tension generated by bi-polar attachments, or both (attachment and tension) to generate a wait anaphase signal. MTs from the opposing spindle poles exert pulling forces in the opposite direction on bi-polar chromosomes aligned at the metaphase plate. These opposing forces generate tension between the two sister kinetochores as well as within the individual kinetochore components (He et al., 2000; Maresca and Salmon, 2009; Uchida et al., 2009; Waters et al., 1996). The kinetochore tension leads to increased distance between the two sister kinetochores upon bi-orientation as well as between the components of inner and outer kinetochore of an individual kinetochore (Figure 1.12).

Reider *et al.*, laser ablated the unattached kinetochore of mono-oriented chromosomes and cells progressed into anaphase in the presence of an unattached chromosome. This finding showed that the kinetochore is the site for the generation of a “wait anaphase” signal and that the mitotic checkpoint senses the kinetochore-MT attachment status (Rieder et al., 1995). However, an elegant study showed that applying tension to an improper kinetochore-MT attachment with a needle resulted in anaphase onset, suggesting that the mitotic checkpoint senses the tension across sister kinetochores (Li and Nicklas, 1995). Several other studies over time have supported either “tension” or “attachment” as the sensing

mechanism for mitotic checkpoint activity, further heating up the debate (Maresca and Salmon, 2010). To resolve this matter, some studies pointed out the role of tension in destabilizing MT attachment and creating unattached kinetochores through Aurora B activity (Cheeseman et al., 2002; DeLuca et al., 2006). However, this matter remains poorly understood and needs further investigation.

Another conundrum in the mitotic checkpoint field is whether the checkpoint generates an on/off switch or a graded response. Two recent reports measured the checkpoint activity in response to different errors (by treating cells with the MT destabilizing drug nocodazole and the MT stabilizing drug taxol) using different approaches and suggested that the checkpoint response is graded since more severe defects generate a stronger response/ mitotic delay (Collin et al., 2013; Dick and Gerlich, 2013). Why cells evolved a graded response as compared to a toggle switch-like response needs further explanation.

Mitotic checkpoint regulation at the molecular level involves various kinetochore proteins, which are discussed next.

1.7.1 Anaphase promoting complex/cyclosome

The mitotic checkpoint prevents anaphase onset by inhibiting the anaphase-promoting complex/cyclosome (APC/C) from ubiquitylating securin and cyclin B (Cdk1 cofactor) (Thornton et al., 2006; Visintin et al., 1997). Degradation of securin activates a protease, separase, which is required for the proteolytic cleavage of cohesin between the sister chromatids, thus allowing the separation of sister chromatids (Musacchio and Salmon, 2007). The mitotic checkpoint inhibits APC/C activity by incorporation of Cdc20 into the MCC as discussed next. The APC/C, a multi-protein complex, functions along with its required coactivators Cdc20 and Cdh1 in the ubiquitin-mediated degradation of various mitotic substrates during mitosis (Figure 1.13). However, degradation of just cyclin B and securin is sufficient for transition from metaphase to anaphase (Pines, 2006; Pines, 2011; Yu, 2007). Cdc20 activity is required for APC/C-mediated securin and cyclin B degradation (Pines, 2011). Cdc20 activity, in turn is regulated by its incorporation into the MCC complex as discussed next.

1.7.2 Mitotic checkpoint complex

The mitotic checkpoint complex (MCC) consists of BubR1, Bub3, Mad2 and Cdc20 and this complex binds and inhibits APC/C activity during mitosis (Sudakin et al., 2001). Initial FRAP studies showed that Mad1 and ~50% of Mad2 are stable kinetochore residents; however, the rest of Mad2 exchanges rapidly with its cytosolic pool (Howell et al., 2004). In metazoan cells, Mad1 also requires the presence of the RZZ complex for kinetochore localization. A key step for the generation of the MCC is the conformational conversion of open Mad2 (O-Mad2) to closed Mad2 (C-Mad2) at unattached kinetochores. The structural conversion of Mad2 has been suggested as the rate-limiting step for checkpoint activation as well as the amplifiable signal. Mad2 was previously believed to be the sole inhibitor of APC/C before the discovery of the MCC. The MCC is highly conserved from yeast to humans and has up to 3000-fold higher APC/C inhibition capacity than individual proteins (Chan et al., 2005; Sudakin et al., 2001).

Mad2 conformational change is the fundamental step for mitotic checkpoint activation. According to the 'template model' Mad1 bound to C-Mad2 at unattached kinetochores recruits cytoplasmic O-Mad2 forming a ternary complex Mad1:C-Mad2: O-Mad2. This complex induces the conversion of O-Mad2 to C-Mad2, which in turn facilitates the interaction of C-Mad2 with Cdc20 (Figure 1.13) (De Antoni et al., 2005; Mapelli et al., 2007). The cytosolic C-Mad2:Cdc20 further converts cytoplasmic O-Mad2 to C-Mad2 similar to the Mad1:C-Mad2 complex at kinetochores albeit at very low levels as demonstrated by in vitro kinetic data (Luo et al., 2002; Luo et al., 2004; Simonetta et al., 2009) but this is still controversial (Mariani et al., 2012). The inhibitory potential of Cdc20:C-Mad2 is significantly increased upon MCC formation with the Bub3/BubR1 complex (Musacchio and Salmon, 2007). However, some studies have suggested that C-Mad2 is not present in the MCC complex and the trimeric complex Bub3:BubR1:Cdc20 is a potent inhibitor of APC/C (Kulukian et al., 2009; Malureanu et al., 2009; Medema, 2009; Tang et al., 2001).

Recently, a mitotic checkpoint factor 2 protein (MCF2) was found to be a potent APC inhibitor (Braunstein et al., 2007; Eytan et al., 2008). The APC/C can also be inhibited by various complexes such as Cdc20:C-Mad2, Bub3:BubR1:Cdc20 and MCC.

The APC/C is readily activated by Cdc20 following the last chromosome attachment to the spindle and triggers the degradation of securin and cyclin B. (Hellmuth et al., 2015; Meadows and Millar, 2015; Sivakumar and Gorbsky, 2015). A recent study showed that APC/C can bind an additional Cdc20 which can activate it but MCC can inhibit APC/C activity even when a second Cdc20 is bound to it (Izawa and Pines, 2015). MCC production is terminated through unclear molecular mechanisms but involves P31^{comet} and dynein as discussed next (Wang et al., 2014).

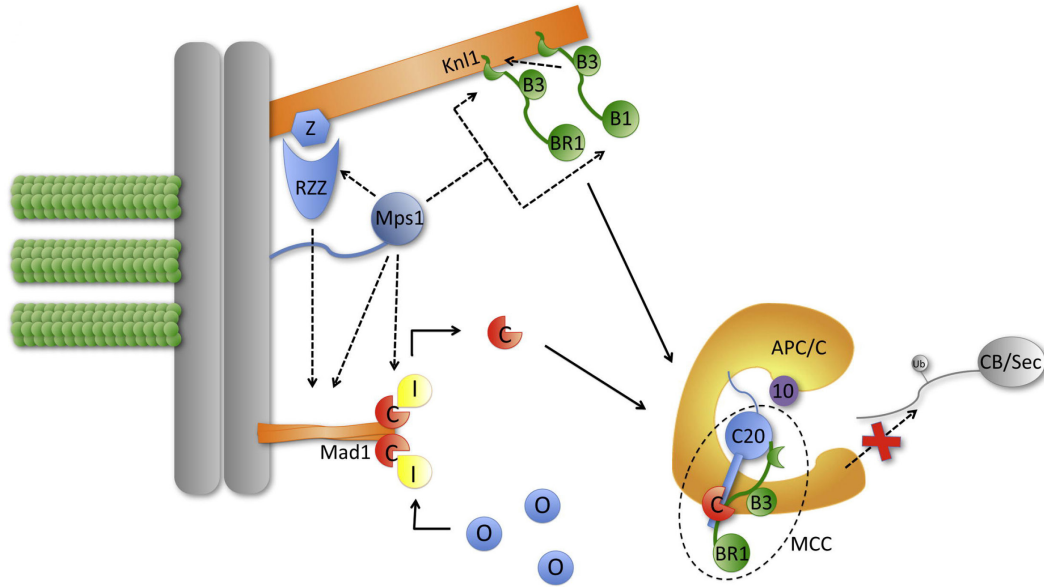


Figure 1.13: MCC complex inhibits APC/C complex.

Unattached kinetochores recruit the RZZ complex through Zwint-1 interaction. Bub1 (B1), BubR1 (BR1) and Bub3 (B3). The RZZ complex with Bub proteins further recruits Mad1 and Mad2 complex, which catalyzes the conversion of Mad2-O to Mad2-C conformation through the formation of an intermediate state (I). Cytosolic Mad2-C binds to BubR1/Bub3 and Cdc20 (APC/C co-activator) forming the MCC complex. The MCC complex binds to APC/C and prevents its activation. Inactivated APC/C cannot ubiquitinate and degrade cyclin B (CB) and securin (Sec). Securin activity is required for cleaving cohesion complexes between sister chromatids. Adapted from (Vleugel et al., 2012).

1.7.3 The RZZ complex and Spindly

The RZZ complex consists of Roughdeal (Rod), Zeste-white 10 (Zw10) and Zwilch proteins and is an essential component of the mitotic checkpoint. Rod was first identified in a *Drosophila* genetic screen for proteins involved in mitosis, with *rod* mutants exhibiting cell death, aneuploidy and chromosome segregation errors (Karess and Glover, 1989). Zw10 was later identified in another *Drosophila* genetic screen where the *zw10* mutant displayed chromosome disjunction and premature anaphase onset (Smith et al., 1985; Williams et al., 1992). Zw10 and rod mutants shared mitotic phenotypes and both proteins were interdependent for kinetochore localization (Scaerou et al., 2001; Williams and Goldberg, 1994). Subsequently, both proteins were shown to be required for mitotic checkpoint activity in *Drosophila* and human cells (Basto et al., 2000; Chan et al., 2000). The third subunit, Zwilch, of the RZZ complex was first identified in *Drosophila* embryo extracts using immunoaffinity chromatography (Williams et al., 2003) followed by identification in human cells (Kops et al., 2005). The RZZ complex lacks homologs in yeast but is conserved in metazoans. The RZZ complex is part of the fibrous corona and is localized to kinetochores in a Zwint-1 (Zeste-white interacting protein) dependent manner as shown in Figure 1.14 (Starr et al., 2000). Zwint-1 is a structural protein of the outer kinetochore and interacts with many outer kinetochore proteins (Ndc80 and Mis12 subunits) and thus serves as a link between outer kinetochore and fibrous corona components (Lin et al., 2006; Obuse et al., 2004a; Vos et al., 2011; Wang et al., 2004a). RZZ complex depletion results in chromosome missegregation, chromatin bridges, premature anaphase and aneuploidy (Basto et al., 2000; Chan et al., 2000; Kops et al., 2005; Lin et al., 2006; Scaerou et al., 2001; Starr et al., 1997; Wang et al., 2004a).

The RZZ complex localizes to kinetochores at prophase and prometaphase, and is seen on MTs of the mitotic spindle upon bi-polar kinetochore-MT attachment and spindle poles during metaphase (Basto et al., 2004; Defachelles et al., 2015; Famulski et al., 2008). *Drosophila* Zw10 is known

to relocate from spindle poles to kinetochores at anaphase; however, such a pattern is not observed in human cells (Williams et al., 1992). Zw10 and Rod are stable residents of kinetochores during prometaphase but their turnover increases at kinetochores during metaphase (Defachelles et al., 2015; Famulski et al., 2008). Inhibition of intra-kinetochore tension with taxol treatment prevents the turnover of Zw10 at metaphase kinetochores indicating that the RZZ complex functions in the tension sensing mechanism of the mitotic checkpoint (Famulski and Chan, 2007; Williams et al., 1996). Recently, CENP-I was shown to stabilize the RZZ complex kinetochore residency at prometaphase (Matson and Stukenberg, 2014). The RZZ complex is further required for the kinetochore localization of Mad1, Mad2, dynein and Spindly (Buffin et al., 2005; Chan et al., 2009; Kops et al., 2005).

Spindly was first discovered in an RNAi screen of *Drosophila* S2 cells for proteins with mitotic checkpoint function. Spindly-depleted S2 cells showed metaphase arrest, chromosome alignment defects and elongated spiky interphase cells with spindle-shaped cell morphology, hence the name Spindly (Griffis et al., 2007). *Drosophila* Spindly localizes to MT plus ends in interphase, to kinetochores in prophase and prometaphase and along MTs but mostly at spindle poles in metaphase. *Drosophila* Spindly localizes to kinetochores at anaphase similar to Zw10 (Griffis et al., 2007). The function of *Drosophila* Spindly during interphase and anaphase needs further investigation. The Spindly homologue in worms was identified shortly thereafter and named SPDL-1 (spindle apparatus coiled-coil protein 1) (Yamamoto et al., 2008).

Human Spindly (hSpindly) also known as CCDC99 (605 amino acids) consists of two coiled-coil domains, which are separated by a conserved Spindly box/motif (32 residues) that is not well characterized. Spindly kinetochore localization is dependent on the RZZ complex since knockdown of Zw10 caused abrogation of Spindly kinetochore localization in *D. melanogaster*, *C. elegans* and humans (Chan et al., 2009; Griffis et al., 2007; Yamamoto et al., 2008). Spindly is further required for the localization of the dynein/dynactin complex (Figure 1.15)

in human cells but only dynein in *C. elegans* and *D. melanogaster* (Chan et al., 2009; Griffis et al., 2007; Yamamoto et al., 2008). An elegant study showed that Spindly physically connects dynein and dynactin and hence is essential to promote the motility of dynein along MTs *in vitro* (Figure 1.15) (McKenney et al., 2014). A comparison of Spindly function between *D. melanogaster*, *C. elegans* and humans is listed in Table 1 showing its conserved function in the recruitment and regulation of dynein at kinetochores during mitosis (Chan et al., 2009; Griffis et al., 2007; Yamamoto et al., 2008). Human Spindly is localized to kinetochores in prophase and prometaphase, moving to the poles during chromosome alignment and is at the poles during metaphase (Chan et al., 2009; Gassmann et al., 2010). Knockdown of hSpindly causes chromosome congression defects, loss of dynein/dynactin kinetochore localization, prometaphase delay, however checkpoint proteins are removed from bi-oriented kinetochores in a delayed manner perhaps by a dynein/dynactin independent mechanism (Chan et al., 2009; Gassmann et al., 2010). In contrast to loss of hSpindly in cells, Spindly box point mutants (S256A and F258A) that localize to kinetochores but uncouple hSpindly from dynein/dynactin recruitment, arrest the cells in metaphase and prevent the removal of Zw10, a proportion of Mad2 protein and hSpindly mutants from kinetochores (Barisic et al., 2010; Gassmann et al., 2010). This metaphase arrest induced by hSpindly box mutants suggests that dynein/dynactin mediated removal of hSpindly from kinetochores is required for mitotic checkpoint silencing and progression into anaphase. In addition, Spindly depletion results in severe chromosome alignment defects in worms and humans as compared to *Drosophila*. These defects were proposed to be the result of the dynein/dynactin complex absence, which helps in the formation of initial lateral kinetochore-MT attachments promoting end-on attachment formation (Chan et al., 2009). Contrary to expectations, Spindly box mutants rescued the chromosome alignment defect in the absence of dynein/dynactin complex at kinetochores indicating a role for hSpindly in kinetochore-MT attachment (Barisic et al., 2010; Gassmann et al., 2010). Furthermore, Gassmann *et al.* showed that the depletion of both the RZZ

complex and Spindly in worms rescued the kinetochore-MT attachment phenotype in worms suggesting a negative role of the RZZ complex in regulating kinetochore-MT attachments in the absence of Spindly (Gassmann et al., 2008). Barisic *et al.* proposed that the RZZ complex destabilizes lateral kinetochore-MT attachments in the absence of hSpindly leading to chromosome congression errors perhaps through Ndc80 regulation (Barisic and Geley, 2011). The authors support their hypothesis by showing that co-depletion of Spindly and Ndc80 leads to gross spindle formation defects as compared to the depletion of individual proteins in both worms and human cells (Barisic and Geley, 2011; Gassmann et al., 2008). Whether this hypothesis is correct needs further examination. According to the present model, Spindly depletion arrests cells in prometaphase (with RZZ complex negatively regulating the lateral kinetochore-MT attachments); however, the Spindly box mutants/dominant negative mutants which are unable to recruit dynein, arrest cells in metaphase (with Spindly inhibiting the negative regulation of the RZZ complex) due to their inability to silence the checkpoint because of the presence of Spindly on kinetochores (Barisic et al., 2010; Gassmann et al., 2010).

Similar to Zw10, hSpindly kinetochore localization is sensitive to both attachment and tension status and is re-recruited to aligned tensionless kinetochores (Chan et al., 2009). To conclude, hSpindly has a conserved function in recruiting dynein to the kinetochore and checkpoint silencing through a dynein/dynactin mediated mechanism. How Spindly is recruited to kinetochores through the RZZ complex and how, in turn, recruits dynein/dynactin complex remains to be investigated.

Table 1.1: Comparison of Spindly function in different organisms shows conserved function in dynein recruitment but differences in terms of checkpoint activation through Mad1/Mad2 recruitment.

	<i>Drosophila</i>	<i>C.elegans</i>	<i>Human</i>
RZZ complex required for hSpindly kinetochore recruitment	Yes	Yes	Yes
Spindly required for Mad1/Mad2 Recruitment	No	Yes	No
Spindly required for Mad1/Mad2 removal	Yes		No
Spindly required for Dynein recruitment	Yes	Yes	Yes
Spindly required for Dynactin recruitment	No	Yes	Yes

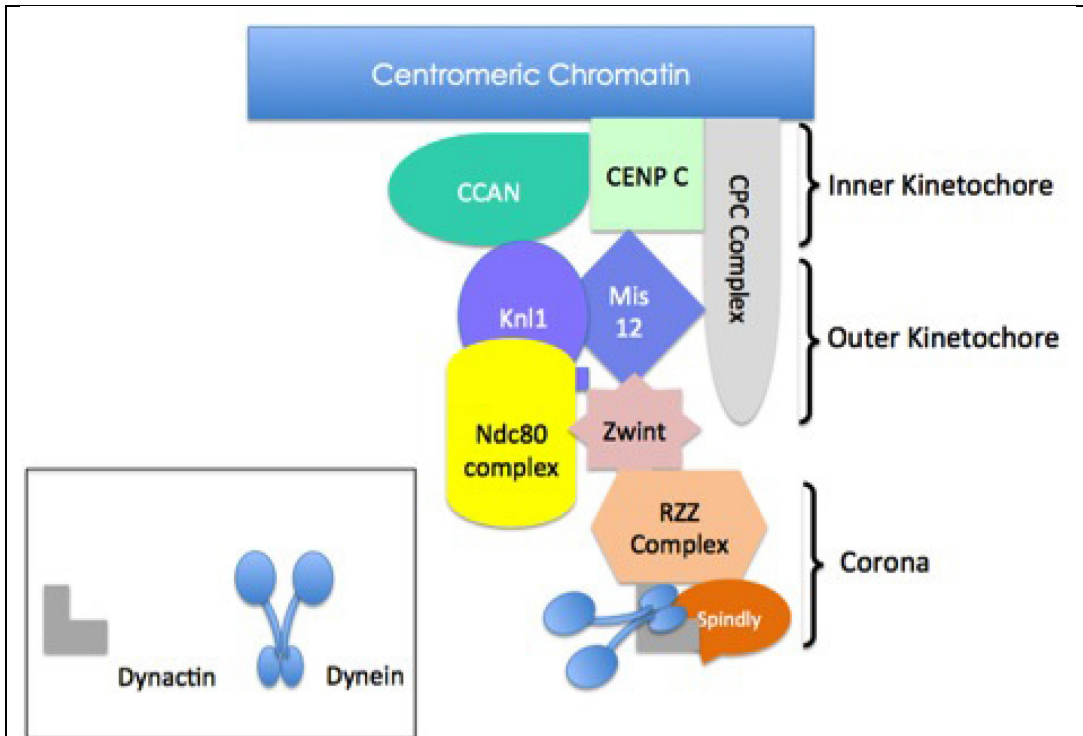


Figure 1.14: A schematic representation of selective proteins in the inner, outer and fibrous corona of the kinetochore.

The RZZ complex is recruited to the kinetochore by Zwint-1 and the RZZ complex recruits Spindly to kinetochores. Recruitment of the dynein/dynactin complex is dependent on the presence of both RZZ and Spindly at kinetochores. CPC, chromosome passenger complex contains Aurora B, Borealin, INCENP, Survivin.

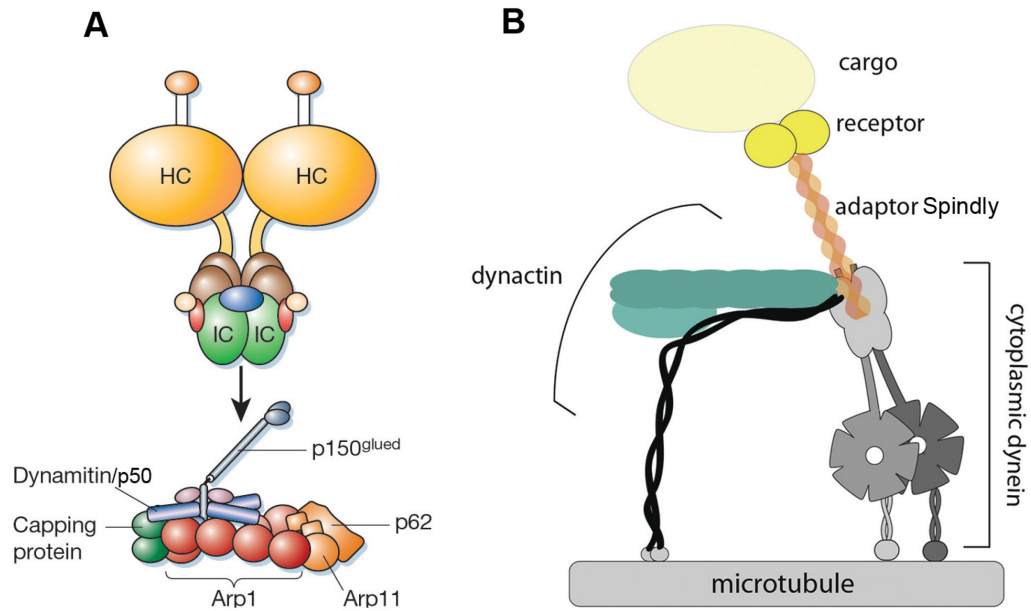


Figure 1.15: A schematic representation of the dynein/dynactin complex subunits and ternary complex between dynein, dynactin and Spindly.

(A) The dynein molecule consists of 2 heavy chain (HC), 2 intermediate (IC) and light chains (not labeled). The dynactin molecule consists of multiple subunits as well and interacts with dynein intermediate chain through its p150^{glued} subunit. Adapted from (Schliwa and Woehlke, 2003). (B) A single dynein molecule forms a complex with adaptor Spindly and dynactin. Cargo proteins associate with the adaptor proteins through their surface receptors or direct association with the adaptor protein. Adapted from (Dodding, 2014)

1.7.4 Mitotic checkpoint and cancer

Numerical and structural chromosome variations are frequently observed in cancer cell genomes. The presence of a greater or lesser than diploid chromosome number in a cell is referred to as aneuploidy. Aneuploidy is a distinguishing characteristic of most solid tumors (~90%) and some hematopoietic cancers (>50%) (Mitelman F, 2015). Aneuploidy can arise in tumor cells due to their inherent ability to undergo and tolerate high rates of chromosome gain or loss during cell division, also referred to as chromosomal instability (CIN). However not all the aneuploid cells undergo CIN, some aneuploid cells display stable chromosome abnormality in reoccurring cell cycle. The role of chromosomal translocations in the development of leukemia and lymphoma is very well understood (Aplan, 2006; Mitelman et al., 2007; Rowley, 1973). Numerical changes in the chromosomes arise due to segregation errors during mitosis and its consequences are not very well understood. One would predict that defective mitotic checkpoint regulation due to altered function of mitotic checkpoint proteins would lead to aneuploidy. However, limited numbers of mutations are found in the mitotic checkpoint genes. Complete loss of mitotic checkpoint activity is embryonic lethal due to massive chromosome segregation errors (Dobles et al., 2000; Kalitsis et al., 2000; Kops et al., 2004). Mosaic variegated aneuploidy (MVA) is a rare disorder with an increased predisposition to cancer and this disorder is associated with germline mutations of *BuBRI* (Hanks et al., 2004; Matsuura et al., 2006). The RZZ complex subunits are mutated in a subset of colorectal cancers and display CIN (Wang et al., 2004b). Haploinsufficiency of Mad1, Mad2 and BubR1 lead to CIN and increases tumor incidence rate (Chi et al., 2009; Dai et al., 2004; Iwanaga et al., 2007; Michel et al., 2001). Therefore, altered expression of checkpoint proteins has been correlated with human cancer although the precise mechanism awaits discovery (Perez de Castro et al., 2007). CENP-F (Clark et al., 1997), CENP-H (Shigeishi et al., 2006) and Hec1 are overexpressed in human cancers. In contrast to complete loss of the checkpoint, a weakened checkpoint allows cells to proceed through

anaphase with missegregation facilitating aneuploidy. In addition to altered mitotic checkpoint function, cohesin defects, centrosome amplification and hyperstable kinetochore-MT attachments during mitosis contribute to the generation of aneuploidy as well (Holland and Cleveland, 2012). Conditional overexpression of Mad2 leads to hyperstable kinetochore-MT attachments and hence promotes aneuploidy through CIN (Kabeche and Compton, 2012). It is proposed that a low CIN rate promotes aneuploidy and that high CIN rates can lead to catastrophic event i.e. cell death (Holland and Cleveland, 2012). Cancer cell lines exhibiting CIN display significantly higher missegregation errors as compared to non-transformed cells and hence promote aneuploidy (Lengauer et al., 1997; Thompson and Compton, 2008).

A long-standing question in the field is to whether aneuploidy is a cause or consequence of cancer. This can only be resolved with more refined aneuploidy animal models and future studies.

1.8 Mitotic Checkpoint Silencing

Mitotic checkpoint signaling is better understood at the molecular level than mitotic checkpoint silencing. How kinetochore-MT attachments shut down checkpoint activity at the molecular level is not very clear. To achieve checkpoint silencing, checkpoint proteins must be removed from kinetochores, further binding of checkpoint proteins to kinetochores must be inhibited, and the pre-existing MCC must be disabled. At present, mitotic checkpoint silencing is thought to be achieved by shutting down the formation of the MCC complex through two pathways as described below.

1.8.1 Dynein/Dynactin stripping

Dynein is a multi-subunit minus end directed MT motor (MW 1.40 MDa) that functions during mitosis in spindle formation/rotation and positioning (Busson et al., 1998; Heald et al., 1996; O'Connell and Wang, 2000; Vaisberg et al., 1993), kinetochore-MT attachment (Pfarr et al., 1990; Steuer et al., 1990), prometaphase and anaphase chromosome movement (Savoian et al., 2000; Sharp et al., 2000a; Yang et al., 2007b) and mitotic checkpoint silencing (Bader and Vaughan, 2010; Howell et al., 2001; Whyte et al., 2008; Wojcik et al., 2001). Dynein consists of heavy, intermediate, light intermediate and light chains (Figure 1.14) (Hirokawa et al., 1998). The dynein motor requires the help of a coactivator that regulates its motility as well as cargo binding. Dynactin is a multi-subunit complex (11 subunits), which interacts with dynein, promotes its motor activity and links dynein to its cargos (King et al., 2000; King and Schroer, 2000). It was recently shown that dynein interacts with dynactin only in the presence of adaptor proteins to form a tripartite complex *in vitro*, Spindly being one of the adaptor proteins identified in the study (Figure 1.14) (McKenney et al., 2014). The formation of this ternary complex is essential for the processive movement along MTs *in vitro* (McKenney et al., 2014). Therefore, dynein motor activity requires its adapter Spindly and dynactin to link to its cargoes and move them along MTs.

Many studies have shown that Mad1 and Mad2 are depleted from kinetochores upon attachment, by dynein/dynactin-mediated stripping (Figure 1.16) (Howell et al., 2001). Dynein/dynactin cargos at the kinetochores were identified using nordihydroguaiaretic acid (NDGA) and ATP reduction assays (Arasaki et al., 2007; Famulski et al., 2011; Silva et al., 2014). NDGA treatment in human cells sustains dynein activity but prevents the release of dynein cargos from spindle poles (Arasaki et al., 2007; Famulski et al., 2011). These studies reported Mad1, Mad2, BubR1, Mps1, CENP-E, RZZ complex, Spindly, cyclin B, a proportion of Hec1 and Mis12 accumulation at spindle poles upon NDGA treatment. In addition, GFP-tagged Mad1, Mad2 and Rod proteins have been reported to move along spindle MTs upon kinetochore-MT attachment (Buffin et al., 2005; Emre et al., 2011; Howell et al., 2000; Wojcik et al., 2001). Dynein/dynactin mediated transport of checkpoint proteins to spindle poles halts the production of the MCC complex since Mad2 conformational change can happen only at kinetochores. Disruption of dynein does not provide a conclusive answer to its role in mitotic checkpoint silencing as dynein has multiple functions during mitosis. Disruption of dynein function by depleting its recruiter Spindly or specifically during early prometaphase by dynactin subunit p50/dynamitin injection resulted in dynein-independent checkpoint silencing (Chan et al., 2009; Howell et al., 2001). The dynein-independent mechanism for checkpoint silencing may involve protein phosphatases similar to plants and fungi lacking kinetochore dynein. Depletion of Spindly, however, results in kinetochore-MT attachment defects and leads to prometaphase arrest. As discussed in section 1.7.1 Spindly point mutants (in conserved Spindly motif) localized to kinetochores and allowed normal formation of kinetochore-MT attachments but prevented dynein kinetochore recruitment (Gassmann et al., 2010). These Spindly mutants in an endogenous Spindly knockdown background induced metaphase arrest rather than prometaphase arrest (as seen with Spindly depletion) and prevented the removal of Mad1 and Mad2 from bi-oriented kinetochores. The identification of such a dynein-independent checkpoint silencing in Spindly box mutant expressing cells

awaits discovery. Furthermore, why this mechanism does not kick in when Spindly mutants are present on the kinetochores is unknown.

In addition to Spindly and dynactin regulating dynein function, other proteins such as NudC (Aumais et al., 2003; Osmani et al., 1990), NudCL (Chen et al., 2015; Zhou et al., 2006), NudE, NudEL (Liang et al., 2007; Moon et al., 2014; Stehman et al., 2007; Wang et al., 2013), CLIP-170 (Dujardin et al., 1998; Tai et al., 2002) and Lis-1 (Faulkner et al., 2000; Tai et al., 2002) have been shown to regulate dynein function during mitosis. Lis-1 depletes p50/dynamitin and therefore dynein from kinetochores (Tai et al., 2002), NudE/EL plays a role in dynein kinetochore recruitment through an unknown interaction (Stehman et al., 2007) and NudC stabilizes dynein intermediate chain (Zhou et al., 2006). CLIP-170 (CAP-Gly domain-containing protein) is a MT plus end binding protein but it also affects dynein function (Dujardin et al., 1998; Tai et al., 2002). Furthermore, CENP-F was proposed to prevent premature stripping of dynein from kinetochores (Yang et al., 2005b). These studies show that dynein interacts with various proteins to perform its function during mitosis. In the next section, I discuss dynein-independent mitotic checkpoint silencing mechanism.

1.8.2 p31^{comet} mediated MCC disassembly

Once all the chromosomes are aligned on the metaphase plate, APC/C is rapidly activated. It is not very clear how the rapid activation is achieved at the molecular level. p31^{comet} (also known as CMT2), identified as a Mad2 interacting protein (Habu et al., 2002) shows increased binding affinity for the Mad2-C form (Date et al., 2014; Xia et al., 2004; Yang et al., 2007a). p31^{comet} resembles Mad2-O in structure and thus prevents the dimerization of Mad2-O and Mad2-C and the Mad2 conformational change, which is a prerequisite for integration into the MCC complex (Figure 1.16) (Vink et al., 2006). p31^{comet} depletion results in metaphase arrest with chromosomes bi-polarly aligned at the metaphase plate indicating that p31^{comet} is required for checkpoint silencing (Hagan et al., 2011). Furthermore, p31^{comet} localizes to prometaphase kinetochores in a Mad1:Mad2-C complex-dependent manner (Fava et al., 2011). Recent studies have suggested that the p31^{comet} kinetochore pool prevents the activation of Mad2-C, thus preventing the formation of the MCC (Xia et al., 2004; Yun et al., 2009) and its cytoplasmic pool extracts Mad2 from the MCC, thereby extinguishing MCC complex activity (Eytan et al., 2014; Fava et al., 2011). All these studies present attractive evidence for p31^{comet} mediated checkpoint silencing but the detailed mechanism remains unknown and p31^{comet} is not conserved in yeast.

In addition to dynein/dynactin and p31^{comet}, ubiquitination of Cdc20 through the E2 enzyme UbcH10 (Reddy et al., 2007; Stegmeier et al., 2007) and PP1 phosphatases in yeast are implicated in checkpoint silencing {reviewed in (Kops and Shah, 2012)}. In yeast, direct binding of PP1 to PP2A is required for phosphatase-mediated checkpoint silencing, however, this has not been observed in human cells (Grallert et al., 2015). PP2A-B56 phosphatases in human cells were shown to play an important role in mitotic checkpoint silencing by creating a negative feedback mechanism (Nijenhuis et al., 2014). In this work, the authors proposed that BubR1 recruits PP2A-B56, which antagonizes Aurora B activity and hence allows PP1 to silence the mitotic checkpoint.

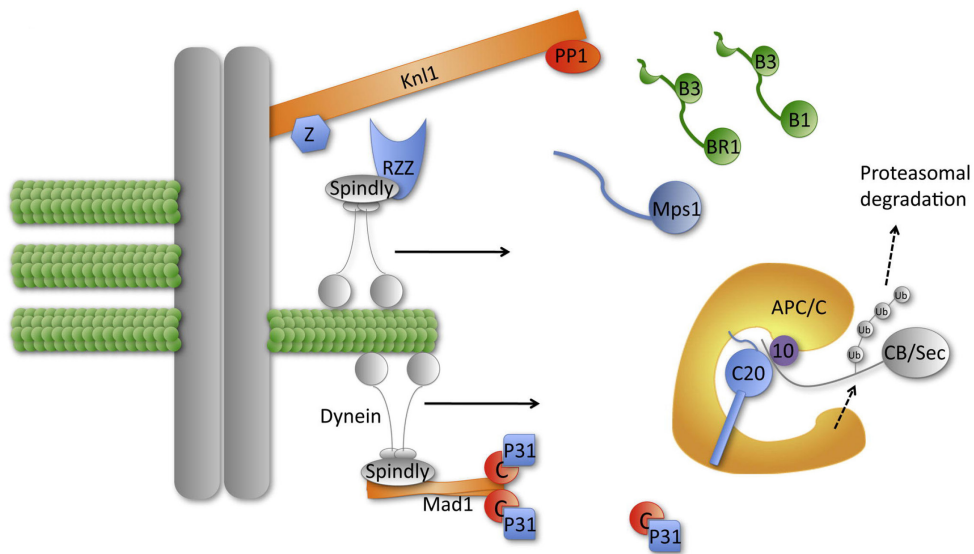


Figure 1.16: Mitotic checkpoint silencing through dynein/dynactin mediated stripping and p31^{comet}.

Spindly recruits dynein complex to kinetochores during prometaphase. Attachment of kinetochores to spindle MTs induces poleward stripping of mitotic checkpoint proteins by minus end directed MT motor dynein. Furthermore, p31^{comet} binds to Mad2 at kinetochores instead of Mad2-O. Both mechanisms prevent formation of the MCC complex and therefore APC/C gets activated. Proteasomal degradation of securin and cyclin B promotes the degradation of cohesion complexes and sister chromatid separation. Mitotic exit also requires the activity of PP1-like phosphatases. Adapted from (Vleugel et al., 2012).

1.9 Protein Prenylation

Multiple protein modifications such as phosphorylation, methylation, sumoylation, ubiquitination and prenylation regulate the function of a protein in a cell. I will be focusing on protein prenylation, since I have shown that Spindly undergoes farnesylation and its kinetochore localization is regulated by this posttranslational lipid modification. Protein prenylation was originally discovered in fungi and it involves an irreversible addition of a farnesyl (15-carbon) or geranylgeranyl (20-carbon) lipid group to one or more cysteine residues located at or near the C-terminus of a protein (Figure 1.17) (Kamiya et al., 1978; Resh, 2006). The presence of a consensus CA₁A₂X motif at the C-terminal of a protein determines its eligibility to undergo prenylation catalyzed by either farnesyl transferase or geranylgeranyl transferase enzyme. The CA₁A₂X motif has a cysteine residue that becomes farnesylated, usually followed by two aliphatic amino acids, and the nature of the last amino acid X determines whether a protein undergoes farnesylation, or geranylgeranylation (Sinensky, 2000). A CA₁A₂X motif with a terminal cysteine, methionine, alanine, serine, or glutamine undergoes farnesylation while leucine, isoleucine, and phenylalanine target the protein to be geranylgeranylated. However, studies have shown that the A₂ residue in combination with the X residue plays an important role in protein farnesylation (Houglund et al., 2010; Houglund et al., 2009).

1.9.1 Farnesylation

The farnesyltransferase (FTase) enzyme catalyzes the addition of a farnesyl group onto the cysteine. This is followed by the cleavage of the AAX by Ras-converting enzyme 1 (Rce1). The C-terminal cysteine next undergoes methylation by isoprenylcysteine carboxymethyl transferase (ICMT) (Porter et al., 2007) (Figure 1.17). These modifications following farnesyl group addition significantly increase the hydrophobicity of proteins facilitating their membrane association (Ghomashchi et al., 1995; Sinensky, 2000; Zhang and Casey, 1996). Nuclear lamin B was the first protein found to undergo farnesylation and since then, more than 150 proteins have been reported to undergo prenylation

(Farnsworth et al., 1989; McTaggart, 2006; Roskoski, 2003). FTase binds to a farnesyl diphosphate (FPP) group forming a binary complex. The binary complex recruits the protein substrate forming a short-lived ternary complex during which cysteine attaches to the farnesyl group through a thioether bond (C-S). A new FPP molecule binds to FTase resulting in the release of the farnesylated substrate protein (Dolence et al., 1995; Pompliano et al., 1993). Zinc and magnesium ions are required for efficient catalysis as well (Huang et al., 1997; Pickett et al., 2003; Tobin et al., 2003). Crystal structures of all these complexes formed during farnesylation catalysis have been determined (Park et al., 1997). The finding that RAS family proteins require farnesylation for membrane binding initiated a multitude of studies investigating the role farnesylation in cancer (Casey et al., 1989; Schafer et al., 1989). RAS is mutated in more than 30% of cancers and for that reason many labs have focused on the development of farnesyl transferase inhibitors (FTIs) to prevent oncogenic RAS activity (Berndt et al., 2011; Downward, 2003; Karnoub and Weinberg, 2008).

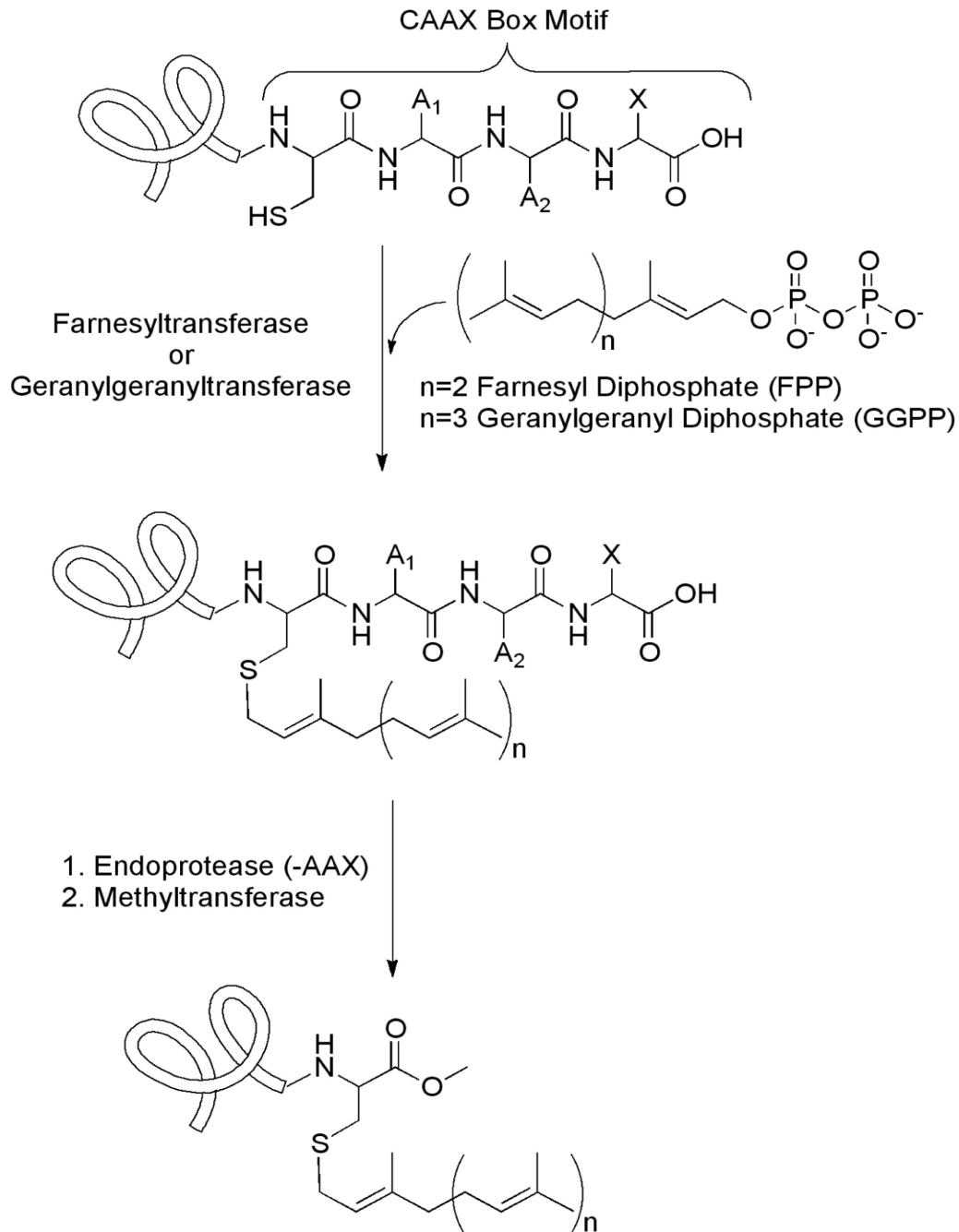


Figure 1.17: Schematic representation of protein prenylation.

Farnesyl or geranylgeranyl transferase enzyme attaches either the farnesyl or geranylgeranyl lipid group onto the cysteine residue following which Ras converting enzyme 1 (RCE1) cleaves the three amino acids preceding the farnesylated cysteine. Farnesylated cysteine further gets methylated by the methyltransferase enzyme. Adapted from (Ochocki and Distefano, 2013)

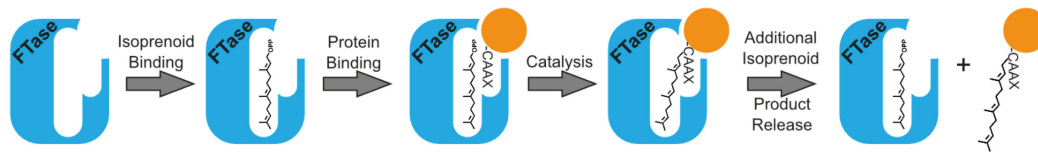


Figure 1.18: Schematic representation of the steps involved in the farnesylation process mediated by FTase.

The FTase enzyme binds to farnesyl diphosphate isoprenoid (FPP) and then catalyzes the attachment of this lipid group to the substrate protein and its release by allowing a second farnesyl diphosphate group to bind. Adapted from (Ochocki and Distefano, 2013).

1.9.2 Farnesyl transferase inhibitors

Farnesyl transferase inhibitors (FTIs) derived from chemical libraries and natural compounds can be classified into three categories based on their mode of action: competitive inhibitors (peptidomimetic compounds), isoprenoid analogs and bi-substrate inhibitors (Reiss et al., 1990; Tamanoi, 1993). Peptidomimetic inhibitors are the most extensively studied and sophisticated FTIs of the three categories due to their potency and ease of synthesis (Ochocki and Distefano, 2013). FTIs efficiently kill tumor cells in culture and in animal models driving the entry of four FTIs (tipifarnib, lonafarnib, BMS-214662 and L-778,123) into clinical trials (Berndt et al., 2011; Kohl et al., 1995). Despite remarkable success in preclinical studies, FTIs did not yield effective results in approximately 75 clinical trials either as monotherapy or in combination with other anti-cancer drugs (Berndt et al., 2011). Importantly, FTIs showed promising results in preclinical studies regardless of RAS mutations (Crespo et al., 2002; Nagasu et al., 1995; Sepp-Lorenzino et al., 1995). Scientists have attributed the failure of FTIs to poor patient selection criteria (Ochocki and Distefano, 2013; Palsuledesai and Distefano, 2015). These FTI trials ignored the observation that K-RAS (the most frequently mutated RAS in cancer patients) and N-RAS proteins can become substrates for Geranylgeranyl transferase and generate geranylgeranylated forms that retain biological function.

Despite disappointing results for cancer patients, FTIs have shown promising results in Hutchinson–Gilford progeria studies (Fong et al., 2006; Yang et al., 2005a). One Phase II clinical trial was successfully completed in 2007 for progeria patients (Gordon et al., 2012) and another Phase II clinical trial using lonafarnib is currently ongoing (Wong and Morse, 2012). In addition to cancer and progeria, FTIs are being explored for parasitic diseases such as malaria (Carrico et al., 2004), African sleeping sickness (Yokoyama et al., 1998) and chagas (Kraus et al., 2010) in which the parasites use their own FTase for pathogenesis. Studies have developed FTIs, which are more selective towards pathogen FTase as compared to mammalian FTase to exclude side effects

(Fletcher et al., 2008; Olepu et al., 2008). Additionally FTIs are being investigated for hepatitis (hepatitis D virus large antigen is farnesylated) and multiple sclerosis (Rho proteins essential for lymphocyte migration undergo farnesylation) diseases {reviewed in (Ochocki and Distefano, 2013)}.

In addition to G1 arrest (characteristic of RAS inhibition), FTI-treated tumor cells exhibit prometaphase delay, defective spindle formation, and chromosome misalignments (Ashar et al., 2000; Crespo et al., 2002; Crespo et al., 2001). These mitotic defects led researchers to postulate that the inhibition of CENP-E and CENP-F farnesylation, two mitotic proteins known to be farnesylated, was responsible for the mitotic FTI phenotype; however, this has been controversial as discussed next (Ashar et al., 2000).

1.9.3 Farnesylated mitotic proteins: CENP-E and CENP-F

Here, I will discuss in detail the functional implication of farnesylation for CENP-E and CENP-F function, which is further addressed in chapter 3 of my thesis. CENP-E is a plus end directed kinesin motor protein and is required for proper chromosome segregation during mitosis (Thrower et al., 1995; Wood et al., 1997; Yen et al., 1991). CENP-E is a 340-kDa coiled-coil protein present at kinetochores during prophase, prometaphase and metaphase and is degraded shortly after mitosis completion. It is a component of the kinetochore fibrous corona and assists mono-oriented chromosomes to glide and align on the spindle equator by forming contacts with the MTs of K-fibers of bi-oriented chromosomes (Cooke et al., 1997; Yao et al., 2000; Yen et al., 1991; Yen et al., 1992). Knock down of CENP-E protein results in unaligned chromosomes closer to spindle poles due to unstable kinetochore-MT attachments leading to metaphase arrest (McEwen et al., 2001; Putkey et al., 2002; Weaver et al., 2003; Yao et al., 2000; Yao et al., 1997). Additionally, CENP-E regulates BubR1 kinase activity as previously discussed in detail in section 1.6.4. In comparison to CENP-E, CENP-F is a less studied protein and was first identified using human autoimmune serum (Rattner et al., 1993). CENP-F is a coiled-coil protein as well

and it shows cell cycle specific localization. It is maintained at low levels in S-phase and during G2 phase it is found in the nucleus. It relocalizes to the nuclear membrane at late G2 and to kinetochores during mitosis until metaphase (Liao et al., 1995; Zhu et al., 1995). At anaphase CENP-F localizes to the spindle mid-zone and is degraded at the end of mitosis (Gurden et al., 2010). Depletion of CENP-F leads to the absence of BubR1 and Mad1 at kinetochores and leads to premature anaphase onset (Feng et al., 2006; Laoukili et al., 2005). CENP-E and CENP-F have been proposed to interact with each other but they are not interdependent for their kinetochore localization (Chan et al., 2005). Both CENP-E and CENP-F possess MT binding domains and have been biochemically shown to bind MTs (Musinipally et al., 2013). The C-terminal end of both CENP-E and CENP-F is required for their kinetochore localization (Chan et al., 1998; Zhu et al., 1995).

Ashar *et al.* originally identified CENP-E and CENP-F as targets of FTase but inhibition of farnesylation did not affect their kinetochore localization (Ashar et al., 2000). However, the mitotic phenotype of FTI-treated cells was attributed to inhibition of CENP-E and CENP-F farnesylation. Additional studies have shown that FTIs do not affect CENP-E or CENP-F kinetochore localization and it has been hypothesized that mitotic effects of FTIs are due to unknown targets (Crespo et al., 2002; Crespo et al., 2001; Verstraeten et al., 2011). This speculation is further supported by the data shows that loss of CENP-F function by siRNA in HeLa cells leads to a very brief mitotic delay rather than prometaphase accumulation as seen with FTI treatment (Feng et al., 2006). In addition, siRNA knock-down of CENP-E or microinjection of function blocking antibodies results in unaligned chromosomes at spindle poles in metaphase cells, thus resembling a metaphase arrest rather than the gross chromosome alignment defects and prometaphase delay observed upon FTI treatment (McEwen et al., 2001; Schaar et al., 1997; Tanudji et al., 2004; Yao et al., 2000).

1.10 Thesis Focus

The RZZ complex is an essential component of mitotic checkpoint in metazoans and it recruits the dynein/dynactin complex through Spindly. I started with a structure-function study of human Spindly (hSpindly) to characterize its role during mitosis. I established an extensive mutant library of hSpindly consisting of truncation, random insertion, deletion and substitution mutants, and mapped the kinetochore localization domain of hSpindly to its C-terminal end. During this mapping study, I found out the hSpindly C-terminus is a potential farnesylation motif and I showed that FTIs inhibited hSpindly kinetochore localization during mitosis. Furthermore, I showed that hSpindly is farnesylated *in vivo* and hSpindly farnesylation is a pre-requisite for its interaction with the RZZ complex explaining hSpindly recruitment to kinetochores. hSpindly does not undergo geranylgeranylation to retain its function upon FTI inhibition unlike some RAS proteins. Additionally, I demonstrated that hSpindly but not CENP-E and CENP-F, is a key mitotic FTase target rather than CENP-E or CENP-F proteins explaining the mitotic phenotype upon FTI treatment. The FTI mitotic phenotype closely resembles hSpindly depletion as shown by our live-cell imaging studies.

I also investigated the kinetochore dynamics of hSpindly during mitosis and discovered that hSpindly turnover increases significantly on metaphase kinetochores and it is moderately stable at prometaphase kinetochores. hSpindly undergoes phosphorylation during mitosis. I showed that hSpindly phospho-mutants have altered kinetochore localization patterns. I have also used the yeast 2-hybrid to demonstrate that p50/dynamitin interacts with hSpindly and identified a novel interaction partner of hSpindly. Through these combined studies, I discovered that hSpindly localization and function is regulated by farnesylation as well as phosphorylation and hSpindly is a key target of FTase during mitosis.

Chapter 2 Experimental Procedures

2.1 Cloning

Full length hSpindly (Gene ID: 54908) and 2581-3210 aa of hCENP-F (Gene ID: 1063) cDNAs were amplified from a human fetal cDNA library (Spring Bioscience) using gene specific primers and cloned into the pDONR221 vector (Invitrogen). hSpindly N- and C-terminal truncation constructs (Figure 3.2) were amplified using pDONR221 hSpindly as a template using specific primers. Truncation constructs were cloned into the pDONR221 vector (Invitrogen) using attB recombination linkers of the Gateway Technology cloning system (Invitrogen). Cloning into the gateway destination pEGFP (CMV promoter) expression vector (Chan et al., 1998) was performed using the Gateway Technology cloning system.

2.2 Mutagenesis and siRNA

The hSpindly random insertion mutant library was generated by transposon-mediated insertion mutagenesis (Mutation Generation System, Finnzymes), which generated mutants of hSpindly protein containing 5 aa in frame insertion. Site-directed hSpindly mutants were generated by using the QuikChange® site-directed mutagenesis kit (Stratagene) using pDONR221 hSpindly as a template. The site of insertion and desired point mutant sequences were confirmed by sequencing using BigDye Terminators v3.1 and an ABI PRISM 310 capillary sequencer (Applied Biosciences). siRNA for Spindly (GAAAGGGUCUCAAACUGAA) or a scrambled control siRNA (UGGUUUACAUGUCGACUAA) from Thermo Scientific was used. The siRNA resistant version of hSpindly containing four silent mutations was generated using the QuikChange® site-directed mutagenesis kit (Stratagene) with the following pair of primer and its antisense (changes shown in bold). 5'-CGTTGCTACAGATGAAGGGATCCCAGACTGAATTTGAGCAGCAGG-3'

2.3 Cell culture and Synchronization

HeLa and HEK (human embryonic kidney)-293 cells were grown as a monolayer in low-glucose DMEM (Dulbecco's modified Eagle's medium) supplemented with 2 L-glutamine and 10% (v/v) FBS (fetal bovine serum) in a humidified incubator at 37 °C with 5% CO₂. T47D cells were grown in RPMI 1640 supplemented with 2 mM L-glutamine and 10% (v/v) FBS and 1 mM sodium pyruvate. MCF7 cells were grown in low-glucose DMEM (Dulbecco's modified Eagle's medium) and high-glucose DMEM (Dulbecco's modified Eagle's medium) in equal volume supplemented with 2 mM L-glutamine and 10% (v/v) FBS (fetal bovine serum) and 0.01 mg/ml insulin. M2 and MeWo cells were grown in low-glucose DMEM F12 media supplemented with 2 mM L-glutamine and 10% (v/v) FBS (fetal bovine serum). Double thymidine cell synchronization was performed by the addition of 2 mM thymidine to cells for 16 hours (h).

2.4 Transient Transfections

HeLa cells were seeded and grown to ~60% confluency on 35-mm dishes. Each dish was transfected with 2 µg of EGFP-Spindly constructs. For each transfection, 2 µg of plasmid DNA was mixed with 100 µl of OPTI-MEM. In a separate tube, 10 µl of PEI was mixed with 100 µl of OPTI-MEM and incubated at room temperature for 5 min. The diluted plasmid DNA and PEI were mixed together and incubated at room temperature for 15 min to allow DNA-PEI complex formation. 2 ml of warmed low glucose DMEM growth media was added to the plasmid-PEI complex mixture, which was then added to the HeLa cell dishes (after removal of growth media). For hSpindly siRNA transfections, Oligofectamine was used according to the manufacturer's instructions. Cells were incubated with 100 nM siRNA and Oligofectamine in OPTI-MEM for 5-6 h followed by the addition of fetal bovine serum to a final concentration of 10%. Transfection media was replaced with fresh media after 24 h.

For hSpindly *in vivo* farnesylation analyses, HeLa cells grown to ~60% confluence in 10 cm diameter dishes were transiently transfected with 10 µg of

the EGFP-Spindly constructs and 40 μ l PEI (1 mg/ml) as described above for ~39 h. HeLa cells were treated with alkynyl-farnesol (50 μ M from 50 mM stock solution in DMSO) for 4 h (Charron et al., 2011). For co-incubation with inhibitors, HeLa cells were pretreated for 1 h with 10 μ M of FTI L-744832 (10 mM stock solution in DMSO; Enzo Lifesciences) or 20 μ M of FTI-277 (20 mM stock solution in DMSO; Sigma-Aldrich) prior to alk-FOH metabolic labeling. Cells were then harvested for immunoprecipitation as previously described (Charron et al., 2011).

2.5 Western Blotting

For Western blotting, HEK-293 cells were seeded at a density of 10^5 cells/ml in 35-mm diameter dishes. Cells were transiently transfected with 1-2 μ g of EGFP-hSpindly mutant constructs as described above for approximately 24h and processed for Western blotting as described previously (Chan et al., 1998). PageRuler Plus Prestained protein ladder (Fermentas; Thermo Scientific) was used as a molecular weight marker.

Blots were blocked with Odyssey blocking buffer (Li-Cor Biosciences) and probed with IR-800-conjugated mouse monoclonal anti-GFP antibodies (1:10000 dilution; Rockland Immunochemicals) and rat polyclonal anti-hSpindly (1:1000 dilution; described below). Rabbit polyclonal anti-hRod (N-terminal 809 aa antigen) and rabbit anti hZw10 (GST full length hZw10-antigen) was used for labeling the blots (Chan et al., 2000). B512 mouse anti-tubulin antibody (1/3000; Sigma) was used to label the blot. Secondary antibodies Alexa Fluor® 680 anti-rat antibody (1:10000 dilution; Invitrogen) and Alexa Fluor® 680 anti-rabbit antibody (1:10000 dilution; Invitrogen) were used. Odyssey IR imager system (Li-Cor Biosciences) was used to scan the blots.

2.6 Fluorescence Microscopy

For hSpindly, hZw10, hRod, hCENP-E and hCENP-F immunofluorescence, HeLa cells were seeded onto 22-mm² coverslips at a density

of 5×10^4 cells/ml in a 35-mm diameter dish for 36–48 h. One set of coverslips was treated with 10 μ M FTI L-744-832 (Enzo Life Sciences) or 20 μ M of FTI-277 (Sigma-Aldrich) and the other set was treated with the same volume of control solvent (DMSO) for 24 h. The cells were fixed with 3.5% (w/v) paraformaldehyde in PBS with 10 mM Pipes (pH 6.8) for 7 min, permeabilized in KB (50 mM Tris/HCl, pH 7.4, 150 mM NaCl and 0.1% BSA) with 0.2% Triton X-100 for 5 min at room temperature (22 °C), and rinsed in KB buffer for 5 min at room temperature without Triton X-100. DNA was stained with 0.1 μ g/ml DAPI (4', 6-diamidino-2-phenylindole). Rat anti-hSpindly (1:1000 dilution) and Alexa Fluor® 488-conjugated anti-rat (1:1000 dilution; Molecular Probes) antibodies were used to detect hSpindly. hZw10, hRod, hCENP-E and hCENP-F were visualized using rat anti-hZw10 sera (1-139 aa-antigen), rabbit anti-hRod (N-terminal 809 aa-antigen) (Chan et al., 2000), rabbit anti-hCENP-E (C-terminal 360 aa-antigen) (Schaar et al., 1997) and rabbit anti-hCENP-F (8445-end nucleotides) (Liao et al., 1995) antibodies. Centromeres were visualized using human ACA (antacentromere antibody) sera (1:4000) (gift from M. Fritzler, University of Calgary, Calgary, Canada). Coverslips were mounted with 1 mg/ml Mowiol 4-88 (Calbiochem) in phosphate buffer (pH 7.4). Alexa Fluor® 488-conjugated anti-rat (1:1000 dilution; Molecular Probes), Alexa Fluor® 555-conjugated anti-rabbit (1:1000 dilution; Molecular Probes), Alexa Fluor® 555-conjugated anti-mouse (1:1000 dilution; Molecular Probes) and Alexa Fluor® 647-conjugated anti-human (1:1000 dilution; Molecular Probes) secondary antibodies were used to visualize protein localization.

For fluorescence microscopy of GFP-tagged hSpindly constructs, HeLa cells were seeded onto 22-mm² coverslips at a density of 5×10^4 cells/ml in 35-mm diameter dishes and grown for 24 h before transfection. Cells were transiently transfected with 1-2 μ g of plasmid DNA as described above for 24-36 h. Cells were fixed and permeabilized as described above. DNA was stained with DAPI (0.1 μ g/ml), and coverslips were mounted with Mowiol 4-88 (Calbiochem).

A microscope (Imager.Z.1; Carl Zeiss, Inc.) equipped with epifluorescence optics was used to collect the images. Cells were visualized with a Zeiss 100X Plan-Apochromat objective with 1.4 numerical aperture. Images were captured with a SensiCam (Cooke) CCD (charge-coupled device) camera (PCO-TECH Inc.) controlled by Metamorph 7.0 software (Universal Imaging Corporation). Images were processed using Adobe Photoshop 7.0. Endogenous Spindly immunofluorescence images (Figure 3.1) were acquired using Zeiss confocal Plan-Apochromat with Zeiss 63X objective (1.4NA) Carl Zeiss, Inc.). Data were collected using the Zeiss Zen software 7.0 (Carl Zeiss, Inc.) and processed using Adobe Photoshop 7.0.

2.7 Fluorescence Quantification

For quantification of fluorescence, fluorescence kinetochore intensities were measured within a 9X9 pixel square. Background fluorescence was measured outside the 9X9 square using 13X13 pixel squares and subtracted (King et al., 2000). For intensity quantifications at kinetochores, the smaller square encompassed a single kinetochore and results were normalized against ACA signals. 20 kinetochores were analyzed for each protein.

2.8 MBP Spindly and Rat anti hSpindly Antibody Production

Recombinant full length MBP-hSpindly fusion protein expression was induced in the *Escherichia coli* strain JM109 (T7 promoter). Protein expression was induced at mid log phase with 2 mM IPTG at 30 °C for 2-3 h. Bacteria were harvested in lysis buffer (50 mM NaPO₄ pH7.6, 0.25 M NaCl, 5 mM MgCl₂, 1 mM EGTA, 10 µg AEBSF protease inhibitor and 0.1 mg/ml lysozyme) and sonicated. The soluble MBP-Spindly fusion protein was bound to an amylose resin (NEB) column washed twice in binding buffer (20 mM Tris-HCL pH7.4, 200 mM NaCl, 1 mM EDTA) following the manufacturer's directions. The recombinant MBP-Spindly protein was eluted using elution buffer (20 mM Tris-HCl pH7.4, 200 mM NaCl, 1 mM EDTA, 10 mM maltose), concentrated in PBS (30,000 MWCO Amicon) and used as an antigen for immunization of rats.

Immunizations of rats were conducted according to the guidelines set by the Cross Cancer Institute Animal Care Committee and Canadian Council of Animal Care. Antibodies were purified by pre-absorbing the rat sera onto an Affigel 15 column (Bio-Rad Laboratories) that was covalently coupled to bacterial lysates containing MBP to remove antibodies against MBP and bacterial proteins. hSpindly antibodies were purified by overnight incubation of pre-adsorbed serum with an Affigel 15 column that was covalently coupled to MBP-hSpindly fusion protein. The column was washed 3 times with at least 10 bed volumes of TBS. Antibodies were eluted with elution buffer (0.2 M glycine-HCl pH 2.5) and immediately neutralized with 1 M Tris-HCl, pH 9.0. Protein concentrations of fractions were monitored by absorbance at 280 nm and antibody containing fractions were pooled, desalted and concentrated by centrifugation with a protein concentrator (30,000 MW cutoff, Amicon). The antibody concentration was determined and diluted with filter sterilized glycerol to a final concentration of 5 µg/ml in 50% glycerol:0.5X PBS. MBP-hZw10 (1-231 aa) recombinant protein was produced, purified and injected into rats using the same protocol as described for MBP-Spindly protein. A rat anti-hZw10 serum was used for IF.

2.9 Metabolic Labeling, Click Chemistry Reactions and In-gel Fluorescence Imaging

HeLa cells were grown and transfected in 10-cm plates as previously described under transient transfection. Cells were gently washed with PBS to remove dead cells or debris followed by trypsinization. Cells were treated with alk-FOH (50 µM, 50 mM stock solution in DMSO) for 4 h using the same volume of solvent (DMSO) in the negative controls (Charron et al., 2011). For co-incubation, HeLa cells were pretreated for 1 h with 10 µM L-744832 FTI prior to alk-FOH metabolic labeling. The cells were pelleted by centrifuging at 1000g for 5 min at RT. The cell pellet was washed twice in ice-cold PBS and pelleted by centrifuging at 1000 g for 5 min at 4 °C. Cells were flash frozen in liquid nitrogen and stored at -80 °C. Cell pellets were lysed in ice-cold Brij lysis buffer (1% Brij97, 50 mM triethanolamine pH 7.4, 150 mM NaCl, 5X EDTA free Roche

protease inhibitor cocktail, 10 mM PMSF) (Charron et al., 2011). Protein concentration was determined by the BCA assay (Pierce). EGFP-hSpindly was immunoprecipitated using 1 μ L anti-GFP rabbit pAb (ab290, Abcam) and 50 μ L of packed protein A-agarose beads (Roche) per sample (Charron et al., 2011). Upon incubation at 4 °C for 2 h on a nutating mixer (Labnet), the beads were washed (3X1 ml) with ice-cold modified RIPA lysis buffer (1% Triton X-100, 1% sodium deoxycholate, 0.1% SDS, 50 mM triethanolamine pH 7.4, 150 mM NaCl).

Cu(I)-catalyzed azide-alkyne cycloaddition (CuAAC)/click reaction was performed as described previously in Charron *et al.* (2011). The purified protein bound to beads was suspended in 47 μ L of ice-cold PBS, to which was added 3 μ L freshly premixed click reaction cocktail [azido-rhodamine (100 μ M, 10 mM stock solution in DMSO), Tris (2-carboxyethyl)phosphine hydrochloride (TCEP) (1 mM, 50 mM freshly prepared stock solution in deionized water), Tris [(1-benzyl-1H-1,2,3-triazol-4-yl) methyl]amine (TBTA) (100 μ M, 10 mM stock solution in DMSO) and CuSO₄·5H₂O (1 mM, 50 mM freshly prepared stock solution in deionized water)] for 1 h at 4 °C on a nutating mixer. The beads were washed (3X1 ml) with ice-cold modified RIPA lysis buffer, resuspended in 40 μ L loading buffer [27.5 μ L (4% SDS, 50 mM triethanolamine pH 7.4, 150 mM NaCl), 10 μ L 4XSDS-loading buffer (40% glycerol, 200 mM Tris-HCl pH 6.8, 8% SDS, 0.4% bromophenol blue) and 2.5 μ L of 0.5 M Bond-Breaker TCEP Solution (Thermo Scientific)], heated for 5 min at 95 °C, and 20 μ L of the supernatant was loaded on 2 separate SDS-PAGE gels (4–20% Bio-Rad Criterion Tris-HCl gel), one for fluorescence detection and the other for immunoblotting.

For cell lysates, 50 μ g protein was clicked in 47 μ L SDS-buffer (4% SDS, 50 mM triethanolamine pH 7.4, 150 mM NaCl) with 3 μ L freshly premixed click reaction cocktail (same as above) for 1 h at room temperature. Proteins were precipitated by adding ice-cold methanol (1 mL), placing at –80 °C overnight, centrifuging at 18000 g for 10 min at 4 °C and discarding the supernatant. The protein pellets were allowed to air-dry, resuspended in 50 μ L loading buffer (same

as above), heated for 5 min at 95 °C, and 20 µg of protein was loaded on 2 separate SDS-PAGE gels.

After SDS-PAGE separation, the gel was soaked in destaining solution (40% MeOH, 10% acetic acid, 50% H₂O) overnight at 4 °C on an orbital shaker, rehydrated with deionized water and visualized by scanning the gel on an Amersham Biosciences Typhoon 9400 variable mode imager (excitation 532 nm, 580 nm filter, 30 nm band-pass).

2.10 Immunoprecipitation and GFP Trap

HeLa cells were grown on 10-cm plates and double thymidine treatment was performed. 24 h before harvesting the cells were treated with either 10 µM of FTI L-744832 FTI or solvent control DMSO. Mitotically arrested HeLa cells (with 0.25 µg/ml nocodazole for 12-16 h) after second thymidine release were collected by shake-off and resuspended in 20 mM HEPES-KOH, pH 7.5, 10 mM KCl, 1 mM MgCl₂, 1 mM EDTA, and 1 mM EGTA, with protease and phosphatase inhibitors (PhosSTOP, Roche), lysed as previously described (Barisic et al., 2010). 500 µg of lysate were then incubated with the rabbit polyclonal anti hSpindly (Bethyl Laboratories Inc.) on a rotator at 4 °C for 1 h. Rabbit. The immunoprecipitates were captured with protein A beads which were blocked overnight with 1% BSA. Western blotting was performed for the identification of Zw10 and Rod pull-down.

For GFP Trap, HeLa cells seeded in the 10 cm plates were transfected with 100 nM hSpindly siRNA for 24 h. After 24 h, the cells were transfected with an siRNA resistant version of either GFP WT hSpindly or GFP C602A mutant hSpindly. Cells were enriched in mitosis by 16 h nocodazole treatment. Mitotic cells were resuspended in buffer as mentioned above in IP. GFP Trap beads (ChromoTek) were used to pull-down hSpindly following manufacturer's instructions with the exception of the buffer used.

2.11 Live-Cell Imaging

For analysis of mitotic timing, a HeLa cell line stably expressing GFP-tubulin and mCherry H2B was used. Cells seeded in a 35-mm glass-bottom dish (MatTek or Flourdish) were placed onto a sample stage within an incubator chamber maintained at a temperature of 37 °C in an atmosphere of 5% CO₂. Cell medium was replaced with imaging medium (OPTI-MEM (Gibco) supplemented with 2 mM L-glutamine, 10% (v/v) FBS (fetal bovine serum) and 14 mM HEPES) before imaging. Imaging was performed using a spinning disk confocal on an inverted microscope Axiovert 200M (Carl Zeiss, Inc.; 40X objective lens; 1.3 NA) equipped with an electron-multiplying charge-coupled device (CCD) camera (ORCA-FLASH-4.0; Hamamatsu Photonics). Images were collected every 5 min for the GFP and Cy3 channels using 100 ms exposure times, for 10-16 h using the velocity software (Perkin Elmer Inc.). Velocity 6.3.0 software was used to collect and export videos in AVI format using Microsoft video 1 compression. Videos were further converted to .mov format with Vegas Pro version 12.0 (Build 394) (Sony Creative Software Inc.) using Sorenson 3 compression. Mitotic timing for cells was calculated manually. Still tiff format images from videos were exported using Velocity 6.3.0 software and processed using Adobe Photoshop 7.0.

2.12 Fluorescent Recovery After Photobleaching (FRAP)

pLV.ExSiP/Neo-CMV-mEGFP-hSpindly vector expressing a siRNA resistant version of hSpindly was constructed by Cyagen. HeLa cells were plated in a 60-mm dish so that they were 50% confluent on the next day. 5 µl of thawed lentivirus was mixed with 2 ml of fresh media, 8 µg/ml of polybrene and transferred onto cells. Cells were incubated in virus containing media for 12-13 h. HeLa cells expressing EGFP-hSpindly were selected by treatment with neomycin following 25 h post transduction. These transduced cells were used for 2-3 weeks for performing FRAP. HeLa cells transiently expressing EGFP-hSpindly were seeded onto 35-mm glass bottomed dishes (MatTek or Flourdish) at a density of 5 X 10⁴ cells/ml for 24 h prior to FRAP analysis.

FRAP experiments were performed using a spinning disk confocal on an inverted microscope Axiovert 200M (Carl Zeiss, Inc.; 63X oil objective lens; 1.4 NA) equipped with an electron-multiplying charge-coupled device (CCD) camera (ORCA-FLASH-4.0; Hamamatsu Photonics). Laser ablation and imaging was controlled using the velocity software (Perkin Elmer Inc.). A circular area 10 X 10 px containing a single kinetochore was photobleached with the 488 nm laser using a single laser pulse. Subsequent images were acquired for 90 seconds at maximum speed followed by 300 seconds at a rate of 12 time points per minute (min) with an exposure time of 200 ms. Fluorescence intensity recovery in the region of interest was quantified using Metaexpress software (Molecular Devices, LLC). The recovered fluorescence intensity signal was corrected for background by a signal obtained from a region outside the cell. Photobleaching was insignificant so I did not correct for photobleaching. The percent recovery and time for half recovery of the fluorescence signal was calculated using excel and graphed using prism (non-linear regression curve).

2.13 Yeast Two-Hybrid

Yeast two-hybrid was performed as described previously (Chan et al., 1998; Estojak et al., 1995; Gyuris et al., 1993). In brief, the SKY473 strain of *S. cerevisiae* was co-transformed with p-Gilda-Spindly mutants and pJG4-5-hp50 along with the pSH18-34 reporter plasmid. Yeast strain SKY473 and plasmids p-Gilda, pJG4-5, and pSH18-34 were provided by E. Golemis (Fox Chase Cancer Center). Transformant yeast colonies were selected by growing yeast on plates with media lacking Tryptophan, Histidine and Uracil. Three transformant colonies were picked from each transformation and restreaked onto plates lacking Tryptophan, Histidine and Uracil but supplemented with D-galactose and raffinose (gal/raf) to induce expression of bait and prey genes. After 2 days, those three colonies were restreaked onto plates lacking Tryptophan, Histidine and Uracil+ gal/raf as well as X-gal, which allowed blue/white selection 2-3 days after streaking. Bait and prey protein expression was confirmed by western blotting. Yeast colonies were picked from plates lacking Tryptophan, Histidine and

Uracil+ gal/raf and yeast was resuspended in 1X SDS-PAGE loading buffer and frozen at -80 °C for 24 h. The samples were boiled for 7 min and SDS-PAGE and western transfer was performed as described in section 2.5. LexA fused hSpindly mutant proteins were detected with rabbit polyclonal anti-LexA antibody followed by Alexa 680 conjugated anti-rabbit antibody. B42 fused hp50 proteins were detected with rabbit polyclonal anti-B42 antibody (Sigma) followed by Alexa 680 conjugated anti-rabbit antibody.

pSH17-4 expresses a lexA fusion with an activation domain that strongly activates transcription in pSH18-34 and this combination was used as a positive control. pRFHM1 expresses a lexA fusion with the N-terminus of bicoid and does not activate transcription in pSH18-34. This combination was used as a negative control. The possibility of false positives was eliminated by checking the interaction between the bait construct with an empty prey vector, and vice versa.

2.13 Statistical Analysis

Statistical analysis was performed using Graphpad Prism version 5.04. P-values were calculated with Student's t test.

2.14 Reagent and Buffer Recipes

3.5% Paraformaldehyde

3.5 g of paraformaldehyde is dissolved in 80 ml of warm ddH₂O (30 sec microwave). Add 20 µl of 10 N NaOH and dissolve paraformaldehyde powder with low stirring. Once completely dissolved, add 10 ml of filter sterile 10X PBS and 2 ml of 0.5 M PIPES (pH 6.9). Adjust paraformaldehyde pH between 6.6 to 6.9 with 0.1 N HCl and bring the final volume up to 100 ml with ddH₂O.

Mowiol Mounting Media

Add 2.4 g of Mowiol powder to 6 g of glycerol and stir to mix.

Add 6 ml of ddH₂O and leave stirring overnight at room temperature.

Add 12 mL of 0.2 M Phosphate Buffer, pH7.4.

Heat to 50 °C for 10 min with gentle stirring to minimize bubbles.

After Mowiol is dissolved, centrifuge at 5000g for 15 min.

Add 0.1% n-propyl gallate.

Aliquot and store at -80 °C.

PEI (1 mg/ml)

Dissolve 100 mg of Polyethylenimine in 80 ml ddH₂O .

Adjust pH to 7.0 with HCl, adjust the final volume to concentration of 1 mg/ml.

Filter through 0.22 µm membrane.

Aliquot and store at -80 °C.

Table 2.1 Composition of buffers and solutions.

Buffer	Composition
KB and KB+TX Buffer	0.01 M Tris-HCl pH 7.5, 0.15 M NaCl, 0.1% BSA (+/- 0.2% Triton X-100)
1% NP40 lysis Buffer	1% NP40, 150 mM NaCl, 50 mM Tris-HCl pH 8, with full protease and phosphatase inhibitors
Lysis Buffer for Spindly IP	20 mM HEPES-KOH, pH 7.5, 10 mM KCl, 1 mM MgCl ₂ , 1 mM EDTA, and 1 mM EGTA, with protease and phosphatase inhibitors
Phosphate buffered Saline (PBS)	137 mM NaCl, 2.7 mM KCl, 4.3 mM Na ₂ HPO ₄ , 1.4 mM KH ₂ PO ₄ , pH 7
1X SDS-PAGE running buffer (10L)	30.3 g Tris-HCl, pH 8.8, 141.7 g glycine, 10 g SDS
1X Western transfer Buffer (4L)	12.12 g Tris-HCl, 57.68 g glycine, 4 g SDS, 10, 800 ml methanol
Coomassie Blue (500ml)	1.25 g of Coomassie blue, 250 ml methanol (10% acetic acid), 50 ml glacial acetic acid (50 % ethanol),
SDS-PAGE sample buffer	20% glycerol, 167 mM Tris-HCl, pH 6.8, 2% SDS, 0.05% bromophenol blue

Table 2.2 Primary antibodies

Antibody	Host Species	IF dilution	Western Blot Dilution	Source
hZW10	Rabbit	1/1000	1/2000	(Chan et al., 2000)
hZW10	Rat	1/1000	ND	This study
hROD	Rabbit	1/1000	1 in 1500	(Chan et al., 2000)
ACA	Human	1/3000	ND	Dr. Fritzler (U of Calgary)
hCENP-E	Rabbit	1/1000	ND	(Chan et al., 1998)
hp50	Rabbit	ND	1/500	Bethyl Laboratories
hTubulin	Mouse	1/2000	1/5000	Sigma (B512)
hPericentrin	Rabbit	1/2000	ND	Abcam (ab4448)
hCENP-F	Rabbit	1/750	ND	(Chan et al., 1998)
Anti GFP-IR800	Mouse	ND	1/10,000	Rockland (600-132-215)
LexA	Rabbit	ND	1/1000	Abcam (50953)
B42	Rabbit	ND	1/1000	Sigma (B9808)
hSpindly	Rat	1/1000	1/2000	(Moudgil et al., 2015)

Table 2.3: hSpindly and hCENP-F cloning and truncation mutant primers

Primer	Gene	Sequence	Description
Ch374	attB1 extension Forward	GGGGACAAGTTTGTACAAAAAAGC AGGCT	attB1
Ch375	attB2 extension Reverse	GGGGACCACTTTGTACAAGAAAGCT GGGT	attB2
Ch717	hSpindly	AAAAAGCAGGCTACATGGAGGCAG ATATAATCAC	hSpindly full-length forward primer
Ch718	hSpindly	AGAAAGCTGGGTTACTGTTGAGGGC ACTGG	hSpindly full-length reverse primer
Ch870	hSpindly	AGAAAGCTGGGTTACATTACGCGCA GTTCCCTC	C-terminal primer aa151
Ch871	hSpindly	AGAAAGCTGGGTTACAACGTGGCA ATTTGTAAC	C-terminal primer aa300
Ch872	hSpindly	AGAAAGCTGGGTTACCTCTTTTTCA GTACAGGCAC	C-terminal primer aa452
Ch873	hSpindly	AAAAAGCAGGCTTAATGTCTGAACG TGTGCAGG	N-terminal primer aa151
Ch874	hSpindly	AAAAAGCAGGCTCCATGTTGGAGCA GAAGAATG	N-terminal primer aa322
Ch875	hSpindly	AAAAAGCAGGCTACATGCGTGAGG TGCTCCC	N-terminal primer aa453
Ch954	hSpindly	AAAAAGCAGGCTCACAGTCCTGCC TAACAG	N-terminal primer aa488
Ch955	hSpindly	AAAAAGCAGGCTACAAAAATCTGC CCGTGG	N-terminal primer aa518
Ch956	hSpindly	AAAAAGCAGGCTCCCCTAACTCTCC CAGG	N-terminal primer aa553
Ch1005	hSpindly	AAAAAGCAGGCTTAACCACCGCTAA AGATGC	N-terminal primer aa461
Ch1006	hSpindly	AAAAAGCAGGCTTCAACAACAGTG CTCTCGG	N-terminal primer aa469
Ch1028	hSpindly	AAAAAGCAGGCTCTAAAGGCAACT CTTTGTTTGC	N-terminal primer aa252
Ch1029	hSpindly	AAAAAGCAGGCTTTAACAGAGAAC AGATGCAGAG	N-terminal primer aa288
Ch1096	hSpindly	GTACAAAAAAGCAGGCATGCAGAG AATGAAG	N-terminal sense primer aa293 (288-605 template)
Ch1097	hSpindly	CTTCATTCTCTGCATGCCTGCTTTTT TGTAC	N-terminal anti-sense primer aa293 (288-605 template)
Ch1224	hCENP-F	AAAAAGCAGGCTTGCTACAAGGCCT TGATG	hCENP-F forward primer aa2581
Ch1225	hCENP-F	AGAAAGCTGGGTCCTGGACCTTAC AGTTCTCAC	hCENP-F reverse primer aa3210

Table 2.4: hSpindly deletion mutant primers

Primer	Gene	Sequence	Description
Ch959	hSpindly	GAGACCCAGTGCCCTTAACAGTAA CCCAG	Q604STOP sense primer
Ch960	hSpindly	CTGGGTTACTGTTAAGGGCACTGG GTCTC	Q604STOP anti sense primer
Ch961	hSpindly	CTACTCCAGAGACCCCTCAACAGT AACC	Δ601-602QC sense primer
Ch962	hSpindly	GGTACTGTTGAGGGGTCTCTGGA GTAG	Δ601-602QC anti-sense primer
Ch963	hSpindly	CCAGTGCCCTCAATAACCCAGCTTT C	D605Q sense primer
Ch964	hSpindly	GAAAGCTGGGTTATTGAGGGCACT GG	D605Q anti-sense primer
Ch991	hSpindly	CCAGAGACCCAGCAACAGTAAAGA C	Δ602-603CP sense primer
Ch992	hSpindly	CCAGAGACCCAGCAACAGTAAAGA C	Δ602-603CP anti-sense primer
Ch993	hSpindly	GTGTCTTCTAAACAGTGCCCTCAAC	Δ596-600STPET sense primer
Ch994	hSpindly	GTTGAGGGCACTGTTTAGAAGACA C	Δ596-600STPET anti- sense primer
Ch995	hSpindly	CCCTATTCTATATACTCCAGAGACC	Δ592-596VSSKS sense primer
Ch996	hSpindly	GGTCTCTGGAGTATATAGAATAGG G	Δ592-596VSSKS anti- sense primer
Ch997	hSpindly	GAAATCACACCCTAAATCTACTCC AG	D589-594ILYVSS sense primer
Ch998	hSpindly	CTGGAGTAGATTTAGGGTGTGATT C	Δ589-594ILYVSS anti- sense primer
Ch1001	hSpindly	CCAGAGACCCAGTGCCCTAACAAC TAAAGACTTTTC	Δ604QQ sense primer
Ch1002	hSpindly	GAAAAGTCTTTAGTTGTTAGGGCA CTGGGTCTCTGG	Δ604QQ anti-sense primer
Ch1031	hSpindly	CTCTGTAAATACATTTGCTTACT ATTGGGATCCAAGGCTTGCTG	Δ253-283 sense primer
Ch1032	hSpindly	GATGCAGAGAATGAAGTTACAAGA ACCTGAAGAGACAGTTGAAG	Δ253-283 anti-sense primer
Ch1033	hSpindly	CTTCAACTGTCTCTTCAGTTCTTG TAACTTCATTCTCTGCATC	Δ298-563 sense primer
Ch1034	hSpindly	GAGAACAGATGCAGAGAATGAAG CTTCAAACAGAAGTTAAAGAAGG	Δ298-563 anti-sense primer

Table 2.5: hSpindly and hCENP-F mutant substitution primers

Primer	Gene	Sequence	Description
Ch1003	hSpindly	GAGACCCAGTGCCCTACCACCTAAAGA CTTTTC	QQ604-605TT sense primer (Q604STOP template)
Ch1004	hSpindly	GAAAAGTCTTTAGGTGGTAGGGCACTG GGTCTC	QQ604-605TT anti-sense primer (Q604STOP template)
Ch1082	hSpindly	CTCAGAAAGAGGAGGCACAGTCCTGCC C	T487A sense primer
Ch1083	hSpindly	GGGCAGGACTGTGCCTCCTCTTTCTGAG	T487A anti-sense primer
Ch1084	hSpindly	CAGTTTCTATACACGCACCAGTAGTCAG TCTCTC	T509A sense primer
Ch1085	hSpindly	GAGAGACTGACTACTGGTGC GTGTATA GAAACTG	T509A anti-sense primer
Ch1086	hSpindly	CTATACACACACCAGTAGTCGCTCTCTC TCCTCAC	S513A sense primer
Ch1087	hSpindly	GTGAGGAGAGAGAGCGACTACTGGTGT GTGTATAG	S513A anti-sense primer
Ch1088	hSpindly	CGCACCAGTAGTCGCTCTCTCTCCTCAC AAAAATC	T509A, S513A sense primer (T509A template)
Ch1089	hSpindly	GATTTTTGTGAGGAGAGAGAGCGACTA CTGGTGCG	T509A, S513A anti-sense primer (T509A template)
Ch1090	hSpindly	CCAGTAGTCAGTCTCGCTCCTCACAAAA ATCTG	S515A sense primer
Ch1091	hSpindly	CAGATTTTTGTGAGGAGCGAGACTGACT ACTGG	S515A anti-sense primer
Ch1092	hSpindly	CCAGTAGTCGCTCTCGCTCCTCACAAAA ATC	S513A/S515A sense primer
Ch1093	hSpindly	GATTTTTGTGAGGAGCGAGAGCGACTA CTGG	S513A/S515A anti-sense primer
Ch1134	hSpindly	CAGTTTCTATACACGAACCAGTAGTCAG TCTCTCTC	T509E sense primer
Ch1135	hSpindly	GAGAGAGACTGACTACTGGTTCGTGTAT AGAAACTG	T509E anti-sense primer
Ch1136	hSpindly	CTATACACACACCAGTAGTCGATCTCTC TCCTCAC	S513D sense primer
Ch1137	hSpindly	GTGAGGAGAGAGATCGACTACTGGTGT GTGTATAG	S513D anti-sense primer
Ch1138	hSpindly	CGAACCAGTAGTCGATCTCTCTCCTCAC AAAAATC	T509E/S513E sense primer
Ch1139	hSpindly	GATTTTTGTGAGGAGAGAGATCGACTAC TGTTTCG	T509E/S513E anti-sense primer
Ch1140	hSpindly	CCAGTAGTCAGTCTCGATCCTCACAAAA ATCTGC	S515D sense primer
Ch1141	hSpindly	GCAGATTTTTGTGAGGATCGAGACTGAC TACTGG	S515D anti-sense primer
Ch1142	hSpindly	CCAGTAGTCGATCTCGATCCTCACAAAA ATCTGC	S513D/S515D sense primer

Ch1143	hSpindly	GCAGATTTTTGTGAGGATCGAGATCGAC TACTGG	S513D/S515D sense primer
Ch1203	hSpindly	CTACTCCAGAGACCCAGTGCAAGCAAC AGTAACCCAGC	P603K sense primer
Ch1204	hSpindly	GCTGGGTTACTGTTGCTTGCCTGGGTC TCTGGAGTAG	P603K anti-sense primer
Ch1205	hSpindly	CCAGAGACCCAGTGCAAGGTACAGTAA CCCAGC	Q604V sense primer
Ch1206	hSpindly	GCTGGGTTACTGTACCTTGCCTGGGTC TCTGG	Q604V anti-sense primer
Ch1207	hSpindly	CCAGAGACCCAGTGCAAGACACAGTAA CCCAGC	Q604T sense primer
Ch1208	hSpindly	CCAGAGACCCAGTGCAAGACACAGTAA CCCAGC	Q604T anti-sense primer
Ch1211	hSpindly	CTAAATCTACTCCAGAGGCCAGTGCAA GCAAC	T600A sense primer
Ch1212	hSpindly	GTTGCTTGCCTGGGCTTGGAGTAGA TTTAG	T600A anti-sense primer
Ch1213	hSpindly	CTTCTAAATCTACTGCAGAGACCCAGTG CCC	P598A sense primer
Ch1214	hSpindly	GGGCACTGGGTCTCTGCAGTAGATTTAG AAG	P598A anti-sense primer
Ch1215	hSpindly	CCAGTGCCCTCAACTGTAACCCAGCTTT C	Q605L sense primer
Ch1216	hSpindly	GAAAGCTGGGTTACAGTTGAGGGCACT GG	Q605L anti-sense primer
Ch1217	hSpindly	GAGACCCAGTGCCCTCAATTCTAACCCA GCTTCTGTAC	L605F sense primer
Ch1218	hSpindly	GTACAAGAAAGCTGGGTTAGAATTGAG GGCACTGGGCTC	L605F anti-sense primer
Ch1226	hCENP-F	CAAGGGCAGTGAGAACCCTAAGGTCCA GTGACC	C3207A sense primer
Ch1227	hCENP-F	GGTCACTGGACCTTAGCGTTCTCACTGC CCTTG	C3207A anti-sense primer
Ch957	hSpindly	CAGAGACCCAGTGCGCTCAACAGTAAC CC	P603A sense primer
Ch958	hSpindly	GGGTTACTGTTGAGCGCACTGGGTCTCT G	P603A anti-sense primer
Ch965	hSpindly	GTGTCTTCTAAATCTGCTCCAGAGACCC AGTG	T597A sense primer
Ch966	hSpindly	CACTGGGTCTCTGGAGCAGATTTAGAAG ACAC	T597A anti-sense primer
Ch979	hSpindly	CCCAATAGTAAAGGCAACGCTTTGTTTG CAGAGG	S256A sense primer
Ch980	hSpindly	CCTCTGCAAACAAGCGTTGCCTTTACT ATTGGG	S256A anti-sense primer
Ch981	hSpindly	GGCAACTCTTTGGCTGCAGAGGTGGAA GATCGAAG	F258A sense primer
Ch982	hSpindly	CTTCGATCTCCACCTCTGCAGCCAAAG AGTTGCC	F258A anti-sense primer
Ch983	hSpindly	CAATAGTAAAGGCAACGCTTTGGCTGC AGAGG	S256A/F258A sense primer
Ch984	hSpindly	CCTCTGCAGCCAAAGCGTTGCCTTTACT	S256A/F258A anti-

		ATTG	sense primer
Ch985	hSpindly	CTACTCCAGAGACCGCGTGCCCTCAACA GTAAC	Q601A sense primer
Ch986	hSpindly	GTTACTGTTGAGGGCAGCGGTCTCTGG AGTAG	Q601A anti-sense primer
Ch987	hSpindly	CTCCAGAGACCCAGGCCGCTCAACAGT AAAG	CP602AA sense primer (P603A template)
Ch988	hSpindly	CTTTACTGTTGAGCGGCCTGGGTCTCTG GAG	CP602AA anti-sense primer (P603A template)
Ch989	hSpindly	CTCCAGAGACCCAGGCCCTCAACAGT AACC	C602A sense primer
Ch990	hSpindly	GGTTACTGTTGAGGGCCTGGGTCTCTG GAG	C602A anti-sense primer

**Chapter 3 A novel role of farnesylation in targeting a
mitotic checkpoint protein, human Spindly, to
kinetochores**

A version of this chapter has been published as Moudgil et al., *Journal of Cell Biology*, 2015, 208(7):881-96

(©Moudgil et al., 2015. Originally published in *Journal of Cell Biology*. doi:
10.1083/jcb.201412085)

3.1 Abstract

Kinetochores localization of mitotic checkpoint proteins is essential for their function during mitosis. hSpindly kinetochores localization is dependent on the RZZ complex and hSpindly recruits the dynein/dynactin complex to kinetochores during mitosis; but the mechanism of hSpindly kinetochores recruitment is unknown. Through domain-mapping studies we characterized the kinetochores localization domain of hSpindly and discovered it undergoes farnesylation at the C-terminal cysteine residue. The N-terminal 293 residues of hSpindly are dispensable for its kinetochores localization. Inhibition of farnesylation using a farnesyl transferase inhibitor (FTI) abrogated hSpindly kinetochores localization without affecting RZZ complex, CENP-E and CENP-F kinetochores localization. We showed that hSpindly is farnesylated *in vivo* and farnesylation is essential for its interaction with the RZZ complex and hence kinetochores localization. FTI treatment and hSpindly knockdown displayed the same mitotic phenotypes, indicating that hSpindly is a key FTI target in mitosis. Our data show a novel role of lipidation in targeting a checkpoint protein to kinetochores through protein-protein interaction.

3.2 Introduction:

Accurate chromosome segregation during mitosis is essential for the maintenance of genomic stability. The mitotic checkpoint is a molecular mechanism that prevents premature segregation until all chromosomes are bioriented and aligned at the metaphase plate. Mitotic checkpoint proteins were first identified in budding yeast (Hoyt et al., 1991; Li and Murray, 1991; Weiss and Winey, 1996) and are conserved from yeast to human (Chan et al., 2005). Mitotic checkpoint proteins assemble at kinetochores during mitosis and include Mad1, Mad2, Bub1, BubR1, Bub3 and Mps1 proteins. The RZZ complex (Roughdeal, ZesteWhite10 and Zwi10) subunits are essential mitotic checkpoint proteins originally identified in flies and are conserved in metazoans (Karess, 2005). The RZZ complex is required for Mad1 and Mad2 kinetochore recruitment, and also recruits hSpindly to kinetochores (Buffin et al., 2005; De Antoni et al., 2005; Fang et al., 1998; Kops et al., 2005). hSpindly plays a critical role in checkpoint silencing by recruiting the dynein/dynactin motor complex that transports checkpoint proteins, such as Mad1, Mad2, RZZ complex and hSpindly, from kinetochores to spindle poles (Barisic et al., 2010; Chan et al., 2009; Famulski et al., 2011; Gassmann et al., 2008; Howell et al., 2001).

hSpindly is a 605 amino acid (aa) protein consisting of two coiled-coil domains separated by a conserved 32 aa spindly motif (Chan et al., 2009; Griffis et al., 2007). Spindly was discovered to be a regulator of dynein at kinetochores during mitosis in *Drosophila* and is also involved in chromosome alignment and mitotic checkpoint silencing in human cells (Barisic et al., 2010; Chan et al., 2009; Gassmann et al., 2010; Griffis et al., 2007). Spindly kinetochore localization is dependent on the RZZ complex since knockdown of Zw10 causes abrogation of Spindly kinetochore localization (Barisic and Geley, 2011; Chan et al., 2009). Knockdown of hSpindly causes chromosome alignment defects, loss of dynein/dynactin kinetochore localization, and prometaphase delay (Barisic et al., 2010; Chan et al., 2009; Gassmann et al., 2008). hSpindly C-terminal residues were previously shown to be important for kinetochore localization and it is

speculated that hSpindly undergoes farnesylation; a post-translational lipid modification (Barisic et al., 2010).

Farnesylation is a type of protein prenylation, where a 15-carbon farnesyl lipid group is transferred onto one or more C-terminal cysteine residues (Zhang and Casey, 1996). A subset of membrane proteins is farnesylated making the C-terminus more hydrophobic, facilitating their membrane binding. A typical farnesylation motif, CAAX, has a C-terminal cysteine that becomes farnesylated, usually followed by two aliphatic aa, and the last aa is typically methionine, serine, glutamine, or alanine (Sinensky, 2000). It is estimated that more than 100 proteins undergo farnesylation including two kinetochore proteins, CENP-E and CENP-F (Ashar et al., 2000; Wright and Philips, 2006). RAS family proteins require farnesylation for membrane binding and, since RAS is mutated in a wide variety of cancers, many farnesyl transferase inhibitors (FTIs) have been developed to inhibit RAS farnesylation (Berndt et al., 2011; Downward, 2003; Karnoub and Weinberg, 2008). FTIs efficiently killed tumor cells in culture and in animal models regardless of RAS mutations suggesting additional unknown farnesylated targets (Crespo et al., 2002; Nagasu et al., 1995; Sepp-Lorenzino et al., 1995). Interestingly, in addition to G1 arrest, FTI-treated tumor cells exhibited prometaphase delay, defective spindle formation, and chromosome misalignments (Ashar et al., 2000; Crespo et al., 2002; Crespo et al., 2001). These mitotic defects have been correlated with the inhibition of CENP-E and CENP-F farnesylation (Ashar et al., 2000; Hussein and Taylor, 2002; Schafer-Hales et al., 2007). Studies have shown, however, that FTIs do not affect CENP-E or CENP-F kinetochore localization and it has been hypothesized that mitotic defects associated with FTIs are due to unknown targets (Crespo et al., 2002; Crespo et al., 2001; Verstraeten et al., 2011). This speculation is further supported by data showing that loss of CENP-F function by siRNA in HeLa cells leads to a very brief mitotic delay rather than prometaphase accumulation as seen with FTI treatment (Feng et al., 2006). In addition, siRNA knock down of CENP-E or microinjection of function blocking antibodies resulted in unaligned chromosomes at spindle poles in

metaphase cells which resembles metaphase arrest rather than the gross chromosome alignment defect and prometaphase delay observed upon FTI-treatment (McEwen et al., 2001; Schaar et al., 1997; Tanudji et al., 2004; Yao et al., 2000). Existence of conflicting data regarding the role of farnesylation in targeting CENP-E and CENP-F proteins to kinetochores warrants further investigation into how FTIs induce prometaphase delay in tumor cells.

Here, we identified hSpindly, a mitotic checkpoint protein as a novel farnesylation substrate. We defined the hSpindly kinetochore localization domain and reported that farnesylation of hSpindly is required for its interaction with the RZZ complex and its kinetochore localization. Furthermore, we showed that loss of hSpindly kinetochore localization following FTI treatment is likely responsible for the prometaphase delay observed in FTI-treated tumor cells rather than CENP-E and CENP-F as reported previously.

3.3 Results

3.3.1 hSpindly kinetochore localization is dependent on its C-terminus

hSpindly localizes to kinetochores in prophase and prometaphase and accumulates at spindle poles during metaphase in HeLa cells consistent with previous immunofluorescence studies (Figure 3.1) (Chan et al., 2009). EGFP fused N- and C-terminal truncation constructs of hSpindly were generated and expression of these constructs was confirmed in HEK293T cells by immunoblots (Figure 3.2 & Figure 3.3). Analysis of transfected prometaphase HeLa cells revealed that the 453-605 aa (construct C1) are required for kinetochore localization but the N-terminal 293 aa (construct N3) are dispensable (Figure 3.2). N-terminal deletion construct N5 did not localize and N4 (322-605 aa) localized to kinetochores only when transfected cells were treated with vinblastine. This microtubule poison disrupts kinetochore-microtubule attachments and maximally enhances checkpoint activity allowing for stringent analysis of kinetochore localization capability of hSpindly mutants (Famulski et al., 2008; Hoffman et al., 2001). The N4 mutant perhaps has very low kinetochore binding affinity (or fast turnover) and is rapidly transported off to spindle poles by dynein (discussed in detail later).

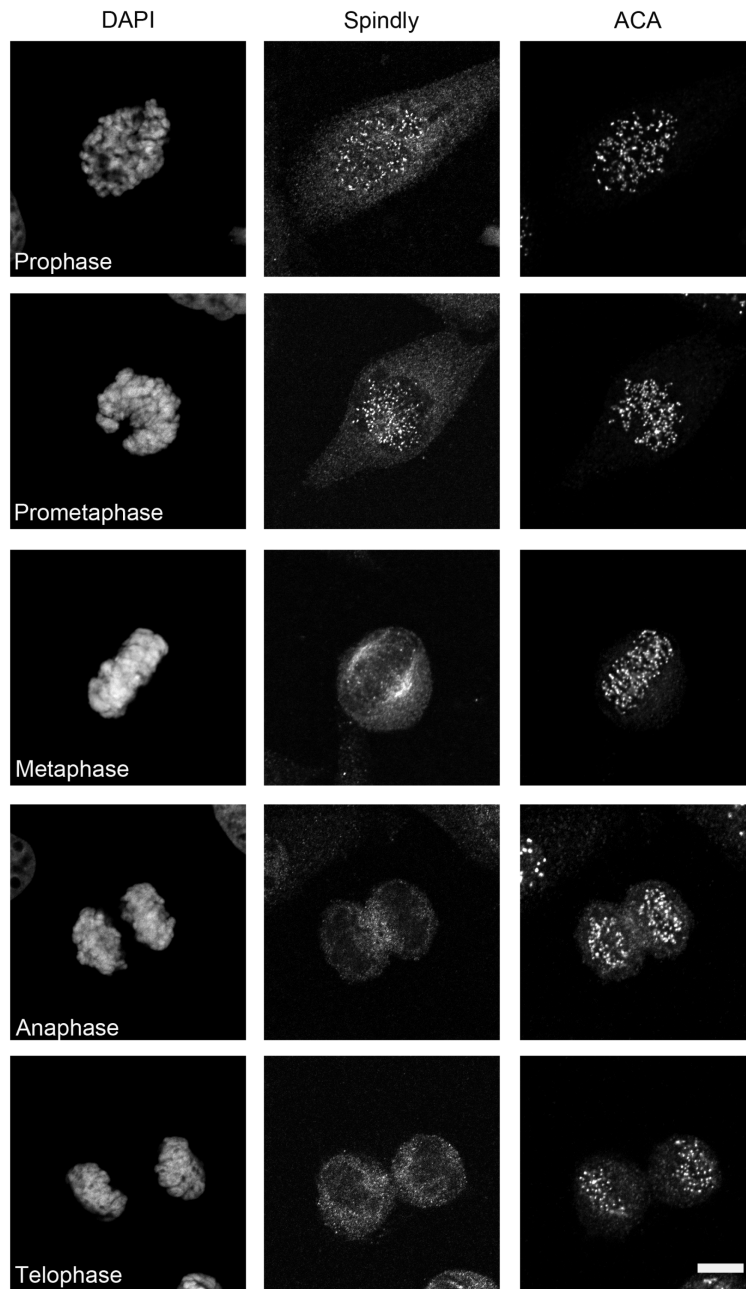


Figure 3.1: Endogenous hSpindly kinetochore localization during mitosis. HeLa cells were immunostained with anti-hSpindly antibody, CREST antisera to immunostain centromeres (ACA) and DAPI to stain DNA. hSpindly localizes to the kinetochores at prophase, prometaphase and at spindle poles in metaphase. Scale bar, 5 μ m

A

	Protein Structure			Kinetochores Localization	
	Colled Coil Domain I 1-252	Spindly motif 253-284	Colled Coil Domain II 300-438	Untreated	Vinblastine
WT	1 ————— 605			+	+
C1	1 ————— 452			-	-
N1	151 —————		605	+	+
N2		288 —————	605	+	+
N3		294 —————	605	+	+
N4		322 —————	605	-	+
N5			453 ————— 605	-	-

B

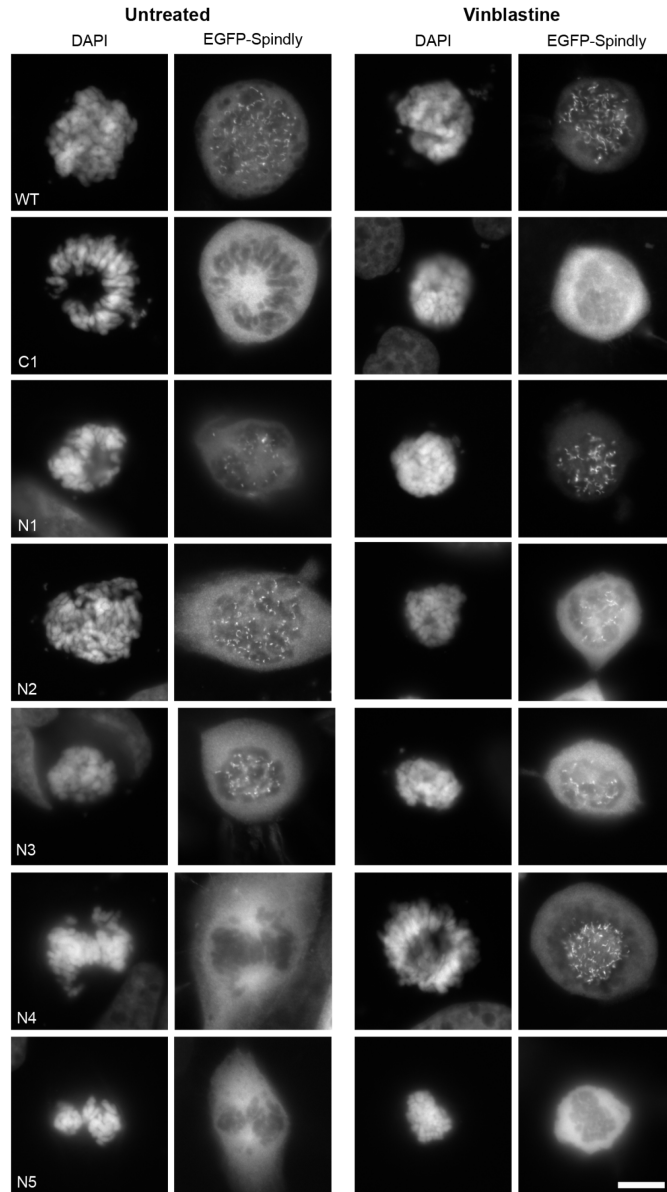


Figure 3.2: hSpindly C-terminal is required for kinetochore localization.

(A) A schematic diagram of hSpindly depicting truncation mutants (+ indicates kinetochore localization and – indicates no kinetochore localization). Kinetochore localizing capability of each construct was analyzed under vinblastine treatment, which maximally load checkpoint proteins on kinetochores. aa numbers are indicated.

(B) HeLa cells were transiently transfected with EGFP-hSpindly fusion constructs (shown in Figure 1A) and the kinetochore localization ability of each construct was analyzed using fluorescence microscopy. DAPI (4',6-diamidino-2-phenylindole) stains chromosomes. Representative images show that the C-terminal aa from 293 to 605 of hSpindly are required for kinetochore localization. Scale bar, 10µm.

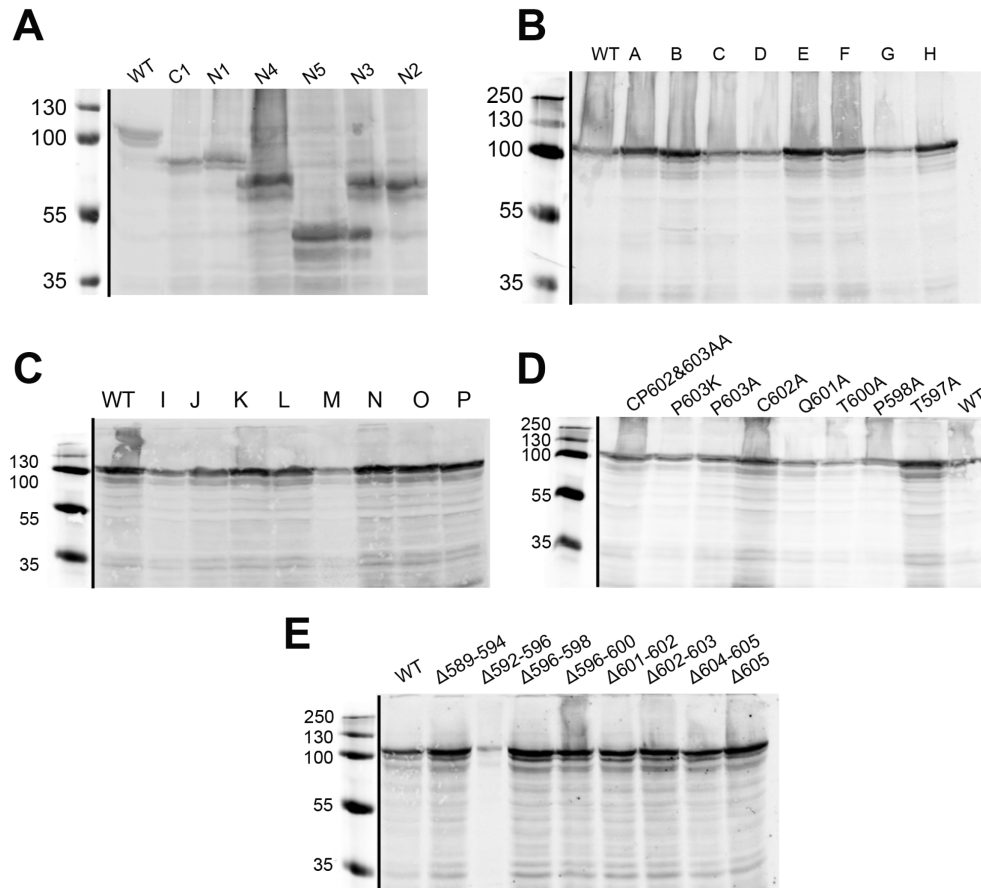


Figure 3.3: Expression of hSpindly mutant library using western blot analysis.

Immunoblots showing the expression of GFP-hSpindly fusion proteins transfected into HEK293 cells (**A**-Truncation mutants, **B&C**-Insertion mutants, **D**-Substitution mutants and **E**- Deletion mutants). GFP-fusion proteins were labeled with IR800-conjugated rabbit anti-GFP antibody. Molecular mass markers detected in the same channel are shown on each blot. (Masses indicated in kD). WT- wild type. All hSpindly mutant constructs expressed at the expected size.

To further define the kinetochore localization domain, a transposon based random insertion mutant library of hSpindly was generated (Table 3.1). hSpindly mutants containing 5 aa in-frame insertions, spanning 151 to 603 aa residues, expressing at the expected size, were screened for kinetochore localization (Figure 3.3 & Figure 3.4). Surprisingly, construct P with an insertion following 603 aa (P603–CGRSP) was the only mutant that completely abrogated kinetochore localization highlighting the importance of the far C-terminal residues (Figure 3.4). In addition, construct O with an insertion following 600 aa (T600–QLRPH) localized to kinetochores only when the cells were treated with vinblastine, indicating that residues immediately adjacent to the C-terminus are also important (Figure 3.4) (discussed in detail later). Kinetochore localization of all the insertion mutants is shown in Figure 3.6.

Table 3.1: hSpindly random insertion mutants show that the far C-terminus is required for kinetochore localization.

Construct	Insertion Site & Sequence (Amino acid)	Kinetochore Localization Untreated	Kinetochore Localization Vinblastine
A	M ¹⁵¹ SAAAM	Positive	Positive
B	R ²³⁰ VCGRS	Positive	Positive
C	N ³⁶⁴ TYAAA	Positive	Positive
D	M ³⁷³ NAAAM	Positive	Positive
E	G ³⁸⁷ ECGRS	Positive	Positive
F	E ⁴⁴¹ CGRTE	Positive	Positive
G	G ⁵³⁷ CGRIG	Positive	Positive
H	S ⁵⁴⁶ AAALS	Positive	Positive
I	E ⁵⁶¹ CGRTE	Positive	Positive
J	T ⁵⁶⁶ AAAQT	Positive	Positive
K	H ⁵⁸⁷ CGRTH	Positive	Positive
L	P ⁵⁸⁸ MRPHP	Positive	Positive
M	T ⁵⁹⁷ PVRPH	Positive	Positive
N	P ⁵⁹⁸ VRPHP	Positive	Positive
O	T⁶⁰⁰QLRPH	Negative	Positive
P	P⁶⁰³CGRSP	Negative	Negative

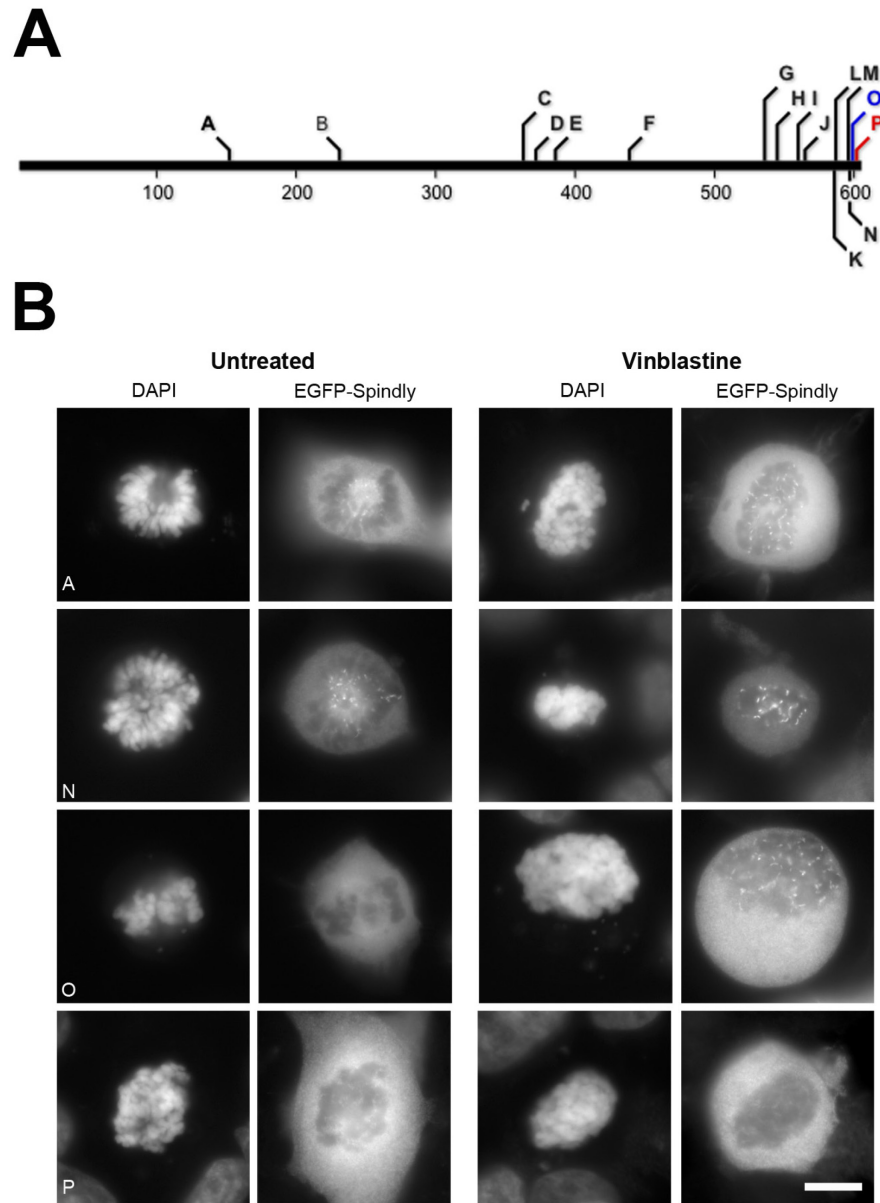


Figure 3.4: hSpindly far C-terminal residues are required for kinetochore localization.

(A) A schematic diagram depicting the location of the insertion mutants generated in the hSpindly protein. Construct shown in red was negative for kinetochore localization and construct shown in blue localized to kinetochores only under vinblastine treatment. Site of insertion and inserted residues are shown in Table 1.

(B) HeLa cells transiently transfected with EGFP-hSpindly insertion constructs were analyzed for their kinetochore localization ability. Representative images show that the far C-terminus is essential for kinetochore localization. For A, N, and P constructs, refer to the constructs depicted in Table 1. Scale bar, 10 μ m

Site-directed mutagenesis was performed to create both deletion and substitution hSpindly mutants to assess the importance of individual C-terminal residues for kinetochore localization (Figure 3.5). I found that all deletions involving the last 10 aa (596-605 aa) abrogated kinetochore localization (Figures 3.5 A & C), but all mutants with substitutions in the far C-terminal residues except cysteine (602 aa) localized to kinetochores (Figures 3.5B & C). Based on deletion and substitution mutants, we concluded that the far C-terminal residues from 596-605 aa were critical for kinetochore localization and the cysteine residue (602 aa) was essential for kinetochore localization. Our kinetochore domain mapping data indicate that the N-terminal 293 aa were dispensable for kinetochore targeting and residues 293-322 contributed to high affinity binding. Expression of all the deletion and substitution mutants is shown in Figure 3.3 and kinetochore localization in Figure 3.7.

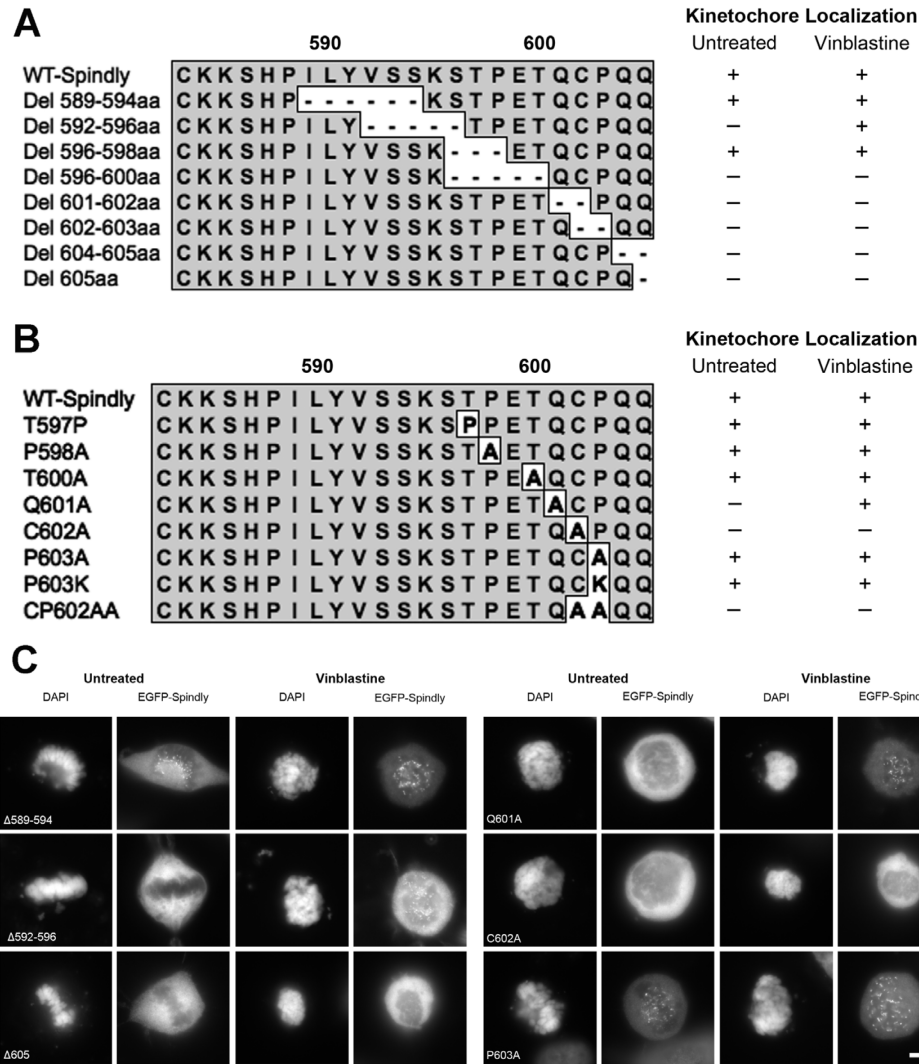


Figure 3.5: Far C-terminal residues of hSpindly are essential for kinetochores localization.

(A) Schematic representation of hSpindly C-terminal deletion mutants (589-605 aa). Kinetochores localization of each EGFP-tagged mutant was analyzed through fluorescence microscopy (+ indicates kinetochores localization and – indicates no kinetochores localization).

(B) Schematic representation of hSpindly C-terminal substitution mutants (597-605 aa). Kinetochores localization of each EGFP-tagged mutant was analyzed through fluorescence microscopy (+ indicates kinetochores localization and – indicates no kinetochores localization).

(C) Representative images of HeLa cells transfected with EGFP-tagged hSpindly deletion or substitution constructs show that the C-terminus of hSpindly is essential for its kinetochores localization. Scale bar, 10 μm

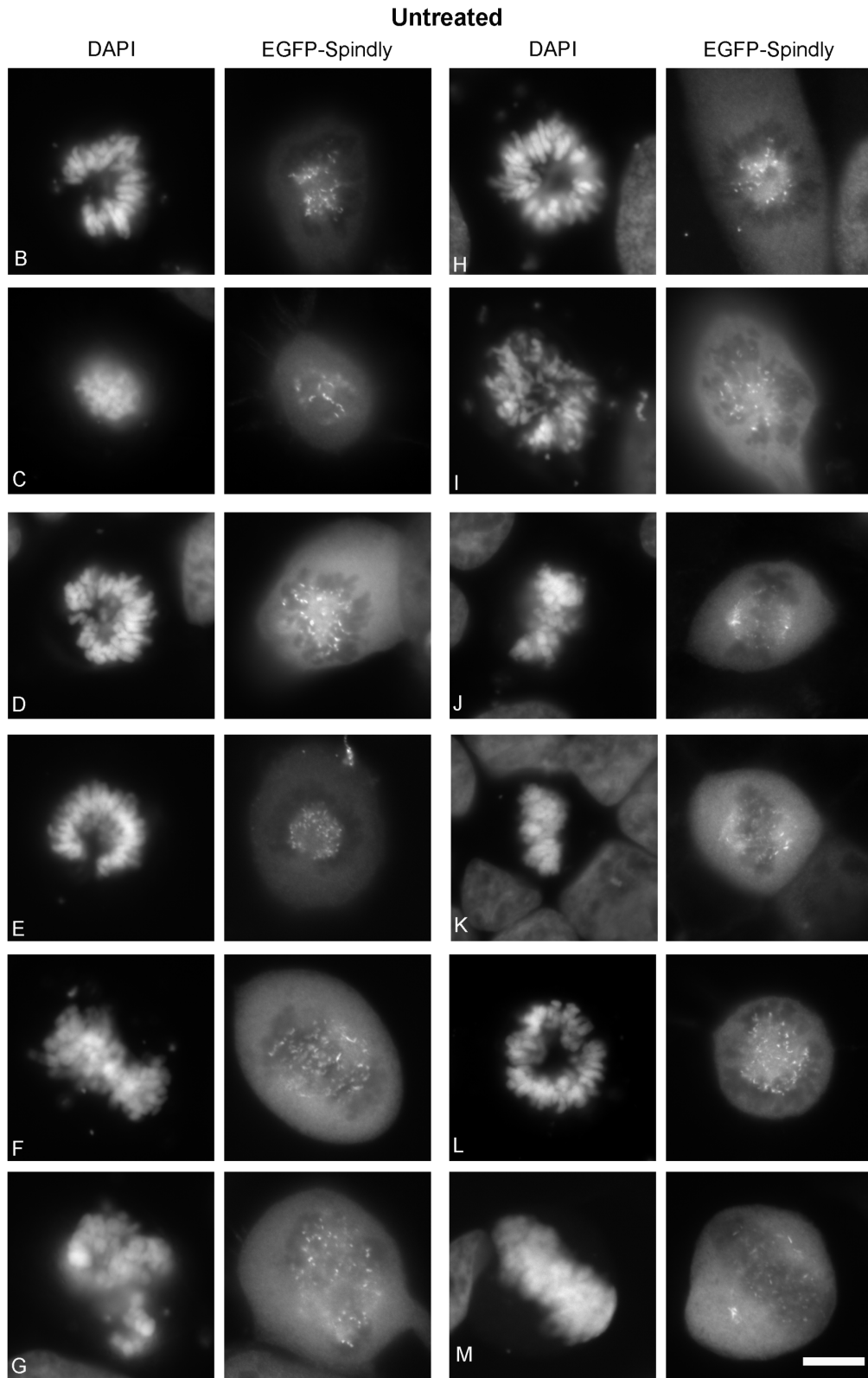


Figure 3.6: Kinetochores localization of GFP-hSpindly insertion mutants.

HeLa cells were transfected with GFP-hSpindly mutants, fixed, stained with DAPI to visualize the DNA and analyzed by fluorescence microscopy for kinetochores localizing ability. Localization results were identical with vinblastine treatment. Positive localization is seen as double-dot staining. Scale bar, 10 μ m.

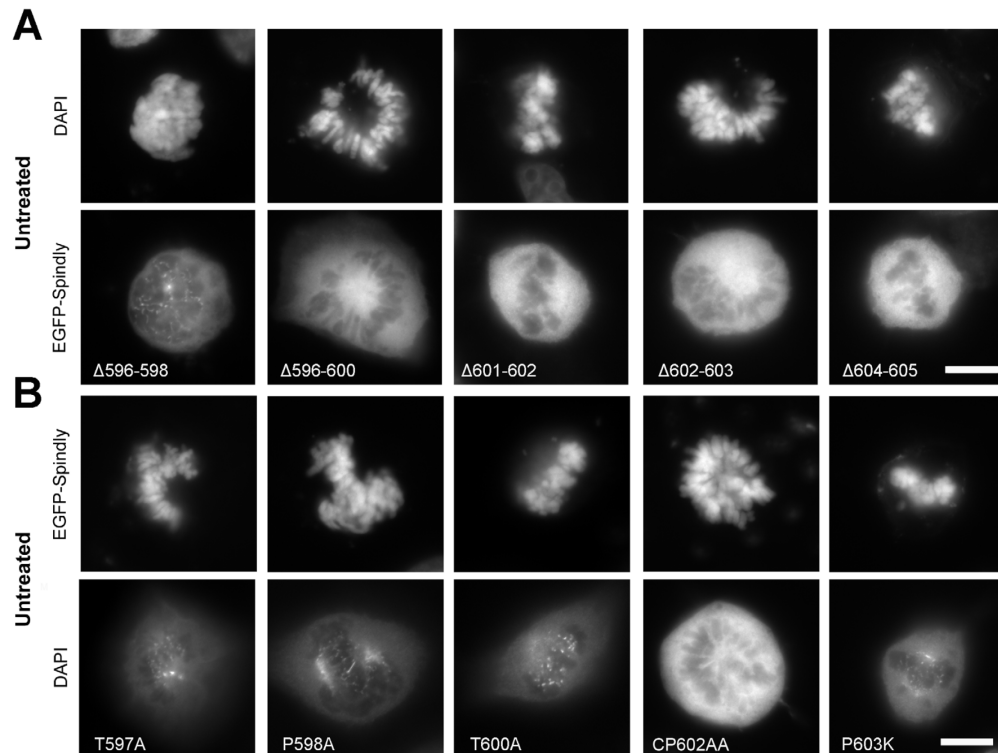


Figure 3.7: Kinetochores localization of EGFP-hSpindly deletion and substitution mutants.

HeLa cells were transfected with GFP-hSpindly mutants, fixed, stained with DAPI to visualize the DNA and analyzed by fluorescence microscopy for kinetochores localizing ability (A- Deletion mutants and B- Substitution mutants). Localization results were identical with vinblastine treatment (not shown). Positive localization is seen as double-dot staining. Scale bar, 10 μ m.

3.3.2 FTI treatment abrogated hSpindly kinetochore localization without affecting the RZZ complex, CENP-E and CENP-F kinetochore localization

The hSpindly C-terminus (CPQQ) is a potential farnesylation site and is highly conserved from zebrafish to humans (Figure 3.8). To investigate if farnesylation plays a role in targeting hSpindly to kinetochores, we examined the effect of a previously validated FTI, L-744-832 (Verstraeten et al., 2011) on kinetochore localization of hSpindly along with Zw10 and Rod since the RZZ complex is required for targeting hSpindly to kinetochores (Barisic et al., 2010; Chan et al., 2009). FTI treatment of HeLa cells led to a complete loss of hSpindly kinetochore localization although Zw10 and Rod localized to kinetochores indicating that farnesylation is normally involved in hSpindly kinetochore localization (Figure 3.9A & B). Vinblastine added to FTI treatment also lacked hSpindly kinetochore localization (Figure 3.9C), indicating that farnesylation is fundamental to hSpindly kinetochore localization and its absence is not a result of rapid dynein-mediated transport. To address the possibility that loss of hSpindly kinetochore localization is a compound-specific effect, we treated HeLa cells with another FTI (FTI-277) (Schafer-Hales et al., 2007) and observed identical results. We observed loss of hSpindly kinetochore localization with FTI treatment in breast cancer (MCF7 & T47D) and melanoma cell lines (M2 and MeWo) confirming that the loss of hSpindly kinetochore localization with FTI treatment is not cell line specific (Figure 3.10). hSpindly protein levels were examined to determine whether the loss of hSpindly kinetochore localization is due to its degradation in the absence of farnesylation. Immunoblots of FTI and DMSO-treated HeLa cell lysates showed an approximately 25% decrease in hSpindly protein level with FTI treatment (Figure 3.9D), which does not account for the complete loss of hSpindly kinetochore localization.

<i>H. Sapiens</i>	H	P	I	L	V	S	S	K	S	T	P	E	T	Q	C	P	Q	Q	
<i>E. caballus</i>	H	P	I	L	V	S	S	K	S	T	P	E	T	Q	C	P	Q	Q	
<i>C. familiaris</i>	H	P	I	L	V	S	S	K	S	T	P	E	T	Q	C	P	Q	Q	
<i>R. norvegicus</i>	H	T	I	M	V	S	S	K	S	T	P	E	M	Q	C	P	Q	Q	
<i>M. musculus</i>	H	N	I	I	V	S	S	K	S	A	P	E	T	Q	C	S	Q	Q	
<i>G. gallus</i>	Y	T	T	L	V	S	S	K	P	T	P	E	T	Q	C	A	Q	Q	
<i>X. tropicalis</i>	P	P	V	L	H	V	P	S	K	P	A	A	T	T	Q	C	P	Q	Q
<i>D. rario</i>	Q	Q	P	T	H	V	S	S	Q	K	T	M	A	N	E	C	A	Q	Q

Figure 3.8: Spindly C-terminal residues are highly conserved in different species.

The far C-terminal cysteine and the last two glutamine residues are conserved in all the organisms shown.

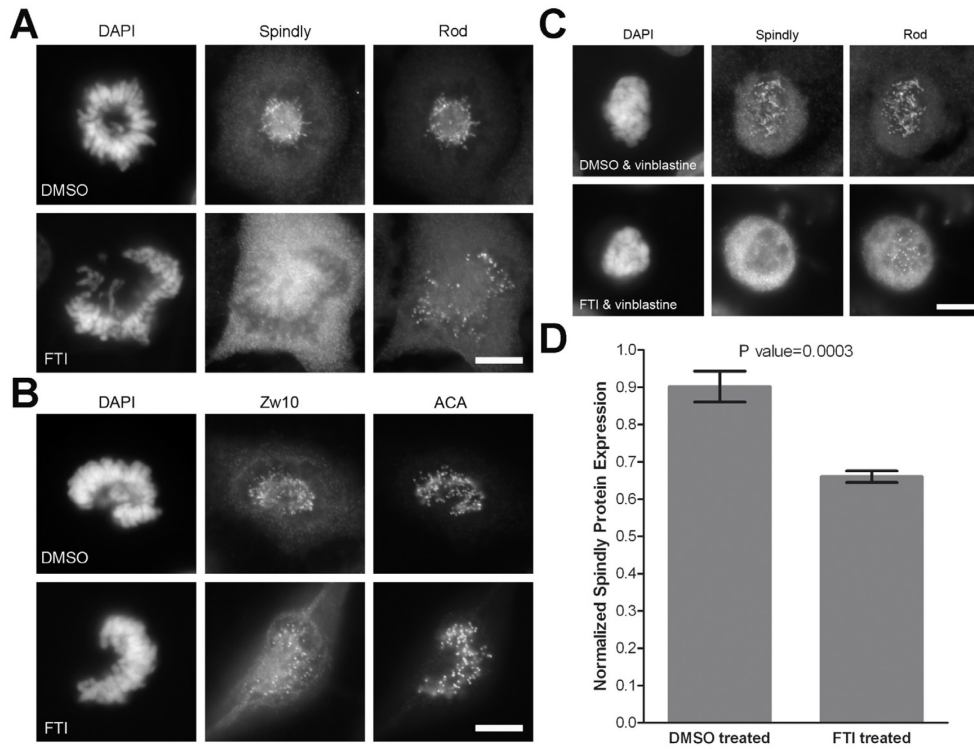


Figure 3.9: Inhibition of farnesylation abrogates kinetochore localization of hSpindly but not the RZZ complex.

(A&B) HeLa cells were treated with 10 μ M of L744832 FTI or DMSO for 24 h, fixed and immunostained for hSpindly, Rod and Zw10. Complete loss of hSpindly kinetochore localization and normal Rod and Zw10 levels on the kinetochores were observed in FTI-treated cells. ACA immunostains centromeres and DAPI stains DNA. Scale bar, 10 μ m.

(C) HeLa cells were treated with FTI or DMSO for 24 h and incubated with 0.5 μ M vinblastine for 30 min before harvesting showing no hSpindly kinetochore localization without affecting Rod kinetochore localization. Scale bar, 10 μ m.

(D) Normalized hSpindly protein expression from HeLa cells shows 25% less expression with FTI treatment as compared to DMSO. n=3. Error bars are SD. P-value indicated a significant difference.

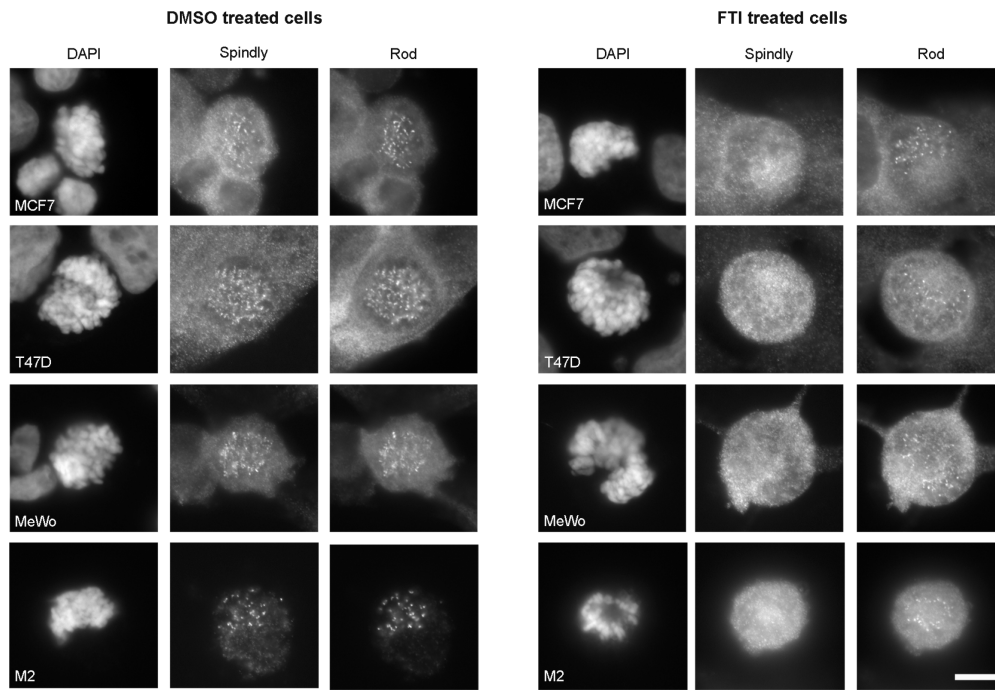


Figure 3.10: hSpindly kinetochore localization is abrogated with FTI treatment in breast cancer and melanoma cell lines without affecting Rod kinetochore localization.

Breast cancer (MCF7 & T47D) and melanoma (MeWo and M2) cell lines were treated with FTI and DMSO for 24 h prior to fixation. The cells were immunostained with anti-hSpindly antibody, anti-hRod antibody and DAPI to stain DNA.

Previous studies have reported conflicting findings regarding whether loss of farnesylation prevents CENP-E and CENP-F kinetochore localization (Ashar et al., 2000; Crespo et al., 2002; Crespo et al., 2001; Hussein and Taylor, 2002; Schafer-Hales et al., 2007; Verstraeten et al., 2011). We observed no effect on CENP-E and CENP-F kinetochore localization in HeLa cells with FTI treatment in prometaphase (Figures 3.11A & B) or metaphase. Quantitative immunofluorescence microscopy of prometaphase HeLa cells showed no significant difference in CENP-E and CENP-F kinetochore localization with FTI treatment compared to DMSO (Figures 3.11C & D). A cysteine-alanine mutant of CENP-F (C3207A of CAAX motif) was reported to be unable to localize to kinetochores (Hussein and Taylor, 2002). We cloned the C-terminal 630 aa kinetochore localizing fragment of CENP-F (2581-3210 aa), and found it localized to kinetochores as expected (Figure 3.12) (Hussein and Taylor, 2002; Zhu et al., 1995), and generated the CENP-F C3207A mutant. In contrast to the Hussein *et al.* 2002 study, the CENP-F C3207A mutant localized to kinetochores during mitosis (Figure 3.12) but was reproducibly reduced in vinblastine treated cells for unknown reasons. These results indicate that FTI mediated mitotic effects cannot be attributed to the loss of CENP-E or CENP-F kinetochore localization. Expression of CENP-F (2581-3210 aa) and CENP-F C3207A mutant is shown in Figure 3.14B.

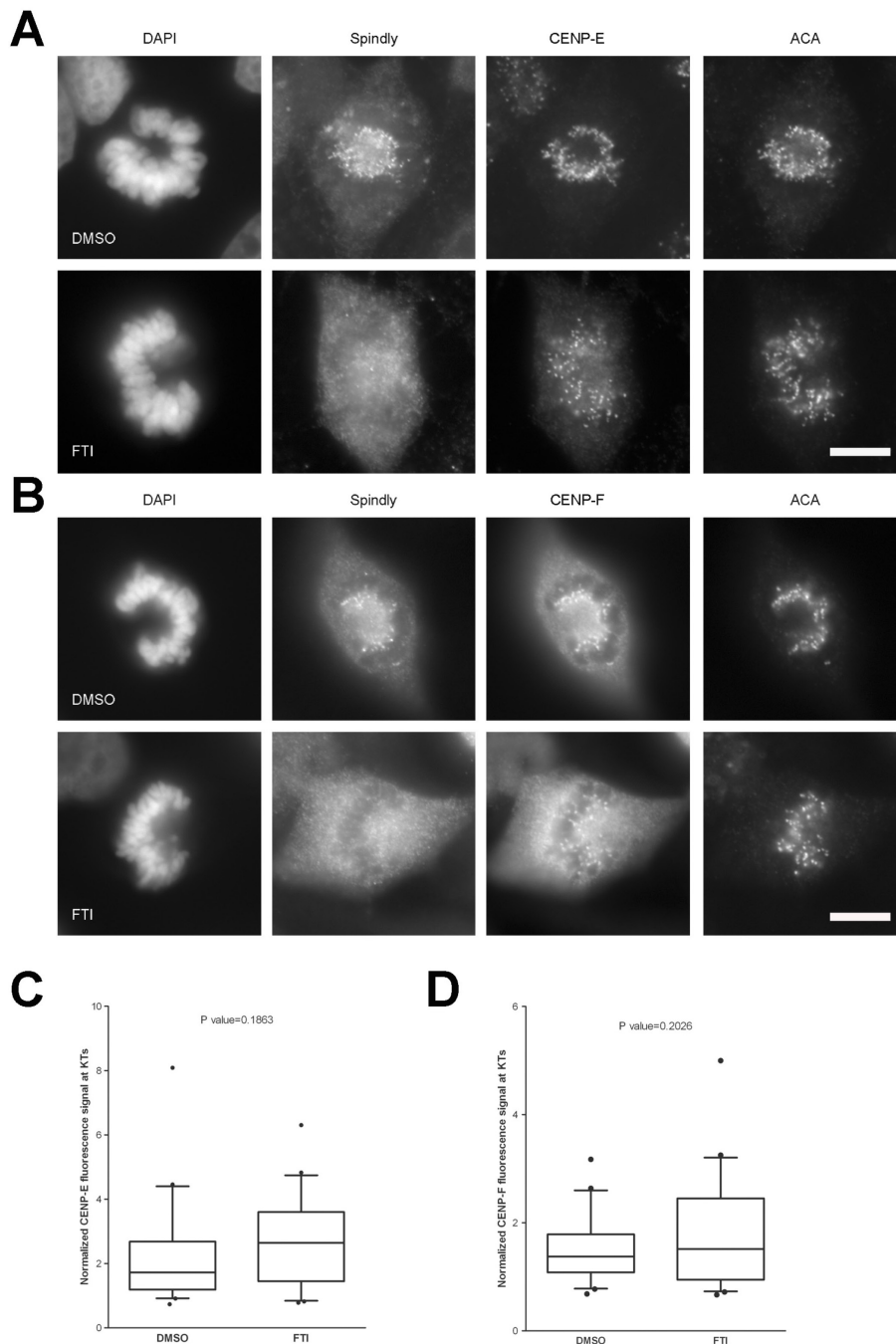




Figure 3.11: Inhibition of farnesylation does not affect CENP-E and CENP-F kinetochore localization.

(A&B) HeLa cells were treated with 10 μ M of L744832 FTI or DMSO for 24 h fixed and immunostained for hSpindly, CENP-E or CENP-F, and ACA. CENP-E and CENP-F localized to kinetochores in FTI-treated HeLa cells whereas hSpindly did not. Scale bar, 10 μ m.

(C&D) Normalized fluorescence signals for CENP-E and CENP-F at kinetochores with 24h DMSO or FTI treatment. n=20. Boxes represent interquartile distributions and whiskers represent 10th and 90th percentiles. FTI-treated cells have slight but not significant increases in CENP-E or CENP-F signal as compared to control DMSO as indicated by P value.

A

		Kinetochores localization of CENP-F	
		Untreated	Vinblastine
2581	3207		
	CPVQ ³²¹⁰	+	+
	APVQ	+	+

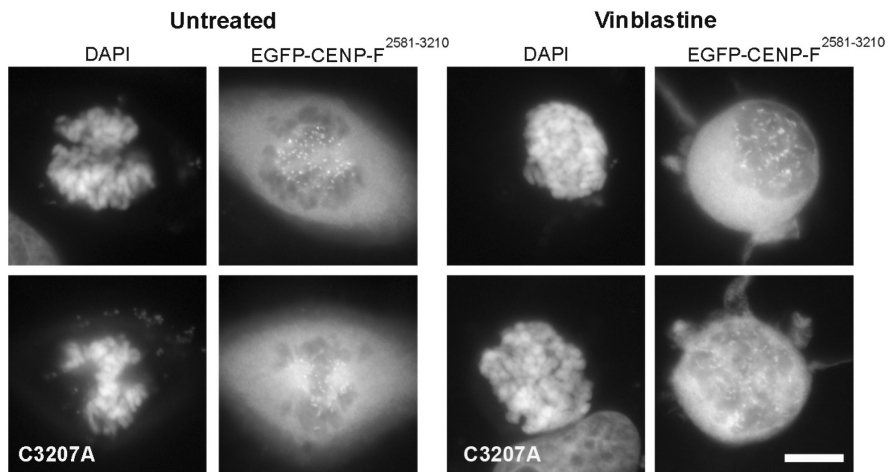
B

Figure 3.12: Farnesylation motif of CENP-F is not required for kinetochore localization.

HeLa cells were transiently transfected with EGFP-hCENP-F fusion constructs (shown in Figure 3E) and the kinetochore localization ability of each construct was analyzed using fluorescence microscopy. Top panel is EGFP-CENP-F²⁵⁸¹⁻³²¹⁰ and lower panel is C3207A mutant of the same fragment. Scale bar, 10 μ m.

3.3.3 hSpindly CPQQ motif can be substituted with other farnesylation motifs

Since the C-terminus of hSpindly is required for kinetochore localization through the CAAX farnesylation motif, we hypothesized that any farnesylation motif on the C-terminus of hSpindly, regardless of the specific sequence should be sufficient for it to undergo farnesylation and target it to kinetochores. We replaced the CPQQ residues of hSpindly with the CKTQ (CENP-E) and CKVQ (CENP-F) farnesylation motifs, referred to as Spindly-E and Spindly-F, respectively. Both Spindly-E and F localized to kinetochores during prometaphase supporting our hypothesis that the exact aa sequence is not important and the ability to be farnesylated is sufficient for hSpindly kinetochore localization (Figure 3.13). Expression of Spindly-E and F is shown in Figure 3.14A.

Geranylgeranylation is a prenylation catalyzed by geranylgeranyl transferase enzymes that attach a 20-carbon geranylgeranyl group to the cysteine of the C-terminal CAAX box (Sinensky, 2000). The nature of the X residue in the CAAX motif determines whether a protein gets farnesylated or geranylgeranylated. Geranylgeranyl transferase enzymes prefer X to be leucine or isoleucine (Zhang and Casey, 1996); however, these rules are not absolute since proteins with phenylalanine at the X position can undergo farnesylation or geranylgeranylation (Carboni et al., 1995). A number of studies have demonstrated that when farnesylation is inhibited, KRAS4B and NRAS become geranylgeranylated and are targeted to the membrane thus retaining their function (Lerner et al., 1997; Rowell et al., 1997; Whyte et al., 1997). Since FTIs inhibit hSpindly kinetochore localization, we predict it cannot inherently be geranylgeranylated to retain its function in the presence of FTIs. We investigated whether a geranylgeranylation motif on the hSpindly C-terminus can target it to kinetochores, assuming it undergoes geranylgeranylation, by replacing the last glutamine of hSpindly with leucine or phenylalanine (referred to as Spindly-GG1 and Spindly-GG2), converting it from a farnesylation substrate to a geranylgeranylation substrate (Figure 3.13). These constructs did not localize to

kinetochores during mitosis in HeLa cells (Figure 3.13) demonstrating that a geranylgeranylation motif on hSpindly cannot functionally substitute for the farnesylation motif making hSpindly a potential clinical target for FTIs unlike RAS proteins. Expression of Spindly-GG1 and Spindly-GG2 is shown in Figure 3.14A.

A

			Kinetochores localization	
	1	601	Untreated	Vinblastine
WT	CPQQ ⁶⁰⁵		+	+
Spindly-E	CPTQ		+	+
Spindly-F	CPVQ		+	+
Spindly-GG1	CPQL		-	-
Spindly-GG2	CPQF		-	-

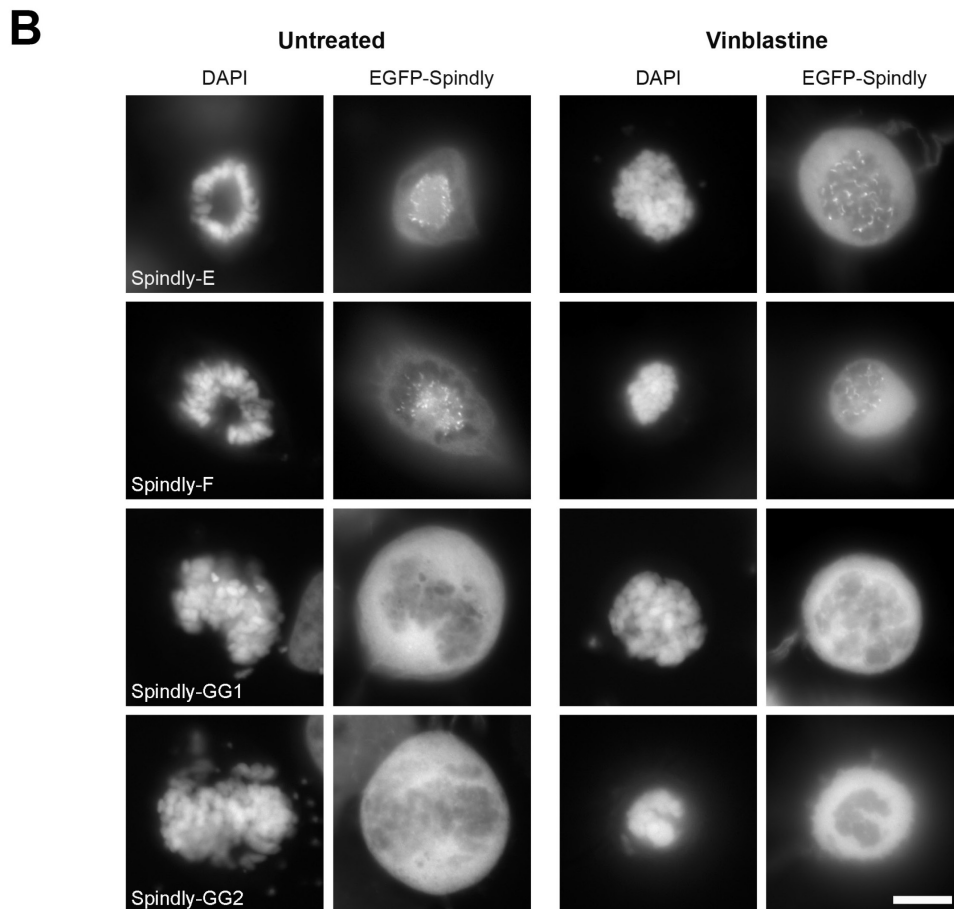


Figure 3.13: hSpindly farnesylation motif can be substituted with CENP-E or CENP-F farnesylation motif but not a geranylgeranylation motif.

(A) A schematic diagram of hSpindly depicting substitution of its farnesylation motif with CENP-E and CENP-F, referred to as Spindly-E and Spindly-F, respectively. The last aa of Spindly is changed such that it is a geranylgeranylation motif instead of farnesylation motif referred to as Spindly-GG1 and Spindly-GG2. The kinetochores localization of each construct is shown (+ indicates kinetochores localization and - indicates non-kinetochores)

localization). aa numbers are indicated.

(B) HeLa cells were transiently transfected with EGFP-hSpindly fusion constructs (shown in Figure 4A) and kinetochore localization ability of each construct was analyzed using fluorescence microscopy. Representative images show that the farnesylation motif of Spindly can be replaced with the farnesylation motif of known farnesylated proteins, CENP-E and CENP-F, but a geranylgeranylation motif cannot target hSpindly to kinetochores. Scale bar, 10 μ m.

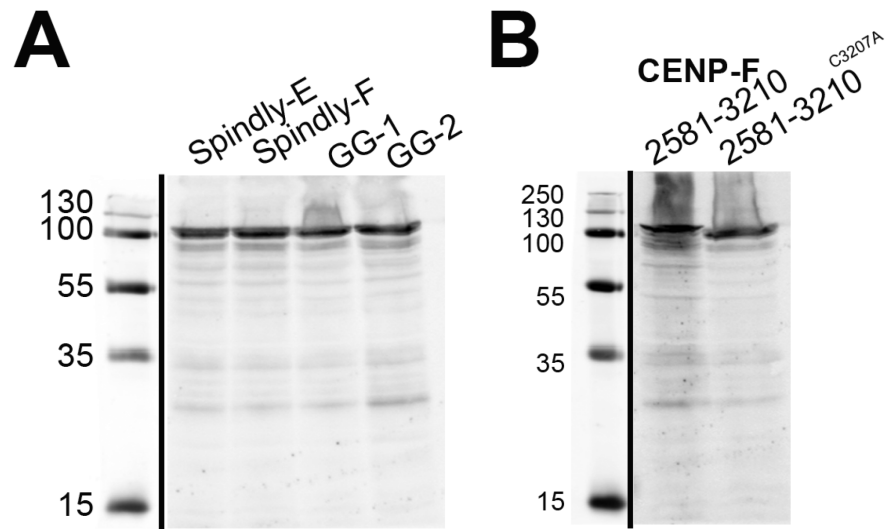


Figure 3.14: Expression of hSpindly mutants and hCENP-F mutant using western blot analysis.

Immunoblots showing the expression of GFP-hSpindly and GFP-hCENP-F fusion proteins transfected into HEK293 cells. GFP-fusion proteins were labeled with IR800-conjugated rabbit anti-GFP antibody. Molecular mass markers detected in the same channel are shown on each blot. (Masses indicated in kD). WT- wild type. All hSpindly and CENP-F mutant constructs migrated at the expected size.

3.3.4 hSpindly is farnesylated on its C-terminal cysteine residue and farnesylation is essential for its interaction with the RZZ complex

To investigate if hSpindly undergoes farnesylation *in vivo*, pEGFP-WT Spindly, pEGFP-C602A hSpindly (of the CAAX motif), pEGFP-Spindly-E and pEGFP-Spindly-F transfected HeLa cells were labeled with alkynyl-farnesol (Alk-FOH), a farnesyl group analogue (Charron et al., 2011), in the presence or absence of FTIs. Farnesylated proteins were detected by performing bioorthogonal ligation (click chemistry) with a fluorescent tag followed by fluorescence signal detection on a western blot. WT-Spindly is farnesylated as indicated by the presence of a fluorescent band (Figure 3.15, lane 5) and farnesylation is inhibited in the presence of FTIs (Figure 3.15, lanes 3 & 4). Furthermore, Spindly-E and Spindly-F undergo farnesylation as expected since these constructs localize to kinetochores (Figure 3.15, lanes 1 & 2). The hSpindly C602A mutant cannot localize to kinetochores and did not undergo farnesylation (lane 6). These results provide an *in vivo* validation of hSpindly farnesylation.

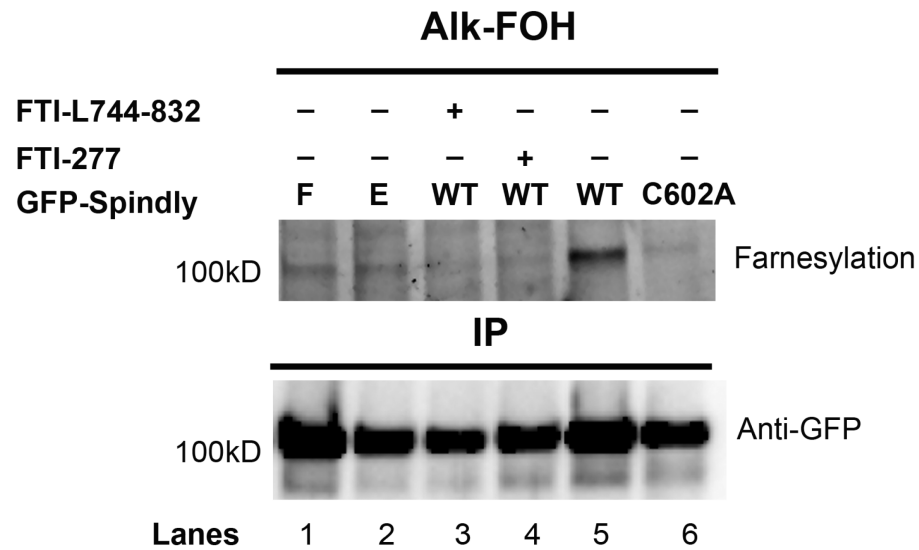


Figure 3.15: hSpindly is farnesylated *in vivo*.

HeLa cells transiently expressing wild type GFP-WT hSpindly, GFP C602A hSpindly (of CAAX motif), GFP-hSpindly-E and GFP-hSpindly-F were metabolically labeled with alkynyl-farnesol (prenylation reporter) and HeLa cells expressing wild-type GFP-Spindly were either treated with FTI or DMSO. Fluorescence detection of farnesylated immunoprecipitated GFP-tagged hSpindly protein as shown on western blot (top panels). The loading control is shown in the lower panel. WT-Spindly, Spindly-E and Spindly-F exhibit bands indicating farnesylation. Farnesylation of WT-Spindly is inhibited in the presence of FTIs (lanes 3 & 4). As expected, C602A mutant of hSpindly is not farnesylated *in vivo* (lane 6).

We have shown that the RZZ complex does not recruit hSpindly to kinetochores when farnesylation is inhibited (Figure 3.9). hSpindly interacts with the RZZ complex and this interaction is sensitive to the presence of detergent in the lysis buffer (Barisic et al., 2010; Chan et al., 2009) suggesting that farnesylation may regulate hSpindly/RZZ complex interaction. To investigate this, we performed co-immunoprecipitation (co-IP) experiments using HeLa cells treated with either DMSO or FTI for 24 h. Mitotic populations were enriched by double thymidine block and nocodazole treatment. We found that hSpindly associated with Zw10 and Rod (RZZ complex subunits) in DMSO-treated cells as shown previously (Figure 3.16) (Barisic et al., 2010; Chan et al., 2009). This interaction, however, is lost in FTI-treated cells indicating that farnesylation of hSpindly is required for its interaction with the RZZ complex (Figure 3.16).

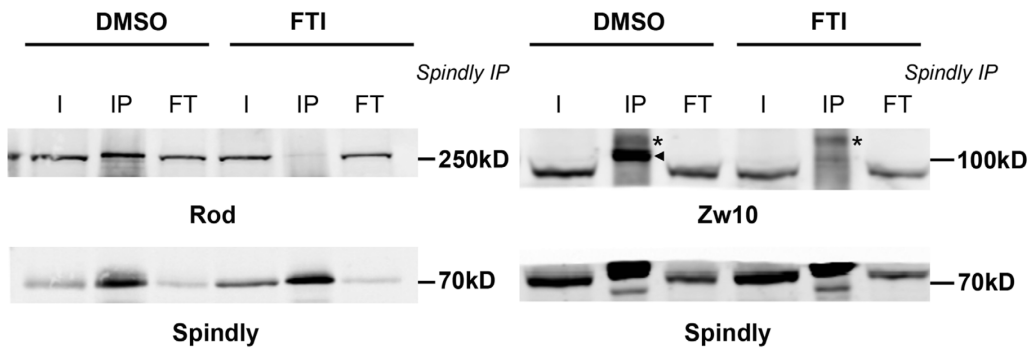


Figure 3.16: Inhibition of farnesylation abrogates hSpindly interaction with the RZZ complex.

IP of hSpindly (70 kD) from mitotic HeLa cell lysates followed by SDS-PAGE and western blot against Zw10 (89 kD) or Rod (250 kD) RZZ complex subunits. I, input; IP, immunoprecipitated; FT, flowthrough. HeLa cells were treated with either DMSO or 10 μ M of FTI-L744832 for 24 h before harvesting and arrested in mitosis with nocodazole treatment. Zw10 and hSpindly are indicated by arrowheads (higher in the IP lanes) and * denotes non-specific band. Inhibition of farnesylation leads to loss of hSpindly and RZZ complex interaction.

Since the C602A hSpindly mutant is not farnesylated *in vivo*, we transfected siRNA resistant GFP-C602A hSpindly or GFP-WT hSpindly into HeLa cells knocked down for endogenous hSpindly (Figure 3.17), immunoprecipitated mitotic cell lysates using GFP Trap and analyzed for Rod and Zw10 pull down. The C602A hSpindly mutant showed complete loss of the RZZ complex pull-down demonstrating that loss of hSpindly farnesylation abrogated the interaction between hSpindly and the RZZ complex subunits (Figure 3.18). This supports the idea that the presence of a farnesyl group on hSpindly is required for its interaction with the RZZ complex and its subsequent recruitment to kinetochores.

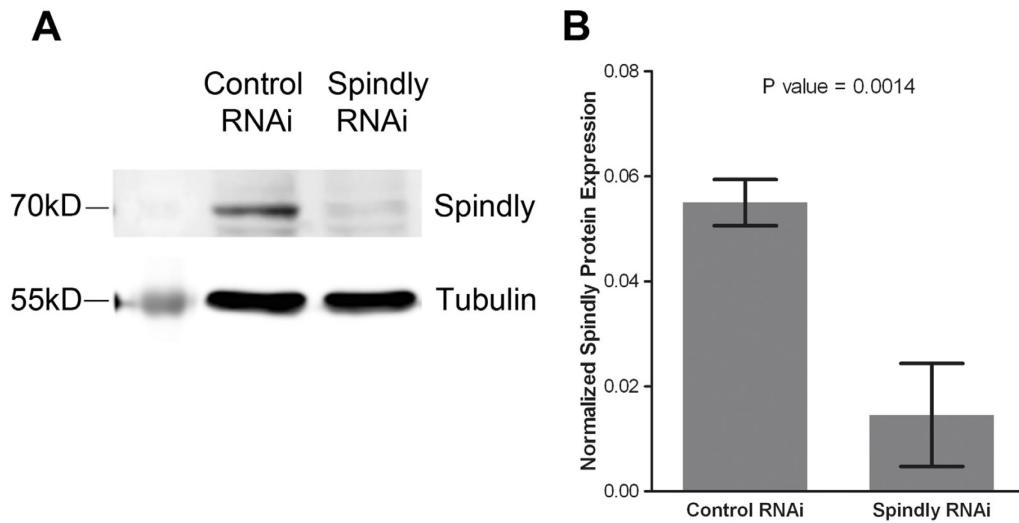


Figure 3.17: Knockdown of hSpindly protein in HeLa cells using siRNA.
(A) Immunoblots of HeLa cells transfected with either control (scrambled) siRNA or hSpindly siRNA for 24 h and harvested after 48 h of transfection. Tubulin is used as a loading control.
(B) Quantitative analysis of hSpindly knockdown shows 73.5% knockdown of hSpindly protein. Bar graphs show the results of three independent experiments and error bars indicate standard deviation from means.

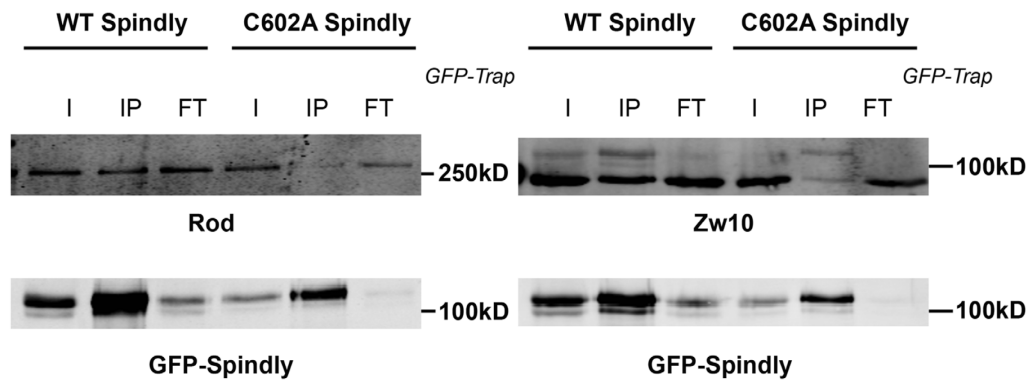


Figure 3.18: Inhibition of hSpindly farnesylation abrogates its interaction with the RZZ complex.

GFP-Trap from mitotic HeLa cells with endogenous hSpindly knockdown and expressing siRNA resistant (siRNA r) GFP-WT hSpindly (98.5 kD) or GFP C602A hSpindly mutant (98.5 kD). GFP-Trap followed by western blot against Zw10 (89 kD) or Rod (250 kD) subunits of the RZZ complex. I, input; IP, immunoprecipitated; FT, flowthrough. Cells were incubated in nocodazole to accumulate in mitosis before harvesting. The cysteine to alanine mutant of GFP-hSpindly (C602A) leads to loss of hSpindly and the RZZ complex interaction.

3.3.5 hSpindly depletion and FTI treatment have similar mitotic phenotype

FTI-treated cells are known to accumulate at the G2-M boundary (Ashar et al., 2000; Crespo et al., 2002; Crespo et al., 2001). We observed prometaphase accumulation, mostly in the rosette arrangement with FTI treatment as compared to control DMSO-treated cells (Figure 3.19A) (Crespo et al., 2001). The percentage of metaphase cells is also significantly reduced indicating that farnesylation is a critical step for transition from prometaphase to metaphase (Figure 3.19B). The cells in metaphase did not show significant lagging chromosomes at the spindle poles, which is a characteristic phenotype of CENP-E knockdown. To examine the mitotic phenotype of FTI treatment and hSpindly depletion in real time, we performed time-lapse imaging experiments using HeLa cells stably expressing GFP-tubulin and mCherry-histone H2B. FTI-treated and hSpindly-depleted cells spent an increased time in mitosis from nuclear envelope breakdown to anaphase onset (mean of 116 and 180 min for FTI treatment and hSpindly siRNA respectively versus a mean of 57 and 55 min for DMSO treatment and scrambled siRNA respectively) (Figure 3.20A & B; Videos 1–4). hSpindly-depleted and FTI-treated cells exhibited prometaphase delay, as a result of prolonged chromosome alignment, and delayed anaphase onset following metaphase with both delays being more pronounced in hSpindly-depleted cells (Figures 3.21A, B & C). A fraction of cells with mitotic arrest due to FTI or hSpindly depletion was observed to undergo cell death or chromatin decondensation. hSpindly-depleted cells spent 2 times longer transitioning from metaphase to anaphase as compared to FTI-treated cells (Figure 3.21). There are two possible explanations for the difference. Firstly, in hSpindly-depleted cells, there is a lack of both hSpindly protein presence and its kinetochore localization. The fact that hSpindly is present but not localized to kinetochores upon FTI treatment suggests farnesylation is not required for checkpoint silencing. Secondly, FTIs have a multitude of targets and we cannot rule out the possibility that some other target is compensating for the prolonged prometaphase and anaphase onset (Sebti, 2005; Sebti and Der, 2003). FTI treatment and hSpindly

knockdown have the same phenotype but differ in severity suggesting that the mitotic effects of FTIs are caused by a lack of hSpindly kinetochore localization.

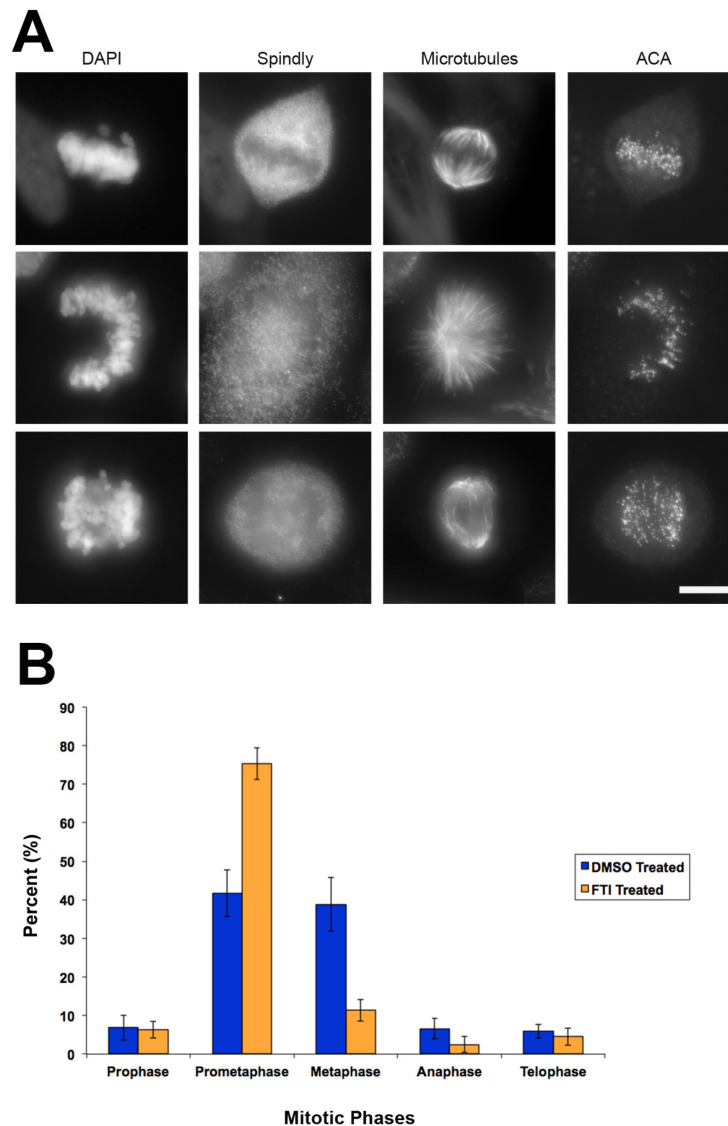


Figure 3.19: FTI treatment leads to mitotic accumulation in HeLa cells.

(A) Representative phenotype of FTI-treated HeLa cells showing prometaphase and metaphase phenotypes. FTI treatment in HeLa cells leads to prometaphase accumulation and very few metaphase cells. HeLa cells treated with FTI for 24 h were immunostained with anti-hSpindly, anti-tubulin and ACA antibodies and stained with DAPI to visualize DNA. Scale bar, 10 μ m.

(B) Accumulation in prometaphase during mitosis was observed in FTI-treated cells as compared to DMSO-treated control. HeLa cells were treated with either 10 μ M of FTI-L744832 or DMSO for 24 h, fixed, and immunostained for hSpindly and tubulin. DNA is visualized by DAPI staining. 100 cells were counted in separate experiments for DMSO (n=8) and FTI-treated cells (n=7). Error bars are SD.

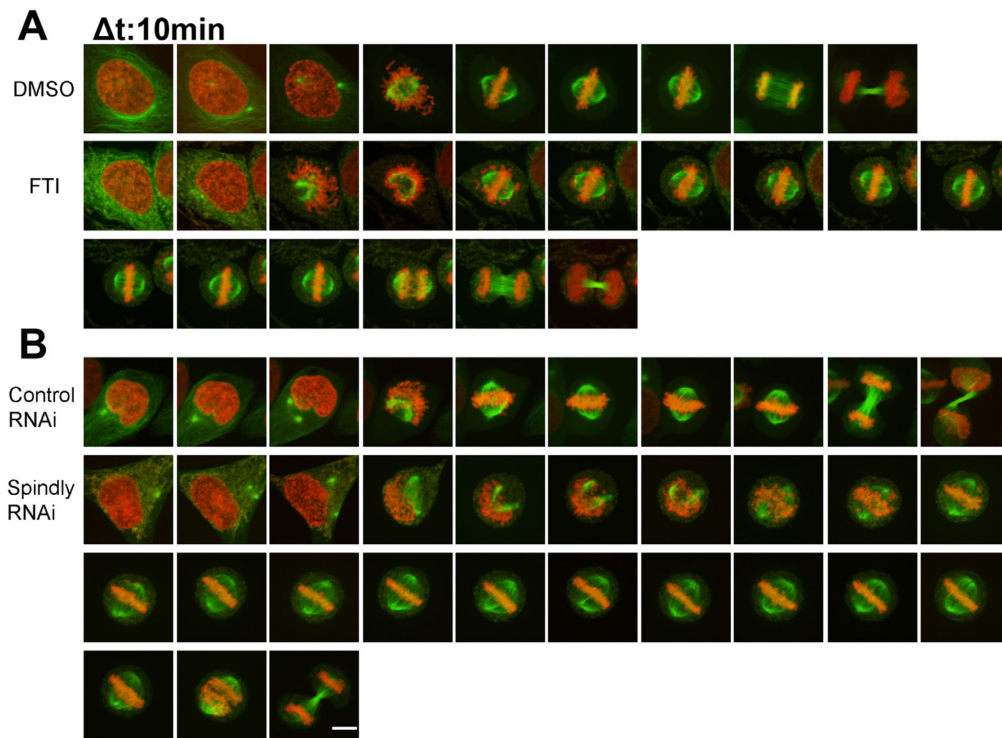


Figure 3.20: Phenocopying of farnesylation inhibition with hSpindly knockdown by siRNA.

(A) Representative stills from videos of GFP-tubulin & mCherry H2B expressing HeLa cells treated with either DMSO or 10 μM of FTI-L744832 for 24 h before filming. Time is shown in 10 min intervals. Scale bar as shown in 3.20B.

(B) Representative stills from videos of GFP-tubulin & mCherry H2B expressing HeLa cells treated with either control (scrambled) siRNA or hSpindly siRNA for 33 h before filming. Time is shown in 10 min intervals. Scale bar, 10 μm

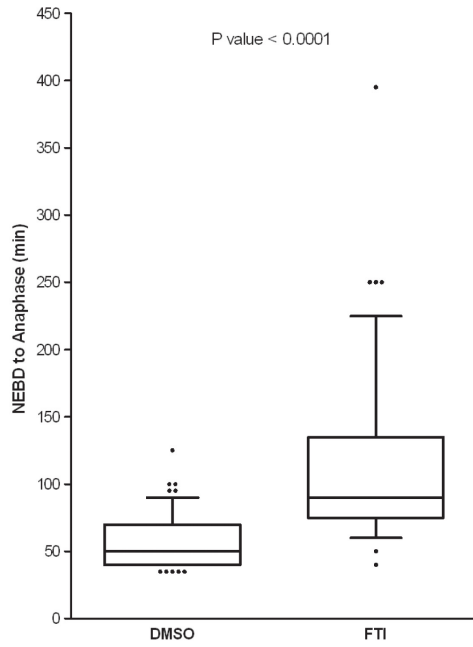
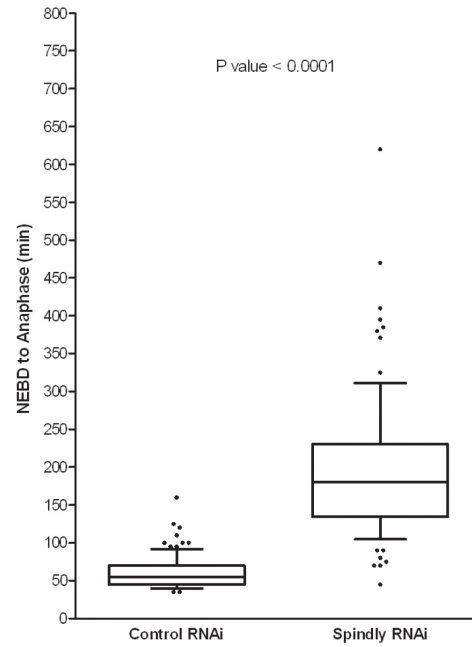
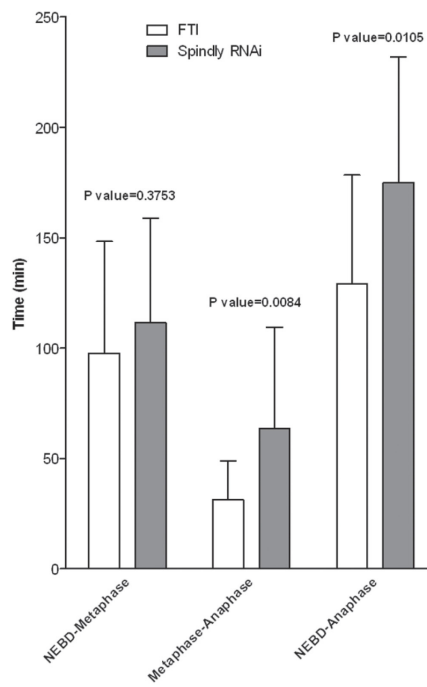
A**B****C**

Figure 3.21: Comparison of mitotic duration of FTI-treated and Spindly knockdown cells show enhanced prometaphase-metaphase delay in Spindly knockdown cells.

(A) Box plots comparing the duration of nuclear envelope breakdown (NEBD) to anaphase between FTI- and DMSO-treated cells show significant mitotic delay in FTI-treated cells. 7 experiments, >60 cells in total were analyzed for each treatment. Boxes represent interquartile distributions and whiskers represent 10th and 90th percentiles.

(B) Box plots comparing the duration of nuclear envelope breakdown (NEBD) to anaphase between control (scrambled) siRNA and hSpindly siRNA treated cells show significant mitotic delay in hSpindly siRNA treated cells. 8 experiments, >80 cells in total were analyzed for each treatment. Boxes represent interquartile distributions and whiskers represent 10th and 90th percentiles.

(C) Duration of NEBD to metaphase, metaphase to anaphase and NEBD-anaphase in FTI and hSpindly siRNA treated HeLa cells shows all are increased in Spindly knockdown cells with metaphase to anaphase time difference being significant. n=18 for FTI and n=22 for hSpindly siRNA. Error bars are SD.

3.4 Discussion

In our current structure function study, we mapped the kinetochore localization domain of hSpindly to its C-terminal 294-605 aa (Figure 3.22). Furthermore, our data showed that hSpindly undergoes farnesylation, which is essential for hSpindly kinetochore localization. Substitution of the farnesylation motif with a geranylgeranylation motif does not support hSpindly kinetochore localization. We found that FTI treatment does not interfere with kinetochore localization of the RZZ complex, CENP-E or CENP-F. Additionally, farnesylation plays a pivotal role in the interaction of hSpindly with the RZZ complex providing insight into lipid modification regulating checkpoint protein assembly. Our results showed that FTI treatment and hSpindly knockdown share the same phenotypes, prolonged prometaphase and metaphase with chromosome alignment defects, differing only in severity. Our analysis indicates that hSpindly is likely a key farnesylation target leading to FTI induced mitotic defects.

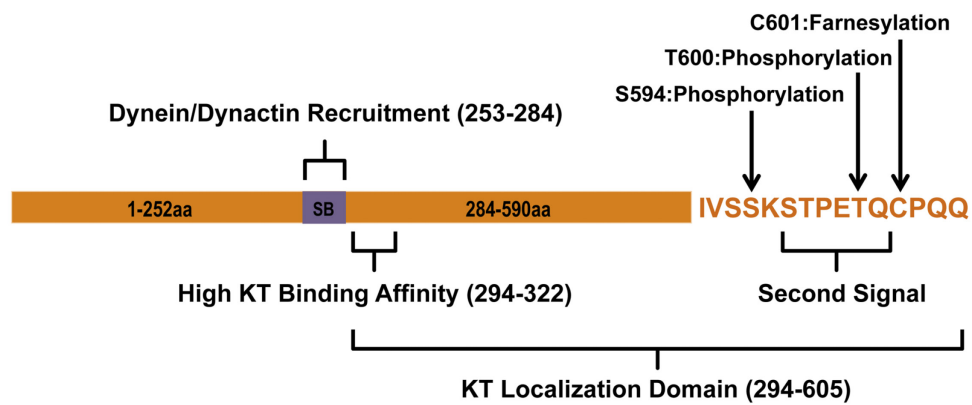


Figure 3.22: A schematic representation of hSpindly domains.

A schematic representation of hSpindly kinetochore localization domain, dynein/dynactin recruitment domain and post-translational modifications. SB;Spindly box.

Kinetochores localization analysis of an extensive hSpindly mutant library consisting of truncation, insertion, deletion, and substitution constructs showed that both the coiled-coil domain II and the C-terminus of hSpindly are required for kinetochores localization (Figure 3.2, Figure 3.4, Figure 3.5). Although Barisic *et al.* (2010) has previously shown that the 293-605 aa fragment of hSpindly did not localize to kinetochores, we found that this specific fragment (N3 construct) does not impair kinetochores localization of hSpindly (Figure 3.2). This discrepancy could be the result of overexpression, differences in fusion tags, or the sensitivity of the two assays. Overexpression of coiled-coil proteins often results in aggregation, which can lead to mislocalization of the protein resulting in a false negative. Immunostaining with anti-FLAG antibody to analyze kinetochores localization by Barisic *et al.* compared to GFP-fusion constructs may influence the detection sensitivity and our assay is maximized for sensitivity with vinblastine treatment. Barisic *et al.* (2010) concluded that both coiled-coil domain II and the Spindly box (253-284 aa) contribute to kinetochores localization. In our study, construct N3 (294-605 aa) lacking the Spindly box localized to kinetochores and we conclude that the Spindly box does not contribute to kinetochores localization. The Spindly box, however, was previously shown to be critical for dynein recruitment (Barisic *et al.*, 2010; Gassmann *et al.*, 2010) suggesting that the hSpindly kinetochores localization domain (294-605 aa) is different from its dynein recruitment domain (Figure 3.22). Additionally, we found that the N4 construct (322-605 aa) localized to kinetochores only when cells were treated with vinblastine suggesting the region between 293-322 aa is important for kinetochores binding affinity (Figure 3.2 & Figure 3.22). Deletion of residues in this region might facilitate premature interaction of hSpindly N4 construct with the dynein/dynactin complex, which transports it off kinetochores to the spindle poles. When kinetochores-microtubule attachment is disrupted by vinblastine, dynein-mediated transport is abolished and the N4 construct is retained on kinetochores. Thus 294-322 aa of hSpindly is required for high affinity binding to kinetochores although the precise mechanism warrants further

investigation. Insertion and site-directed hSpindly mutants revealed that deletions in residues 596-605, or substitution of the C-terminal cysteine were not tolerated indicating 596-605 aa are important and the C-terminal cysteine is essential for hSpindly kinetochore localization (Figure 3.4 & Figure 3.5). These results are in agreement with Barisic *et al.* (2010) where deletion mutant 604-605 aa (Δ QQ) and substitution mutant C602S both did not localize to kinetochores. It also revealed that C-terminus residues constitute a potential CAAX farnesylation motif.

The role of farnesylation in targeting proteins to the membrane is well known. It was first realized with the discovery of CENP-E and CENP-F farnesylation, that lipid modifications regulate mitotic protein functions. The hSpindly CPQQ farnesylation motif is conserved in vertebrates but not in *Drosophila* and *C. elegans* (Figure 3.8). Inhibition of farnesylation led to complete loss of hSpindly kinetochore localization but had no effect on kinetochore localization of the RZZ complex (Figure 3.9). The 25% decrease in hSpindly protein expression upon FTI treatment is not responsible for the absence of hSpindly kinetochore localization and suggests that hSpindly may be slightly more susceptible to degradation in the absence of farnesylation. hSpindly was shown to be degraded when it is not localized to kinetochores, however, interaction between hSpindly and the RZZ complex and not kinetochore localization stabilizes the hSpindly protein (Chan *et al.*, 2009). Our *in vivo* labeling experiment results confirmed that hSpindly is farnesylated on the cysteine of its CAAX motif and farnesylation is abolished in the C602A mutant of hSpindly (Figure 3.15). These results show that farnesylation is required for hSpindly kinetochore localization.

The presence of the RZZ complex on kinetochores when farnesylation is inhibited indicates that it is unable to recruit hSpindly. Farnesylation has been reported to regulate protein-protein interactions, two key examples being RAS and Lamin B (Bhattacharya *et al.*, 1995; Kisselev *et al.*, 1995; Kitten and Nigg, 1991; Kuroda *et al.*, 1993; Mical and Monteiro, 1998; Porfiri *et al.*, 1994; Rubio

et al., 1999). Farnesylated RAS interacts with and activates Raf-1 kinase, however if RAS is not farnesylated, it can still interact with Raf-1, but Raf-1 is poorly activated (Booden et al., 2000; Luo et al., 1997). Lamin B localizes to the nuclear membrane and is postulated to bind the lamin B receptor on the membrane. Lamin B cofractionation with lamin B receptor was abolished in cells with lamin B lacking a CAAX farnesylation motif (Mical and Monteiro, 1998). It remains unclear if the farnesyl group binds directly with the interacting protein or if the presence of the farnesyl group induces a conformational change and creates a binding site for its interacting protein. Rubio *et al.* proposed that farnesylation induces a conformational change in RAS creating a binding site for the G-protein responsive phosphoinositide 3-kinase p110 γ . Our co-IP and GFP Trap results showed hSpindly farnesylation is a prerequisite for its interaction with the RZZ complex (Figure 3.16 & Figure 3.18). Farnesylation remodels the C-terminus of a protein from hydrophilic to hydrophobic. Insight into the role of the farnesyl group in binding to a hydrophobic pocket on the RZZ complex could be obtained from the crystal structure of the RZZ complex. The crystal structure of the hZwilch split construct (1-334 & 335-591 aa) and *in vitro* experiments showed that hZwilch binds to the N-terminus of Rod and hZw10 bind to the C-terminus of Rod (Civril et al., 2010). Super-resolution microscopy mapping has suggested that the C-terminus of hSpindly binds Zwilch and/or the N-terminus of Rod since they are spatially close to each other (Varma et al., 2013). The main goal of future studies is to identify how farnesylation regulates hSpindly and RZZ complex interaction and which RZZ subunit interacts with hSpindly. Absence of a farnesylation motif in Spindly in *Drosophila* and *C. elegans* (Figure 3.8) suggests that farnesylation is not required for its interaction with the RZZ complex in these organisms. We found that the hSpindly/RZZ complex interaction, mediated through hSpindly farnesylation is essential for its kinetochore recruitment (Figure 3.23). We propose that farnesylation induces a conformational change in hSpindly such that it can interact with the RZZ complex (Figure 3.23). Co-IP and GFP Trap experiments showed that non-farnesylated hSpindly is unable to interact with the

RZZ complex subunits Zw10 and Rod. In our model, we predict that the RZZ complex acts as a kinetochore recruitment factor for hSpindly, and Zwilch and/or Rod interacts directly with hSpindly based on recent super-resolution microscopy findings (Varma et al., 2013) (Figure 3.23). RZZ in complex with hSpindly is recruited to unattached kinetochores whereby hSpindly recruits the dynein/dynactin complex (Figure 3.23) although which subunit interacts directly with hSpindly is not clear. Once all chromosomes are bi-oriented, the dynein/dynactin complex transports the checkpoint proteins from the kinetochores to the spindle poles.

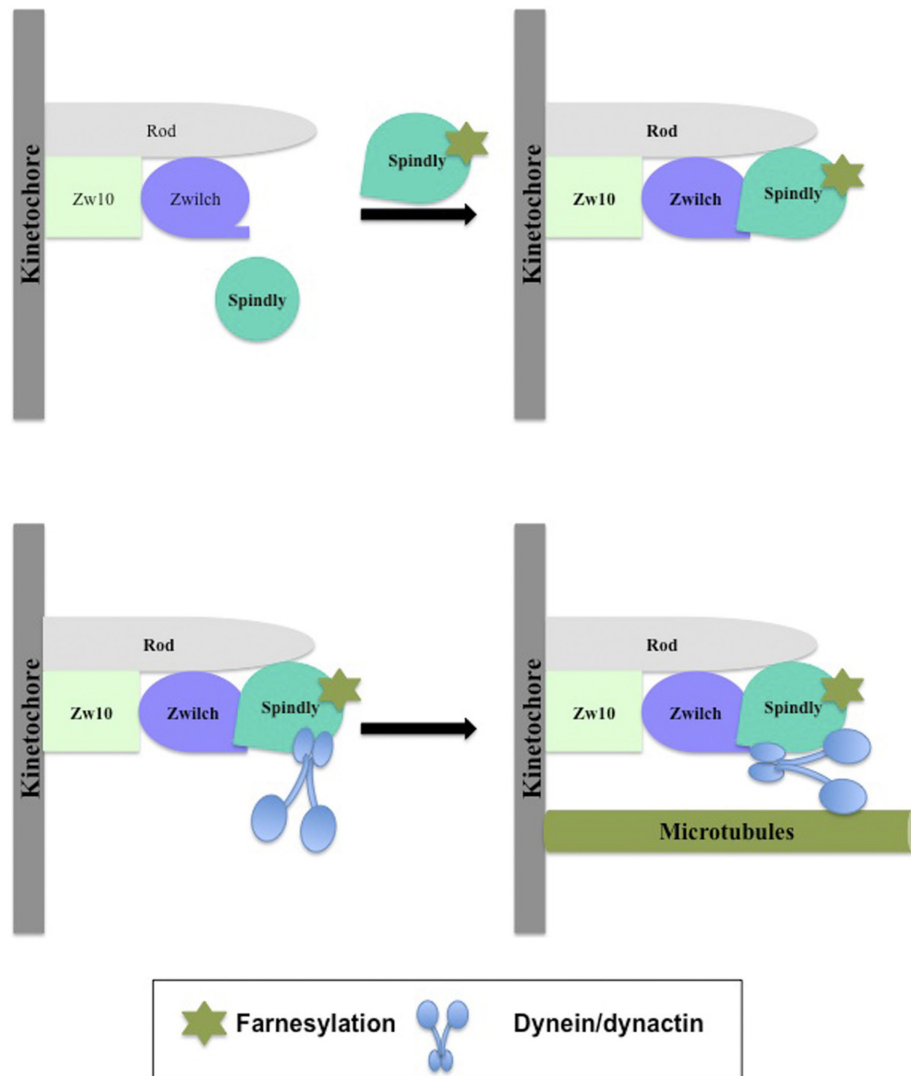


Figure 3.23: A proposed model of hSpindly kinetochore localization.

hSpindly farnesylation induces a conformational change such that it can interact with the RZZ complex subunits Rod and Zwilch, which recruits hSpindly to kinetochores during mitosis. hSpindly further recruits Dynein/Dynactin complex to kinetochores. Once all the chromosomes are aligned on the metaphase plate, hSpindly and the RZZ complex is transported from the kinetochores to spindle poles.

Interestingly, hSpindly constructs O (insertion T600-QLRPH), del592-596 aa, and Q601A that contained mutations upstream of the CAAX motif, localized to kinetochores only when cells were treated with vinblastine (Figure 3.2, Figure 3.4, Figure 3.5 & Table 3.1). These results suggest that the hydrophobicity, charge, and/or posttranslational modifications of the residues upstream of the farnesylation motif might play a role in binding affinity. Insertion mutant O (T600-QLRPH) places a basic residue (H) where there is an acidic residue (E) in WT hSpindly. Del592-596 aa replaces hydrophilic serine residues (SSKS) and a basic lysine with hydrophobic residues (PIL). Q601A replaces a polar hydrophilic residue (Q) with an amphiphilic residue (A). These changes likely have further consequences in the 3D structure of the protein leading to reduced binding affinity. Our results reflect a system similar to membrane binding in RAS proteins, where the CAAX farnesylation motif requires an upstream second signal, which in HRAS, NRAS and KRAS4A is an upstream cysteine residue, that is palmitoylated (Apolloni et al., 2000; Choy et al., 1999). In KRAS4B, however, the second signal is an upstream lysine rich polybasic region with a net positive charge of eight (Hancock et al., 1990). Farnesylation and the polybasic region work together with either one alone being insufficient for membrane binding (Ahearn et al., 2012). hSpindly has two residues upstream of the CAAX motif that are phosphorylated; serine⁵⁹⁴ and threonine⁶⁰⁰ (Hornbeck et al., 2012). Mutants with a deletion encompassing serine⁵⁹⁴ (Del592-596 aa) and substitution of threonine⁶⁰⁰ with alanine (T600A) localized to kinetochores although Del592-596 aa localized to kinetochores only with vinblastine (Figure 3.5). We propose that the region upstream of the hSpindly CAAX motif (hydrophilic and acidic) acts as a second signal for binding affinity due to its charge properties since there is no upstream cysteine that can undergo a second lipid modification (Figure 3.22).

Evidence regarding the effect of FTI on CENP-E and CENP-F kinetochore localization is controversial. Several studies have shown that inhibition of farnesylation does not affect CENP-E and CENP-F kinetochore localization (Ashar et al., 2000; Crespo et al., 2002; Crespo et al., 2001; Verstraeten et al.,

2011). Ashar *et al.* and Verstraeten *et al.* treated A549 cells (for 4 days) and human skin fibroblasts (for 3 days) with FTI and did not observe any effect on CENP-E or CENP-F kinetochore localization. Crespo *et al.* treated Calu-1 and A549 cells with FTI for 48 h and observed CENP-E and CENP-F kinetochore localization. Schafer-Hales *et al.* showed that 16 h FTI treatment of 1A9 ovarian cancer cells disrupts CENP-E and CENP-F kinetochore localization at metaphase but not at prometaphase. Hussein *et al.* reported the inability of a CENP-F cysteine to alanine C3207A mutant (of the CAAX motif) to localize to kinetochores indicating that farnesylation is essential for CENP-F kinetochore localization (Hussein and Taylor, 2002). In the same study, however, FTI treatment did not affect endogenous CENP-F kinetochore localization in agreement with other studies (Crespo *et al.*, 2001; Hussein and Taylor, 2002; Schafer-Hales *et al.*, 2007). In our analysis, inhibition of farnesylation using FTIs did not impair CENP-E or CENP-F kinetochore localization as indicated by quantitative analysis (Figure 3.11). In contrast to Hussein *et al.*, our CENP-F C3207A mutant localized to kinetochores (Figure 3.12). Thus, the mitotic effects of FTIs cannot be attributed to loss of CENP-E and CENP-F kinetochore localization.

FTIs were originally developed to prevent RAS farnesylation; however, it was soon realized that not all the effects of FTIs were due to inhibition of RAS farnesylation as RAS can alternatively undergo geranylgeranylation in the presence of FTIs. Additionally, cell lines lacking any RAS mutations responded to FTIs (Sepp-Lorenzino *et al.*, 1995). Prometaphase delay and chromosome alignment defects in FTI-treated cells were previously hypothesized to be due to CENP-E and CENP-F farnesylation inhibition. One study disputed this hypothesis and suggested the mitotic effects were caused by additional unknown farnesylation targets (Crespo *et al.*, 2001). Our live-cell imaging results showed striking similarities between FTI treatment and the hSpindly knockdown phenotype, such as prolonged prometaphase, chromosome alignment defects and delayed anaphase onset following biorientation, differing only in severity. Unlike

KRAS and NRAS, geranylgeranylation does not appear to substitute for farnesylation in hSpindly kinetochore localization, making hSpindly a potentially good target for FTIs as anti-cancer drugs (Figure 3.13). Extensive clinical trials using tipifarnib, lonafarnib, BMS-214662 and L-7778123 have mostly demonstrated little efficacy in cancer patients except a subset of patients with hematological malignancies (Berndt et al., 2011). Tipifarnib has shown efficacy against breast cancer in addition to acute myeloid leukemia and chronic myelogenous leukemia (Gotlib, 2005; Johnston et al., 2003). Two studies used a two-gene signature (RASGRP1/APTX ratio) to select which acute myeloid leukemia patients could receive tipifarnib treatment (Karp et al., 2012; Raponi et al., 2008). Similarly, lonafarnib has shown efficacy in acute myeloid leukemia and chronic myelogenous leukemia. Recently FTI therapy showed very promising results in patients with Hutchinson-Gilford Progeria syndrome and a clinical trial is ongoing (Wong and Morse, 2012). The biggest challenge to the development of FTI drugs is the lack of knowledge of their target effectors. Here, we propose hSpindly as a novel FTI mitotic target and potential prognostic marker for using FTIs as a therapeutic treatment.

We therefore propose a novel role of farnesylation in targeting a checkpoint protein, hSpindly, to kinetochores. Here, we showed that farnesylation of hSpindly regulates its interaction with the RZZ complex and its recruitment to kinetochores through this interaction. Our data also explains the mitotic effects observed upon FTI treatment. Further research is required to investigate if hSpindly expression is altered in specific cancers.

**Chapter 4 Phospho Regulation of hSpindly and
dynein/dynactin complex recruitment through hp50
subunit**

4.1 Abstract

Kinetochores localization of mitotic checkpoint proteins is essential for their function during mitosis. Among the several checkpoint proteins is hSpindly, an adapter for the dynein/dynactin complex at kinetochores. hSpindly is phosphorylated during mitosis and here I describe a role for phosphorylation in hSpindly kinetochore binding affinity and its transport to spindle poles during mitosis. I showed that inhibition of hSpindly phosphorylation does not affect its kinetochore localization capability but it induces premature transport of hSpindly to kinetochores. The premature transport to the spindle poles is dependent on kinetochore-MT attachments. I also showed that hSpindly is a dynamic kinetochore component with a moderate exchange rate at prometaphase and very high turnover at metaphase kinetochores using fluorescence recovery after photobleaching. In addition, I revealed a novel interaction partner of hSpindly by showing that hSpindly interacts with the hp50 subunit of dynactin by the yeast 2-hybrid assay.

4.2 Introduction:

Mitosis is a cell cycle process by which one cell divides and equally distributes its chromosomes into two daughter cells. During cell division, the faithful segregation of genetic material into two daughter cells is controlled by the mitotic checkpoint (Musacchio and Salmon, 2007). Failure of the mitotic checkpoint has been closely linked to aneuploidy, which is a hallmark of most solid tumors, and mutations in mitotic checkpoint proteins have been linked to mitotic checkpoint dysfunction and cancer (Cahill et al., 1998; Dai et al., 2004; Michel et al., 2001; Wang et al., 2004b). After nuclear envelope breakdown, microtubules (MTs) emanating from the two spindle poles establish links with the kinetochores of sister chromatids. During this process, the sister kinetochores often establish aberrant kinetochore-MT attachments (Kelly and Funabiki, 2009; Silva et al., 2011). The kinetochore-MT error correction mechanism is mediated by Aurora B kinase, which localizes to the inner centromere and de-stabilizes erroneous kinetochore-MT attachments (Kelly and Funabiki, 2009). The mitotic checkpoint is kept in an on state until all the kinetochore-MT attachments are corrected and all chromosomes are aligned on the metaphase plate, and are under tension. The presence of even a single unaligned chromosome delays anaphase onset by keeping the checkpoint in an active state (Rieder et al., 1994). Alignment of chromosomes at the metaphase plate gives rise to tension across sister kinetochores (Musacchio and Salmon, 2007).

In budding yeast, core components of the checkpoint include Bub1, Bub3, Mad1, Mad2, Mad3 and Mps1. However, in metazoans, additional well-conserved proteins such as the RZZ complex and hZwint-1 are also essential components of the mitotic checkpoint (Chan et al., 2000; Karess, 2005; Starr et al., 1998). Kinetochore recruitment of the RZZ complex is dependent on the KMN (KNL1, Mis12, and Ndc80) network and Zwint-1 during late prophase (Cheeseman et al., 2006; Vos et al., 2011). The RZZ complex is required for kinetochore localization of checkpoint proteins Mad1, Mad2, hSpindly and the dynein/dynactin complex (Chan et al., 2009; Starr et al., 1998; Vos et al., 2011; Williams et al., 2003). The

mitotic checkpoint generates a “wait” signal to delay anaphase initiation in the form of the mitotic checkpoint complex (MCC) composed of Mad2, Bub3, BubR1 and Cdc20 (Sudakin et al., 2001; Tang et al., 2001), that directly inhibits the anaphase promoting complex/cyclosome (APC/C) (De Antoni et al., 2005; Fang et al., 1998; Luo et al., 2004; Tipton et al., 2011). APC/C is an E3 ubiquitin ligase required to direct the degradation of securin and cyclin B to exit mitosis (King et al., 1995; Sudakin et al., 1995).

As mentioned earlier, hSpindly kinetochore localization is dependent on the RZZ complex. hSpindly plays a critical role in checkpoint silencing by recruiting the dynein/dynactin motor complex that transports checkpoint proteins, such as Mad1, Mad2, the RZZ complex and hSpindly, from kinetochores to spindle poles thus inactivating the checkpoint (Barisic et al., 2010; Chan et al., 2009; Famulski et al., 2011; Gassmann et al., 2008; Howell et al., 2001). The dynein/dynactin complex localizes to kinetochores during prometaphase but not at metaphase (Echeverri et al., 1996; Pfarr et al., 1990). Dynein is a multi-subunit minus end directed MT motor that functions during mitosis in kinetochore-MT attachment, mitotic checkpoint silencing, and chromosome movement during prometaphase and anaphase (Bader and Vaughan, 2010) and requires dynactin for all its functions (King and Schroer, 2000). Once sister kinetochores are bi-oriented, dynein/dynactin transports the checkpoint proteins to the spindle poles prior to the onset of anaphase leading to mitotic checkpoint silencing (Howell et al., 2001; King et al., 2000; Wojcik et al., 2001). hSpindly is proposed to act as an adapter linking dynein and dynactin as well as their cargos, and this association (dynein-Spindly-dynactin) facilitates the motor activity of dynein along MTs (McKenney et al., 2014). Knockdown of hSpindly causes chromosome congression defects, loss of dynein/dynactin kinetochore localization and prometaphase delay. However, in hSpindly-depleted cells, the checkpoint proteins are removed from the kinetochores of bi-oriented chromosomes in a delayed manner perhaps by a dynein/dynactin independent mechanism (Chan et al., 2009; Gassmann et al., 2010). In contrast, Spindly box point mutants of hSpindly

(S256A and F258A) that localize to kinetochores but uncouple hSpindly from dynein/dynactin recruitment, arrest the cells in metaphase and prevents the removal of Zw10, a proportion of Mad2 protein and hSpindly mutants from kinetochores (Barisic et al., 2010; Gassmann et al., 2010). This metaphase arrest induced by hSpindly's box mutants suggests that dynein/dynactin mediated removal of hSpindly from kinetochores is required for mitotic checkpoint silencing and progression into anaphase. hSpindly has a conserved function of dynein kinetochore recruitment in *Drosophila*, *C. elegans* and humans but there is a significant gap in the knowledge of how hSpindly recruits dynein to kinetochores as no direct interaction has been reported to date (Chan et al., 2009). To define the dynein/dynactin recruitment by hSpindly, I set out to investigate and characterize the dynein/dynactin subunit interacting with hSpindly.

Protein phosphorylation is known to temporally target proteins to the mitotic spindle and kinetochores in addition to functionally regulate the mitotic checkpoint (Elia et al., 2003; Malik et al., 2009; Whyte et al., 2008). Phosphorylation of checkpoint proteins is the most common modification regulating their structure and function (Kang and Yu, 2009; Kemmler et al., 2009). Phosphorylation of checkpoint proteins plays a pivotal role not only in the regulation of checkpoint function but all phases of mitosis (Elowe et al., 2007; Kraft et al., 2003; Malik et al., 2009; Nousiainen et al., 2006). Entry into mitosis is dependent on the activation of Cdk1 (cyclin dependent kinase 1) in complex with cyclin B (Porter and Donoghue, 2003). Additional prominent checkpoint kinases include Plk1, Aurora A and B, Mps1 and BubR1 (Abrieu et al., 2001; Nigg, 2001). hSpindly has been reported to undergo phosphorylation during mitosis in two different studies as a slower migrating band in nocodazole-treated cells that disappeared after treatment with λ -phosphatase (Barisic et al., 2010; Chan et al., 2009). Therefore, I sought to examine the role of hSpindly phosphorylation on its kinetochore localization and checkpoint function.

4.4 Results

4.4.1 hSpindly has numerous phosphorylation sites within the kinetochore localization domain.

As mentioned earlier, hSpindly is phosphorylated during mitosis (Barisic et al., 2010). Phosphorylation prediction software program Group based Prediction System 3.0 (GPS 3.0) was used to identify hSpindly potential phosphorylation sites for mitotic kinases (Cdk1, Aurora kinase family, Mps1/TTK, Nek2 & Plk1) (Xue et al., 2011). This software program predicted 29 sites in total with 13 serines and 16 threonines (Table 4.1). To narrow down the list, I used PhosphoSitePlus (PSP) to identify the residues phosphorylated *in vivo* based on mass spectrometry results (Hornbeck et al., 2012). Currently, PSP reports 13 phosphorylation sites on hSpindly protein with most sites being clustered in the C-terminal end (Figure 4.1). All of these sites are within the kinetochore localization domain of hSpindly (294-605aa). Some of the PSP sites are not included in the GPS 3.0 prediction if I set the prediction threshold to high (Table 4.1); however, if I use the medium threshold for GPS 3.0 prediction then those sites are predicted to be phosphorylated as well. Kinases predicted to phosphorylate the PSP residues are shown in Table 4.2. I examined if PSP phosphorylation sites are conserved in vertebrates (Figure 4.2). Out of the 13 residues, S576 and S594 are evolutionarily conserved, and T600 and S515 are conserved in some organisms.

To investigate the functional aspect of phosphorylation of hSpindly, I chose four phosphorylation sites for mutagenesis: T487, S509, S513 and S515. I did not include other sites in our studies, as those sites were not listed in PSP database at the time I started this study. Most of these sites have been reported recently on PSP and I am in the process of generating more phospho mutants of hSpindly. T600A was generated in the previous study (Figure 3.5B) and it did not affect the kinetochore localization. The S515 site is conserved in mouse and rat whereas the other 3 sites are not conserved in these organisms. The selected 4 phosphorylation sites in hSpindly were mutated to either an unphosphorylatable

residue (alanine) or a phospho-mimic residue (asparatic or glutamic acid). These phospho mutant constructs were cloned into a C-terminal GFP vector to analyze their ability to localize to kinetochores when transfected into HeLa cells.

Table 4.1: Predicted serine (S) and threonine (T) phosphorylation sites in hSpindly using GPS 3.0.

Only residues above high threshold (with a predicted false positive rate of 10%) are shown. Score represents the value calculated by the GPS algorithm to evaluate the potential of phosphorylation. Higher score represents higher probability to undergo phosphorylation.

Position	Code	Kinase	Score
52	T	Other/PLK	15.987
126	S	Other/AUR/AurB	9.944
171	T	Other/PLK	16.409
175	S	Other/PLK	12.779
349	S	Other/NEK	6.536
365	T	Other/TTK/MPS1	8.333
385	T	Other/TTK	5.75
390	S	Other/PLK	11.208
443	T	Other/TTK	6.688
443	T	Other/PLK/PLK1	6.862
443	T	Other/PLK/PLK1/CDC5	7.833
443	T	Other/PLK/PLK1/PLK1	4.264
461	T	Other/TTK/MPS1	7.667
471	S	Other/PLK	12.565
487	T	Other/TTK	6.625
504	S	Other/PLK/PLK1	7.826
504	S	Other/PLK/PLK1/PLK1	4.242
509	T	CMGC/CDK/CDC2	9.315
509	T	CMGC/CDK/CDC2/CDK1	14.528
515	S	CMGC/CDK	6.841
515	S	CMGC/CDK/CDC2/CDK1	10.234
552	T	CMGC/CDK/CDC2	10.268
552	T	CMGC/CDK/CDC2/CDK1	12.192
555	S	CMGC/CDK	7.457
555	S	Other/PLK	10.695
555	S	CMGC/CDK/CDC2	10.297
576	S	Other/PLK	11.24
597	T	CMGC/CDK	6.386
597	T	CMGC/CDK/CDC2/CDK1	11.659

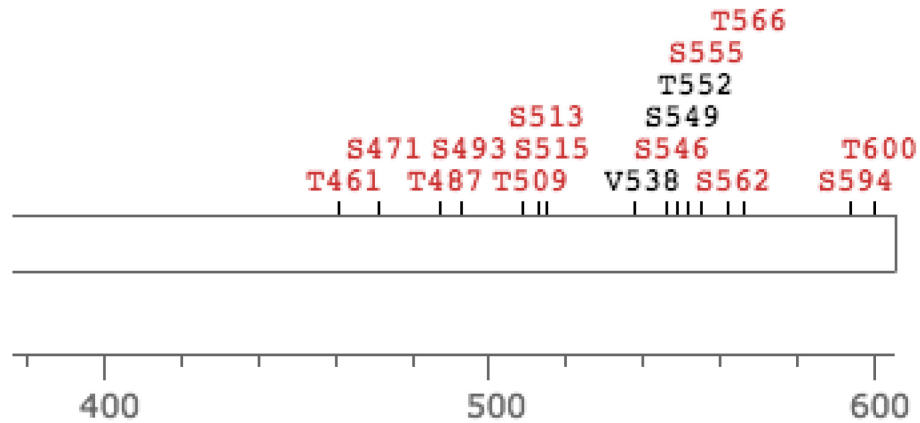


Figure 4.1: Schematic of hSpindly C-terminus showing phosphorylation sites.

Residues shown in red are reported to be phosphorylated *in vivo* and residues shown in black are predicted to be phosphorylated based on mouse and rat phosphorylation sites. (Adapted from PhosphoSitePlus).

Table 4.2: Kinases predicted by GPS3.0 to phosphorylate sites reported by PhosphoSite Plus.

If more than one kinase was predicted to phosphorylate a site, the kinase with the higher potential (score) to phosphorylate a given site was chosen.

Position	Code	Kinase	Score
461	T	MPS1	7.667
471	S	PLK	12.565
487	T	MPS1	6.625
493	S	PLK/PLK2	7.605
509	T	CDK/CDK5/CDK5	17.938
513	S	CDK/CDK7/CDK7	0.242
515	S	CDK/CDK2/CDK2	27.154
546	S	PLK/PLK2/PLK3	4.722
555	S	CDK/CDK2/CDK2	19.584
576	S	CDK/CDC2/CDK1	4.966
594	S	PLK	10.409
600	T	CDK/CDK9/CDK9	8.737

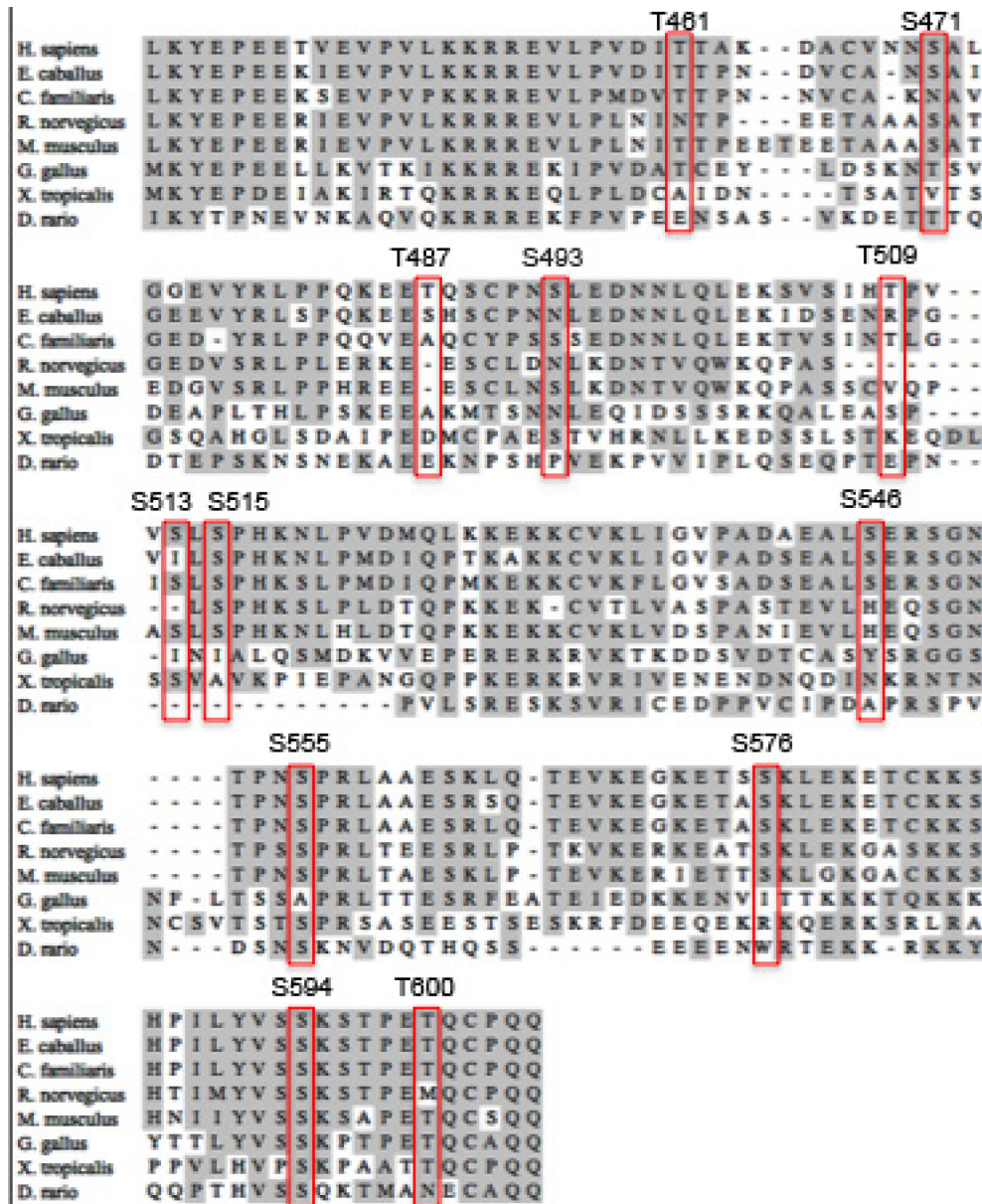


Figure 4.2: hSpindly PSP phospho-sites are not conserved in different species.

ClustalW alignment of hSpindly protein with PSP phosphorylation sites highlighted in red shows S555, S594 and T600 conserved during evolution. Species shown are *Homo sapiens* (human), *Equus caballus* (horse), *Canis familiaris* (dog), *Rattus norvegicus* (rat), *Mus musculus* (mouse), *Gallus gallus* (chicken), *Xenopus tropicalis* (Western clawed frog) and *Danio rerio* (Zebrafish).

4.4.2 Mutation of hSpindly phosphorylation sites leads to altered kinetochore localization.

I mutated the 4 phosphorylation sites (T487A, S509A, S513A and S515A) within the kinetochore localization domain of hSpindly to alanine and analyzed their kinetochore localization ability. All these non-phosphorylatable mutants retained their ability to localize to kinetochores but showed premature accumulation at poles in prometaphase (Figure 4.3). In some cells these mutants were noticed at the spindle poles in anaphase whereas in wild type hSpindly accumulation at the poles is observed only during metaphase (data not shown). I further created two double non-phosphorylatable mutants encompassing 3 of the phosphorylation sites: T509A/S513A and S513A/S515A. These double mutants also showed premature accumulation at spindle poles similar to the single phospho mutants (Figure 4.4). I treated phospho mutant transfected HeLa cells with vinblastine to allow maximal accumulation of checkpoint proteins at kinetochores. In the presence of vinblastine, these mutants localized only to kinetochores indicating that polar localization is MT dependent (Figure 4.5). Cells transfected with hSpindly non-phosphorylatable mutants frequently displayed unaligned chromosomes at metaphase and lagging chromosomes at anaphase. These results indicate that these mutants might be exerting a dominant negative phenotype in these cells.

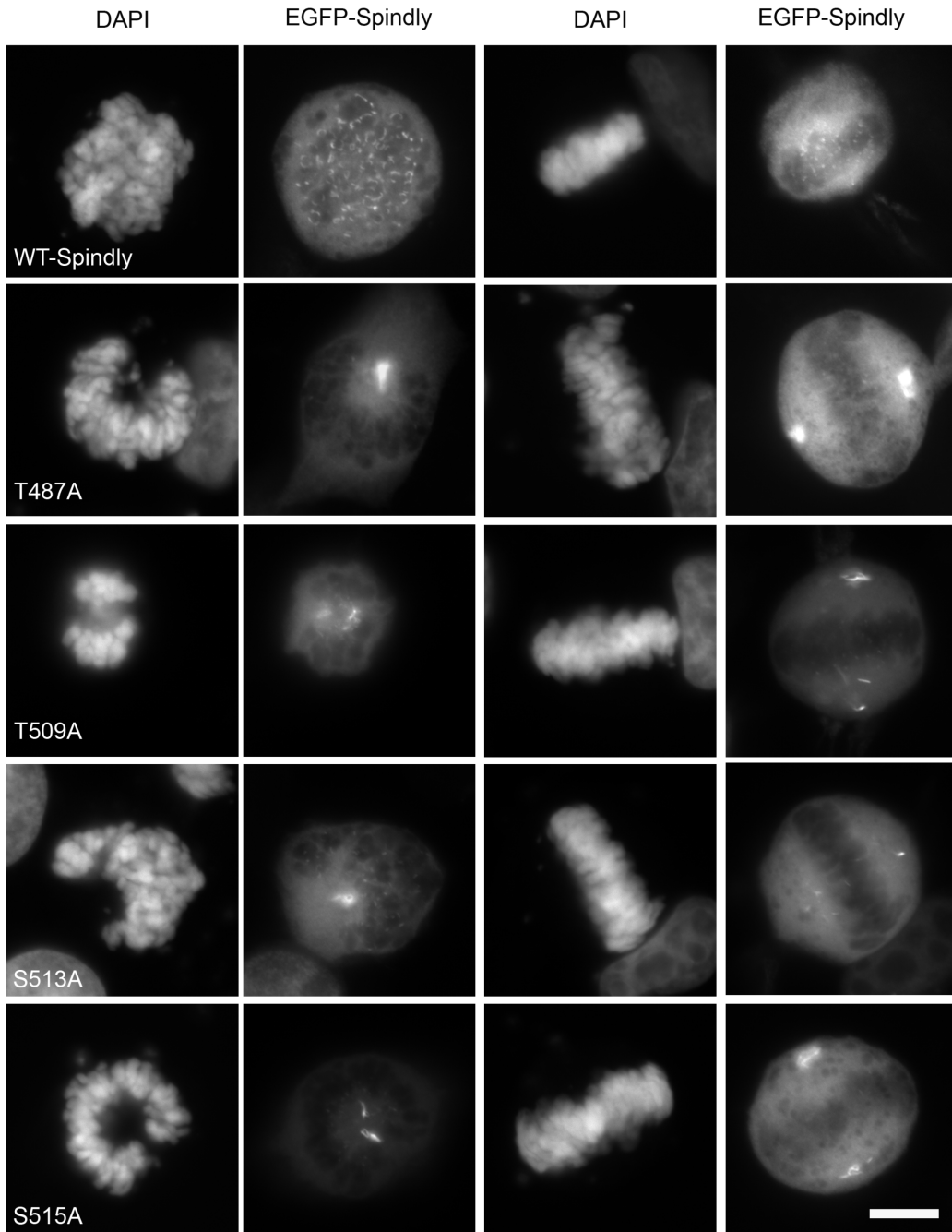


Figure 4.3: Enhanced localization of hSpindly non-phosphorylatable mutants at spindle poles during prometaphase and metaphase.

Fluorescence microscopy of GFP-tagged phospho mutants transfected into HeLa cells. DNA is visualized using DAPI. Scale bar, 10 μ m.

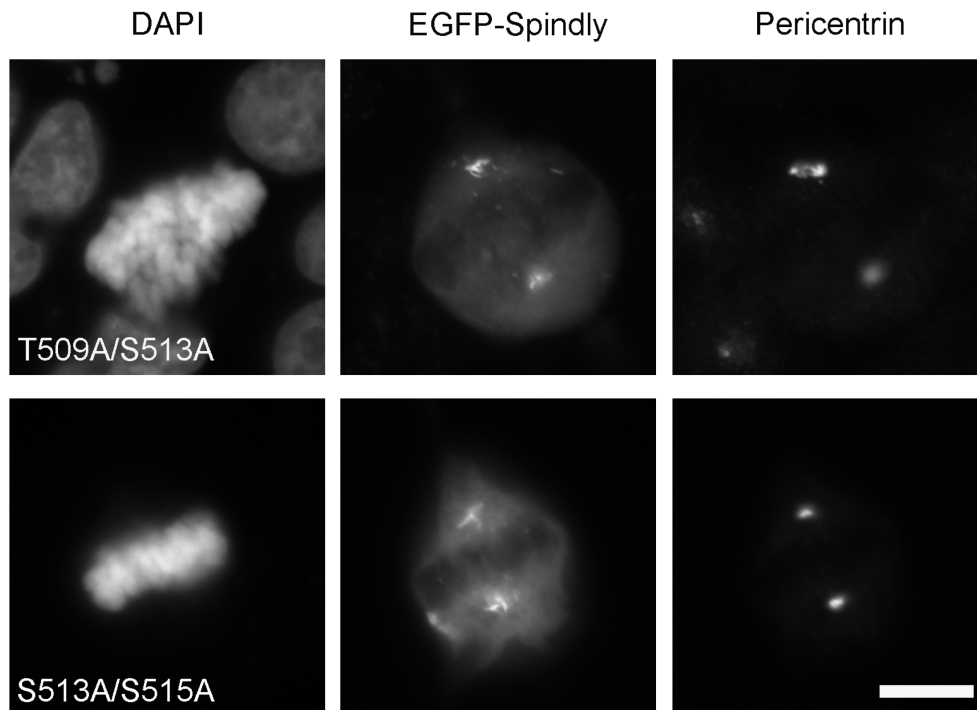


Figure 4.4: Enhanced localization of hSpindly double non-phosphorylatable mutants at spindle poles.

Fluorescence microscopy of GFP-tagged phospho mutants transfected into HeLa cells. Pericentrin staining shows spindle poles. DNA is visualized using DAPI. Scale bar, 10 μm .

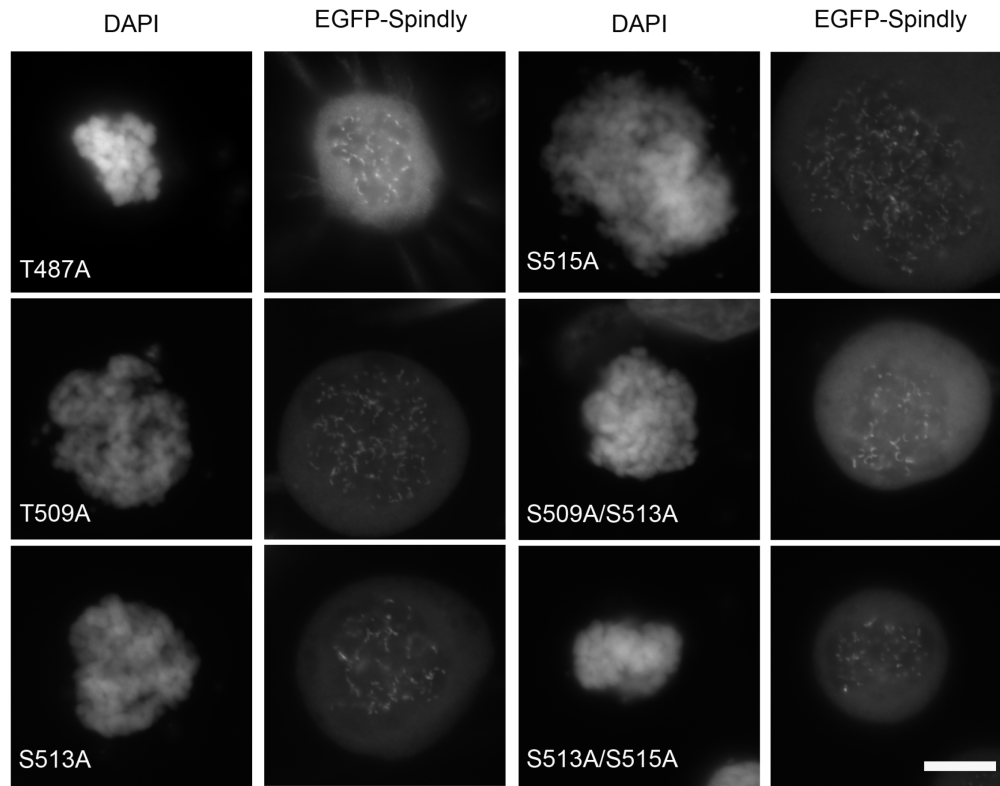


Figure 4.5: hSpindly non-phosphorylatable mutants localized to kinetochores under vinblastine treatment showing polar localization is MT dependent. Fluorescence microscopy of GFP-tagged phospho mutants transfected into HeLa cells. Strong localization at kinetochores was observed upon treatment with vinblastine. DNA is visualized using DAPI. Scale bar, 10 μ m.

I generated 3 single and 3 double phospho-mimic mutants of hSpindly as shown in Table 4.3. EGFP-tagged hSpindly phospho-mimic mutants were transfected into HeLa cells and I found that single phospho-mimics localized to kinetochores in untreated and vinblastine treated cells similar to WT-hSpindly. Double phospho-mimics (T509E/ S513D, T509E/ S513D and S513D/S515D) showed enhanced streaming along mitotic spindle MTs (Figure 4.7) as well as normal kinetochore localization (Figure 4.8). The streaming of EGFP-hSpindly double non-phosphorylatable mutants suggests that these mutants might be unable to leave the MTs and accumulate at poles.

Table 4.3: hSpindly phospho-mimics and their kinetochore localization.

Mutated Site	Kinetochore Localization
T509E	Normal
S513D	Normal
S515D	Normal
T509E/ S513D	Premature accumulation at poles in prometaphase
T509E/ S515D	Premature accumulation at poles in prometaphase
S513D/ S515D	Premature accumulation at poles in prometaphase

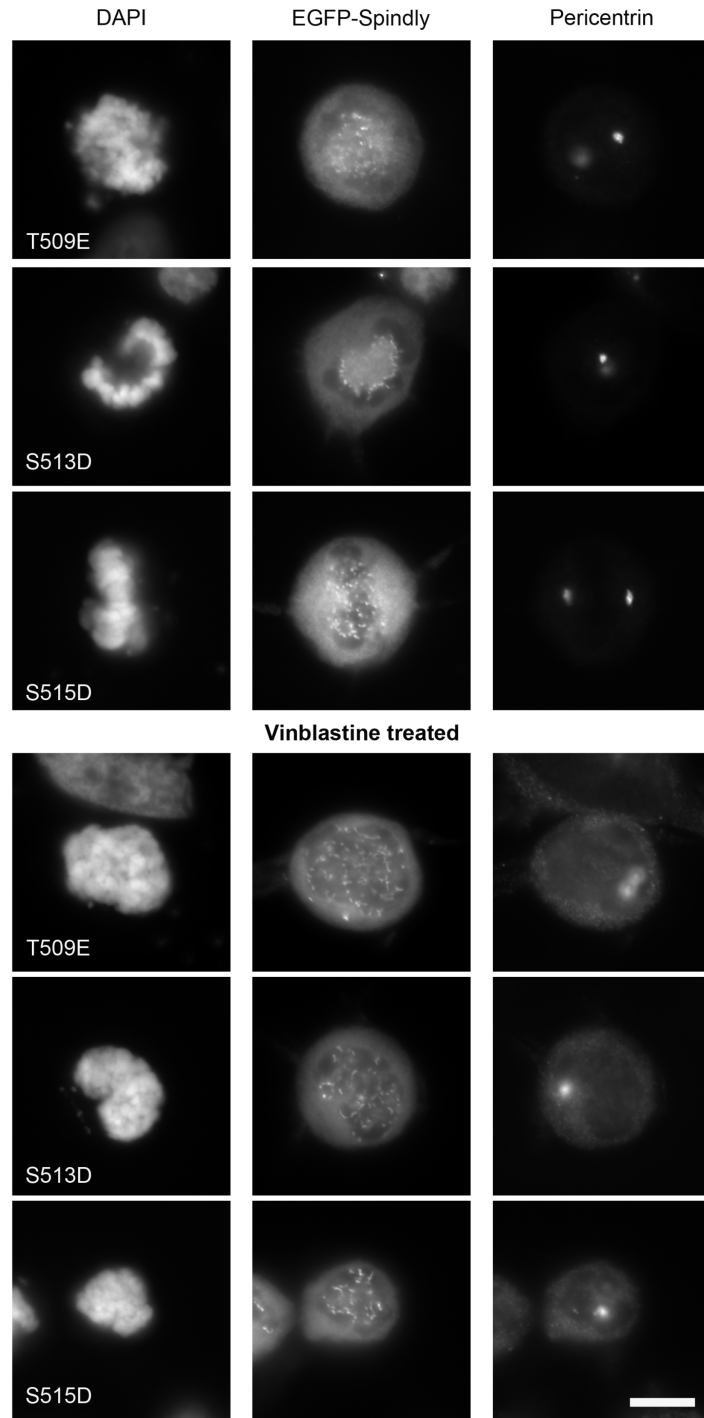


Figure 4.6: hSpindly single phospho-mimics localized to kinetochores in untreated and vinblastine treated HeLa cells similar to WT-hSpindly. Fluorescence microscopy of GFP-tagged hSpindly phospho-mimics transfected into HeLa cells. DNA is visualized using DAPI. Scale bar, 10 μ m.

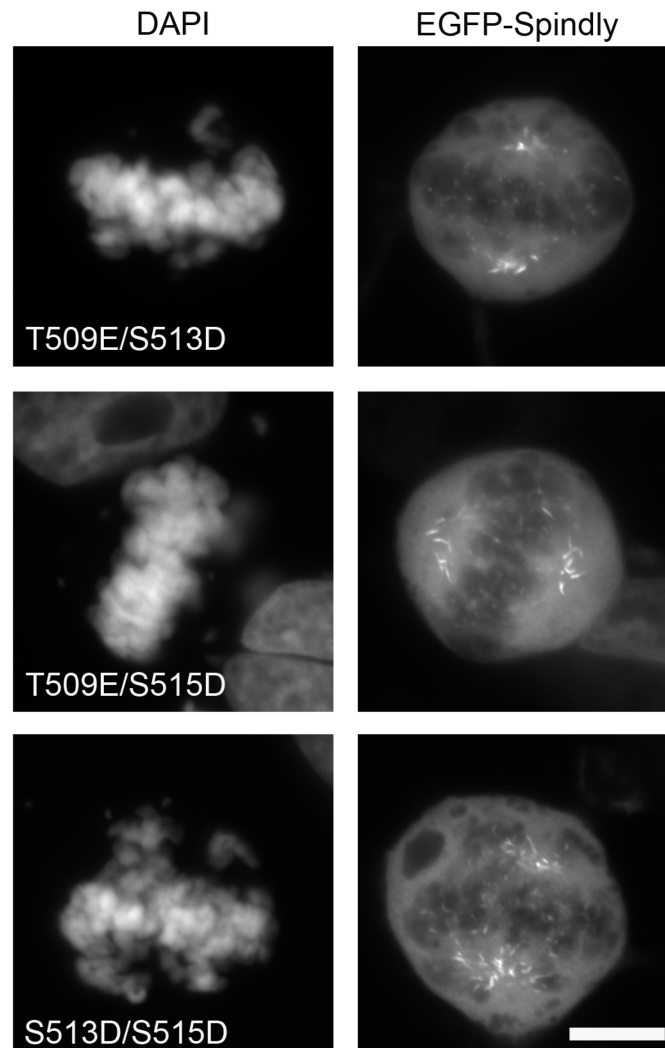


Figure 4.7: hSpindly double phospho-mimics showing enhanced streaming on the mitotic spindle, transport to spindle poles at prometaphase but not accumulation at poles.

Fluorescence microscopy of GFP-tagged hSpindly phospho-mimics transfected into HeLa cells. DNA is visualized using DAPI. Scale bar, 10 μm .

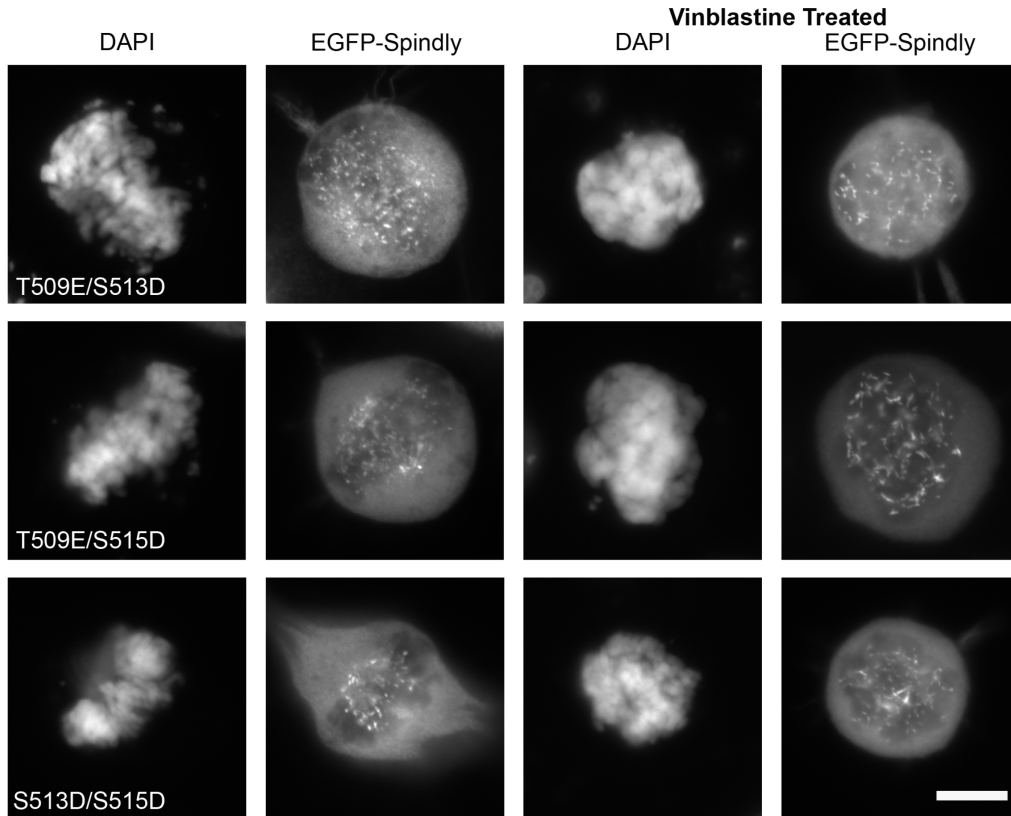


Figure 4.8: hSpindly double phospho-mimics showing normal kinetochore localization.

Fluorescence microscopy of GFP-tagged hSpindly phospho-mimics transfected into HeLa cells. DNA is visualized using DAPI. Scale bar, 10 μm .

4.4.3 Kinetochores dynamics of WT-hSpindly and phospho mutants

To better understand if phosphorylation affects the kinetochore dynamics of hSpindly, I attempted to understand the WT-hSpindly kinetochore dynamics. Checkpoint proteins are usually transient kinetochore components with kinetochore-MT attachment status affecting their kinetochore residency patterns (Howell et al., 2004). Kinetochore proteins can be classified into two categories based on their kinetochore residency pattern; stable and transient. The structural components of kinetochores such as Zwint-1 (Vos et al., 2011) and Spc25 (Schittenhelm et al., 2007) are stable. Other kinetochore proteins show turnover during mitosis such as Zw10 (Famulski et al., 2008), Mps1 (Howell et al., 2004; Jelluma et al., 2010) and Mad2 (Defachelles et al., 2015; Howell et al., 2004). Zw10 has a rapid recovery rate ($t_{1/2}$ = 13.8 seconds) at metaphase kinetochores compared to no recovery at prometaphase kinetochores (Famulski et al., 2008). In contrast to human Zw10, *Drosophila* GFP-Rod was shown to be a transient kinetochore component ($t_{1/2}$ = 1 minute) in prometaphase cells (Basto et al., 2004), however recently the same lab showed that both Zw10 and Rod are stable at prometaphase and become dynamic at metaphase in *Drosophila* larval neuroblasts (Defachelles et al., 2015). The latter observation is in agreement with human RZZ kinetochore dynamics (Famulski et al., 2008). It is not clear if hSpindly kinetochore dynamics are similar to Zw10 and no one has examined if kinetochore-MT attachments affects hSpindly dynamics.

To analyze hSpindly kinetochore dynamics, I performed FRAP on EGFP-hSpindly expressing HeLa cells (Figure 4.9). EGFP-hSpindly recovered ~30% of the initial pre-bleach signal in vinblastine treated HeLa cells showing hSpindly has 70% immobile fraction at prometaphase. However, the turnover of hSpindly at unattached kinetochores is moderate compared to Zw10. At metaphase kinetochores, I observed very rapid turnover of hSpindly with $t_{1/2}$ of 0.98 seconds, which is much faster than Zw10 ($t_{1/2}$ = 13.8 seconds) (Famulski et al., 2008). These results suggest that hSpindly becomes a dynamic kinetochore component upon microtubule attachment similar to Zw10. The fluorescent time-lapse imaging

from FRAP experiments in metaphase cells revealed the transport of EGFP-hSpindly (in the form of streaks) along mitotic spindle MTs and accumulation at spindle poles. This polar transport was mostly unidirectional but I observed that hSpindly particles sporadically switched direction towards kinetochores or paused movement along MTs. Similar transport patterns were observed for Mad2 at metaphase kinetochores (Howell et al., 2000).

I selected a subset of our hSpindly phospho mutants to study their kinetochore dynamics using FRAP in endogenous hSpindly-depleted cells. I made siRNA resistant versions of hSpindly non-phosphorylatable and phospho-mimics to investigate if kinetochore dynamics of these mutants are altered. Expression of these mutants in cells transfected with hSpindly siRNA is shown in Figure 4.10. Kinetochore localization of these phospho mutants except for T509A & S513A^R and S515D^R is shown in Figure 4.11. Kinetochore dynamics of hSpindly phospho mutants remains to be investigated.

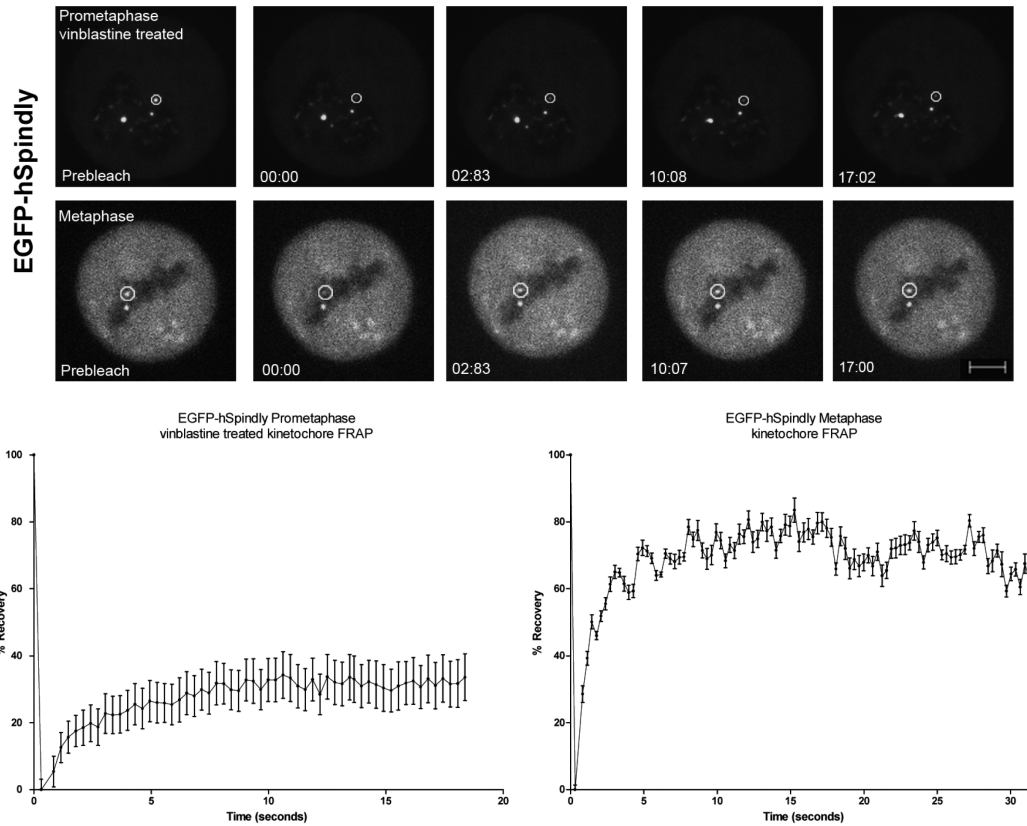


Figure 4.9: hSpindly shows rapid turnover at metaphase but not at prometaphase.

EGFP-hSpindly expressing HeLa cells were treated with 0.1 μM vinblastine or untreated (for metaphase cells) and time lapse imaging was performed before and after photobleaching encompassing a single kinetochore. Bleached kinetochores are shown in a white circle. Bottom panels show kinetics of fluorescence percent recovery at prometaphase (left) and metaphase (right) using nonlinear regression curves plotted as a fraction of initial prebleach signal ($n=5$). Time scale is in seconds: milliseconds. Error bars are S.E.M. Scale bar, 5 μm .

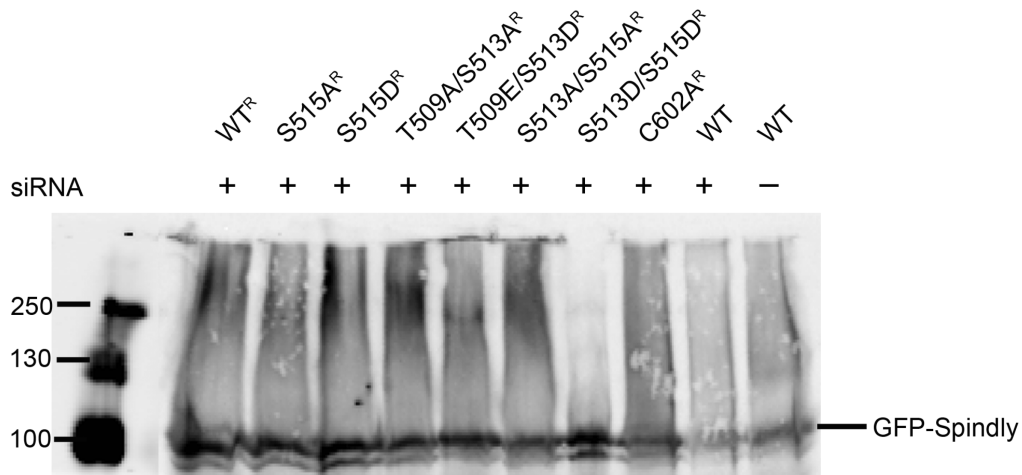


Figure 4.10: Correct expression of siRNA resistant WT-hSpindly and hSpindly phospho mutants using western blot analysis.

Immunoblot showing the expression of GFP-hSpindly fusion proteins transfected into HEK293 cells, HEK293 cells were previously transfected with hSpindly siRNA. GFP-fusion proteins were labeled with IR800-conjugated rabbit anti-GFP antibody. Molecular mass markers detected in the same channel are shown on the blot. (Masses indicated in kD). WT- wild type.

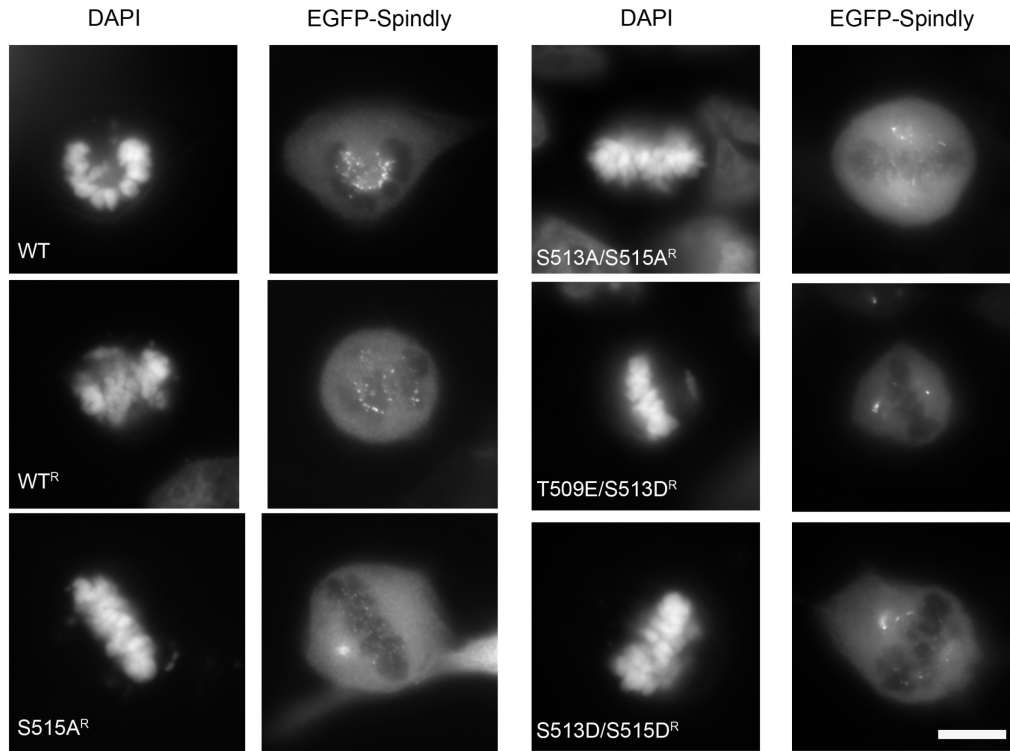


Figure 4.11: Kinetochore localization of siRNA resistant hSpindly phospho mutants.

Fluorescence microscopy of GFP-tagged hSpindly phospho mutants transfected into HeLa cells; HeLa cells were previously transfected with 100 nM hSpindly siRNA to knockdown endogenous hSpindly. DNA is visualized using DAPI. WT refers to wild type and WT^R is siRNA resistant WT version of hSpindly. Scale bar, 10 μ m.

4.4.4 Inhibition of Plk1 and Mps1 kinase affects hSpindly kinetochore localization.

hSpindly PSP phosphorylation sites are predicted to be target sites for Plk1 kinase (S471, S493, S546 and S594) and Mps1 kinase (T461 and T487) in addition to CDK as shown in Table 4.2. Inhibition of Mps1 kinase using Reversine demonstrated that Mps1 kinase activity is required for RZZ complex kinetochore recruitment (Santaguida et al., 2010). Since hSpindly kinetochore recruitment is dependent on the RZZ complex, I predict loss of hSpindly kinetochore localization in cells treated with Mps1 inhibitor. Treatment of HeLa cells with AZ 3146, an Mps1 kinase inhibitor, led to complete loss of hSpindly kinetochore localization (Figure 4.12).

Treatment of HeLa cells with BI2536 (Choi et al., 2015), a Plk1 small molecule inhibitor, led to abnormal kinetochore localization of the RZZ complex and hSpindly. In prometaphase, the RZZ complex and hSpindly localized to kinetochores similar to WT. In early metaphase cells, the RZZ complex is absent from kinetochores and hSpindly is absent from both kinetochores and spindle poles. In anaphase, the RZZ complex and hSpindly were found to be present at the kinetochores again. Normally, the RZZ complex and hSpindly are absent from kinetochores or spindle poles at anaphase. Abnormal RZZ complex kinetochore localization in response to Plk1 inhibition was observed by a previous graduate student in the lab as well (unpublished results).

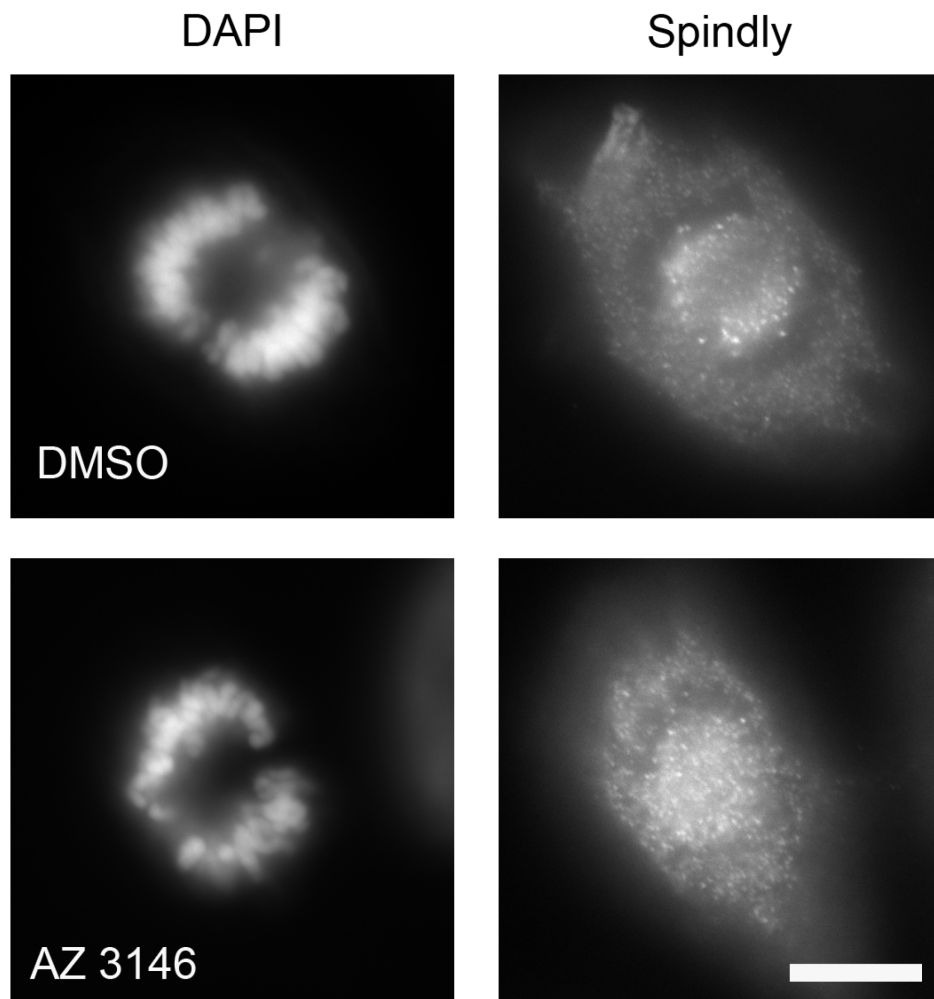


Figure 4.12: Mps1 inhibitor treatment leads to loss of hSpindly kinetochore localization.

HeLa cells treated with 2 μ M of AZ 3146 for 2 h, fixed and immunostained for Spindly. DAPI stains DNA. Scale bar, 10 μ m.

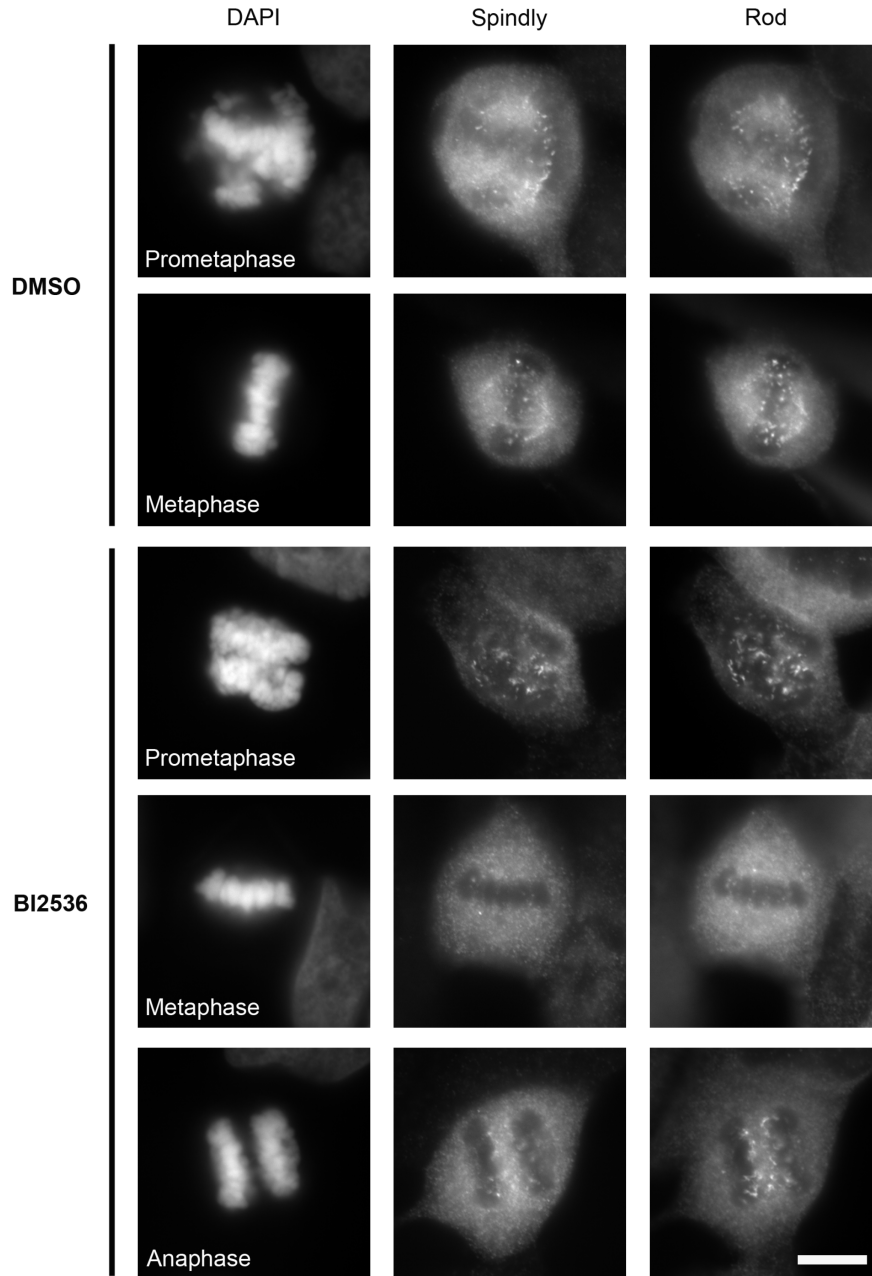


Figure 4.13: Plk1 kinase regulates the RZZ complex and hSpindly kinetochore localization.

HeLa cells treated with 100 nM of BI2536 for 30 min, fixed and immunostained for hSpindly and Rod. BI2536 treatment led to loss of the RZZ complex and hSpindly kinetochore localization at metaphase, and retention of both at kinetochores in anaphase kinetochores. DAPI stains DNA. Scale bar, 10 μ m.

4.4.5 hSpindly interacts with human p50/dynamitin (hp50), a subunit of the dynactin complex in the yeast 2-hybrid system.

hSpindly recruits the dynein/dynactin complex to the kinetochores but there is no evidence of direct interaction between hSpindly and dynein/dynactin subunits. I tested hp50/dynamitin, a subunit of dynactin, for interaction with hSpindly using the Lex-A based yeast 2-hybrid assay and discovered that hSpindly readily interacts with hp50/dynamitin. Expression of bait and prey constructs in yeast colonies screened for blue/white color was confirmed by western blot and is shown in Figure 4.16. Furthermore, I screened truncation mutants of hSpindly for interaction with the wild type hp50/dynamitin and found that two domains of hSpindly interact with hp50 (Figures 4.14 and 4.15). hSpindly mutant I (151-452) lacking both the N and C terminal end but containing the Spindly motif is able to interact with hp50 indicating that the Spindly motif may be part of the hSpindly interaction domain for hp50, in agreement with previous studies (Figure 4.14) (Gassmann et al., 2010). Furthermore, the C1 hSpindly mutant containing a Spindly motif but lacking the coiled-coil domain II, does not interact with hp50 indicating that the Spindly motif requires the coiled-coil domain II for interaction with hp50 (Figure 4.14). In addition, the C-terminal N8 mutant of hSpindly is sufficient for interaction with hp50. These results indicate that two domains of hSpindly; domain comprising of Spindly motif with coiled-coil II, and hSpindly C-terminus, might be interacting with hp50 independent of each other. I further investigated hSpindly insertion mutant P with an insertion following aa 603 (P603-CGRSP) for its ability to interact with hp50. This mutant has an insertion upstream of the farnesylation motif and does not localize to the kinetochore (Table 3.1); however, the hp50 interaction results are not conclusive since the yeast colony transfected with this mutant did not grow very well.

		Coiled Coil Domain I 1-252	Spindly motif 253 - 284	Coiled Coil Domain II 300-438		Y-2-H interaction with p50	Kinetochores localization		
WT	1	—————			605	+	+		
C1	1	————— 300				-	-		
I		151	————— 452			+	-		
N1		151	—————		605	+	+		
N2			322	—————		605	+/-		
N3				453	—————		605	+	-
N4				461	—————		605	+	-
N5				469	—————		605	+	-
N6				488	—————		605	+	-
N7				518	—————		605	+	-
N8				553	—————		605	+	-

Figure 4.14: hSpindly interacts with the hp50 subunit of dynactin through the Spindly motif and its C-terminus.

Schematic diagram of hSpindly truncation mutant library showing their ability to interact with hp50 and kinetochores localization (+ indicates positive for interaction with hp50 and kinetochores localization, - indicates negative for interaction with hp50 and no kinetochores localization and +/- indicates localizes to kinetochores only under vinblastine treatment). aa numbers are indicated.

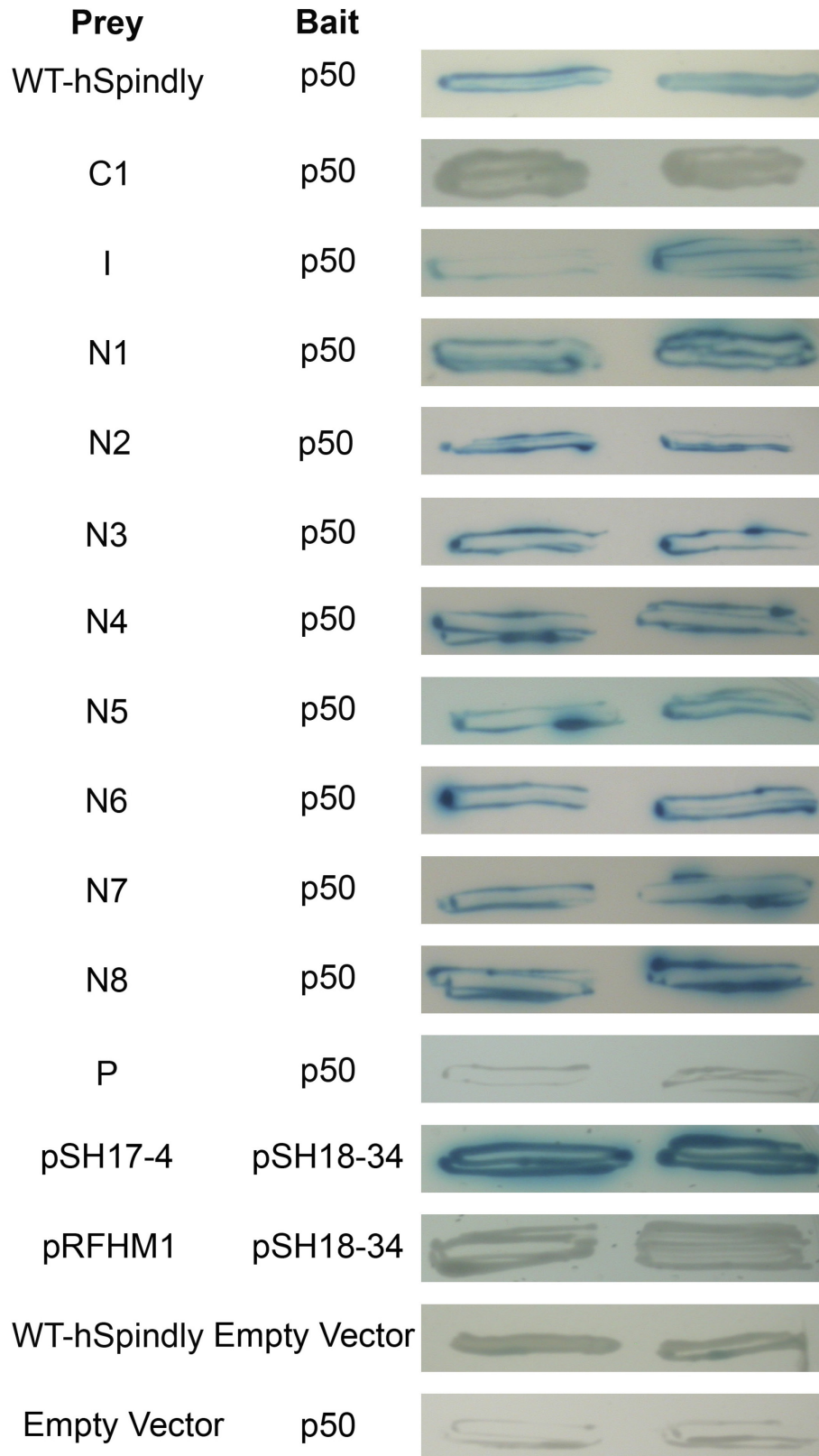
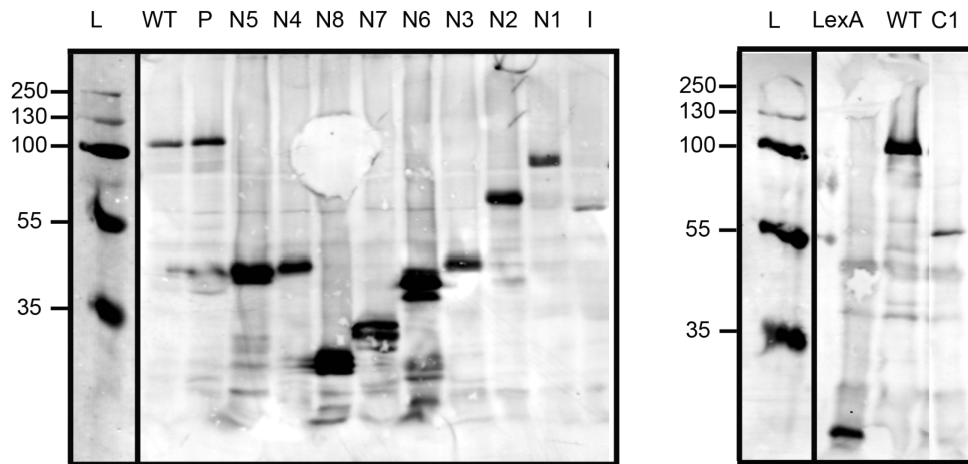


Figure 4.15: hSpindly interacts with hp50 subunit of dynactin complex.

Representative results of LexA yeast 2-hybrid experiment between wild type p50 (bait) and hSpindly truncation mutants (prey). Interactions between bait and prey proteins were scored by blue (positive) and white (negative) color on X-gal dropout plates. P is an insertion mutant with an insertion following aa 603 (P603-CGRSP). pSH17-4 expresses a lexA fusion with an activation domain that strongly activates transcription in pSH18-34 and this combination was used as a positive control. pRFHM1 expresses a LexA fusion with the N-terminus of bicoid and does not activate transcription in pSH18-34. This combination was used as a negative control. The possibility of false positive was eliminated by checking the interaction between bait construct with empty prey vector, and vice versa.

LexA fused hSpindly Truncation and Insertion Mutants Expression



B42 fused WT-hp50 Expression

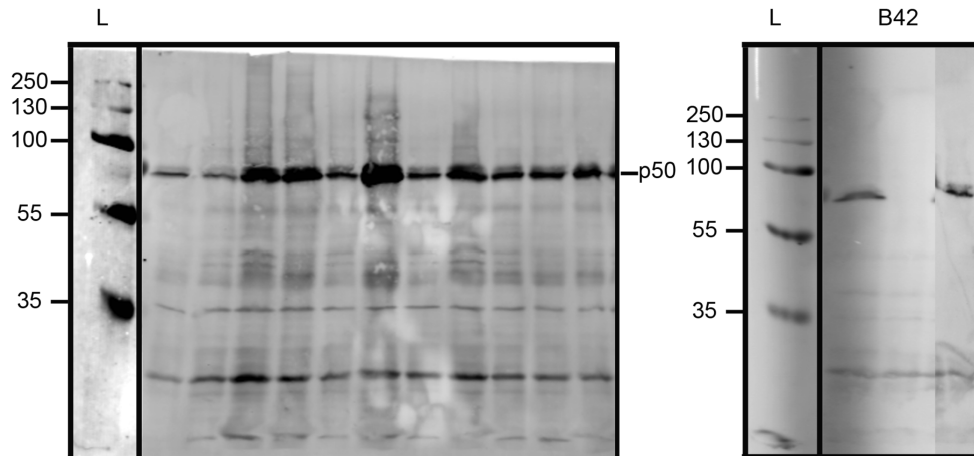


Figure 4.16: Immunoblots showing correct size expression of hSpindly mutants (prey) and p50 (bait).

LexA fused hSpindly mutant proteins were labeled with rabbit polyclonal anti-LexA antibody followed by Alexa 680 conjugated anti-rabbit antibody. B42 fused hp50 proteins were labeled with rabbit polyclonal anti-B42 antibody followed by Alexa 680 conjugated anti-rabbit antibody. Molecular mass markers detected in the same channel are shown on each blot. (Masses indicated in kD). WT- wild type. All hSpindly mutant constructs and WT-hp50 expressed at the expected size. (LexA fused WT-hSpindly= 95 kD, P=95 kD, C1= 41.7 kD, I=54.34 kD, N1= 76 kD, N2=55.8 kD, N3=40.6 kD, N4=39.6 kD, N5=38.8 kD, N6=36.6 kD, N7=33.5 kD, N8= 29.6 kD, lexA alone=22.35 kD, B42 alone=10.28 kD and B42 fused WT-p50=55.09 kD). L denotes molecular mass ladder.

4.5 Discussion

hSpindly non-phosphorylatable mutants (S509, S513, S515, T509A/S513A and S513A/S515A) localized to kinetochores indicating that phosphorylation is not a requirement for hSpindly kinetochore localization (Figure 4.3). However, inhibition of hSpindly phosphorylation promotes its premature transport to spindle poles in prometaphase indicating that removal of a phospho group upon MT attachment might be the catalytic step for streaming hSpindly along the MTs via the dynein/dynactin complex and accumulation at poles (Figure 4.3 & 4.4). I did not observe accumulation of hSpindly non-phosphorylatable mutants at spindle poles in cells treated with the MT destabilizing drug vinblastine indicating that these mutants accumulate at poles through streaming along MTs of the mitotic spindle. Unlike hSpindly non-phosphorylatable mutants, one would expect that phospho-mimic mutants of hSpindly should not be removed from kinetochores since they carry a permanent negative charge similar to a phospho group. However, I observed that double phospho-mimics of hSpindly showed spindle pole accumulation albeit to a lesser extent and less frequently compared to non-phosphorylatable mutants. These hSpindly phospho-mimic mutants might be transported to the poles through dimerization with endogenous hSpindly (Holland et al., 2015) facilitating their transport along the MTs. To conclude, I propose that non-phosphorylatable Spindly can be recruited to kinetochores but the stable association with the kinetochores requires hSpindly phosphorylation.

In KRAS4B, farnesylation and the upstream polybasic region (lysine rich region with a net positive charge of eight) cooperate for membrane binding (Ahearn et al., 2012; Hancock et al., 1990). Furthermore, KRAS4B undergoes phosphorylation at the serine in the polybasic region, and this facilitates its translocation from the plasma membrane to the endomembranes, referred to as farnesyl-electrostatic switch (Bivona et al., 2006). However, I hypothesize an alternative to the farnesyl-electrostatic switch for hSpindly, based on our observations, where removal of phosphorylation (upstream of CAAX motif)

reduces its affinity for kinetochores or increases affinity for dynein and acts as a signal for translocation from kinetochores to spindle poles along mitotic spindle MTs (Figure 4.17). This hypothesis can be tested by performing live-cell imaging and FRAP, comparing the dynamics of WT-hSpindly and its phospho mutants.

I discovered that hSpindly is a transient kinetochore component with a highly increased turnover rate at metaphase as compared to prometaphase (Figure 4.9). These results show that kinetochore-MT attachment affects the hSpindly kinetochore dynamics similar to Zw10. Rod and Zw10 are stably associated with kinetochores at prometaphase but becomes dynamic at metaphase (Defachelles et al., 2015; Famulski et al., 2008). GFP-Zw10 does not show turnover at prometaphase kinetochores whereas hSpindly recovers to some extent (~30%) at prometaphase kinetochores, suggesting that hSpindly disassembles from the RZZ complex at prometaphase kinetochores and exchanges with its cytoplasmic pool. However, the RZZ complex recruits hSpindly to kinetochores and it seems unlikely that hSpindly exchanges with its cytoplasmic pool without its adaptor the RZZ complex. The moderate EGFP-hSpindly turnover in vinblastine treated prometaphase cells should be confirmed in untreated prometaphase cells since saturation of EGFP signal at kinetochores due to maximal accumulation of checkpoint proteins at kinetochores in vinblastine treated cells could lead to some errors in signal quantification. Another explanation for the difference between Zw10 and hSpindly prometaphase dynamics is that the initial hSpindly kinetochore recruitment is dependent on the RZZ complex following which hSpindly dynamics are RZZ complex independent. Based on our FRAP data, I can conclude that hSpindly turnover significantly increases on metaphase kinetochores and I believe that this is dependent upon its streaming along the MTs of mitotic spindle and transfer to the spindle poles. Mps1 kinase phosphorylation inhibition reduces Mps1's exchange rate at prometaphase kinetochores indicating that phosphorylation regulation plays a major role in the dynamics of checkpoint proteins (Jelluma et al., 2010). The dynamics of hSpindly phospho mutants remain to be investigated.

The yeast 2-hybrid assay results show that hSpindly interacts with the hp50 subunit of the dynactin complex. In agreement with other studies, I have not been able to confirm hSpindly's interaction with p50 in co-immunoprecipitation or GST pull-down experiments (Barisic et al., 2010; Chan et al., 2009). However a recent study showed the hSpindly immunoprecipitated the dynein/dynactin complex (McKenney et al., 2014). The interaction between hSpindly and hp50 is a potential mechanism for dynein/dynactin recruitment to the kinetochores through hSpindly. Our next step is to investigate this interaction with the proximity ligation assay using the Duolink II kit (Olink Biosciences) to confirm this interaction *in situ* (Naegle et al., 2012; Zhu et al., 2012). In addition, it would be of great interest to examine if hSpindly alone is sufficient to recruit dynein/dynactin to the kinetochores in the absence of the RZZ complex or whether the two co-operate with each other to recruit the dynein/dynactin complex.

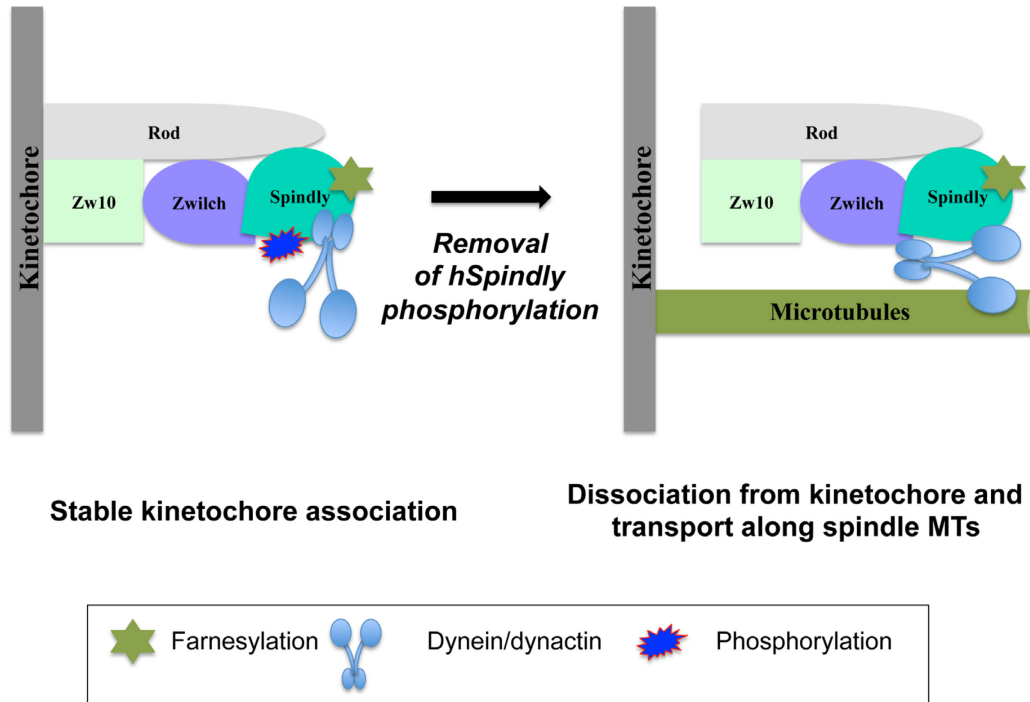


Figure 4.17: Model of hSpindly phosphorylation regulating its kinetochore localization pattern.

hSpindly localizes to unattached kinetochores at prophase downstream of the RZZ complex through an interaction mediated by hSpindly farnesylation. hSpindly further recruits dynein/dynactin complex through its interaction with the hp50 subunit of dynactin (not depicted). Once the kinetochore establishes an attachment with MTs, hSpindly is unphosphorylated which promotes its dissociation from the kinetochores and transport along the MTs through an unknown mechanism.

Chapter 5 Discussion

Portions of this chapter have been reproduced from Moudgil et al., *Cell Cycle*, 2015, Volume 14, Issue 14, pp 2185-2186

5.1 Synopsis

The mitotic checkpoint, conserved from yeast to humans, delays the onset of anaphase until all chromosomes are aligned at the metaphase plate ensuring equal chromosome segregation. The RZZ complex, an essential mitotic checkpoint component present only in higher eukaryotes regulates checkpoint activation and silencing. Checkpoint activation occurs by RZZ mediated Mad1-Mad2 kinetochore recruitment (through an unknown mechanism) whereas checkpoint silencing is by dynein/dynactin kinetochore recruitment through Spindly (Figure 5.1). Human Spindly recruits dynein to kinetochores facilitating dynein binding to dynactin, a regulatory factor of dynein (Chan et al., 2009; McKenney et al., 2014). Exactly how hSpindly is recruited to kinetochores remains unknown.

I undertook a structure-function study of hSpindly. The work presented in this thesis defines the kinetochore localization domain of Spindly, thereby establishing a novel role for protein lipidation, specifically farnesylation, in regulating human kinetochore protein assembly and checkpoint signaling. I have demonstrated that hSpindly is farnesylated *in vivo* and that this lipid modification is required for its interaction with the RZZ complex (Figure 3.23). To date, farnesylation has only been reported to modulate protein-protein interaction strength but here I present for the first time that farnesylation is essential for the interaction of hSpindly with the RZZ complex and its subsequent kinetochore localization. Furthermore, I concluded that the mitotic effects of FTIs are essentially due to the loss of hSpindly function. In the second half of this thesis, I have shown that the hSpindly kinetochore residency pattern varies between prometaphase and metaphase and is perhaps regulated by phosphorylation (Figure 4.17). I also showed that hSpindly interacts with the p50 subunit of dynactin. In the next sections, I will discuss the results and their implications in a broader perspective along with speculations on future directions.

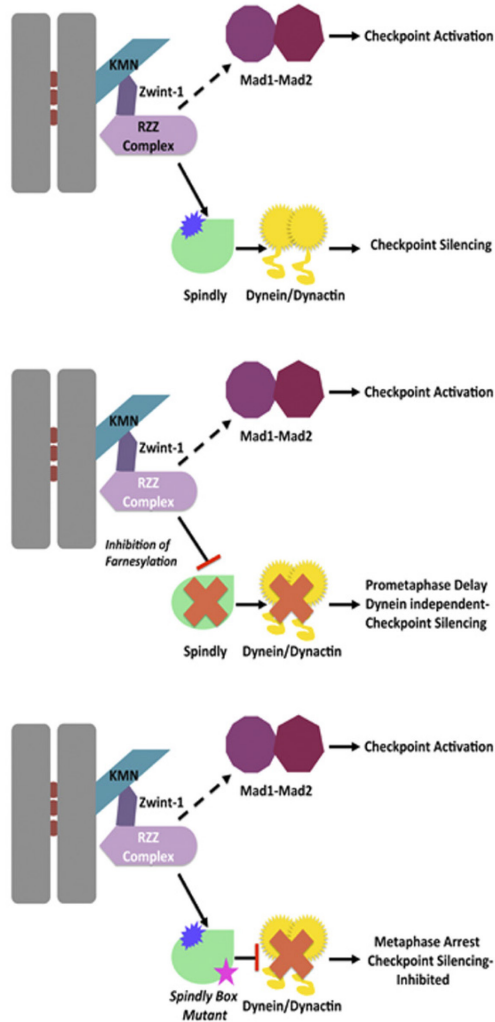


Figure 5.1: Farnesylation targets hSpindly to kinetochores and hSpindly regulates the checkpoint silencing pathways.

The RZZ complex recruits hSpindly to kinetochores and this interaction is regulated by hSpindly farnesylation. Mad1-Mad2 kinetochore localization is also dependent on the RZZ complex through an unknown mechanism (indicated by dotted line). hSpindly acts as an adapter for the dynein/dynactin complex and recruits it to the kinetochores. Inhibition of farnesylation prevents RZZ/hSpindly interaction, and the kinetochore localization of hSpindly and the dynein/dynactin complex leading to prometaphase delay. The checkpoint is silenced by a dynein independent mechanism in the absence of hSpindly kinetochore localization. Spindly box point mutants localize to kinetochores but do not recruit dynein/dynactin and the checkpoint is not silenced. (Moudgil and Chan, 2015)

5.2 hSpindly Kinetochores Localization

The kinetochore recruitment of hSpindly relies on RZZ complex kinetochore localization (Chan et al., 2009). Using a hSpindly mutant library (truncations, random insertions, deletions and substitutions), I have determined that 294-605 aa of hSpindly are required and sufficient for kinetochore localization. Mutations of the phosphorylation sites within the kinetochore localization domain do not affect its kinetochore localization ability (chapter 4) indicating that hSpindly phosphorylation is not required for its kinetochore localization. Interestingly, I found hSpindly mutants (N4, O, del592-596aa, and Q601A) localized to kinetochores only in cells treated with vinblastine, indicating that when these residues are mutated, hSpindly has low kinetochore binding affinity (Moudgil et al., 2015). These mutants are of particular interest since they show that hSpindly kinetochore binding is more like a graded phenomenon rather than a simple on/off mechanism. Multiple residues contribute to efficient binding and these specific mutants have the capability to bind kinetochores only under stringent conditions (vinblastine treatment). There are a few explanations for the kinetochore localization of these mutants. The simplest idea is that these residues may be required for the proper folding of the protein and somehow modulate hSpindly/RZZ complex interaction. Considering that membrane proteins undergoing farnesylation also require certain specific residues upstream of the CAAX motif for efficient membrane binding, the C-terminal hSpindly mutants with mutations upstream of the CAAX motif might be modulating its kinetochore binding affinity (Ahearn et al., 2012; Apolloni et al., 2000; Choy et al., 1999; Hancock et al., 1990). One cannot rule out the possibility that these mutants are readily transported to spindle poles from kinetochores resulting in no accumulation at kinetochores in untreated prometaphase cells. Future live-cell imaging studies of cells transfected with these mutants will distinguish between these possibilities and help us understand the contribution of these residues in kinetochore binding affinity.

5.3 hSpindly and the RZZ Complex Connections

Deletions in residues 596-605, or substitution of the C-terminal cysteine were not tolerated indicating their importance in hSpindly kinetochore localization, with the C-terminal cysteine being essential (Barisic et al., 2010; Moudgil et al., 2015). These hSpindly C-terminal residues contain a CAAX farnesylation motif that is conserved in vertebrates but not in worms and insects (Holland et al., 2015; Moudgil et al., 2015). Farnesyl transferase inhibitor (FTI) treatment prevents hSpindly kinetochore localization but not RZZ complex formation and kinetochore localization, and two previously known farnesylated mitotic proteins CENP-E and CENP-F localize to kinetochores (Moudgil et al., 2015). Holland et al. observed the same results in HeLa and DLD-1 cells (with loss of kinetochore dynein as expected) in a parallel study, although they reported CENP-E and CENP-F kinetochore levels were affected albeit to a lesser extent than hSpindly (Holland et al., 2015). The observed differences in the two studies pertaining to CENP-E and CENP-F kinetochore levels can be attributed to 48 h FTI treatment compared to 24 h in our study and these effects were more prominent in DLD-1 cells compared to HeLa. In addition, I showed that the CENP-F cysteine to alanine mutant (of the farnesylation motif) localized to kinetochores suggesting that CENP-F farnesylation is not essential for its kinetochore localization (Moudgil et al., 2015). I showed that hSpindly undergoes farnesylation *in vivo* and farnesylation is a pre-requisite for its interaction with the RZZ complex since hSpindly C602A mutant did not pull down RZZ complex subunits. Since *Drosophila* and *C. elegans* lack the farnesylation motif, the Spindly/RZZ interaction must be regulated by an unknown mechanism. It must be noted that both *Drosophila* and *C. elegans* Spindly contain a non-conventional CAAX motif in the middle of the protein and farnesylation is only reported to occur at the C-terminal cysteine residues. *Drosophila* Spindly is 782 aa with CVQQ (374:377 aa) and *C. elegans* Spindly is 480 aa with CQKY (124:127 aa). Whether these proteins are farnesylated on these motifs is not known or these motifs have lost their ability to undergo farnesylation during evolution is not

clear. Next, the focus should be on identifying the RZZ subunit that directly interacts with hSpindly and the domains of the proteins involved in the interaction.

Swapping Spindly's farnesylation motif with the CENP-E or CENP-F farnesylation motif did not affect its ability to undergo farnesylation and kinetochore localization. Since substitution with a geranylgeranylation motif did not target hSpindly to kinetochores, I concluded that hSpindly specifically requires farnesylation for kinetochore localization. I proposed that farnesylation induces a conformational change in hSpindly, which promotes its association with the RZZ complex. This possibility remains hypothetical and we shall also consider that the farnesyl group on hSpindly directly interacts with the RZZ complex. This idea is supported by the observation that RZZ/hSpindly interaction is inhibited by high salt and low amounts of detergent in the lysis buffer suggesting that ionic interactions are holding the two proteins together. We do not know whether RZZ/hSpindly interaction occurs in the cytosol or at kinetochores, which mandates further investigation. I showed that residues upstream of the hSpindly farnesylation motif are important for kinetochore binding affinity, which is analogous to membrane binding in RAS proteins. KRAS4B undergoes serine phosphorylation in the polybasic region upstream of the farnesylation site that facilitates its translocation from the plasma membrane to the endomembranes referred to as farnesyl-electrostatic switch (Bivona et al., 2006). In the case of hSpindly the hydrophobicity, charge and perhaps phosphorylation of CAAX upstream residues may contribute to kinetochore binding affinity. I observed that hSpindly non-phosphorylatable mutants showed premature transport to spindle poles indicating phosphorylation delays/inhibits hSpindly transport to poles (Chapter 4). Whether hSpindly undergoes a farnesyl-electrostatic switch to promote its release from kinetochores upon bi-orientation of chromosomes remains to be investigated.

Another important unknown is whether farnesylation of hSpindly is just targeting it to kinetochores or is involved in mitotic checkpoint signaling as well.

This is challenging to test since the non-farnesylated form of hSpindly does not localize to kinetochores. Carboxy-methylation on the farnesylated cysteine residue was shown to be important for RAS membrane localization as well as for RAS dependent ERK pathway activation (Chiu et al., 2004). The role of carboxy-methylation (following the attachment of farnesyl group on cysteine) in hSpindly kinetochore localization and signaling remains to be investigated.

Previous studies suggested that there is cross talk between hSpindly and the RZZ complex and that hSpindly stabilizes kinetochore-MT interactions by regulating the KMN complex MT-binding function through the RZZ complex (Barisic and Geley, 2011; Barisic et al., 2010; Gassmann et al., 2008; Gassmann et al., 2010). The hSpindly box point mutants that are unable to recruit the dynein/dynactin complex to kinetochores ameliorate kinetochore-MT attachment defects seen in hSpindly knockdown cells (Gassmann et al., 2010). In addition, co-depletion of the RZZ complex with hSpindly eliminated the kinetochore-MT defects seen in cells lacking hSpindly (Barisic et al., 2010). These studies suggest that the RZZ complex is negatively regulating kinetochore-MT attachment in the absence of hSpindly. Furthermore, Holland *et al.* reported that FTI treatment led to decreased kinetochore levels of the Zwilch subunit of the RZZ complex (Holland et al., 2015). However this study do not address if the decrease is due to loss of hSpindly kinetochore localization or an indirect effect of FTI treatment. Nonetheless, there is sufficient evidence to suggest that hSpindly affects the functions of the RZZ complex. Thus, hSpindly is not just a dynein/dynactin recruitment factor at kinetochores but also appears to contribute to checkpoint signaling through its kinetochore-MT attachment function. At present, it is unknown how Spindly regulates the RZZ complex function at the molecular level and this warrants further investigation.

5.3 hSpindly Kinetochore Residency Patterns

The RZZ complex subunits, Zw10 and Rod are dynamic at kinetochores (Defachelles et al., 2015; Famulski et al., 2008). Our lab showed that human Zw10 shows high turnover at metaphase kinetochores and is stable at

prometaphase kinetochores (Famulski et al., 2008). Since hSpindly interacts with the RZZ complex, I hypothesized that hSpindly kinetochore dynamics would be similar to that of hZw10. Strikingly, I discovered that hSpindly has a moderate exchange rate at prometaphase kinetochores with no kinetochore-MT attachments (treated with vinblastine) and only recovered to ~30% (Chapter 4). Similar to Zw10, hSpindly exchange rate was significantly increased at metaphase kinetochores with a $t_{1/2}$ of 0.98 seconds.

The underlying mechanism of regulation of hSpindly kinetochore dynamics is not clear but based on our hSpindly phospho mutants, I propose that dephosphorylation of hSpindly triggers its release from kinetochores. Since hSpindly is suggested to act as an adaptor between dynein and its cargo proteins, I propose that hSpindly release from kinetochores must be regulated to prevent premature transport of checkpoint proteins to kinetochores leading to premature checkpoint silencing. Specifically, I envision a scenario where establishment of bi-polar attachments results in removal of hSpindly phosphorylation and the unphosphorylated form of hSpindly is released rapidly from the kinetochores along with other checkpoint proteins. This can be achieved in two different ways: first, phosphorylation of hSpindly might be merely required for strong kinetochore binding affinity due to its charge properties and second, removal of hSpindly phosphorylation may induce a conformational change promoting its interaction with the dynein/dynactin complex and transport to spindle poles. Live-cell imaging and FRAP studies of hSpindly phospho mutants will shed more light on the mechanism of hSpindly kinetochore turnover.

It also appears that premature transport of hSpindly mutants affects its release from spindle poles since I observed that the hSpindly non-phosphorylatable mutants were present at spindle poles in some anaphase cells (Chapter 4). I predict that the premature fast turnover of hSpindly phospho mutants at prometaphase may override the rate of its dissociation from spindle poles. The RZZ complex present at spindle poles has been shown to remain active in terms of checkpoint signaling (Famulski et al., 2011). Similarly, I speculate that

the presence of hSpindly at spindle poles in anaphase cells might prevent the dissociation of some other checkpoint proteins as well. Future work to study the effects of persistent hSpindly presence at spindle poles during anaphase could address this possibility.

5.4 Role of hSpindly in Checkpoint Silencing

hSpindly recruits the dynein/dynactin complex to kinetochores (Chan et al., 2009) and has been shown to act as an adapter protein between dynein and dynactin (McKenney et al., 2014). The physical association of dynein with its co-activator dynactin through Spindly promotes its motility along MTs. Therefore, one would predict that Spindly directly interacts with both dynein and dynactin. Indeed, using yeast 2-hybrid I was able to show that hSpindly interacts directly with the p50 subunit of dynactin. In a recent study, recombinant Spindly immunoprecipitated dynein and dynactin from pig brain lysates and RPE1 cell lysates (McKenney et al., 2014). Our results suggest that hSpindly interacts with hp50 through two independent domains, one of which is different from its kinetochore localization domain. I reveal hp50/dynamitin as a novel interaction partner of hSpindly although this interaction needs to be confirmed in a biochemical assay.

Cells rely on dynein-mediated transport of checkpoint proteins to spindle poles for checkpoint silencing. In hSpindly-depleted cells, dynein/dynactin does not localize to kinetochores, but checkpoint silences through an unknown mechanisms, perhaps involving phosphatases or p31^{comet} (Habu et al., 2002; Hagan et al., 2011). Preventing hSpindly kinetochore dissociation at metaphase prevents checkpoint inactivation as seen with Spindly box mutants. Linking these two observations, I propose that hSpindly acts as a guard that allows removal of checkpoint proteins only through dynein/dynactin. Alternative checkpoint silencing pathways can participate only when hSpindly is removed from kinetochores. How does hSpindly kinetochore localization restrict the activation of dynein-independent checkpoint activation is not clear. Checkpoint proteins are removed only from bi-oriented chromosomes in hSpindly knockdown cells. How

the dynein independent checkpoint silencing pathway is activated in a timely manner in hSpindly-depleted cells is poorly understood. This model infers that hSpindly kinetochore localization regulates both dynein checkpoint silencing as well as dynein independent checkpoint silencing. Since hSpindly plays such a crucial role in checkpoint silencing, in future it will be important to understand hSpindly checkpoint signaling in depth.

5.5 hSpindly Cytoplasmic Function

Live-cell imaging studies comparing the mitotic phenotype of hSpindly knockdown and FTI-treated cells concluded that the mitotic effects of FTIs are essentially due to the loss of hSpindly function although CENP-E and CENP-F may also contribute to some extent (Holland et al., 2015; Moudgil et al., 2015). Our results showed that the prolonged duration of mitosis is more pronounced in hSpindly knockdown cells compared to FTI-treated cells (with no hSpindly kinetochore localization). For most checkpoint proteins including hSpindly, checkpoint signaling ability is contingent upon their kinetochore localization. However, our data show that the presence of cytoplasmic hSpindly in FTI-treated cells leads to faster checkpoint silencing compared to loss of hSpindly protein in hSpindly knockdown cells. This idea is further supported by the Holland *et al.* study, where they showed that the mitotic duration of 79 min in hSpindly-depleted cells was decreased to 64 min when rescued with hSpindly C602A mutant (unable to undergo farnesylation). Combining these two observations, cytoplasmic hSpindly appears to contribute to checkpoint silencing through an unknown mechanism. Since C602A and cytosolic hSpindly in FTI-treated cells is not farnesylated, I propose that the cytosolic function of hSpindly is not dependent on its farnesylation. Consistent with our hypothesis of cytosolic function of hSpindly, a few studies have previously reported cytosolic functions of BubR1 and Mps1, independent of their kinetochore localization. A BubR1 non-kinetochore-localizing mutant retains its mitotic function of cdc20 inhibition (Malureanu et al., 2009). Cytosolic Mps1 was shown to be required for cdc20 inhibition during interphase (Maciejowski et al., 2010). In agreement with these

studies, a later study showed that nuclear pore bound Mad-1-Mad-2 can generate MCC in interphase cells and inhibit APC/C^{cdc20} in the cytoplasm (Rodriguez-Bravo et al., 2014). Further investigation is needed to determine whether cytoplasmic hSpindly plays a role in checkpoint silencing.

5.6 Farnesylation and mitotic checkpoint inhibition through Spindly for cancer treatment

FTIs were enthusiastically developed to prevent Ras protein family activation as Ras is mutated in 30% of all human cancers. K-Ras and N-Ras mutations are more prevalent in cancer as compared to H-Ras, and both K-Ras and N-Ras are geranyl-geranylated in the presence of FTIs to retain their biological function. Surprisingly, FTIs showed significant anti-tumor activity in a large subset of cell lines without Ras mutations in pre-clinical in vitro studies (End et al., 2001; Sepp-Lorenzino et al., 1995). FTIs also variably modulated cell cycle in human tumor cell lines inducing either G2-M arrest in most of the cell lines or G1 arrest in cell lines with activated H-Ras (Ashar et al., 2001). FTIs were effective against both sets of cell lines in the latter study indicating FTIs can prevent tumor progression by targeting two different biological pathways. Furthermore, Crespo et al. have shown that FTI-2153 delays prometaphase to metaphase transition during mitosis by inhibiting the formation of bipolar spindle (Crespo et al., 2001). FTIs have shown anti-tumor activity in transgenic mouse models with spontaneous tumor occurrence (Liu et al., 1998; Mangues et al., 1998; Omer et al., 2000) as well as in mice with chemically induced lung tumors (Gunning et al., 2003; Lantry et al., 2000). FTIs induced tumor regression in in vivo xenograft tumor mouse models with or without Ras mutations (End et al., 2001; Liu et al., 1998; Rose et al., 2001). Regardless of the evidence demonstrating Ras independent effectiveness of FTIs, most studies considered Ras as a main FTI target for evaluating FTIs as anti-cancer drugs. In spite of significant success in preclinical studies, FTIs showed effectiveness in hematological malignancies in phase II (Cortes et al., 2005) but not in phase III trials (Hamilton et al., 2010), malignant glioma (Cloughesy et al., 2006) and in

breast cancer (Johnston and Kelland, 2001). FTI phase III studies reported negative results but these studies were conducted in advanced or relapsed tumors. These negative results led to the ultimate demise of FTIs as anti-cancer drugs. It is not clear why FTIs failed in clinical trials despite of impressive preclinical results. FTIs inhibited tumor progression in certain specific types of cancers but their molecular targets remained unknown. We still lack a biological understanding of FTI mechanism of action in responsive versus non-responsive tumors.

Here we show that hSpindly, a kinetochore protein with mitotic checkpoint function, requires farnesylation to become functionally active. Knockdown of hSpindly has been shown to cause chromosome missegregation and delayed mitosis with prolonged prometaphase and metaphase (Chan et al., 2009; Gassmann et al., 2010; Moudgil et al., 2015). Chromosome missegregation often leads to aneuploidy, which is a hallmark of most solid tumors. The mitotic checkpoint has been an attractive target for many successful clinical chemotherapy agents such as taxanes (microtubule-destabilizing agents) and the vinca alkaloids (microtubule-destabilizing agents). These drugs induce mitotic-checkpoint dependent arrest, which leads to cell death. These anti-mitotic drugs are effective against a wide variety of cancers but also cause side effects affecting vesicular trafficking, axonal transport and maintenance of cytoskeleton functions (Schmidt and Bastians, 2007). These side effects can be eliminated with the development of novel drugs that inhibit the progression of mitosis but do not affect microtubules in non-dividing cells. FTIs targeting hSpindly function represent an important novel avenue. Since previous FTI led clinical studies have demonstrated negative results, it will be important to analyze if hSpindly can be used as a prognostic marker for the selection of patients receiving FTI treatment. Interestingly, FTIs have been shown to sensitize tumor cells to paclitaxel-induced mitotic arrest (Moasser et al., 1998; Shi et al., 2000), and work synergistically with epothilones (MT destabilizing drug) (Sepp-Lorenzino et al., 1999) and cisplatin (Adjei et al., 2001). Furthermore, FTI SCH66336 in combination with paclitaxel demonstrated partial response in taxane resistant patients (Mazieres et

al., 2004). Scientists in the past have attributed the failure of FTIs to poor patient selection criteria and to an unidentified farnesylation target (Ochocki and Distefano, 2013; Palsuledesai and Distefano, 2015). These FTI trials ignored the observation that K-RAS (the most frequently mutated Ras in cancer patients) and N-RAS proteins can become substrates for geranylgeranyl transferase and generate geranylgeranylated forms that retain biological function. This raises the question whether hSpindly is a potential biomarker especially in FTI sensitive cancer cell lines in which FTIs induced cell death by G2-M arrest (Ashar et al., 2001). Therefore, we propose that expression of hSpindly shall be examined in various cancers and furthermore investigate if hSpindly can be used as a prognostic marker in future for FTI treatment. FTIs have shown therapeutic potential in Progeria patients, and are being explored for malaria, African sleeping sickness and hepatitis diseases {reviewed in (Ochocki and Distefano, 2013)}. However the effect of FTIs on hSpindly function in mitosis, and hence in the maintenance of genomic integrity should not be ignored.

In spite of vast advances in the field of kinetochore assembly mechanism and mitotic checkpoint signaling, we still strive for answers to many questions. Based on our and other groups' studies, hSpindly likely plays multiple roles in checkpoint signaling rather than just recruiting the dynein/dynactin complex as originally proposed. My work supports an important novel role of farnesylation in kinetochore assembly and reinforces the role of phosphorylation in the regulation of checkpoint signaling.

References

- Abrieu, A., L. Magnaghi-Jaulin, J.A. Kahana, M. Peter, A. Castro, S. Vigneron, T. Lorca, D.W. Cleveland, and J.C. Labbe. 2001. Mps1 is a kinetochore-associated kinase essential for the vertebrate mitotic checkpoint. *Cell*. 106:83-93.
- Adjei, A.A., J.N. Davis, L.M. Bruzek, C. Erlichman, and S.H. Kaufmann. 2001. Synergy of the protein farnesyltransferase inhibitor SCH66336 and cisplatin in human cancer cell lines. *Clin Cancer Res*. 7:1438-1445.
- Ahearn, I.M., K. Haigis, D. Bar-Sagi, and M.R. Philips. 2012. Regulating the regulator: post-translational modification of RAS. *Nat Rev Mol Cell Biol*. 13:39-51.
- Ahonen, L.J., M.J. Kallio, J.R. Daum, M. Bolton, I.A. Manke, M.B. Yaffe, P.T. Stukenberg, and G.J. Gorbsky. 2005. Polo-like kinase 1 creates the tension-sensing 3F3/2 phosphoepitope and modulates the association of spindle-checkpoint proteins at kinetochores. *Curr Biol*. 15:1078-1089.
- Albertson, D.G., and J.N. Thomson. 1993. Segregation of holocentric chromosomes at meiosis in the nematode, *Caenorhabditis elegans*. *Chromosome Res*. 1:15-26.
- Alonso, A., R. Mahmood, S. Li, F. Cheung, K. Yoda, and P.E. Warburton. 2003. Genomic microarray analysis reveals distinct locations for the CENP-A binding domains in three human chromosome 13q32 neocentromeres. *Hum Mol Genet*. 12:2711-2721.
- Amano, M., A. Suzuki, T. Hori, C. Backer, K. Okawa, I.M. Cheeseman, and T. Fukagawa. 2009. The CENP-S complex is essential for the stable assembly of outer kinetochore structure. *J Cell Biol*. 186:173-182.
- Aplan, P.D. 2006. Causes of oncogenic chromosomal translocation. *Trends Genet*. 22:46-55.
- Apolloni, A., I.A. Prior, M. Lindsay, R.G. Parton, and J.F. Hancock. 2000. H-ras but not K-ras traffics to the plasma membrane through the exocytic pathway. *Mol Cell Biol*. 20:2475-2487.
- Arasaki, K., K. Tani, T. Yoshimori, D.J. Stephens, and M. Tagaya. 2007. Nordihydroguaiaretic acid affects multiple dynein-dynactin functions in interphase and mitotic cells. *Mol Pharmacol*. 71:454-460.
- Archambault, V., and D.M. Glover. 2009. Polo-like kinases: conservation and divergence in their functions and regulation. *Nat Rev Mol Cell Biol*. 10:265-275.
- Ashar, H.R., L. James, K. Gray, D. Carr, S. Black, L. Armstrong, W.R. Bishop, and P. Kirschmeier. 2000. Farnesyl transferase inhibitors block the farnesylation of CENP-E and CENP-F and alter the association of CENP-E with the microtubules. *J Biol Chem*. 275:30451-30457.
- Ashar, H.R., L. James, K. Gray, D. Carr, M. McGuirk, E. Maxwell, S. Black, L. Armstrong, R.J. Doll, A.G. Taveras, W.R. Bishop, and P. Kirschmeier. 2001. The farnesyl transferase inhibitor SCH 66336 induces a G(2) --> M or G(1) pause in sensitive human tumor cell lines. *Exp Cell Res*. 262:17-27.

- Aumais, J.P., S.N. Williams, W. Luo, M. Nishino, K.A. Caldwell, G.A. Caldwell, S.H. Lin, and L.Y. Yu-Lee. 2003. Role for NudC, a dynein-associated nuclear movement protein, in mitosis and cytokinesis. *J Cell Sci.* 116:1991-2003.
- Bader, J.R., and K.T. Vaughan. 2010. Dynein at the kinetochore: Timing, Interactions and Functions. *Semin Cell Dev Biol.* 21:269-275.
- Barisic, M., and S. Geley. 2011. Spindly switch controls anaphase: spindly and RZZ functions in chromosome attachment and mitotic checkpoint control. *Cell Cycle.* 10:449-456.
- Barisic, M., B. Sohm, P. Mikolcevic, C. Wandke, V. Rauch, T. Ringer, M. Hess, G. Bonn, and S. Geley. 2010. Spindly/CCDC99 is required for efficient chromosome congression and mitotic checkpoint regulation. *Mol Biol Cell.* 21:1968-1981.
- Barr, A.R., and F. Gergely. 2007. Aurora-A: the maker and breaker of spindle poles. *J Cell Sci.* 120:2987-2996.
- Basto, R., R. Gomes, and R.E. Karess. 2000. Rough deal and Zw10 are required for the metaphase checkpoint in *Drosophila*. *Nat Cell Biol.* 2:939-943.
- Basto, R., J. Lau, T. Vinogradova, A. Gardiol, C.G. Woods, A. Khodjakov, and J.W. Raff. 2006. Flies without centrioles. *Cell.* 125:1375-1386.
- Basto, R., F. Scaerou, S. Mische, E. Wojcik, C. Lefebvre, R. Gomes, T. Hays, and R. Karess. 2004. In vivo dynamics of the rough deal checkpoint protein during *Drosophila* mitosis. *Curr Biol.* 14:56-61.
- Basu, J., H. Bousbaa, E. Logarinho, Z. Li, B.C. Williams, C. Lopes, C.E. Sunkel, and M.L. Goldberg. 1999. Mutations in the essential spindle checkpoint gene *bub1* cause chromosome missegregation and fail to block apoptosis in *Drosophila*. *J Cell Biol.* 146:13-28.
- Bayliss, R., T. Sardon, I. Vernos, and E. Conti. 2003. Structural basis of Aurora-A activation by TPX2 at the mitotic spindle. *Mol Cell.* 12:851-862.
- Berndt, N., A.D. Hamilton, and S.M. Sebti. 2011. Targeting protein prenylation for cancer therapy. *Nat Rev Cancer.* 11:775-791.
- Bettencourt-Dias, M., and D.M. Glover. 2007. Centrosome biogenesis and function: centrosomes brings new understanding. *Nat Rev Mol Cell Biol.* 8:451-463.
- Bhattacharya, S., L. Chen, J.R. Broach, and S. Powers. 1995. Ras membrane targeting is essential for glucose signaling but not for viability in yeast. *Proc Natl Acad Sci U S A.* 92:2984-2988.
- Bivona, T.G., S.E. Quatela, B.O. Bodemann, I.M. Ahearn, M.J. Soskis, A. Mor, J. Miura, H.H. Wiener, L. Wright, S.G. Saba, D. Yim, A. Fein, I. Perez de Castro, C. Li, C.B. Thompson, A.D. Cox, and M.R. Philips. 2006. PKC regulates a farnesyl-electrostatic switch on K-Ras that promotes its association with Bcl-XL on mitochondria and induces apoptosis. *Mol Cell.* 21:481-493.
- Blangy, A., H.A. Lane, P. d'Herin, M. Harper, M. Kress, and E.A. Nigg. 1995. Phosphorylation by p34cdc2 regulates spindle association of human Eg5, a

- kinesin-related motor essential for bipolar spindle formation in vivo. *Cell*. 83:1159-1169.
- Blower, M.D., and G.H. Karpen. 2001. The role of *Drosophila* CID in kinetochore formation, cell-cycle progression and heterochromatin interactions. *Nat Cell Biol*. 3:730-739.
- Blower, M.D., B.A. Sullivan, and G.H. Karpen. 2002. Conserved organization of centromeric chromatin in flies and humans. *Dev Cell*. 2:319-330.
- Bock, L.J., C. Pagliuca, N. Kobayashi, R.A. Grove, Y. Oku, K. Shrestha, C. Alfieri, C. Golfieri, A. Oldani, M. Dal Maschio, R. Bermejo, T.R. Hazbun, T.U. Tanaka, and P. De Wulf. 2012. Cnn1 inhibits the interactions between the KMN complexes of the yeast kinetochore. *Nat Cell Biol*. 14:614-624.
- Bolzer, A., G. Kreth, I. Solovei, D. Koehler, K. Saracoglu, C. Fauth, S. Muller, R. Eils, C. Cremer, M.R. Speicher, and T. Cremer. 2005. Three-dimensional maps of all chromosomes in human male fibroblast nuclei and prometaphase rosettes. *PLoS Biol*. 3:e157.
- Booden, M.A., D.S. Sakaguchi, and J.E. Buss. 2000. Mutation of Ha-Ras C terminus changes effector pathway utilization. *J Biol Chem*. 275:23559-23568.
- Braunstein, I., S. Miniowitz, Y. Moshe, and A. Hershko. 2007. Inhibitory factors associated with anaphase-promoting complex/cylosome in mitotic checkpoint. *Proc Natl Acad Sci U S A*. 104:4870-4875.
- Brenner, S., D. Pepper, M.W. Berns, E. Tan, and B.R. Brinkley. 1981. Kinetochore structure, duplication, and distribution in mammalian cells: analysis by human autoantibodies from scleroderma patients. *J Cell Biol*. 91:95-102.
- Brinkley, B.R., and E. Stubblefield. 1966. The fine structure of the kinetochore of a mammalian cell in vitro. *Chromosoma*. 19:28-43.
- Brust-Mascher, I., G. Civelekoglu-Scholey, M. Kwon, A. Mogilner, and J.M. Scholey. 2004. Model for anaphase B: role of three mitotic motors in a switch from poleward flux to spindle elongation. *Proc Natl Acad Sci U S A*. 101:15938-15943.
- Bucciarelli, E., M.G. Giansanti, S. Bonaccorsi, and M. Gatti. 2003. Spindle assembly and cytokinesis in the absence of chromosomes during *Drosophila* male meiosis. *J Cell Biol*. 160:993-999.
- Buchwitz, B.J., K. Ahmad, L.L. Moore, M.B. Roth, and S. Henikoff. 1999. A histone-H3-like protein in *C. elegans*. *Nature*. 401:547-548.
- Buffin, E., C. Lefebvre, J. Huang, M.E. Gagou, and R.E. Karess. 2005. Recruitment of Mad2 to the kinetochore requires the Rod/Zw10 complex. *Curr Biol*. 15:856-861.
- Busson, S., D. Dujardin, A. Moreau, J. Dompierre, and J.R. De Mey. 1998. Dynein and dynactin are localized to astral microtubules and at cortical sites in mitotic epithelial cells. *Curr Biol*. 8:541-544.

- Cahill, D.P., C. Lengauer, J. Yu, G.J. Riggins, J.K. Willson, S.D. Markowitz, K.W. Kinzler, and B. Vogelstein. 1998. Mutations of mitotic checkpoint genes in human cancers. *Nature*. 392:300-303.
- Carazo-Salas, R.E., O.J. Gruss, I.W. Mattaj, and E. Karsenti. 2001. Ran-GTP coordinates regulation of microtubule nucleation and dynamics during mitotic-spindle assembly. *Nat Cell Biol*. 3:228-234.
- Carboni, J.M., N. Yan, A.D. Cox, X. Bustelo, S.M. Graham, M.J. Lynch, R. Weinmann, B.R. Seizinger, C.J. Der, M. Barbacid, and et al. 1995. Farnesyltransferase inhibitors are inhibitors of Ras but not R-Ras2/TC21, transformation. *Oncogene*. 10:1905-1913.
- Carrico, D., J. Ohkanda, H. Kendrick, K. Yokoyama, M.A. Blaskovich, C.J. Bucher, F.S. Buckner, W.C. Van Voorhis, D. Chakrabarti, S.L. Croft, M.H. Gelb, S.M. Sebt, and A.D. Hamilton. 2004. In vitro and in vivo antimalarial activity of peptidomimetic protein farnesyltransferase inhibitors with improved membrane permeability. *Bioorg Med Chem*. 12:6517-6526.
- Carroll, C.W., K.J. Milks, and A.F. Straight. 2010. Dual recognition of CENP-A nucleosomes is required for centromere assembly. *J Cell Biol*. 189:1143-1155.
- Casey, P.J., P.A. Solski, C.J. Der, and J.E. Buss. 1989. p21ras is modified by a farnesyl isoprenoid. *Proc Natl Acad Sci U S A*. 86:8323-8327.
- Chan, C.S., and D. Botstein. 1993. Isolation and characterization of chromosome-gain and increase-in-ploidy mutants in yeast. *Genetics*. 135:677-691.
- Chan, G.K., S.A. Jablonski, D.A. Starr, M.L. Goldberg, and T.J. Yen. 2000. Human Zw10 and ROD are mitotic checkpoint proteins that bind to kinetochores. *Nat Cell Biol*. 2:944-947.
- Chan, G.K., S.A. Jablonski, V. Sudakin, J.C. Hittle, and T.J. Yen. 1999. Human BUBR1 is a mitotic checkpoint kinase that monitors CENP-E functions at kinetochores and binds the cyclosome/APC. *J Cell Biol*. 146:941-954.
- Chan, G.K., S.T. Liu, and T.J. Yen. 2005. Kinetochores structure and function. *Trends Cell Biol*. 15:589-598.
- Chan, G.K., B.T. Schaar, and T.J. Yen. 1998. Characterization of the kinetochores binding domain of CENP-E reveals interactions with the kinetochores proteins CENP-F and hBUBR1. *J Cell Biol*. 143:49-63.
- Chan, G.K., and T.J. Yen. 2003. The mitotic checkpoint: a signaling pathway that allows a single unattached kinetochores to inhibit mitotic exit. *Prog Cell Cycle Res*. 5:431-439.
- Chan, J.Y. 2011. A clinical overview of centrosome amplification in human cancers. *Int J Biol Sci*. 7:1122-1144.
- Chan, Y.W., L.L. Fava, A. Uldschmid, M.H. Schmitz, D.W. Gerlich, E.A. Nigg, and A. Santamaria. 2009. Mitotic control of kinetochores-associated dynein and spindle orientation by human Spindly. *J Cell Biol*. 185:859-874.
- Chan, Y.W., A.A. Jeyapakash, E.A. Nigg, and A. Santamaria. 2012. Aurora B controls kinetochores-microtubule attachments by inhibiting Ska complex-KMN network interaction. *J Cell Biol*. 196:563-571.

- Charron, G., L.K. Tsou, W. Maguire, J.S. Yount, and H.C. Hang. 2011. Alkynyl-farnesol reporters for detection of protein S-prenylation in cells. *Mol Biosyst.* 7:67-73.
- Cheeseman, I.M. 2014. The kinetochore. *Cold Spring Harb Perspect Biol.* 6:a015826.
- Cheeseman, I.M., S. Anderson, M. Jwa, E.M. Green, J. Kang, J.R. Yates, 3rd, C.S. Chan, D.G. Drubin, and G. Barnes. 2002. Phospho-regulation of kinetochore-microtubule attachments by the Aurora kinase Ipl1p. *Cell.* 111:163-172.
- Cheeseman, I.M., J.S. Chappie, E.M. Wilson-Kubalek, and A. Desai. 2006. The conserved KMN network constitutes the core microtubule-binding site of the kinetochore. *Cell.* 127:983-997.
- Cheeseman, I.M., and A. Desai. 2008. Molecular architecture of the kinetochore-microtubule interface. *Nat Rev Mol Cell Biol.* 9:33-46.
- Cheeseman, I.M., S. Niessen, S. Anderson, F. Hyndman, J.R. Yates, 3rd, K. Oegema, and A. Desai. 2004. A conserved protein network controls assembly of the outer kinetochore and its ability to sustain tension. *Genes Dev.* 18:2255-2268.
- Chen, D., S. Ito, H. Yuan, T. Hyodo, K. Kadomatsu, M. Hamaguchi, and T. Senga. 2015. EML4 promotes the loading of NUDC to the spindle for mitotic progression. *Cell Cycle*:0.
- Chen, R.H. 2002. BubR1 is essential for kinetochore localization of other spindle checkpoint proteins and its phosphorylation requires Mad1. *J Cell Biol.* 158:487-496.
- Chi, Y.H., J.M. Ward, L.I. Cheng, J. Yasunaga, and K.T. Jeang. 2009. Spindle assembly checkpoint and p53 deficiencies cooperate for tumorigenesis in mice. *Int J Cancer.* 124:1483-1489.
- Chiu, V.K., J. Silletti, V. Dinsell, H. Wiener, K. Loukeris, G. Ou, M.R. Philips, and M.H. Pillinger. 2004. Carboxyl methylation of Ras regulates membrane targeting and effector engagement. *J Biol Chem.* 279:7346-7352.
- Choi, M., W. Kim, M.G. Cheon, C.W. Lee, and J.E. Kim. 2015. Polo-like kinase 1 inhibitor BI2536 causes mitotic catastrophe following activation of the spindle assembly checkpoint in non-small cell lung cancer cells. *Cancer Lett.* 357:591-601.
- Choy, E., V.K. Chiu, J. Silletti, M. Feoktistov, T. Morimoto, D. Michaelson, I.E. Ivanov, and M.R. Philips. 1999. Endomembrane trafficking of ras: the CAAX motif targets proteins to the ER and Golgi. *Cell.* 98:69-80.
- Ciferri, C., J. De Luca, S. Monzani, K.J. Ferrari, D. Ristic, C. Wyman, H. Stark, J. Kilmartin, E.D. Salmon, and A. Musacchio. 2005. Architecture of the human ndc80-hec1 complex, a critical constituent of the outer kinetochore. *J Biol Chem.* 280:29088-29095.
- Ciferri, C., S. Pasqualato, E. Screpanti, G. Varetto, S. Santaguida, G. Dos Reis, A. Maiolica, J. Polka, J.G. De Luca, P. De Wulf, M. Salek, J. Rappsilber, C.A. Moores, E.D. Salmon, and A. Musacchio. 2008. Implications for

- kinetochore-microtubule attachment from the structure of an engineered Ndc80 complex. *Cell*. 133:427-439.
- Cimini, D., and F. Degrossi. 2005. Aneuploidy: a matter of bad connections. *Trends Cell Biol*. 15:442-451.
- Civril, F., A. Wehenkel, F.M. Giorgi, S. Santaguida, A. Di Fonzo, G. Grigorean, F.D. Ciccarelli, and A. Musacchio. 2010. Structural analysis of the RZZ complex reveals common ancestry with multisubunit vesicle tethering machinery. *Structure*. 18:616-626.
- Clark, G.M., D.C. Allred, S.G. Hilsenbeck, G.C. Chamness, C.K. Osborne, D. Jones, and W.H. Lee. 1997. Mitosin (a new proliferation marker) correlates with clinical outcome in node-negative breast cancer. *Cancer Res*. 57:5505-5508.
- Clarke, L., and J. Carbon. 1983. Genomic substitutions of centromeres in *Saccharomyces cerevisiae*. *Nature*. 305:23-28.
- Cloughesy, T.F., P.Y. Wen, H.I. Robins, S.M. Chang, M.D. Groves, K.L. Fink, L. Junck, D. Schiff, L. Abrey, M.R. Gilbert, F. Lieberman, J. Kuhn, L.M. DeAngelis, M. Mehta, J.J. Raizer, W.K. Yung, K. Aldape, J. Wright, K.R. Lamborn, and M.D. Prados. 2006. Phase II trial of tipifarnib in patients with recurrent malignant glioma either receiving or not receiving enzyme-inducing antiepileptic drugs: a North American Brain Tumor Consortium Study. *J Clin Oncol*. 24:3651-3656.
- Collin, P., O. Nashchekina, R. Walker, and J. Pines. 2013. The spindle assembly checkpoint works like a rheostat rather than a toggle switch. *Nat Cell Biol*. 15:1378-1385.
- Compton, D.A. 1998. Focusing on spindle poles. *J Cell Sci*. 111 (Pt 11):1477-1481.
- Compton, D.A. 2000. Spindle assembly in animal cells. *Annu Rev Biochem*. 69:95-114.
- Cooke, C.A., B. Schaar, T.J. Yen, and W.C. Earnshaw. 1997. Localization of CENP-E in the fibrous corona and outer plate of mammalian kinetochores from prometaphase through anaphase. *Chromosoma*. 106:446-455.
- Cortes, J., S. Faderl, E. Estey, R. Kurzrock, D. Thomas, M. Beran, G. Garcia-Manero, A. Ferrajoli, F. Giles, C. Koller, S. O'Brien, J. Wright, S.A. Bai, and H. Kantarjian. 2005. Phase I study of BMS-214662, a farnesyl transferase inhibitor in patients with acute leukemias and high-risk myelodysplastic syndromes. *J Clin Oncol*. 23:2805-2812.
- Crespo, N.C., F. Delarue, J. Ohkanda, D. Carrico, A.D. Hamilton, and S.M. Sebt. 2002. The farnesyltransferase inhibitor, FTI-2153, inhibits bipolar spindle formation during mitosis independently of transformation and Ras and p53 mutation status. *Cell Death Differ*. 9:702-709.
- Crespo, N.C., J. Ohkanda, T.J. Yen, A.D. Hamilton, and S.M. Sebt. 2001. The farnesyltransferase inhibitor, FTI-2153, blocks bipolar spindle formation and chromosome alignment and causes prometaphase accumulation during mitosis of human lung cancer cells. *J Biol Chem*. 276:16161-16167.

- Dai, W., Q. Wang, T. Liu, M. Swamy, Y. Fang, S. Xie, R. Mahmood, Y.M. Yang, M. Xu, and C.V. Rao. 2004. Slippage of mitotic arrest and enhanced tumor development in mice with BubR1 haploinsufficiency. *Cancer Res.* 64:440-445.
- Date, D.A., A.C. Burrows, and M.K. Summers. 2014. Phosphorylation regulates the p31Comet-mitotic arrest-deficient 2 (Mad2) interaction to promote spindle assembly checkpoint (SAC) activity. *J Biol Chem.* 289:11367-11373.
- Daum, J.R., J.D. Wren, J.J. Daniel, S. Sivakumar, J.N. McAvoy, T.A. Potapova, and G.J. Gorbsky. 2009. Ska3 is required for spindle checkpoint silencing and the maintenance of chromosome cohesion in mitosis. *Curr Biol.* 19:1467-1472.
- De Antoni, A., C.G. Pearson, D. Cimini, J.C. Canman, V. Sala, L. Nezi, M. Mapelli, L. Sironi, M. Faretta, E.D. Salmon, and A. Musacchio. 2005. The Mad1/Mad2 complex as a template for Mad2 activation in the spindle assembly checkpoint. *Curr Biol.* 15:214-225.
- Defachelles, L., N. Raich, R. Terracol, X. Baudin, B. Williams, M. Goldberg, and R.E. Karess. 2015. RZZ and Mad1 dynamics in *Drosophila* mitosis. *Chromosome Res.*
- DeLuca, J.G., W.E. Gall, C. Ciferri, D. Cimini, A. Musacchio, and E.D. Salmon. 2006. Kinetochores microtubule dynamics and attachment stability are regulated by Hec1. *Cell.* 127:969-982.
- DeLuca, J.G., B. Moree, J.M. Hickey, J.V. Kilmartin, and E.D. Salmon. 2002. hNuf2 inhibition blocks stable kinetochores-microtubule attachment and induces mitotic cell death in HeLa cells. *J Cell Biol.* 159:549-555.
- Desai, A., P.S. Maddox, T.J. Mitchison, and E.D. Salmon. 1998. Anaphase A chromosome movement and poleward spindle microtubule flux occur at similar rates in *Xenopus* extract spindles. *J Cell Biol.* 141:703-713.
- Desai, A., and T.J. Mitchison. 1997. Microtubule polymerization dynamics. *Annu Rev Cell Dev Biol.* 13:83-117.
- Dick, A.E., and D.W. Gerlich. 2013. Kinetic framework of spindle assembly checkpoint signalling. *Nat Cell Biol.* 15:1370-1377.
- Dinarina, A., C. Pugieux, M.M. Corral, M. Loose, J. Spatz, E. Karsenti, and F. Nedelec. 2009. Chromatin shapes the mitotic spindle. *Cell.* 138:502-513.
- Ditchfield, C., V.L. Johnson, A. Tighe, R. Ellston, C. Haworth, T. Johnson, A. Mortlock, N. Keen, and S.S. Taylor. 2003. Aurora B couples chromosome alignment with anaphase by targeting BubR1, Mad2, and Cenp-E to kinetochores. *J Cell Biol.* 161:267-280.
- Dobles, M., V. Liberal, M.L. Scott, R. Benezra, and P.K. Sorger. 2000. Chromosome missegregation and apoptosis in mice lacking the mitotic checkpoint protein Mad2. *Cell.* 101:635-645.
- Dodding, M.P. 2014. Backseat drivers: Regulation of dynein motility. *Cell Res.* 24:1385-1386.

- Dolence, J.M., P.B. Cassidy, J.R. Mathis, and C.D. Poulter. 1995. Yeast protein farnesyltransferase: steady-state kinetic studies of substrate binding. *Biochemistry*. 34:16687-16694.
- Dong, Y., K.J. Vanden Beldt, X. Meng, A. Khodjakov, and B.F. McEwen. 2007. The outer plate in vertebrate kinetochores is a flexible network with multiple microtubule interactions. *Nat Cell Biol*. 9:516-522.
- Downward, J. 2003. Targeting RAS signalling pathways in cancer therapy. *Nat Rev Cancer*. 3:11-22.
- Doxsey, S. 2001. Re-evaluating centrosome function. *Nat Rev Mol Cell Biol*. 2:688-698.
- du Sart, D., M.R. Cancilla, E. Earle, J.I. Mao, R. Saffery, K.M. Tainton, P. Kalitsis, J. Martyn, A.E. Barry, and K.H. Choo. 1997. A functional neocentromere formed through activation of a latent human centromere and consisting of non-alpha-satellite DNA. *Nat Genet*. 16:144-153.
- Dujardin, D., U.I. Wacker, A. Moreau, T.A. Schroer, J.E. Rickard, and J.R. De Mey. 1998. Evidence for a role of CLIP-170 in the establishment of metaphase chromosome alignment. *J Cell Biol*. 141:849-862.
- Dumont, S., and T.J. Mitchison. 2009. Force and length in the mitotic spindle. *Curr Biol*. 19:R749-761.
- Earnshaw, W.C., and R.L. Bernat. 1991. Chromosomal passengers: toward an integrated view of mitosis. *Chromosoma*. 100:139-146.
- Earnshaw, W.C., and M. Carmena. 2003. A perfect funeral with no corpse. *J Cell Biol*. 160:989-990.
- Earnshaw, W.C., and N. Rothfield. 1985. Identification of a family of human centromere proteins using autoimmune sera from patients with scleroderma. *Chromosoma*. 91:313-321.
- Echeverri, C.J., B.M. Paschal, K.T. Vaughan, and R.B. Vallee. 1996. Molecular characterization of the 50-kD subunit of dynactin reveals function for the complex in chromosome alignment and spindle organization during mitosis. *J Cell Biol*. 132:617-633.
- Elia, A.E., P. Rellos, L.F. Haire, J.W. Chao, F.J. Ivins, K. Hoepker, D. Mohammad, L.C. Cantley, S.J. Smerdon, and M.B. Yaffe. 2003. The molecular basis for phosphodependent substrate targeting and regulation of Plks by the Polo-box domain. *Cell*. 115:83-95.
- Elledge, S.J. 1996. Cell cycle checkpoints: preventing an identity crisis. *Science*. 274:1664-1672.
- Elowe, S., K. Dulla, A. Uldschmid, X. Li, Z. Dou, and E.A. Nigg. 2010. Uncoupling of the spindle-checkpoint and chromosome-congression functions of BubR1. *J Cell Sci*. 123:84-94.
- Elowe, S., S. Hummer, A. Uldschmid, X. Li, and E.A. Nigg. 2007. Tension-sensitive Plk1 phosphorylation on BubR1 regulates the stability of kinetochore microtubule interactions. *Genes Dev*. 21:2205-2219.
- Elting, M.W., C.L. Hueschen, D.B. Udy, and S. Dumont. 2014. Force on spindle microtubule minus ends moves chromosomes. *J Cell Biol*. 206:245-256.

- Emre, D., R. Terracol, A. Poncet, Z. Rahmani, and R.E. Karess. 2011. A mitotic role for Mad1 beyond the spindle checkpoint. *J Cell Sci.* 124:1664-1671.
- End, D.W., G. Smets, A.V. Todd, T.L. Applegate, C.J. Fuery, P. Angibaud, M. Venet, G. Sanz, H. Poignet, S. Skrzat, A. Devine, W. Wouters, and C. Bowden. 2001. Characterization of the antitumor effects of the selective farnesyl protein transferase inhibitor R115777 in vivo and in vitro. *Cancer Res.* 61:131-137.
- Espeut, J., A. Gaussen, P. Bieling, V. Morin, S. Prieto, D. Fesquet, T. Surrey, and A. Abrieu. 2008. Phosphorylation relieves autoinhibition of the kinetochore motor Cenp-E. *Mol Cell.* 29:637-643.
- Estojak, J., R. Brent, and E.A. Golemis. 1995. Correlation of two-hybrid affinity data with in vitro measurements. *Mol Cell Biol.* 15:5820-5829.
- Eytan, E., I. Braunstein, D. Ganoh, A. Teichner, J.C. Hittle, T.J. Yen, and A. Hershko. 2008. Two different mitotic checkpoint inhibitors of the anaphase-promoting complex/cyclosome antagonize the action of the activator Cdc20. *Proc Natl Acad Sci U S A.* 105:9181-9185.
- Eytan, E., K. Wang, S. Miniowitz-Shemtov, D. Sitry-Shevah, S. Kaisari, T.J. Yen, S.T. Liu, and A. Hershko. 2014. Disassembly of mitotic checkpoint complexes by the joint action of the AAA-ATPase TRIP13 and p31(comet). *Proc Natl Acad Sci U S A.* 111:12019-12024.
- Famulski, J.K., and G.K. Chan. 2007. Aurora B kinase-dependent recruitment of hZW10 and hROD to tensionless kinetochores. *Curr Biol.* 17:2143-2149.
- Famulski, J.K., L. Vos, X. Sun, and G. Chan. 2008. Stable hZW10 kinetochore residency, mediated by hZwint-1 interaction, is essential for the mitotic checkpoint. *J Cell Biol.* 180:507-520.
- Famulski, J.K., L.J. Vos, J.B. Rattner, and G.K. Chan. 2011. Dynein/Dynactin-mediated transport of kinetochore components off kinetochores and onto spindle poles induced by nordihydroguaiaretic acid. *PLoS One.* 6:e16494.
- Fang, G., H. Yu, and M.W. Kirschner. 1998. The checkpoint protein MAD2 and the mitotic regulator CDC20 form a ternary complex with the anaphase-promoting complex to control anaphase initiation. *Genes Dev.* 12:1871-1883.
- Farnsworth, C.C., S.L. Wolda, M.H. Gelb, and J.A. Glomset. 1989. Human lamin B contains a farnesylated cysteine residue. *J Biol Chem.* 264:20422-20429.
- Faulkner, N.E., D.L. Dujardin, C.Y. Tai, K.T. Vaughan, C.B. O'Connell, Y. Wang, and R.B. Vallee. 2000. A role for the lissencephaly gene LIS1 in mitosis and cytoplasmic dynein function. *Nat Cell Biol.* 2:784-791.
- Fava, L.L., M. Kaulich, E.A. Nigg, and A. Santamaria. 2011. Probing the in vivo function of Mad1:C-Mad2 in the spindle assembly checkpoint. *Embo J.* 30:3322-3336.
- Feng, J., H. Huang, and T.J. Yen. 2006. CENP-F is a novel microtubule-binding protein that is essential for kinetochore attachments and affects the duration of the mitotic checkpoint delay. *Chromosoma.* 115:320-329.

- Fletcher, S., C.G. Cummings, K. Rivas, W.P. Katt, C. Horney, F.S. Buckner, D. Chakrabarti, S.M. Sebti, M.H. Gelb, W.C. Van Voorhis, and A.D. Hamilton. 2008. Potent, Plasmodium-selective farnesyltransferase inhibitors that arrest the growth of malaria parasites: structure-activity relationships of ethylenediamine-analogue scaffolds and homology model validation. *J Med Chem.* 51:5176-5197.
- Foltz, D.R., L.E. Jansen, B.E. Black, A.O. Bailey, J.R. Yates, 3rd, and D.W. Cleveland. 2006. The human CENP-A centromeric nucleosome-associated complex. *Nat Cell Biol.* 8:458-469.
- Fong, L.G., D. Frost, M. Meta, X. Qiao, S.H. Yang, C. Coffinier, and S.G. Young. 2006. A protein farnesyltransferase inhibitor ameliorates disease in a mouse model of progeria. *Science.* 311:1621-1623.
- Fourest-Lieuvin, A., L. Peris, V. Gache, I. Garcia-Saez, C. Juillan-Binard, V. Lantez, and D. Job. 2006. Microtubule regulation in mitosis: tubulin phosphorylation by the cyclin-dependent kinase Cdk1. *Mol Biol Cell.* 17:1041-1050.
- Fujita, Y., T. Hayashi, T. Kiyomitsu, Y. Toyoda, A. Kokubu, C. Obuse, and M. Yanagida. 2007. Priming of centromere for CENP-A recruitment by human hMis18alpha, hMis18beta, and M18BP1. *Dev Cell.* 12:17-30.
- Gascoigne, K.E., and I.M. Cheeseman. 2013. CDK-dependent phosphorylation and nuclear exclusion coordinately control kinetochore assembly state. *J Cell Biol.* 201:23-32.
- Gascoigne, K.E., K. Takeuchi, A. Suzuki, T. Hori, T. Fukagawa, and I.M. Cheeseman. 2011. Induced ectopic kinetochore assembly bypasses the requirement for CENP-A nucleosomes. *Cell.* 145:410-422.
- Gassmann, R., A. Essex, J.S. Hu, P.S. Maddox, F. Motegi, A. Sugimoto, S.M. O'Rourke, B. Bowerman, I. McLeod, J.R. Yates, 3rd, K. Oegema, I.M. Cheeseman, and A. Desai. 2008. A new mechanism controlling kinetochore-microtubule interactions revealed by comparison of two dynein-targeting components: SPDL-1 and the Rod/Zwilch/Zw10 complex. *Genes Dev.* 22:2385-2399.
- Gassmann, R., A.J. Holland, D. Varma, X. Wan, F. Civril, D.W. Cleveland, K. Oegema, E.D. Salmon, and A. Desai. 2010. Removal of Spindly from microtubule-attached kinetochores controls spindle checkpoint silencing in human cells. *Genes Dev.* 24:957-971.
- Ghomashchi, F., X. Zhang, L. Liu, and M.H. Gelb. 1995. Binding of prenylated and polybasic peptides to membranes: affinities and intervesicle exchange. *Biochemistry.* 34:11910-11918.
- Golan, A., Y. Yudkovsky, and A. Hershko. 2002. The cyclin-ubiquitin ligase activity of cyclosome/APC is jointly activated by protein kinases Cdk1-cyclin B and Plk. *J Biol Chem.* 277:15552-15557.
- Gordon, L.B., M.E. Kleinman, D.T. Miller, D.S. Neuberger, A. Giobbie-Hurder, M. Gerhard-Herman, L.B. Smoot, C.M. Gordon, R. Cleveland, B.D. Snyder, B. Fligor, W.R. Bishop, P. Statkevich, A. Regen, A. Sonis, S. Riley, C. Ploski, A. Correia, N. Quinn, N.J. Ullrich, A. Nazarian, M.G. Liang, S.Y.

- Huh, A. Schwartzman, and M.W. Kieran. 2012. Clinical trial of a farnesyltransferase inhibitor in children with Hutchinson-Gilford progeria syndrome. *Proc Natl Acad Sci U S A*. 109:16666-16671.
- Goshima, G., T. Kiyomitsu, K. Yoda, and M. Yanagida. 2003. Human centromere chromatin protein hMis12, essential for equal segregation, is independent of CENP-A loading pathway. *J Cell Biol*. 160:25-39.
- Gotlib, J. 2005. Farnesyltransferase inhibitor therapy in acute myelogenous leukemia. *Curr Hematol Rep*. 4:77-84.
- Grallert, A., E. Boke, A. Hagting, B. Hodgson, Y. Connolly, J.R. Griffiths, D.L. Smith, J. Pines, and I.M. Hagan. 2015. A PP1-PP2A phosphatase relay controls mitotic progression. *Nature*. 517:94-98.
- Gray, K.M., J.W. White, C. Costanzi, D. Gillespie, W.T. Schroeder, B. Calabretta, and G.F. Saunders. 1985. Recent amplification of an alpha satellite DNA in humans. *Nucleic Acids Res*. 13:521-535.
- Griffis, E.R., N. Stuurman, and R.D. Vale. 2007. Spindly, a novel protein essential for silencing the spindle assembly checkpoint, recruits dynein to the kinetochore. *J Cell Biol*. 177:1005-1015.
- Guacci, V., D. Koshland, and A. Strunnikov. 1997. A direct link between sister chromatid cohesion and chromosome condensation revealed through the analysis of MCD1 in *S. cerevisiae*. *Cell*. 91:47-57.
- Guimaraes, G.J., Y. Dong, B.F. McEwen, and J.G. Deluca. 2008. Kinetochore-microtubule attachment relies on the disordered N-terminal tail domain of Hec1. *Curr Biol*. 18:1778-1784.
- Gunawardane, R.N., S.B. Lizarraga, C. Wiese, A. Wilde, and Y. Zheng. 2000. gamma-Tubulin complexes and their role in microtubule nucleation. *Curr Top Dev Biol*. 49:55-73.
- Gunning, W.T., P.M. Kramer, R.A. Lubet, V.E. Steele, D.W. End, W. Wouters, and M.A. Pereira. 2003. Chemoprevention of benzo(a)pyrene-induced lung tumors in mice by the farnesyltransferase inhibitor R115777. *Clin Cancer Res*. 9:1927-1930.
- Gurden, M.D., A.J. Holland, W. van Zon, A. Tighe, M.A. Vergnolle, D.A. Andres, H.P. Spielmann, M. Malumbres, R.M. Wolthuis, D.W. Cleveland, and S.S. Taylor. 2010. Cdc20 is required for the post-anaphase, KEN-dependent degradation of centromere protein F. *J Cell Sci*. 123:321-330.
- Gyuris, J., E. Golemis, H. Chertkov, and R. Brent. 1993. Cdi1, a human G1 and S phase protein phosphatase that associates with Cdk2. *Cell*. 75:791-803.
- Habu, T., S.H. Kim, J. Weinstein, and T. Matsumoto. 2002. Identification of a MAD2-binding protein, CMT2, and its role in mitosis. *Embo J*. 21:6419-6428.
- Hagan, R.S., M.S. Manak, H.K. Buch, M.G. Meier, P. Meraldi, J.V. Shah, and P.K. Sorger. 2011. p31(comet) acts to ensure timely spindle checkpoint silencing subsequent to kinetochore attachment. *Mol Biol Cell*. 22:4236-4246.
- Hamilton, A., P. Gallipoli, E. Nicholson, and T.L. Holyoake. 2010. Targeted therapy in haematological malignancies. *J Pathol*. 220:404-418.

- Hancock, J.F., H. Paterson, and C.J. Marshall. 1990. A polybasic domain or palmitoylation is required in addition to the CAAX motif to localize p21ras to the plasma membrane. *Cell*. 63:133-139.
- Hanisch, A., H.H. Sillje, and E.A. Nigg. 2006. Timely anaphase onset requires a novel spindle and kinetochore complex comprising Ska1 and Ska2. *Embo J*. 25:5504-5515.
- Hanks, S., K. Coleman, S. Reid, A. Plaja, H. Firth, D. Fitzpatrick, A. Kidd, K. Mehes, R. Nash, N. Robin, N. Shannon, J. Tolmie, J. Swansbury, A. Irrthum, J. Douglas, and N. Rahman. 2004. Constitutional aneuploidy and cancer predisposition caused by biallelic mutations in BUB1B. *Nat Genet*. 36:1159-1161.
- Hardwick, K.G., E. Weiss, F.C. Luca, M. Winey, and A.W. Murray. 1996. Activation of the budding yeast spindle assembly checkpoint without mitotic spindle disruption. *Science*. 273:953-956.
- Harrington, J.J., G. Van Bokkelen, R.W. Mays, K. Gustashaw, and H.F. Willard. 1997. Formation of de novo centromeres and construction of first-generation human artificial microchromosomes. *Nat Genet*. 15:345-355.
- He, D., and B.R. Brinkley. 1996. Structure and dynamic organization of centromeres/prekinetochores in the nucleus of mammalian cells. *J Cell Sci*. 109 (Pt 11):2693-2704.
- He, X., S. Asthana, and P.K. Sorger. 2000. Transient sister chromatid separation and elastic deformation of chromosomes during mitosis in budding yeast. *Cell*. 101:763-775.
- Heald, R., R. Tournebize, T. Blank, R. Sandaltzopoulos, P. Becker, A. Hyman, and E. Karsenti. 1996. Self-organization of microtubules into bipolar spindles around artificial chromosomes in *Xenopus* egg extracts. *Nature*. 382:420-425.
- Heald, R., R. Tournebize, A. Habermann, E. Karsenti, and A. Hyman. 1997. Spindle assembly in *Xenopus* egg extracts: respective roles of centrosomes and microtubule self-organization. *J Cell Biol*. 138:615-628.
- Hellmuth, S., C. Pohlmann, A. Brown, F. Bottger, M. Sprinzl, and O. Stemmann. 2015. Positive and negative regulation of vertebrate separase by cdk1-cyclin b1 may explain why securin is dispensable. *J Biol Chem*. 290:8002-8010.
- Hemmerich, P., S. Weidtkamp-Peters, C. Hoischen, L. Schmiedeberg, I. Erliandri, and S. Diekmann. 2008. Dynamics of inner kinetochore assembly and maintenance in living cells. *J Cell Biol*. 180:1101-1114.
- Henley, S.A., and F.A. Dick. 2012. The retinoblastoma family of proteins and their regulatory functions in the mammalian cell division cycle. *Cell Div*. 7:10.
- Hirano, T. 2015. Chromosome Dynamics during Mitosis. *Cold Spring Harb Perspect Biol*.
- Hirokawa, N., Y. Noda, and Y. Okada. 1998. Kinesin and dynein superfamily proteins in organelle transport and cell division. *Curr Opin Cell Biol*. 10:60-73.

- Hoffman, D.B., C.G. Pearson, T.J. Yen, B.J. Howell, and E.D. Salmon. 2001. Microtubule-dependent changes in assembly of microtubule motor proteins and mitotic spindle checkpoint proteins at PtK1 kinetochores. *Mol Biol Cell*. 12:1995-2009.
- Holland, A.J., and D.W. Cleveland. 2012. Losing balance: the origin and impact of aneuploidy in cancer. *EMBO Rep*. 13:501-514.
- Holland, A.J., R.M. Reis, S. Niessen, C. Pereira, D.A. Andres, H.P. Spielmann, D.W. Cleveland, A. Desai, and R. Gassmann. 2015. Preventing farnesylation of the dynein adaptor spindly contributes to the mitotic defects caused by farnesyltransferase inhibitors. *Mol Biol Cell*.
- Holy, T.E., and S. Leibler. 1994. Dynamic instability of microtubules as an efficient way to search in space. *Proc Natl Acad Sci U S A*. 91:5682-5685.
- Hornbeck, P.V., J.M. Kornhauser, S. Tkachev, B. Zhang, E. Skrzypek, B. Murray, V. Latham, and M. Sullivan. 2012. PhosphoSitePlus: a comprehensive resource for investigating the structure and function of experimentally determined post-translational modifications in man and mouse. *Nucleic Acids Res*. 40:D261-270.
- Houglund, J.L., K.A. Hicks, H.L. Hartman, R.A. Kelly, T.J. Watt, and C.A. Fierke. 2010. Identification of novel peptide substrates for protein farnesyltransferase reveals two substrate classes with distinct sequence selectivities. *J Mol Biol*. 395:176-190.
- Houglund, J.L., C.L. Lamphear, S.A. Scott, R.A. Gibbs, and C.A. Fierke. 2009. Context-dependent substrate recognition by protein farnesyltransferase. *Biochemistry*. 48:1691-1701.
- Howell, B.J., D.B. Hoffman, G. Fang, A.W. Murray, and E.D. Salmon. 2000. Visualization of Mad2 dynamics at kinetochores, along spindle fibers, and at spindle poles in living cells. *J Cell Biol*. 150:1233-1250.
- Howell, B.J., B.F. McEwen, J.C. Canman, D.B. Hoffman, E.M. Farrar, C.L. Rieder, and E.D. Salmon. 2001. Cytoplasmic dynein/dynactin drives kinetochore protein transport to the spindle poles and has a role in mitotic spindle checkpoint inactivation. *J Cell Biol*. 155:1159-1172.
- Howell, B.J., B. Moree, E.M. Farrar, S. Stewart, G. Fang, and E.D. Salmon. 2004. Spindle checkpoint protein dynamics at kinetochores in living cells. *Curr Biol*. 14:953-964.
- Howman, E.V., K.J. Fowler, A.J. Newson, S. Redward, A.C. MacDonald, P. Kalitsis, and K.H. Choo. 2000. Early disruption of centromeric chromatin organization in centromere protein A (Cenpa) null mice. *Proc Natl Acad Sci U S A*. 97:1148-1153.
- Hoyt, M.A., L. Totis, and B.T. Roberts. 1991. *S. cerevisiae* genes required for cell cycle arrest in response to loss of microtubule function. *Cell*. 66:507-517.
- Huang, C.C., P.J. Casey, and C.A. Fierke. 1997. Evidence for a catalytic role of zinc in protein farnesyltransferase. Spectroscopy of Co²⁺-farnesyltransferase indicates metal coordination of the substrate thiolate. *J Biol Chem*. 272:20-23.

- Hussein, D., and S.S. Taylor. 2002. Farnesylation of Cenp-F is required for G2/M progression and degradation after mitosis. *J Cell Sci.* 115:3403-3414.
- Ishii, K., Y. Ogiyama, Y. Chikashige, S. Soejima, F. Masuda, T. Kakuma, Y. Hiraoka, and K. Takahashi. 2008. Heterochromatin integrity affects chromosome reorganization after centromere dysfunction. *Science.* 321:1088-1091.
- Iwanaga, Y., Y.H. Chi, A. Miyazato, S. Sheleg, K. Haller, J.M. Peloponese, Jr., Y. Li, J.M. Ward, R. Benezra, and K.T. Jeang. 2007. Heterozygous deletion of mitotic arrest-deficient protein 1 (MAD1) increases the incidence of tumors in mice. *Cancer Res.* 67:160-166.
- Izawa, D., and J. Pines. 2015. The mitotic checkpoint complex binds a second CDC20 to inhibit active APC/C. *Nature.* 517:631-634.
- Izuta, H., M. Ikeno, N. Suzuki, T. Tomonaga, N. Nozaki, C. Obuse, Y. Kisu, N. Goshima, F. Nomura, N. Nomura, and K. Yoda. 2006. Comprehensive analysis of the ICEN (Interphase Centromere Complex) components enriched in the CENP-A chromatin of human cells. *Genes Cells.* 11:673-684.
- Jelluma, N., A.B. Brenkman, N.J. van den Broek, C.W. Cruijsen, M.H. van Osch, S.M. Lens, R.H. Medema, and G.J. Kops. 2008. Mps1 phosphorylates Borealin to control Aurora B activity and chromosome alignment. *Cell.* 132:233-246.
- Jelluma, N., T.B. Dansen, T. Sliedrecht, N.P. Kwiatkowski, and G.J. Kops. 2010. Release of Mps1 from kinetochores is crucial for timely anaphase onset. *J Cell Biol.* 191:281-290.
- Joglekar, A.P., K. Bloom, and E.D. Salmon. 2009. In vivo protein architecture of the eukaryotic kinetochore with nanometer scale accuracy. *Curr Biol.* 19:694-699.
- Joglekar, A.P., D. Bouck, K. Finley, X. Liu, Y. Wan, J. Berman, X. He, E.D. Salmon, and K.S. Bloom. 2008. Molecular architecture of the kinetochore-microtubule attachment site is conserved between point and regional centromeres. *J Cell Biol.* 181:587-594.
- Joglekar, A.P., D.C. Bouck, J.N. Molk, K.S. Bloom, and E.D. Salmon. 2006. Molecular architecture of a kinetochore-microtubule attachment site. *Nat Cell Biol.* 8:581-585.
- Johnson, V.L., M.I. Scott, S.V. Holt, D. Hussein, and S.S. Taylor. 2004. Bub1 is required for kinetochore localization of BubR1, Cenp-E, Cenp-F and Mad2, and chromosome congression. *J Cell Sci.* 117:1577-1589.
- Johnston, S.R., T. Hickish, P. Ellis, S. Houston, L. Kelland, M. Dowsett, J. Salter, B. Michiels, J.J. Perez-Ruixo, P. Palmer, and A. Howes. 2003. Phase II study of the efficacy and tolerability of two dosing regimens of the farnesyl transferase inhibitor, R115777, in advanced breast cancer. *J Clin Oncol.* 21:2492-2499.
- Johnston, S.R., and L.R. Kelland. 2001. Farnesyl transferase inhibitors--a novel therapy for breast cancer. *Endocr Relat Cancer.* 8:227-235.

- Jokelainen, P.T. 1967. The ultrastructure and spatial organization of the metaphase kinetochore in mitotic rat cells. *J Ultrastruct Res.* 19:19-44.
- Jordan, M.A., D. Thrower, and L. Wilson. 1992. Effects of vinblastine, podophyllotoxin and nocodazole on mitotic spindles. Implications for the role of microtubule dynamics in mitosis. *J Cell Sci.* 102 (Pt 3):401-416.
- Kabeche, L., and D.A. Compton. 2012. Checkpoint-independent stabilization of kinetochore-microtubule attachments by Mad2 in human cells. *Curr Biol.* 22:638-644.
- Kalab, P., K. Weis, and R. Heald. 2002. Visualization of a Ran-GTP gradient in interphase and mitotic *Xenopus* egg extracts. *Science.* 295:2452-2456.
- Kalantzaki, M., E. Kitamura, T. Zhang, A. Mino, B. Novak, and T.U. Tanaka. 2015. Kinetochore-microtubule error correction is driven by differentially regulated interaction modes. *Nat Cell Biol.* 17:421-433.
- Kalitsis, P., E. Earle, K.J. Fowler, and K.H. Choo. 2000. Bub3 gene disruption in mice reveals essential mitotic spindle checkpoint function during early embryogenesis. *Genes Dev.* 14:2277-2282.
- Kallio, M.J., M.L. McClelland, P.T. Stukenberg, and G.J. Gorbsky. 2002. Inhibition of aurora B kinase blocks chromosome segregation, overrides the spindle checkpoint, and perturbs microtubule dynamics in mitosis. *Curr Biol.* 12:900-905.
- Kamiya, Y., A. Sakurai, S. Tamura, and N. Takahashi. 1978. Structure of rhodotorucine A, a novel lipopeptide, inducing mating tube formation in *Rhodosporidium toruloides*. *Biochem Biophys Res Commun.* 83:1077-1083.
- Kang, J., and H. Yu. 2009. Kinase signaling in the spindle checkpoint. *J Biol Chem.* 284:15359-15363.
- Kapoor, T.M., M.A. Lampson, P. Hergert, L. Cameron, D. Cimini, E.D. Salmon, B.F. McEwen, and A. Khodjakov. 2006. Chromosomes can congress to the metaphase plate before biorientation. *Science.* 311:388-391.
- Karess, R. 2005. Rod-Zw10-Zwilch: a key player in the spindle checkpoint. *Trends Cell Biol.* 15:386-392.
- Karess, R.E., and D.M. Glover. 1989. rough deal: a gene required for proper mitotic segregation in *Drosophila*. *J Cell Biol.* 109:2951-2961.
- Karnoub, A.E., and R.A. Weinberg. 2008. Ras oncogenes: split personalities. *Nat Rev Mol Cell Biol.* 9:517-531.
- Karp, J.E., T.I. Vener, M. Raponi, E.K. Ritchie, B.D. Smith, S.D. Gore, L.E. Morris, E.J. Feldman, J.M. Greer, S. Malek, H.E. Carraway, V. Ironside, S. Galkin, M.J. Levis, M.A. McDevitt, G.R. Roboz, C.D. Gocke, C. Derecho, J. Palma, Y. Wang, S.H. Kaufmann, J.J. Wright, and E. Garret-Mayer. 2012. Multi-institutional phase 2 clinical and pharmacogenomic trial of tipifarnib plus etoposide for elderly adults with newly diagnosed acute myelogenous leukemia. *Blood.* 119:55-63.
- Karsenti, E., J. Newport, and M. Kirschner. 1984. Respective roles of centrosomes and chromatin in the conversion of microtubule arrays from interphase to metaphase. *J Cell Biol.* 99:47s-54s.

- Kasuboski, J.M., J.R. Bader, P.S. Vaughan, S.B. Tauhata, M. Winding, M.A. Morrissey, M.V. Joyce, W. Boggess, L. Vos, G.K. Chan, E.H. Hinchcliffe, and K.T. Vaughan. 2011. Zwint-1 is a novel Aurora B substrate required for the assembly of a dynein-binding platform on kinetochores. *Mol Biol Cell*. 22:3318-3330.
- Kato, H., J. Jiang, B.R. Zhou, M. Rozendaal, H. Feng, R. Ghirlando, T.S. Xiao, A.F. Straight, and Y. Bai. 2013. A conserved mechanism for centromeric nucleosome recognition by centromere protein CENP-C. *Science*. 340:1110-1113.
- Kawashima, S.A., Y. Yamagishi, T. Honda, K. Ishiguro, and Y. Watanabe. 2010. Phosphorylation of H2A by Bub1 prevents chromosomal instability through localizing shugoshin. *Science*. 327:172-177.
- Kelly, A.E., and H. Funabiki. 2009. Correcting aberrant kinetochore microtubule attachments: an Aurora B-centric view. *Curr Opin Cell Biol*. 21:51-58.
- Kemmler, S., M. Stach, M. Knapp, J. Ortiz, J. Pfannstiel, T. Ruppert, and J. Lechner. 2009. Mimicking Ndc80 phosphorylation triggers spindle assembly checkpoint signalling. *Embo J*. 28:1099-1110.
- Khodjakov, A., R.W. Cole, B.R. Oakley, and C.L. Rieder. 2000. Centrosome-independent mitotic spindle formation in vertebrates. *Curr Biol*. 10:59-67.
- Khodjakov, A., L. Copenagle, M.B. Gordon, D.A. Compton, and T.M. Kapoor. 2003. Minus-end capture of preformed kinetochore fibers contributes to spindle morphogenesis. *J Cell Biol*. 160:671-683.
- Khodjakov, A., S. La Terra, and F. Chang. 2004. Laser microsurgery in fission yeast; role of the mitotic spindle midzone in anaphase B. *Curr Biol*. 14:1330-1340.
- Khodjakov, A., and C.L. Rieder. 2001. Centrosomes enhance the fidelity of cytokinesis in vertebrates and are required for cell cycle progression. *J Cell Biol*. 153:237-242.
- Kim, S., and H. Yu. 2015. Multiple assembly mechanisms anchor the KMN spindle checkpoint platform at human mitotic kinetochores. *J Cell Biol*. 208:181-196.
- King, J.M., T.S. Hays, and R.B. Nicklas. 2000. Dynein is a transient kinetochore component whose binding is regulated by microtubule attachment, not tension. *J Cell Biol*. 151:739-748.
- King, R.W., J.M. Peters, S. Tugendreich, M. Rolfe, P. Hieter, and M.W. Kirschner. 1995. A 20S complex containing CDC27 and CDC16 catalyzes the mitosis-specific conjugation of ubiquitin to cyclin B. *Cell*. 81:279-288.
- King, S.J., and T.A. Schroer. 2000. Dynactin increases the processivity of the cytoplasmic dynein motor. *Nat Cell Biol*. 2:20-24.
- Kirschner, M., and T. Mitchison. 1986. Beyond self-assembly: from microtubules to morphogenesis. *Cell*. 45:329-342.
- Kisselev, O., M. Ermolaeva, and N. Gautam. 1995. Efficient interaction with a receptor requires a specific type of prenyl group on the G protein gamma subunit. *J Biol Chem*. 270:25356-25358.

- Kitajima, T.S., S. Hauf, M. Ohsugi, T. Yamamoto, and Y. Watanabe. 2005. Human Bub1 defines the persistent cohesion site along the mitotic chromosome by affecting Shugoshin localization. *Curr Biol.* 15:353-359.
- Kitten, G.T., and E.A. Nigg. 1991. The CaaX motif is required for isoprenylation, carboxyl methylation, and nuclear membrane association of lamin B2. *J Cell Biol.* 113:13-23.
- Kiyomitsu, T., C. Obuse, and M. Yanagida. 2007. Human Blinkin/AF15q14 is required for chromosome alignment and the mitotic checkpoint through direct interaction with Bub1 and BubR1. *Dev Cell.* 13:663-676.
- Kline, S.L., I.M. Cheeseman, T. Hori, T. Fukagawa, and A. Desai. 2006. The human Mis12 complex is required for kinetochore assembly and proper chromosome segregation. *J Cell Biol.* 173:9-17.
- Knowlton, A.L., W. Lan, and P.T. Stukenberg. 2006. Aurora B is enriched at merotelic attachment sites, where it regulates MCAK. *Curr Biol.* 16:1705-1710.
- Kohl, N.E., C.A. Omer, M.W. Conner, N.J. Anthony, J.P. Davide, S.J. deSolms, E.A. Giuliani, R.P. Gomez, S.L. Graham, K. Hamilton, and et al. 1995. Inhibition of farnesyltransferase induces regression of mammary and salivary carcinomas in ras transgenic mice. *Nat Med.* 1:792-797.
- Kops, G.J., D.R. Foltz, and D.W. Cleveland. 2004. Lethality to human cancer cells through massive chromosome loss by inhibition of the mitotic checkpoint. *Proc Natl Acad Sci U S A.* 101:8699-8704.
- Kops, G.J., Y. Kim, B.A. Weaver, Y. Mao, I. McLeod, J.R. Yates, 3rd, M. Tagaya, and D.W. Cleveland. 2005. ZW10 links mitotic checkpoint signaling to the structural kinetochore. *J Cell Biol.* 169:49-60.
- Kops, G.J., and J.V. Shah. 2012. Connecting up and clearing out: how kinetochore attachment silences the spindle assembly checkpoint. *Chromosoma.* 121:509-525.
- Kraft, C., F. Herzog, C. Gieffers, K. Mechtler, A. Hagting, J. Pines, and J.M. Peters. 2003. Mitotic regulation of the human anaphase-promoting complex by phosphorylation. *Embo J.* 22:6598-6609.
- Kraus, J.M., H.B. Tatipaka, S.A. McGuffin, N.K. Chennamaneni, M. Karimi, J. Arif, C.L. Verlinde, F.S. Buckner, and M.H. Gelb. 2010. Second generation analogues of the cancer drug clinical candidate tipifarnib for anti-Chagas disease drug discovery. *J Med Chem.* 53:3887-3898.
- Krenn, V., K. Overlack, I. Primorac, S. van Gerwen, and A. Musacchio. 2014. KI motifs of human Knl1 enhance assembly of comprehensive spindle checkpoint complexes around MELT repeats. *Curr Biol.* 24:29-39.
- Kulukian, A., J.S. Han, and D.W. Cleveland. 2009. Unattached kinetochores catalyze production of an anaphase inhibitor that requires a Mad2 template to prime Cdc20 for BubR1 binding. *Dev Cell.* 16:105-117.
- Kuroda, Y., N. Suzuki, and T. Kataoka. 1993. The effect of posttranslational modifications on the interaction of Ras2 with adenylyl cyclase. *Science.* 259:683-686.

- Lagana, A., J.F. Dorn, V. De Rop, A.M. Ladouceur, A.S. Maddox, and P.S. Maddox. 2010. A small GTPase molecular switch regulates epigenetic centromere maintenance by stabilizing newly incorporated CENP-A. *Nat Cell Biol.* 12:1186-1193.
- Lan, W., X. Zhang, S.L. Kline-Smith, S.E. Rosasco, G.A. Barrett-Wilt, J. Shabanowitz, D.F. Hunt, C.E. Walczak, and P.T. Stukenberg. 2004. Aurora B phosphorylates centromeric MCAK and regulates its localization and microtubule depolymerization activity. *Curr Biol.* 14:273-286.
- Lantry, L.E., Z. Zhang, R. Yao, K.A. Crist, Y. Wang, J. Ohkanda, A.D. Hamilton, S.M. Sebti, R.A. Lubet, and M. You. 2000. Effect of farnesyltransferase inhibitor FTI-276 on established lung adenomas from A/J mice induced by 4-(methylnitrosamino)-1-(3-pyridyl)-1-butanone. *Carcinogenesis.* 21:113-116.
- Laoukili, J., M.R. Kooistra, A. Bras, J. Kauw, R.M. Kerkhoven, A. Morrison, H. Clevers, and R.H. Medema. 2005. FoxM1 is required for execution of the mitotic programme and chromosome stability. *Nat Cell Biol.* 7:126-136.
- Lengauer, C., K.W. Kinzler, and B. Vogelstein. 1997. Genetic instability in colorectal cancers. *Nature.* 386:623-627.
- Lerner, E.C., T.T. Zhang, D.B. Knowles, Y. Qian, A.D. Hamilton, and S.M. Sebti. 1997. Inhibition of the prenylation of K-Ras, but not H- or N-Ras, is highly resistant to CAAX peptidomimetics and requires both a farnesyltransferase and a geranylgeranyltransferase I inhibitor in human tumor cell lines. *Oncogene.* 15:1283-1288.
- Li, R., and A.W. Murray. 1991. Feedback control of mitosis in budding yeast. *Cell.* 66:519-531.
- Li, X., and R.B. Nicklas. 1995. Mitotic forces control a cell-cycle checkpoint. *Nature.* 373:630-632.
- Liang, Y., W. Yu, Y. Li, L. Yu, Q. Zhang, F. Wang, Z. Yang, J. Du, Q. Huang, X. Yao, and X. Zhu. 2007. Nudel modulates kinetochore association and function of cytoplasmic dynein in M phase. *Mol Biol Cell.* 18:2656-2666.
- Liao, H., R.J. Winkfein, G. Mack, J.B. Rattner, and T.J. Yen. 1995. CENP-F is a protein of the nuclear matrix that assembles onto kinetochores at late G2 and is rapidly degraded after mitosis. *J Cell Biol.* 130:507-518.
- Lin, Y.T., Y. Chen, G. Wu, and W.H. Lee. 2006. Hec1 sequentially recruits Zwint-1 and ZW10 to kinetochores for faithful chromosome segregation and spindle checkpoint control. *Oncogene.* 25:6901-6914.
- Lioutas, A., and I. Vernos. 2013. Aurora A kinase and its substrate TACC3 are required for central spindle assembly. *EMBO Rep.* 14:829-836.
- Lischetti, T., G. Zhang, G.G. Sedgwick, V.M. Bolanos-Garcia, and J. Nilsson. 2014. The internal Cdc20 binding site in BubR1 facilitates both spindle assembly checkpoint signalling and silencing. *Nat Commun.* 5:5563.
- Liu, D., G. Vader, M.J. Vromans, M.A. Lampson, and S.M. Lens. 2009. Sensing chromosome bi-orientation by spatial separation of aurora B kinase from kinetochore substrates. *Science.* 323:1350-1353.

- Liu, M., M.S. Bryant, J. Chen, S. Lee, B. Yaremko, P. Lipari, M. Malkowski, E. Ferrari, L. Nielsen, N. Prioli, J. Dell, D. Sinha, J. Syed, W.A. Korfmacher, A.A. Nomeir, C.C. Lin, L. Wang, A.G. Taveras, R.J. Doll, F.G. Njoroge, A.K. Mallams, S. Remiszewski, J.J. Catino, V.M. Girijavallabhan, W.R. Bishop, and et al. 1998. Antitumor activity of SCH 66336, an orally bioavailable tricyclic inhibitor of farnesyl protein transferase, in human tumor xenograft models and wap-ras transgenic mice. *Cancer Res.* 58:4947-4956.
- Liu, S.T., J.B. Rattner, S.A. Jablonski, and T.J. Yen. 2006. Mapping the assembly pathways that specify formation of the trilaminar kinetochore plates in human cells. *J Cell Biol.* 175:41-53.
- Liu, X., and M. Winey. 2012. The MPS1 family of protein kinases. *Annu Rev Biochem.* 81:561-585.
- London, N., S. Ceto, J.A. Ranish, and S. Biggins. 2012. Phosphoregulation of Spc105 by Mps1 and PP1 regulates Bub1 localization to kinetochores. *Curr Biol.* 22:900-906.
- Lu, L.Y., J.L. Wood, K. Minter-Dykhouse, L. Ye, T.L. Saunders, X. Yu, and J. Chen. 2008. Polo-like kinase 1 is essential for early embryonic development and tumor suppression. *Mol Cell Biol.* 28:6870-6876.
- Luo, X., Z. Tang, J. Rizo, and H. Yu. 2002. The Mad2 spindle checkpoint protein undergoes similar major conformational changes upon binding to either Mad1 or Cdc20. *Mol Cell.* 9:59-71.
- Luo, X., Z. Tang, G. Xia, K. Wassmann, T. Matsumoto, J. Rizo, and H. Yu. 2004. The Mad2 spindle checkpoint protein has two distinct natively folded states. *Nat Struct Mol Biol.* 11:338-345.
- Luo, Z., B. Diaz, M.S. Marshall, and J. Avruch. 1997. An intact Raf zinc finger is required for optimal binding to processed Ras and for ras-dependent Raf activation in situ. *Mol Cell Biol.* 17:46-53.
- Ma, H.T., and R.Y. Poon. 2011. How protein kinases co-ordinate mitosis in animal cells. *Biochem J.* 435:17-31.
- Maciejowski, J., K.A. George, M.E. Terret, C. Zhang, K.M. Shokat, and P.V. Jallepalli. 2010. Mps1 directs the assembly of Cdc20 inhibitory complexes during interphase and mitosis to control M phase timing and spindle checkpoint signaling. *J Cell Biol.* 190:89-100.
- Maddox, P.S., F. Hyndman, J. Monen, K. Oegema, and A. Desai. 2007. Functional genomics identifies a Myb domain-containing protein family required for assembly of CENP-A chromatin. *J Cell Biol.* 176:757-763.
- Maddox, P.S., K. Oegema, A. Desai, and I.M. Cheeseman. 2004. "Holo"er than thou: chromosome segregation and kinetochore function in *C. elegans*. *Chromosome Res.* 12:641-653.
- Maiato, H., C.L. Rieder, and A. Khodjakov. 2004a. Kinetochore-driven formation of kinetochore fibers contributes to spindle assembly during animal mitosis. *J Cell Biol.* 167:831-840.
- Maiato, H., P. Sampaio, and C.E. Sunkel. 2004b. Microtubule-associated proteins and their essential roles during mitosis. *Int Rev Cytol.* 241:53-153.

- Malik, R., R. Lenobel, A. Santamaria, A. Ries, E.A. Nigg, and R. Korner. 2009. Quantitative analysis of the human spindle phosphoproteome at distinct mitotic stages. *J Proteome Res.* 8:4553-4563.
- Malureanu, L.A., K.B. Jeganathan, M. Hamada, L. Wasilewski, J. Davenport, and J.M. van Deursen. 2009. BubR1 N terminus acts as a soluble inhibitor of cyclin B degradation by APC/C(Cdc20) in interphase. *Dev Cell.* 16:118-131.
- Mangués, R., T. Corral, N.E. Kohl, W.F. Symmans, S. Lu, M. Malumbres, J.B. Gibbs, A. Oliff, and A. Pellicer. 1998. Antitumor effect of a farnesyl protein transferase inhibitor in mammary and lymphoid tumors overexpressing N-ras in transgenic mice. *Cancer Res.* 58:1253-1259.
- Manuelidis, L. 1976. Repeating restriction fragments of human DNA. *Nucleic Acids Res.* 3:3063-3076.
- Mao, Y., A. Abrieu, and D.W. Cleveland. 2003. Activating and silencing the mitotic checkpoint through CENP-E-dependent activation/inactivation of BubR1. *Cell.* 114:87-98.
- Mao, Y., A. Desai, and D.W. Cleveland. 2005. Microtubule capture by CENP-E silences BubR1-dependent mitotic checkpoint signaling. *J Cell Biol.* 170:873-880.
- Mapelli, M., L. Massimiliano, S. Santaguida, and A. Musacchio. 2007. The Mad2 conformational dimer: structure and implications for the spindle assembly checkpoint. *Cell.* 131:730-743.
- Maresca, T.J., and E.D. Salmon. 2009. Intrakinetochores stretch is associated with changes in kinetochore phosphorylation and spindle assembly checkpoint activity. *J Cell Biol.* 184:373-381.
- Maresca, T.J., and E.D. Salmon. 2010. Welcome to a new kind of tension: translating kinetochore mechanics into a wait-anaphase signal. *J Cell Sci.* 123:825-835.
- Mariani, L., E. Chiroli, L. Nezi, H. Muller, S. Piatti, A. Musacchio, and A. Ciliberto. 2012. Role of the Mad2 dimerization interface in the spindle assembly checkpoint independent of kinetochores. *Curr Biol.* 22:1900-1908.
- Maskell, D.P., X.W. Hu, and M.R. Singleton. 2010. Molecular architecture and assembly of the yeast kinetochore MIND complex. *J Cell Biol.* 190:823-834.
- Matson, D.R., and P.T. Stukenberg. 2014. CENP-I and Aurora B act as a molecular switch that ties RZZ/Mad1 recruitment to kinetochore attachment status. *J Cell Biol.* 205:541-554.
- Matsusaka, T., and J. Pines. 2004. Chfr acts with the p38 stress kinases to block entry to mitosis in mammalian cells. *J Cell Biol.* 166:507-516.
- Matsuura, S., Y. Matsumoto, K. Morishima, H. Izumi, H. Matsumoto, E. Ito, K. Tsutsui, J. Kobayashi, H. Tauchi, Y. Kajiwara, S. Hama, K. Kurisu, H. Tahara, M. Oshimura, K. Komatsu, T. Ikeuchi, and T. Kajii. 2006. Monoallelic BUB1B mutations and defective mitotic-spindle checkpoint

- in seven families with premature chromatid separation (PCS) syndrome. *Am J Med Genet A*. 140:358-367.
- Mattison, C.P., W.M. Old, E. Steiner, B.J. Huneycutt, K.A. Resing, N.G. Ahn, and M. Winey. 2007. Mps1 activation loop autophosphorylation enhances kinase activity. *J Biol Chem*. 282:30553-30561.
- Mazia, D. 1961. Mitosis and the physiology of cell division. *The Cell. Biochemistry, Physiology, Morphology*:77-412.
- Mazieres, J., A. Pradines, and G. Favre. 2004. Perspectives on farnesyl transferase inhibitors in cancer therapy. *Cancer Lett*. 206:159-167.
- McClelland, S.E., S. Borusu, A.C. Amaro, J.R. Winter, M. Belwal, A.D. McAinsh, and P. Meraldi. 2007. The CENP-A NAC/CAD kinetochore complex controls chromosome congression and spindle bipolarity. *Embo J*. 26:5033-5047.
- McEwen, B.F., G.K. Chan, B. Zubrowski, M.S. Savoian, M.T. Sauer, and T.J. Yen. 2001. CENP-E is essential for reliable bioriented spindle attachment, but chromosome alignment can be achieved via redundant mechanisms in mammalian cells. *Mol Biol Cell*. 12:2776-2789.
- McEwen, B.F., A.B. Heagle, G.O. Cassels, K.F. Buttle, and C.L. Rieder. 1997. Kinetochore fiber maturation in PtK1 cells and its implications for the mechanisms of chromosome congression and anaphase onset. *J Cell Biol*. 137:1567-1580.
- McEwen, B.F., C.E. Hsieh, A.L. Matheyses, and C.L. Rieder. 1998. A new look at kinetochore structure in vertebrate somatic cells using high-pressure freezing and freeze substitution. *Chromosoma*. 107:366-375.
- McKenney, R.J., W. Huynh, M.E. Tanenbaum, G. Bhabha, and R.D. Vale. 2014. Activation of cytoplasmic dynein motility by dynactin-cargo adapter complexes. *Science*. 345:337-341.
- McKim, K.S., and R.S. Hawley. 1995. Chromosomal control of meiotic cell division. *Science*. 270:1595-1601.
- McTaggart, S.J. 2006. Isoprenylated proteins. *Cell Mol Life Sci*. 63:255-267.
- Meadows, J.C., and J.B. Millar. 2015. Sharpening the anaphase switch. *Biochem Soc Trans*. 43:19-22.
- Medema, R.H. 2009. Relaying the checkpoint signal from kinetochore to APC/C. *Dev Cell*. 16:6-8.
- Mical, T.I., and M.J. Monteiro. 1998. The role of sequences unique to nuclear intermediate filaments in the targeting and assembly of human lamin B: evidence for lack of interaction of lamin B with its putative receptor. *J Cell Sci*. 111 (Pt 23):3471-3485.
- Michaelis, C., R. Ciosk, and K. Nasmyth. 1997. Cohesins: chromosomal proteins that prevent premature separation of sister chromatids. *Cell*. 91:35-45.
- Michel, L.S., V. Liberal, A. Chatterjee, R. Kirchwegger, B. Pasche, W. Gerald, M. Dobles, P.K. Sorger, V.V. Murty, and R. Benezra. 2001. MAD2 haplo-insufficiency causes premature anaphase and chromosome instability in mammalian cells. *Nature*. 409:355-359.

- Miniowitz-Shemtov, S., E. Eytan, D. Ganoth, D. Sitry-Shevah, E. Dumin, and A. Hershko. 2012. Role of phosphorylation of Cdc20 in p31(comet)-stimulated disassembly of the mitotic checkpoint complex. *Proc Natl Acad Sci U S A*. 109:8056-8060.
- Minoshima, Y., T. Hori, M. Okada, H. Kimura, T. Haraguchi, Y. Hiraoka, Y.C. Bao, T. Kawashima, T. Kitamura, and T. Fukagawa. 2005. The constitutive centromere component CENP-50 is required for recovery from spindle damage. *Mol Cell Biol*. 25:10315-10328.
- Mitchison, T., and M. Kirschner. 1984. Dynamic instability of microtubule growth. *Nature*. 312:237-242.
- Mitchison, T.J., and E.D. Salmon. 1992. Poleward kinetochore fiber movement occurs during both metaphase and anaphase-A in newt lung cell mitosis. *J Cell Biol*. 119:569-582.
- Mitelman F, J.B.a.M.F.E. 2015. Mitelman Database of Chromosome Aberrations and Gene Fusions in Cancer. <http://cgap.nci.nih.gov/Chromosomes/Mitelman>.
- Mitelman, F., B. Johansson, and F. Mertens. 2007. The impact of translocations and gene fusions on cancer causation. *Nat Rev Cancer*. 7:233-245.
- Moasser, M.M., L. Sepp-Lorenzino, N.E. Kohl, A. Oliff, A. Balog, D.S. Su, S.J. Danishefsky, and N. Rosen. 1998. Farnesyl transferase inhibitors cause enhanced mitotic sensitivity to taxol and epothilones. *Proc Natl Acad Sci U S A*. 95:1369-1374.
- Mogilner, A., and E. Craig. 2010. Towards a quantitative understanding of mitotic spindle assembly and mechanics. *J Cell Sci*. 123:3435-3445.
- Moon, H.M., Y.H. Youn, H. Pemble, J. Yingling, T. Wittmann, and A. Wynshaw-Boris. 2014. LIS1 controls mitosis and mitotic spindle organization via the LIS1-NDEL1-dynein complex. *Hum Mol Genet*. 23:449-466.
- Morrow, C.J., A. Tighe, V.L. Johnson, M.I. Scott, C. Ditchfield, and S.S. Taylor. 2005. Bub1 and aurora B cooperate to maintain BubR1-mediated inhibition of APC/CCdc20. *J Cell Sci*. 118:3639-3652.
- Moudgil, D.K., and G.K. Chan. 2015. Lipids beyond membranes; farnesylation targets Spindly to kinetochores. *Cell Cycle*. 14:2185-2186.
- Moudgil, D.K., N. Westcott, J.K. Famulski, K. Patel, D. Macdonald, H. Hang, and G.K. Chan. 2015. A novel role of farnesylation in targeting a mitotic checkpoint protein, human Spindly, to kinetochores. *J Cell Biol*. 208:881-896.
- Murray, A.W. 1992. Creative blocks: cell-cycle checkpoints and feedback controls. *Nature*. 359:599-604.
- Musacchio, A., and E.D. Salmon. 2007. The spindle-assembly checkpoint in space and time. *Nat Rev Mol Cell Biol*. 8:379-393.
- Musinipally, V., S. Howes, G.M. Alushin, and E. Nogales. 2013. The microtubule binding properties of CENP-E's C-terminus and CENP-F. *J Mol Biol*. 425:4427-4441.
- Musio, A., C. Montagna, D. Zambroni, E. Indino, O. Barbieri, L. Citti, A. Villa, T. Ried, and P. Vezioni. 2003. Inhibition of BUB1 results in genomic

- instability and anchorage-independent growth of normal human fibroblasts. *Cancer Res.* 63:2855-2863.
- Naegle, K.M., F.M. White, D.A. Lauffenburger, and M.B. Yaffe. 2012. Robust co-regulation of tyrosine phosphorylation sites on proteins reveals novel protein interactions. *Mol Biosyst.* 8:2771-2782.
- Nagasu, T., K. Yoshimatsu, C. Rowell, M.D. Lewis, and A.M. Garcia. 1995. Inhibition of human tumor xenograft growth by treatment with the farnesyl transferase inhibitor B956. *Cancer Res.* 55:5310-5314.
- Nagele, R., T. Freeman, L. McMorro, and H.Y. Lee. 1995. Precise spatial positioning of chromosomes during prometaphase: evidence for chromosomal order. *Science.* 270:1831-1835.
- Nahaboo, W., M. Zouak, P. Askjaer, and M. Delattre. 2015. Chromatids segregate without centrosomes during *C. elegans* mitosis in a Ran and CLASP dependent manner. *Mol Biol Cell.*
- Nigg, E.A. 2001. Mitotic kinases as regulators of cell division and its checkpoints. *Nat Rev Mol Cell Biol.* 2:21-32.
- Niikura, Y., R. Kitagawa, H. Ogi, R. Abdulle, V. Pagala, and K. Kitagawa. 2015. CENP-A K124 Ubiquitylation Is Required for CENP-A Deposition at the Centromere. *Dev Cell.* 32:589-603.
- Nijenhuis, W., G. Vallardi, A. Teixeira, G.J. Kops, and A.T. Saurin. 2014. Negative feedback at kinetochores underlies a responsive spindle checkpoint signal. *Nat Cell Biol.* 16:1257-1264.
- Nishihashi, A., T. Haraguchi, Y. Hiraoka, T. Ikemura, V. Regnier, H. Dodson, W.C. Earnshaw, and T. Fukagawa. 2002. CENP-I is essential for centromere function in vertebrate cells. *Dev Cell.* 2:463-476.
- Nishino, T., K. Takeuchi, K.E. Gascoigne, A. Suzuki, T. Hori, T. Oyama, K. Morikawa, I.M. Cheeseman, and T. Fukagawa. 2012. CENP-T-W-S-X forms a unique centromeric chromatin structure with a histone-like fold. *Cell.* 148:487-501.
- Nogales, E., M. Whittaker, R.A. Milligan, and K.H. Downing. 1999. High-resolution model of the microtubule. *Cell.* 96:79-88.
- Nousiainen, M., H.H. Sillje, G. Sauer, E.A. Nigg, and R. Korner. 2006. Phosphoproteome analysis of the human mitotic spindle. *Proc Natl Acad Sci U S A.* 103:5391-5396.
- O'Connell, C.B., and Y.L. Wang. 2000. Mammalian spindle orientation and position respond to changes in cell shape in a dynein-dependent fashion. *Mol Biol Cell.* 11:1765-1774.
- Obuse, C., O. Iwasaki, T. Kiyomitsu, G. Goshima, Y. Toyoda, and M. Yanagida. 2004a. A conserved Mis12 centromere complex is linked to heterochromatic HP1 and outer kinetochore protein Zwint-1. *Nat Cell Biol.* 6:1135-1141.
- Obuse, C., H. Yang, N. Nozaki, S. Goto, T. Okazaki, and K. Yoda. 2004b. Proteomics analysis of the centromere complex from HeLa interphase cells: UV-damaged DNA binding protein 1 (DDB-1) is a component of

- the CEN-complex, while BMI-1 is transiently co-localized with the centromeric region in interphase. *Genes Cells*. 9:105-120.
- Ochocki, J.D., and M.D. Distefano. 2013. Prenyltransferase Inhibitors: Treating Human Ailments from Cancer to Parasitic Infections. *Medchemcomm*. 4:476-492.
- Ohba, T., M. Nakamura, H. Nishitani, and T. Nishimoto. 1999. Self-organization of microtubule asters induced in *Xenopus* egg extracts by GTP-bound Ran. *Science*. 284:1356-1358.
- Ohi, R., M.L. Coughlin, W.S. Lane, and T.J. Mitchison. 2003. An inner centromere protein that stimulates the microtubule depolymerizing activity of a KinI kinesin. *Dev Cell*. 5:309-321.
- Ohta, S., J.C. Bukowski-Wills, L. Sanchez-Pulido, L. Alves Fde, L. Wood, Z.A. Chen, M. Platani, L. Fischer, D.F. Hudson, C.P. Ponting, T. Fukagawa, W.C. Earnshaw, and J. Rappsilber. 2010. The protein composition of mitotic chromosomes determined using multiclassifier combinatorial proteomics. *Cell*. 142:810-821.
- Okada, M., I.M. Cheeseman, T. Hori, K. Okawa, I.X. McLeod, J.R. Yates, 3rd, A. Desai, and T. Fukagawa. 2006. The CENP-H-I complex is required for the efficient incorporation of newly synthesized CENP-A into centromeres. *Nat Cell Biol*. 8:446-457.
- Olepu, S., P.K. Suryadevara, K. Rivas, K. Yokoyama, C.L. Verlinde, D. Chakrabarti, W.C. Van Voorhis, and M.H. Gelb. 2008. 2-Oxo-tetrahydro-1,8-naphthyridines as selective inhibitors of malarial protein farnesyltransferase and as anti-malarials. *Bioorg Med Chem Lett*. 18:494-497.
- Olmsted, J.B. 1986. Microtubule-associated proteins. *Annu Rev Cell Biol*. 2:421-457.
- Olszak, A.M., D. van Essen, A.J. Pereira, S. Diehl, T. Manke, H. Maiato, S. Saccani, and P. Heun. 2011. Heterochromatin boundaries are hotspots for de novo kinetochore formation. *Nat Cell Biol*. 13:799-808.
- Omer, C.A., Z. Chen, R.E. Diehl, M.W. Conner, H.Y. Chen, M.E. Trumbauer, S. Gopal-Truter, G. Seeburger, H. Bhimnathwala, M.T. Abrams, J.P. Davide, M.S. Ellis, J.B. Gibbs, I. Greenberg, K.S. Koblan, A.M. Kral, D. Liu, R.B. Lobell, P.J. Miller, S.D. Mosser, T.J. O'Neill, E. Rands, M.D. Schaber, E.T. Senderak, A. Oliff, and N.E. Kohl. 2000. Mouse mammary tumor virus-Ki-rasB transgenic mice develop mammary carcinomas that can be growth-inhibited by a farnesyl:protein transferase inhibitor. *Cancer Res*. 60:2680-2688.
- Osmani, A.H., S.A. Osmani, and N.R. Morris. 1990. The molecular cloning and identification of a gene product specifically required for nuclear movement in *Aspergillus nidulans*. *J Cell Biol*. 111:543-551.
- Palmer, D.K., K. O'Day, H.L. Trong, H. Charbonneau, and R.L. Margolis. 1991. Purification of the centromere-specific protein CENP-A and demonstration that it is a distinctive histone. *Proc Natl Acad Sci U S A*. 88:3734-3738.

- Palsuledesai, C.C., and M.D. Distefano. 2015. Protein prenylation: enzymes, therapeutics, and biotechnology applications. *ACS Chem Biol.* 10:51-62.
- Park, H.W., S.R. Boduluri, J.F. Moomaw, P.J. Casey, and L.S. Beese. 1997. Crystal structure of protein farnesyltransferase at 2.25 angstrom resolution. *Science.* 275:1800-1804.
- Perez de Castro, I., G. de Carcer, and M. Malumbres. 2007. A census of mitotic cancer genes: new insights into tumor cell biology and cancer therapy. *Carcinogenesis.* 28:899-912.
- Perpelescu, M., N. Nozaki, C. Obuse, H. Yang, and K. Yoda. 2009. Active establishment of centromeric CENP-A chromatin by RSF complex. *J Cell Biol.* 185:397-407.
- Peters, A.H., D. O'Carroll, H. Scherthan, K. Mechtler, S. Sauer, C. Schofer, K. Weipoltshammer, M. Pagani, M. Lachner, A. Kohlmaier, S. Opravil, M. Doyle, M. Sibilia, and T. Jenuwein. 2001. Loss of the Suv39h histone methyltransferases impairs mammalian heterochromatin and genome stability. *Cell.* 107:323-337.
- Petersen, J., and I.M. Hagan. 2003. S. pombe aurora kinase/survivin is required for chromosome condensation and the spindle checkpoint attachment response. *Curr Biol.* 13:590-597.
- Petrovic, A., S. Mosalaganti, J. Keller, M. Mattiuzzo, K. Overlack, V. Krenn, A. De Antoni, S. Wohlgemuth, V. Cecatiello, S. Pasqualato, S. Raunser, and A. Musacchio. 2014. Modular assembly of RWD domains on the Mis12 complex underlies outer kinetochore organization. *Mol Cell.* 53:591-605.
- Petrovic, A., S. Pasqualato, P. Dube, V. Krenn, S. Santaguida, D. Cittaro, S. Monzani, L. Massimiliano, J. Keller, A. Tarricone, A. Maiolica, H. Stark, and A. Musacchio. 2010. The MIS12 complex is a protein interaction hub for outer kinetochore assembly. *J Cell Biol.* 190:835-852.
- Pfarr, C.M., M. Coue, P.M. Grissom, T.S. Hays, M.E. Porter, and J.R. McIntosh. 1990. Cytoplasmic dynein is localized to kinetochores during mitosis. *Nature.* 345:263-265.
- Pickett, J.S., K.E. Bowers, H.L. Hartman, H.W. Fu, A.C. Embry, P.J. Casey, and C.A. Fierke. 2003. Kinetic studies of protein farnesyltransferase mutants establish active substrate conformation. *Biochemistry.* 42:9741-9748.
- Pines, J. 2006. Mitosis: a matter of getting rid of the right protein at the right time. *Trends Cell Biol.* 16:55-63.
- Pines, J. 2011. Cubism and the cell cycle: the many faces of the APC/C. *Nat Rev Mol Cell Biol.* 12:427-438.
- Pompliano, D.L., M.D. Schaber, S.D. Mosser, C.A. Omer, J.A. Shafer, and J.B. Gibbs. 1993. Isoprenoid diphosphate utilization by recombinant human farnesyl:protein transferase: interactive binding between substrates and a preferred kinetic pathway. *Biochemistry.* 32:8341-8347.
- Porfiri, E., T. Evans, P. Chardin, and J.F. Hancock. 1994. Prenylation of Ras proteins is required for efficient hSOS1-promoted guanine nucleotide exchange. *J Biol Chem.* 269:22672-22677.

- Porter, L.A., and D.J. Donoghue. 2003. Cyclin B1 and CDK1: nuclear localization and upstream regulators. *Prog Cell Cycle Res.* 5:335-347.
- Porter, S.B., E.R. Hildebrandt, S.R. Breevoort, D.Z. Mokry, T.M. Dore, and W.K. Schmidt. 2007. Inhibition of the CaaX proteases Rce1p and Ste24p by peptidyl (acyloxy)methyl ketones. *Biochim Biophys Acta.* 1773:853-862.
- Primorac, I., J.R. Weir, E. Chiroli, F. Gross, I. Hoffmann, S. van Gerwen, A. Ciliberto, and A. Musacchio. 2013. Bub3 reads phosphorylated MELT repeats to promote spindle assembly checkpoint signaling. *Elife.* 2:e01030.
- Przewloka, M.R., Z. Venkei, V.M. Bolanos-Garcia, J. Debski, M. Dadlez, and D.M. Glover. 2011. CENP-C is a structural platform for kinetochore assembly. *Curr Biol.* 21:399-405.
- Putkey, F.R., T. Cramer, M.K. Morphew, A.D. Silk, R.S. Johnson, J.R. McIntosh, and D.W. Cleveland. 2002. Unstable kinetochore-microtubule capture and chromosomal instability following deletion of CENP-E. *Dev Cell.* 3:351-365.
- Raponi, M., J.E. Lancet, H. Fan, L. Dossey, G. Lee, I. Gojo, E.J. Feldman, J. Gotlib, L.E. Morris, P.L. Greenberg, J.J. Wright, J.L. Harousseau, B. Lowenberg, R.M. Stone, P. De Porre, Y. Wang, and J.E. Karp. 2008. A 2-gene classifier for predicting response to the farnesyltransferase inhibitor tipifarnib in acute myeloid leukemia. *Blood.* 111:2589-2596.
- Rattner, J.B., A. Rao, M.J. Fritzler, D.W. Valencia, and T.J. Yen. 1993. CENP-F is a ca 400 kDa kinetochore protein that exhibits a cell-cycle dependent localization. *Cell Motil Cytoskeleton.* 26:214-226.
- Reddy, S.K., M. Rape, W.A. Margansky, and M.W. Kirschner. 2007. Ubiquitination by the anaphase-promoting complex drives spindle checkpoint inactivation. *Nature.* 446:921-925.
- Regnier, V., P. Vagnarelli, T. Fukagawa, T. Zerjal, E. Burns, D. Trouche, W. Earnshaw, and W. Brown. 2005. CENP-A is required for accurate chromosome segregation and sustained kinetochore association of BubR1. *Mol Cell Biol.* 25:3967-3981.
- Reiss, Y., J.L. Goldstein, M.C. Seabra, P.J. Casey, and M.S. Brown. 1990. Inhibition of purified p21ras farnesyl:protein transferase by Cys-AAX tetrapeptides. *Cell.* 62:81-88.
- Resh, M.D. 2006. Trafficking and signaling by fatty-acylated and prenylated proteins. *Nat Chem Biol.* 2:584-590.
- Rieder, C.L., R.W. Cole, A. Khodjakov, and G. Sluder. 1995. The checkpoint delaying anaphase in response to chromosome monoorientation is mediated by an inhibitory signal produced by unattached kinetochores. *J Cell Biol.* 130:941-948.
- Rieder, C.L., S. Faruki, and A. Khodjakov. 2001. The centrosome in vertebrates: more than a microtubule-organizing center. *Trends Cell Biol.* 11:413-419.
- Rieder, C.L., A. Schultz, R. Cole, and G. Sluder. 1994. Anaphase onset in vertebrate somatic cells is controlled by a checkpoint that monitors sister kinetochore attachment to the spindle. *J Cell Biol.* 127:1301-1310.

- Rodriguez-Bravo, V., J. Maciejowski, J. Corona, H.K. Buch, P. Collin, M.T. Kanemaki, J.V. Shah, and P.V. Jallepalli. 2014. Nuclear pores protect genome integrity by assembling a premitotic and Mad1-dependent anaphase inhibitor. *Cell*. 156:1017-1031.
- Rogers, G.C., S.L. Rogers, T.A. Schwimmer, S.C. Ems-McClung, C.E. Walczak, R.D. Vale, J.M. Scholey, and D.J. Sharp. 2004. Two mitotic kinesins cooperate to drive sister chromatid separation during anaphase. *Nature*. 427:364-370.
- Rose, W.C., F.Y. Lee, C.R. Fairchild, M. Lynch, T. Monticello, R.A. Kramer, and V. Manne. 2001. Preclinical antitumor activity of BMS-214662, a highly apoptotic and novel farnesyltransferase inhibitor. *Cancer Res*. 61:7507-7517.
- Roshak, A.K., E.A. Capper, C. Imburgia, J. Fornwald, G. Scott, and L.A. Marshall. 2000. The human polo-like kinase, PLK, regulates cdc2/cyclin B through phosphorylation and activation of the cdc25C phosphatase. *Cell Signal*. 12:405-411.
- Roskoski, R., Jr. 2003. Protein prenylation: a pivotal posttranslational process. *Biochem Biophys Res Commun*. 303:1-7.
- Rowell, C.A., J.J. Kowalczyk, M.D. Lewis, and A.M. Garcia. 1997. Direct demonstration of geranylgeranylation and farnesylation of Ki-Ras in vivo. *J Biol Chem*. 272:14093-14097.
- Rowley, J.D. 1973. Identification of a translocation with quinacrine fluorescence in a patient with acute leukemia. *Ann Genet*. 16:109-112.
- Rubio, I., U. Wittig, C. Meyer, R. Heinze, D. Kadereit, H. Waldmann, J. Downward, and R. Wetzker. 1999. Farnesylation of Ras is important for the interaction with phosphoinositide 3-kinase gamma. *Eur J Biochem*. 266:70-82.
- Rudd, M.K., and H.F. Willard. 2004. Analysis of the centromeric regions of the human genome assembly. *Trends Genet*. 20:529-533.
- Sanchez, Y., C. Wong, R.S. Thoma, R. Richman, Z. Wu, H. Piwnica-Worms, and S.J. Elledge. 1997. Conservation of the Chk1 checkpoint pathway in mammals: linkage of DNA damage to Cdk regulation through Cdc25. *Science*. 277:1497-1501.
- Santaguida, S., and A. Musacchio. 2009. The life and miracles of kinetochores. *Embo J*. 28:2511-2531.
- Santaguida, S., A. Tighe, A.M. D'Alise, S.S. Taylor, and A. Musacchio. 2010. Dissecting the role of MPS1 in chromosome biorientation and the spindle checkpoint through the small molecule inhibitor reversine. *J Cell Biol*. 190:73-87.
- Sasai, K., H. Katayama, D.L. Stenoien, S. Fujii, R. Honda, M. Kimura, Y. Okano, M. Tatsuka, F. Suzuki, E.A. Nigg, W.C. Earnshaw, W.R. Brinkley, and S. Sen. 2004. Aurora-C kinase is a novel chromosomal passenger protein that can complement Aurora-B kinase function in mitotic cells. *Cell Motil Cytoskeleton*. 59:249-263.

- Saunders, W.S., C. Chue, M. Goebel, C. Craig, R.F. Clark, J.A. Powers, J.C. Eissenberg, S.C. Elgin, N.F. Rothfield, and W.C. Earnshaw. 1993. Molecular cloning of a human homologue of Drosophila heterochromatin protein HP1 using anti-centromere autoantibodies with anti-chromosome specificity. *J Cell Sci.* 104 (Pt 2):573-582.
- Savoian, M.S., M.L. Goldberg, and C.L. Rieder. 2000. The rate of poleward chromosome motion is attenuated in Drosophila *zw10* and rod mutants. *Nat Cell Biol.* 2:948-952.
- Scaerou, F., D.A. Starr, F. Piano, O. Papoulas, R.E. Karess, and M.L. Goldberg. 2001. The ZW10 and Rough Deal checkpoint proteins function together in a large, evolutionarily conserved complex targeted to the kinetochore. *J Cell Sci.* 114:3103-3114.
- Schaar, B.T., G.K. Chan, P. Maddox, E.D. Salmon, and T.J. Yen. 1997. CENP-E function at kinetochores is essential for chromosome alignment. *J Cell Biol.* 139:1373-1382.
- Schafer, W.R., R. Kim, R. Sterne, J. Thorner, S.H. Kim, and J. Rine. 1989. Genetic and pharmacological suppression of oncogenic mutations in *ras* genes of yeast and humans. *Science.* 245:379-385.
- Schafer-Hales, K., J. Iaconelli, J.P. Snyder, A. Prussia, J.H. Nettles, A. El-Naggar, F.R. Khuri, P. Giannakakou, and A.I. Marcus. 2007. Farnesyl transferase inhibitors impair chromosomal maintenance in cell lines and human tumors by compromising CENP-E and CENP-F function. *Mol Cancer Ther.* 6:1317-1328.
- Schittenhelm, R.B., S. Heeger, F. Althoff, A. Walter, S. Heidmann, K. Mechtler, and C.F. Lehner. 2007. Spatial organization of a ubiquitous eukaryotic kinetochore protein network in Drosophila chromosomes. *Chromosoma.* 116:385-402.
- Schleiffer, A., M. Maier, G. Litos, F. Lampert, P. Hornung, K. Mechtler, and S. Westermann. 2012. CENP-T proteins are conserved centromere receptors of the Ndc80 complex. *Nat Cell Biol.* 14:604-613.
- Schliwa, M., and G. Woehlke. 2003. Molecular motors. *Nature.* 422:759-765.
- Schmidt, M., and H. Bastians. 2007. Mitotic drug targets and the development of novel anti-mitotic anticancer drugs. *Drug Resist Updat.* 10:162-181.
- Schuh, M., C.F. Lehner, and S. Heidmann. 2007. Incorporation of Drosophila CID/CENP-A and CENP-C into centromeres during early embryonic anaphase. *Curr Biol.* 17:237-243.
- Screpanti, E., A. De Antoni, G.M. Alushin, A. Petrovic, T. Melis, E. Nogales, and A. Musacchio. 2011. Direct binding of Cenp-C to the Mis12 complex joins the inner and outer kinetochore. *Curr Biol.* 21:391-398.
- Sebti, S.M. 2005. Protein farnesylation: implications for normal physiology, malignant transformation, and cancer therapy. *Cancer Cell.* 7:297-300.
- Sebti, S.M., and C.J. Der. 2003. Opinion: Searching for the elusive targets of farnesyltransferase inhibitors. *Nat Rev Cancer.* 3:945-951.
- Sepp-Lorenzino, L., A. Balog, D.S. Su, D. Meng, N. Timaul, H.I. Scher, S.J. Danishefsky, and N. Rosen. 1999. The microtubule-stabilizing agents

- epothilones A and B and their desoxy-derivatives induce mitotic arrest and apoptosis in human prostate cancer cells. *Prostate Cancer Prostatic Dis.* 2:41-52.
- Sepp-Lorenzino, L., Z. Ma, E. Rands, N.E. Kohl, J.B. Gibbs, A. Oliff, and N. Rosen. 1995. A peptidomimetic inhibitor of farnesyl:protein transferase blocks the anchorage-dependent and -independent growth of human tumor cell lines. *Cancer Res.* 55:5302-5309.
- Sharp, D.J., G.C. Rogers, and J.M. Scholey. 2000a. Cytoplasmic dynein is required for poleward chromosome movement during mitosis in *Drosophila* embryos. *Nat Cell Biol.* 2:922-930.
- Sharp, D.J., G.C. Rogers, and J.M. Scholey. 2000b. Microtubule motors in mitosis. *Nature.* 407:41-47.
- Shepherd, L.A., J.C. Meadows, A.M. Sochaj, T.C. Lancaster, J. Zou, G.J. Buttrick, J. Rappsilber, K.G. Hardwick, and J.B. Millar. 2012. Phosphodependent recruitment of Bub1 and Bub3 to Spc7/KNL1 by Mph1 kinase maintains the spindle checkpoint. *Curr Biol.* 22:891-899.
- Shi, B., B. Yaremko, G. Hajian, G. Terracina, W.R. Bishop, M. Liu, and L.L. Nielsen. 2000. The farnesyl protein transferase inhibitor SCH66336 synergizes with taxanes in vitro and enhances their antitumor activity in vivo. *Cancer Chemother Pharmacol.* 46:387-393.
- Shigeishi, H., K. Higashikawa, S. Ono, K. Mizuta, Y. Ninomiya, S. Yoneda, M. Taki, and N. Kamata. 2006. Increased expression of CENP-H gene in human oral squamous cell carcinomas harboring high-proliferative activity. *Oncol Rep.* 16:1071-1075.
- Shimogawa, M.M., B. Graczyk, M.K. Gardner, S.E. Francis, E.A. White, M. Ess, J.N. Molk, C. Ruse, S. Niessen, J.R. Yates, 3rd, E.G. Muller, K. Bloom, D.J. Odde, and T.N. Davis. 2006. Mps1 phosphorylation of Dam1 couples kinetochores to microtubule plus ends at metaphase. *Curr Biol.* 16:1489-1501.
- Sikirzhytski, V., V. Magidson, J.B. Steinman, J. He, M. Le Berre, I. Tikhonenko, J.G. Ault, B.F. McEwen, J.K. Chen, H. Sui, M. Piel, T.M. Kapoor, and A. Khodjakov. 2014. Direct kinetochore-spindle pole connections are not required for chromosome segregation. *J Cell Biol.* 206:231-243.
- Silk, A.D., A.J. Holland, and D.W. Cleveland. 2009. Requirements for NuMA in maintenance and establishment of mammalian spindle poles. *J Cell Biol.* 184:677-690.
- Silva, P., J. Barbosa, A.V. Nascimento, J. Faria, R. Reis, and H. Bousbaa. 2011. Monitoring the fidelity of mitotic chromosome segregation by the spindle assembly checkpoint. *Cell Prolif.* 44:391-400.
- Silva, P.M., R.M. Reis, V.M. Bolanos-Garcia, C. Florindo, A.A. Tavares, and H. Bousbaa. 2014. Dynein-dependent transport of spindle assembly checkpoint proteins off kinetochores toward spindle poles. *FEBS Lett.* 588:3265-3273.

- Simonetta, M., R. Manzoni, R. Mosca, M. Mapelli, L. Massimiliano, M. Vink, B. Novak, A. Musacchio, and A. Ciliberto. 2009. The influence of catalysis on mad2 activation dynamics. *PLoS Biol.* 7:e10.
- Sinensky, M. 2000. Recent advances in the study of prenylated proteins. *Biochim Biophys Acta.* 1484:93-106.
- Sivakumar, S., and G.J. Gorbsky. 2015. Spatiotemporal regulation of the anaphase-promoting complex in mitosis. *Nat Rev Mol Cell Biol.* 16:82-94.
- Skibbens, R.V., V.P. Skeen, and E.D. Salmon. 1993. Directional instability of kinetochore motility during chromosome congression and segregation in mitotic newt lung cells: a push-pull mechanism. *J Cell Biol.* 122:859-875.
- Sluder, G. 1979. Role of spindle microtubules in the control of cell cycle timing. *J Cell Biol.* 80:674-691.
- Smith, D.A., B.S. Baker, and M. Gatti. 1985. Mutations in genes encoding essential mitotic functions in *Drosophila melanogaster*. *Genetics.* 110:647-670.
- Spencer, F., and P. Hieter. 1992. Centromere DNA mutations induce a mitotic delay in *Saccharomyces cerevisiae*. *Proc Natl Acad Sci U S A.* 89:8908-8912.
- Starr, D.A., R. Saffery, Z. Li, A.E. Simpson, K.H. Choo, T.J. Yen, and M.L. Goldberg. 2000. HZWint-1, a novel human kinetochore component that interacts with HZW10. *J Cell Sci.* 113 (Pt 11):1939-1950.
- Starr, D.A., B.C. Williams, T.S. Hays, and M.L. Goldberg. 1998. ZW10 helps recruit dynactin and dynein to the kinetochore. *J Cell Biol.* 142:763-774.
- Starr, D.A., B.C. Williams, Z. Li, B. Etemad-Moghadam, R.K. Dawe, and M.L. Goldberg. 1997. Conservation of the centromere/kinetochore protein ZW10. *J Cell Biol.* 138:1289-1301.
- Stegmeier, F., M. Rape, V.M. Draviam, G. Nalepa, M.E. Sowa, X.L. Ang, E.R. McDonald, 3rd, M.Z. Li, G.J. Hannon, P.K. Sorger, M.W. Kirschner, J.W. Harper, and S.J. Elledge. 2007. Anaphase initiation is regulated by antagonistic ubiquitination and deubiquitination activities. *Nature.* 446:876-881.
- Stehman, S.A., Y. Chen, R.J. McKenney, and R.B. Vallee. 2007. NudE and NudEL are required for mitotic progression and are involved in dynein recruitment to kinetochores. *J Cell Biol.* 178:583-594.
- Steuer, E.R., L. Wordeman, T.A. Schroer, and M.P. Sheetz. 1990. Localization of cytoplasmic dynein to mitotic spindles and kinetochores. *Nature.* 345:266-268.
- Sudakin, V., G.K. Chan, and T.J. Yen. 2001. Checkpoint inhibition of the APC/C in HeLa cells is mediated by a complex of BUBR1, BUB3, CDC20, and MAD2. *J Cell Biol.* 154:925-936.
- Sudakin, V., D. Ganoth, A. Dahan, H. Heller, J. Hershko, F.C. Luca, J.V. Ruderman, and A. Hershko. 1995. The cyclosome, a large complex containing cyclin-selective ubiquitin ligase activity, targets cyclins for destruction at the end of mitosis. *Mol Biol Cell.* 6:185-197.

- Sumara, I., E. Vorlauffer, P.T. Stukenberg, O. Kelm, N. Redemann, E.A. Nigg, and J.M. Peters. 2002. The dissociation of cohesin from chromosomes in prophase is regulated by Polo-like kinase. *Mol Cell*. 9:515-525.
- Szollosi, D., P. Calarco, and R.P. Donahue. 1972. Absence of centrioles in the first and second meiotic spindles of mouse oocytes. *J Cell Sci*. 11:521-541.
- Tai, C.Y., D.L. Dujardin, N.E. Faulkner, and R.B. Vallee. 2002. Role of dynein, dynactin, and CLIP-170 interactions in LIS1 kinetochore function. *J Cell Biol*. 156:959-968.
- Takahashi, K., S. Murakami, Y. Chikashige, H. Funabiki, O. Niwa, and M. Yanagida. 1992. A low copy number central sequence with strict symmetry and unusual chromatin structure in fission yeast centromere. *Mol Biol Cell*. 3:819-835.
- Tamanai, F. 1993. Inhibitors of Ras farnesyltransferases. *Trends Biochem Sci*. 18:349-353.
- Tang, Z., R. Bharadwaj, B. Li, and H. Yu. 2001. Mad2-Independent inhibition of APCCdc20 by the mitotic checkpoint protein BubR1. *Dev Cell*. 1:227-237.
- Tang, Z., H. Shu, D. Oncel, S. Chen, and H. Yu. 2004. Phosphorylation of Cdc20 by Bub1 provides a catalytic mechanism for APC/C inhibition by the spindle checkpoint. *Mol Cell*. 16:387-397.
- Tanudji, M., J. Shoemaker, L. L'Italien, L. Russell, G. Chin, and X.M. Schebye. 2004. Gene silencing of CENP-E by small interfering RNA in HeLa cells leads to missegregation of chromosomes after a mitotic delay. *Mol Biol Cell*. 15:3771-3781.
- Theurkauf, W.E., and R.S. Hawley. 1992. Meiotic spindle assembly in *Drosophila* females: behavior of nonexchange chromosomes and the effects of mutations in the nod kinesin-like protein. *J Cell Biol*. 116:1167-1180.
- Thompson, S.L., and D.A. Compton. 2008. Examining the link between chromosomal instability and aneuploidy in human cells. *J Cell Biol*. 180:665-672.
- Thornton, B.R., T.M. Ng, M.E. Matyskiela, C.W. Carroll, D.O. Morgan, and D.P. Toczyski. 2006. An architectural map of the anaphase-promoting complex. *Genes Dev*. 20:449-460.
- Thrower, D.A., M.A. Jordan, B.T. Schaar, T.J. Yen, and L. Wilson. 1995. Mitotic HeLa cells contain a CENP-E-associated minus end-directed microtubule motor. *Embo J*. 14:918-926.
- Tipton, A.R., M. Tipton, T. Yen, and S.T. Liu. 2011. Closed MAD2 (C-MAD2) is selectively incorporated into the mitotic checkpoint complex (MCC). *Cell Cycle*. 10:3740-3750.
- Tobin, D.A., J.S. Pickett, H.L. Hartman, C.A. Fierke, and J.E. Penner-Hahn. 2003. Structural characterization of the zinc site in protein farnesyltransferase. *J Am Chem Soc*. 125:9962-9969.

- Tolic-Norrelykke, I.M., L. Sacconi, G. Thon, and F.S. Pavone. 2004. Positioning and elongation of the fission yeast spindle by microtubule-based pushing. *Curr Biol.* 14:1181-1186.
- Tooley, J.G., S.A. Miller, and P.T. Stukenberg. 2011. The Ndc80 complex uses a tripartite attachment point to couple microtubule depolymerization to chromosome movement. *Mol Biol Cell.* 22:1217-1226.
- Tulu, U.S., C. Fagerstrom, N.P. Ferenz, and P. Wadsworth. 2006. Molecular requirements for kinetochore-associated microtubule formation in mammalian cells. *Curr Biol.* 16:536-541.
- Uchida, K.S., K. Takagaki, K. Kumada, Y. Hirayama, T. Noda, and T. Hirota. 2009. Kinetochore stretching inactivates the spindle assembly checkpoint. *J Cell Biol.* 184:383-390.
- Urbani, L., and T. Stearns. 1999. The centrosome. *Curr Biol.* 9:R315-317.
- Vagnarelli, P., and W.C. Earnshaw. 2004. Chromosomal passengers: the four-dimensional regulation of mitotic events. *Chromosoma.* 113:211-222.
- Vaisberg, E.A., M.P. Koonce, and J.R. McIntosh. 1993. Cytoplasmic dynein plays a role in mammalian mitotic spindle formation. *J Cell Biol.* 123:849-858.
- Varma, D., X. Wan, D. Cheerambathur, R. Gassmann, A. Suzuki, J. Lawrimore, A. Desai, and E.D. Salmon. 2013. Spindle assembly checkpoint proteins are positioned close to core microtubule attachment sites at kinetochores. *J Cell Biol.* 202:735-746.
- Vermeulen, K., D.R. Van Bockstaele, and Z.N. Berneman. 2003. The cell cycle: a review of regulation, deregulation and therapeutic targets in cancer. *Cell Prolif.* 36:131-149.
- Verstraeten, V.L., L.A. Peckham, M. Olive, B.C. Capell, F.S. Collins, E.G. Nabel, S.G. Young, L.G. Fong, and J. Lammerding. 2011. Protein farnesylation inhibitors cause donut-shaped cell nuclei attributable to a centrosome separation defect. *Proc Natl Acad Sci U S A.* 108:4997-5002.
- Vink, M., M. Simonetta, P. Transidico, K. Ferrari, M. Mapelli, A. De Antoni, L. Massimiliano, A. Ciliberto, M. Faretta, E.D. Salmon, and A. Musacchio. 2006. In vitro FRAP identifies the minimal requirements for Mad2 kinetochore dynamics. *Curr Biol.* 16:755-766.
- Visintin, R., S. Prinz, and A. Amon. 1997. CDC20 and CDH1: a family of substrate-specific activators of APC-dependent proteolysis. *Science.* 278:460-463.
- Vitre, B., N. Gudimchuk, R. Borda, Y. Kim, J.E. Heuser, D.W. Cleveland, and E.L. Grishchuk. 2014. Kinetochore-microtubule attachment throughout mitosis potentiated by the elongated stalk of the kinetochore kinesin CENP-E. *Mol Biol Cell.* 25:2272-2281.
- Vleugel, M., E. Hoogendoorn, B. Snel, and G.J. Kops. 2012. Evolution and function of the mitotic checkpoint. *Dev Cell.* 23:239-250.
- Vleugel, M., E. Tromer, M. Omerzu, V. Groenewold, W. Nijenhuis, B. Snel, and G.J. Kops. 2013. Arrayed BUB recruitment modules in the kinetochore scaffold KNL1 promote accurate chromosome segregation. *J Cell Biol.* 203:943-955.

- Vos, L.J., J.K. Famulski, and G.K. Chan. 2006. How to build a centromere: from centromeric and pericentromeric chromatin to kinetochore assembly. *Biochem Cell Biol.* 84:619-639.
- Vos, L.J., J.K. Famulski, and G.K. Chan. 2011. hZwint-1 bridges the inner and outer kinetochore: identification of the kinetochore localization domain and the hZw10-interaction domain. *Biochem J.* 436:157-168.
- Voullaire, L.E., H.R. Slater, V. Petrovic, and K.H. Choo. 1993. A functional marker centromere with no detectable alpha-satellite, satellite III, or CENP-B protein: activation of a latent centromere? *Am J Hum Genet.* 52:1153-1163.
- Wadsworth, P., and A. Khodjakov. 2004. E pluribus unum: towards a universal mechanism for spindle assembly. *Trends Cell Biol.* 14:413-419.
- Walczak, C.E., S. Cai, and A. Khodjakov. 2010. Mechanisms of chromosome behaviour during mitosis. *Nat Rev Mol Cell Biol.* 11:91-102.
- Walczak, C.E., and R. Heald. 2008. Mechanisms of mitotic spindle assembly and function. *Int Rev Cytol.* 265:111-158.
- Wan, X., R.P. O'Quinn, H.L. Pierce, A.P. Joglekar, W.E. Gall, J.G. DeLuca, C.W. Carroll, S.T. Liu, T.J. Yen, B.F. McEwen, P.T. Stukenberg, A. Desai, and E.D. Salmon. 2009. Protein architecture of the human kinetochore microtubule attachment site. *Cell.* 137:672-684.
- Wang, H., X. Hu, X. Ding, Z. Dou, Z. Yang, A.W. Shaw, M. Teng, D.W. Cleveland, M.L. Goldberg, L. Niu, and X. Yao. 2004a. Human Zwint-1 specifies localization of Zeste White 10 to kinetochores and is essential for mitotic checkpoint signaling. *J Biol Chem.* 279:54590-54598.
- Wang, S., S.A. Ketcham, A. Schon, B. Goodman, Y. Wang, J. Yates, 3rd, E. Freire, T.A. Schroer, and Y. Zheng. 2013. Nudel/NudE and Lis1 promote dynein and dynactin interaction in the context of spindle morphogenesis. *Mol Biol Cell.* 24:3522-3533.
- Wang, Y., and D.J. Burke. 1995. Checkpoint genes required to delay cell division in response to nocodazole respond to impaired kinetochore function in the yeast *Saccharomyces cerevisiae*. *Mol Cell Biol.* 15:6838-6844.
- Wang, Y., F. Jin, R. Higgins, and K. McKnight. 2014. The current view for the silencing of the spindle assembly checkpoint. *Cell Cycle.* 13:1694-1701.
- Wang, Z., J.M. Cummins, D. Shen, D.P. Cahill, P.V. Jallepalli, T.L. Wang, D.W. Parsons, G. Traverso, M. Awad, N. Silliman, J. Ptak, S. Szabo, J.K. Willson, S.D. Markowitz, M.L. Goldberg, R. Karess, K.W. Kinzler, B. Vogelstein, V.E. Velculescu, and C. Lengauer. 2004b. Three classes of genes mutated in colorectal cancers with chromosomal instability. *Cancer Res.* 64:2998-3001.
- Warburton, P.E., C.A. Cooke, S. Bourassa, O. Vafa, B.A. Sullivan, G. Stetten, G. Gimelli, D. Warburton, C. Tyler-Smith, K.F. Sullivan, G.G. Poirier, and W.C. Earnshaw. 1997. Immunolocalization of CENP-A suggests a distinct nucleosome structure at the inner kinetochore plate of active centromeres. *Curr Biol.* 7:901-904.

- Waters, J.C., R.V. Skibbens, and E.D. Salmon. 1996. Oscillating mitotic newt lung cell kinetochores are, on average, under tension and rarely push. *J Cell Sci.* 109 (Pt 12):2823-2831.
- Weaver, B.A., Z.Q. Bonday, F.R. Putkey, G.J. Kops, A.D. Silk, and D.W. Cleveland. 2003. Centromere-associated protein-E is essential for the mammalian mitotic checkpoint to prevent aneuploidy due to single chromosome loss. *J Cell Biol.* 162:551-563.
- Wei, R.R., J. Al-Bassam, and S.C. Harrison. 2007. The Ndc80/HEC1 complex is a contact point for kinetochore-microtubule attachment. *Nat Struct Mol Biol.* 14:54-59.
- Wei, R.R., P.K. Sorger, and S.C. Harrison. 2005. Molecular organization of the Ndc80 complex, an essential kinetochore component. *Proc Natl Acad Sci U S A.* 102:5363-5367.
- Weiss, E., and M. Winey. 1996. The *Saccharomyces cerevisiae* spindle pole body duplication gene MPS1 is part of a mitotic checkpoint. *J Cell Biol.* 132:111-123.
- Welburn, J.P., E.L. Grishchuk, C.B. Backer, E.M. Wilson-Kubalek, J.R. Yates, 3rd, and I.M. Cheeseman. 2009. The human kinetochore Ska1 complex facilitates microtubule depolymerization-coupled motility. *Dev Cell.* 16:374-385.
- Whyte, D.B., P. Kirschmeier, T.N. Hockenberry, I. Nunez-Oliva, L. James, J.J. Catino, W.R. Bishop, and J.K. Pai. 1997. K- and N-Ras are geranylgeranylated in cells treated with farnesyl protein transferase inhibitors. *J Biol Chem.* 272:14459-14464.
- Whyte, J., J.R. Bader, S.B. Tauhata, M. Raycroft, J. Hornick, K.K. Pfister, W.S. Lane, G.K. Chan, E.H. Hinchcliffe, P.S. Vaughan, and K.T. Vaughan. 2008. Phosphorylation regulates targeting of cytoplasmic dynein to kinetochores during mitosis. *J Cell Biol.* 183:819-834.
- Wilde, A., and Y. Zheng. 1999. Stimulation of microtubule aster formation and spindle assembly by the small GTPase Ran. *Science.* 284:1359-1362.
- Willard, H.F. 1991. Evolution of alpha satellite. *Curr Opin Genet Dev.* 1:509-514.
- Williams, B.C., M. Gatti, and M.L. Goldberg. 1996. Bipolar spindle attachments affect redistributions of ZW10, a *Drosophila* centromere/kinetochore component required for accurate chromosome segregation. *J Cell Biol.* 134:1127-1140.
- Williams, B.C., and M.L. Goldberg. 1994. Determinants of *Drosophila* zw10 protein localization and function. *J Cell Sci.* 107 (Pt 4):785-798.
- Williams, B.C., T.L. Karr, J.M. Montgomery, and M.L. Goldberg. 1992. The *Drosophila* l(1)zw10 gene product, required for accurate mitotic chromosome segregation, is redistributed at anaphase onset. *J Cell Biol.* 118:759-773.
- Williams, B.C., Z. Li, S. Liu, E.V. Williams, G. Leung, T.J. Yen, and M.L. Goldberg. 2003. ZwiCh, a new component of the ZW10/ROD complex required for kinetochore functions. *Mol Biol Cell.* 14:1379-1391.

- Wojcik, E., R. Basto, M. Serr, F. Scaerou, R. Karess, and T. Hays. 2001. Kinetochores dynein: its dynamics and role in the transport of the Rough deal checkpoint protein. *Nat Cell Biol.* 3:1001-1007.
- Wollman, R., E.N. Cytrynbaum, J.T. Jones, T. Meyer, J.M. Scholey, and A. Mogilner. 2005. Efficient chromosome capture requires a bias in the 'search-and-capture' process during mitotic-spindle assembly. *Curr Biol.* 15:828-832.
- Wong, N.S., and M.A. Morse. 2012. Lonafarnib for cancer and progeria. *Expert Opin Investig Drugs.* 21:1043-1055.
- Wong, O.K., and G. Fang. 2007. Cdk1 phosphorylation of BubR1 controls spindle checkpoint arrest and Plk1-mediated formation of the 3F3/2 epitope. *J Cell Biol.* 179:611-617.
- Wood, K.W., R. Sakowicz, L.S. Goldstein, and D.W. Cleveland. 1997. CENP-E is a plus end-directed kinetochore motor required for metaphase chromosome alignment. *Cell.* 91:357-366.
- Wright, L.P., and M.R. Philips. 2006. Thematic review series: lipid posttranslational modifications. CAAX modification and membrane targeting of Ras. *J Lipid Res.* 47:883-891.
- Xia, G., X. Luo, T. Habu, J. Rizo, T. Matsumoto, and H. Yu. 2004. Conformation-specific binding of p31(comet) antagonizes the function of Mad2 in the spindle checkpoint. *Embo J.* 23:3133-3143.
- Xue, Y., Z. Liu, J. Cao, Q. Ma, X. Gao, Q. Wang, C. Jin, Y. Zhou, L. Wen, and J. Ren. 2011. GPS 2.1: enhanced prediction of kinase-specific phosphorylation sites with an algorithm of motif length selection. *Protein Eng Des Sel.* 24:255-260.
- Yamagishi, Y., T. Honda, Y. Tanno, and Y. Watanabe. 2010. Two histone marks establish the inner centromere and chromosome bi-orientation. *Science.* 330:239-243.
- Yamagishi, Y., T. Sakuno, Y. Goto, and Y. Watanabe. 2014. Kinetochore composition and its function: lessons from yeasts. *FEMS Microbiol Rev.* 38:185-200.
- Yamagishi, Y., C.H. Yang, Y. Tanno, and Y. Watanabe. 2012. MPS1/Mph1 phosphorylates the kinetochore protein KNL1/Spc7 to recruit SAC components. *Nat Cell Biol.* 14:746-752.
- Yamamoto, T.G., S. Watanabe, A. Essex, and R. Kitagawa. 2008. SPDL-1 functions as a kinetochore receptor for MDF-1 in *Caenorhabditis elegans*. *J Cell Biol.* 183:187-194.
- Yang, M., B. Li, D.R. Tomchick, M. Machius, J. Rizo, H. Yu, and X. Luo. 2007a. p31comet blocks Mad2 activation through structural mimicry. *Cell.* 131:744-755.
- Yang, S.H., M.O. Bergho, J.I. Toth, X. Qiao, Y. Hu, S. Sandoval, M. Meta, P. Bendale, M.H. Gelb, S.G. Young, and L.G. Fong. 2005a. Blocking protein farnesyltransferase improves nuclear blebbing in mouse fibroblasts with a targeted Hutchinson-Gilford progeria syndrome mutation. *Proc Natl Acad Sci U S A.* 102:10291-10296.

- Yang, Y., F. Wu, T. Ward, F. Yan, Q. Wu, Z. Wang, T. McGlothen, W. Peng, T. You, M. Sun, T. Cui, R. Hu, Z. Dou, J. Zhu, W. Xie, Z. Rao, X. Ding, and X. Yao. 2008. Phosphorylation of HsMis13 by Aurora B kinase is essential for assembly of functional kinetochore. *J Biol Chem.* 283:26726-26736.
- Yang, Z., J. Guo, Q. Chen, C. Ding, J. Du, and X. Zhu. 2005b. Silencing mitosis induces misaligned chromosomes, premature chromosome decondensation before anaphase onset, and mitotic cell death. *Mol Cell Biol.* 25:4062-4074.
- Yang, Z., U.S. Tulu, P. Wadsworth, and C.L. Rieder. 2007b. Kinetochore dynein is required for chromosome motion and congression independent of the spindle checkpoint. *Curr Biol.* 17:973-980.
- Yao, X., A. Abrieu, Y. Zheng, K.F. Sullivan, and D.W. Cleveland. 2000. CENP-E forms a link between attachment of spindle microtubules to kinetochores and the mitotic checkpoint. *Nat Cell Biol.* 2:484-491.
- Yao, X., K.L. Anderson, and D.W. Cleveland. 1997. The microtubule-dependent motor centromere-associated protein E (CENP-E) is an integral component of kinetochore corona fibers that link centromeres to spindle microtubules. *J Cell Biol.* 139:435-447.
- Yen, T.J., D.A. Compton, D. Wise, R.P. Zinkowski, B.R. Brinkley, W.C. Earnshaw, and D.W. Cleveland. 1991. CENP-E, a novel human centromere-associated protein required for progression from metaphase to anaphase. *Embo J.* 10:1245-1254.
- Yen, T.J., G. Li, B.T. Schaar, I. Szilak, and D.W. Cleveland. 1992. CENP-E is a putative kinetochore motor that accumulates just before mitosis. *Nature.* 359:536-539.
- Yokoyama, K., P. Trobridge, F.S. Buckner, J. Scholten, K.D. Stuart, W.C. Van Voorhis, and M.H. Gelb. 1998. The effects of protein farnesyltransferase inhibitors on trypanosomatids: inhibition of protein farnesylation and cell growth. *Mol Biochem Parasitol.* 94:87-97.
- Yu, H. 2007. Cdc20: a WD40 activator for a cell cycle degradation machine. *Mol Cell.* 27:3-16.
- Yun, M., Y.H. Han, S.H. Yoon, H.Y. Kim, B.Y. Kim, Y.J. Ju, C.M. Kang, S.H. Jang, H.Y. Chung, S.J. Lee, M.H. Cho, G. Yoon, G.H. Park, S.H. Kim, and K.H. Lee. 2009. p31^{comet} Induces cellular senescence through p21 accumulation and Mad2 disruption. *Mol Cancer Res.* 7:371-382.
- Zhai, Y., P.J. Kronebusch, and G.G. Borisy. 1995. Kinetochore microtubule dynamics and the metaphase-anaphase transition. *J Cell Biol.* 131:721-734.
- Zhang, F.L., and P.J. Casey. 1996. Protein prenylation: molecular mechanisms and functional consequences. *Annu Rev Biochem.* 65:241-269.
- Zheng, Y., M.L. Wong, B. Alberts, and T. Mitchison. 1995. Nucleation of microtubule assembly by a gamma-tubulin-containing ring complex. *Nature.* 378:578-583.

- Zhou, T., W. Zimmerman, X. Liu, and R.L. Erikson. 2006. A mammalian NudC-like protein essential for dynein stability and cell viability. *Proc Natl Acad Sci U S A*. 103:9039-9044.
- Zhu, L., S. Jaamaa, T.M. Af Hallstrom, M. Laiho, A. Sankila, S. Nordling, U.H. Stenman, and H. Koistinen. 2012. PSA forms complexes with alpha(1) - antichymotrypsin in prostate. *Prostate*.
- Zhu, X., K.H. Chang, D. He, M.A. Mancini, W.R. Brinkley, and W.H. Lee. 1995. The C terminus of mitotin is essential for its nuclear localization, centromere/kinetochore targeting, and dimerization. *J Biol Chem*. 270:19545-19550.

Appendix

Presented within this Appendix are results of a follow up of a study initiated by a former graduate student 'Dr. Larissa Joy Vos' and has been published in her thesis under '*hZwint-1, but not hZw10, is overexpressed and both have altered kinetochores localization in a subset of breast cancer cell lines*'. These results are not a part of any of the preceding results chapters contained within this thesis.

D.K. Moudgil performed all the experiments for the figures shown in this chapter with the exception of lentivirus transduction procedure, which was performed by Dr. Dawn MacDonald.

A study reported higher expression of hZwint-1 protein in a subset of pulmonary adenocarcinomas and correlated it with poor prognosis. Our lab discovered ~1.5-2 times higher levels of hZwint-1 protein expression in breast cancer cell lines in comparison to a non-tumorigenic breast cell line (MCF10A) and HeLa (unpublished results). Furthermore, Zwint-1 displayed an aberrant kinetochore localization pattern in MCF10A and breast cancer cell lines as it remained at the kinetochore in telophase, while no Zwint-1 kinetochore localization is observed in HeLa cells at telophase. A former graduate student in our laboratory examined Zw10 kinetochore localization in a subset of breast cancer cell lines and reported it has reduced or no kinetochore localization in a subset of breast cancer cell lines even though it expressed at similar levels in all the breast cancer cell lines. Zw10 kinetochore localization is normal in HeLa, MCF10A, MCF7 and ZR-75-1 cell lines. It has reduced kinetochore localization in BT-20, BT-549, SK-BR-3 and MDA-MB-175-VII cell lines and is almost absent from prometaphase kinetochores in MDA-MB-231, MDA-MB-435s, HCC1937 and T-47D. However, Zw10 robustly localized to kinetochores in all the breast cancer cells treated with vinblastine, a MT destabilizing drug.

Since hSpindly kinetochore localization is dependent on the RZZ complex, I examined the kinetochore localization pattern of hSpindly in a panel of breast cancer cell lines previously used for the study. I observed hSpindly prometaphase kinetochore localization is normal in HeLa, MCF10A, and MCF7 cell lines (Figure A.1). It has reduced kinetochore localization in MDA-MB-231 and BT-20 cell lines and is almost absent from prometaphase kinetochores in, MDA-MB-435s, BT-549 and T-47D (Figure A.1). Similar to Zw10, hSpindly robustly localized to kinetochores in cells treated with vinblastine (Figure A.2). I compared hSpindly protein expression levels and found no correlation with its kinetochore localization pattern (Figure A.3). To determine if the reduced Zw10 kinetochore localization is due to Zw10 mutation/misregulation or lies upstream of Zw10, we infected breast cancer cell lines displaying reduced or null Zw10 kinetochore localization (MDA-MB-231 and T47D) with lentivirus containing

wild type GFP-Zw10. While Zw10 kinetochore localization was rescued in MDA-MB-231 cells, it showed heterogeneous population of T47D cells with both GFP-Zw10 positive and negative kinetochore localization. Therefore, I speculate that multiple checkpoint components might be misregulated in the breast cancer cell lines leading to a weakened mitotic checkpoint activity.

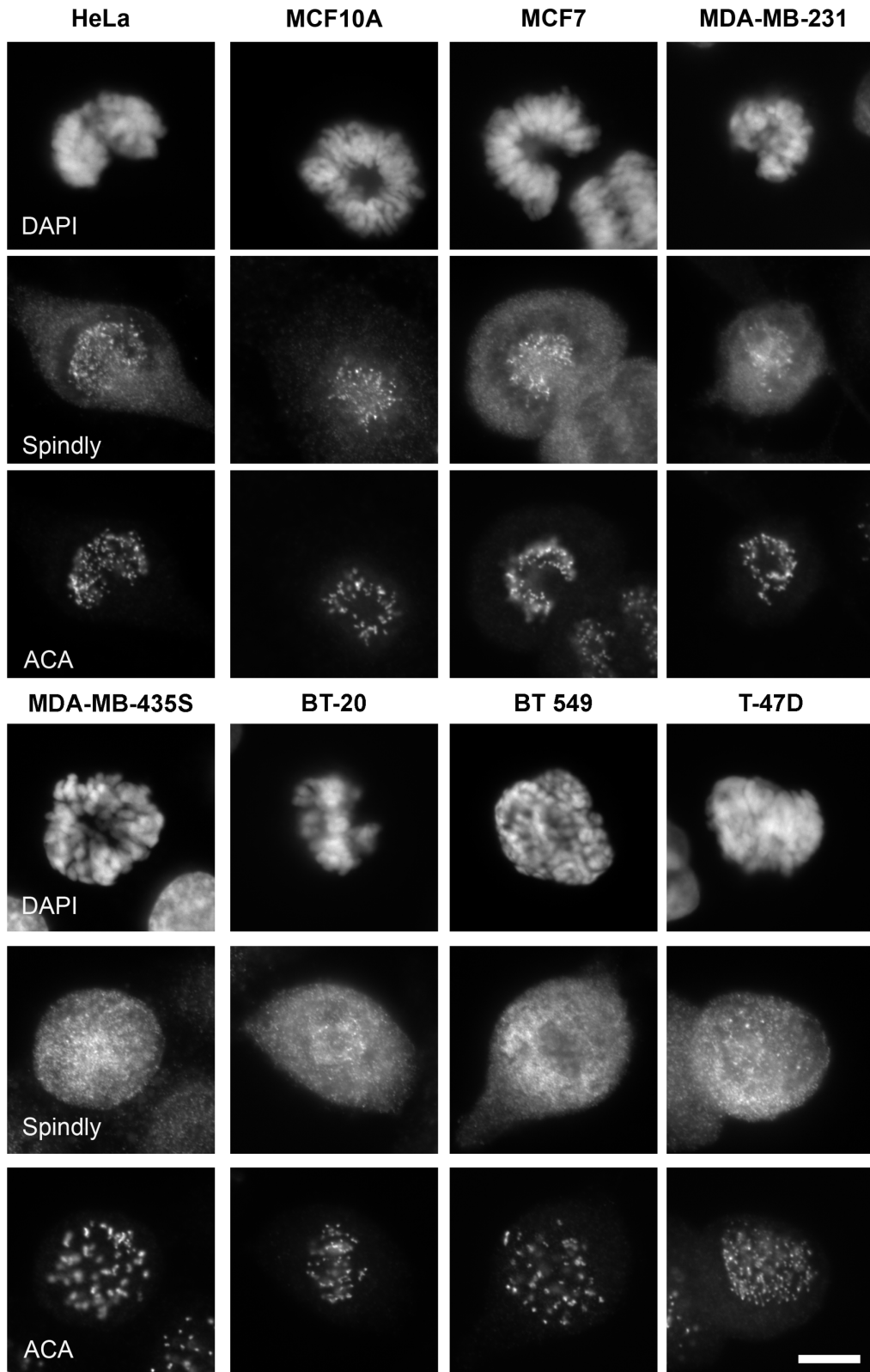


Figure A.1: hSpindly has reduced kinetochore occupancy in a subset of breast cancer cell lines similar to Zw10.

hSpindly prometaphase kinetochore localization is normal in HeLa, MCF10A, and MCF7 cell lines. It has reduced kinetochore localization in MDA-MB-231 and BT-20 cell lines and is almost absent from prometaphase kinetochores in, MDA-MB-435s, BT-549 and T-47D. Cells were labeled with rat anti-hSpindly and ACA antibodies and chromosomes stained with DAPI. Scale bar = 10 μ m.

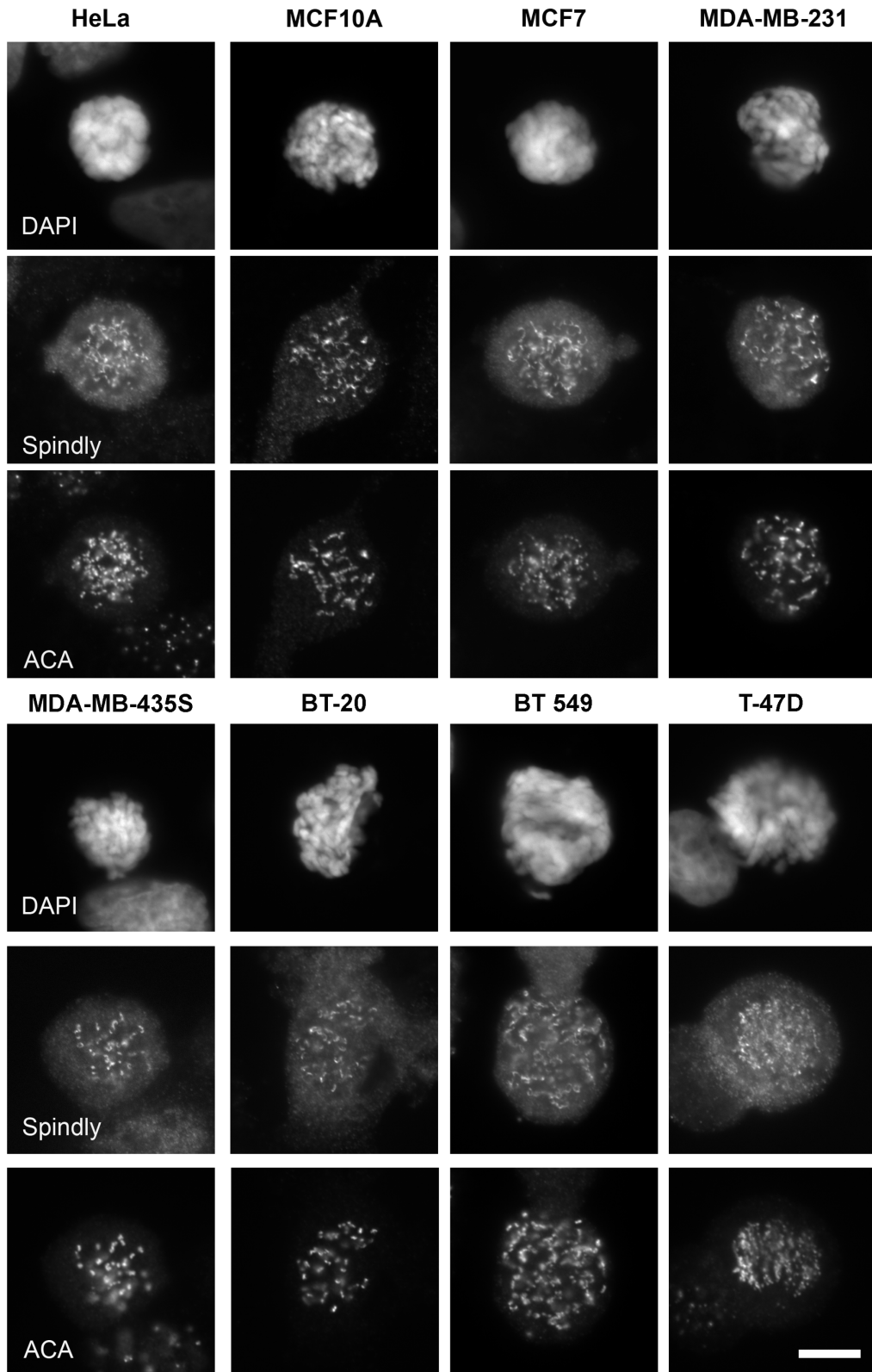


Figure A.2: hSpindly robustly localizes to kinetochores devoid of MT attachments.

Cells were treated with 0.5 10 μ M vinblastine before fixation. hSpindly strongly localized to kinetochores in all the cell lines including breast cancer cell lines that showed reduced or no hSpindly kinetochore localization under normal mitotic conditions (MDA-MB-231, BT-20, MDA-MB-435s, BT-549 and T-47D). Cells were labeled with rat anti-hSpindly and ACA antibodies and chromosomes stained with DAPI. Scale bar = 10 μ m.

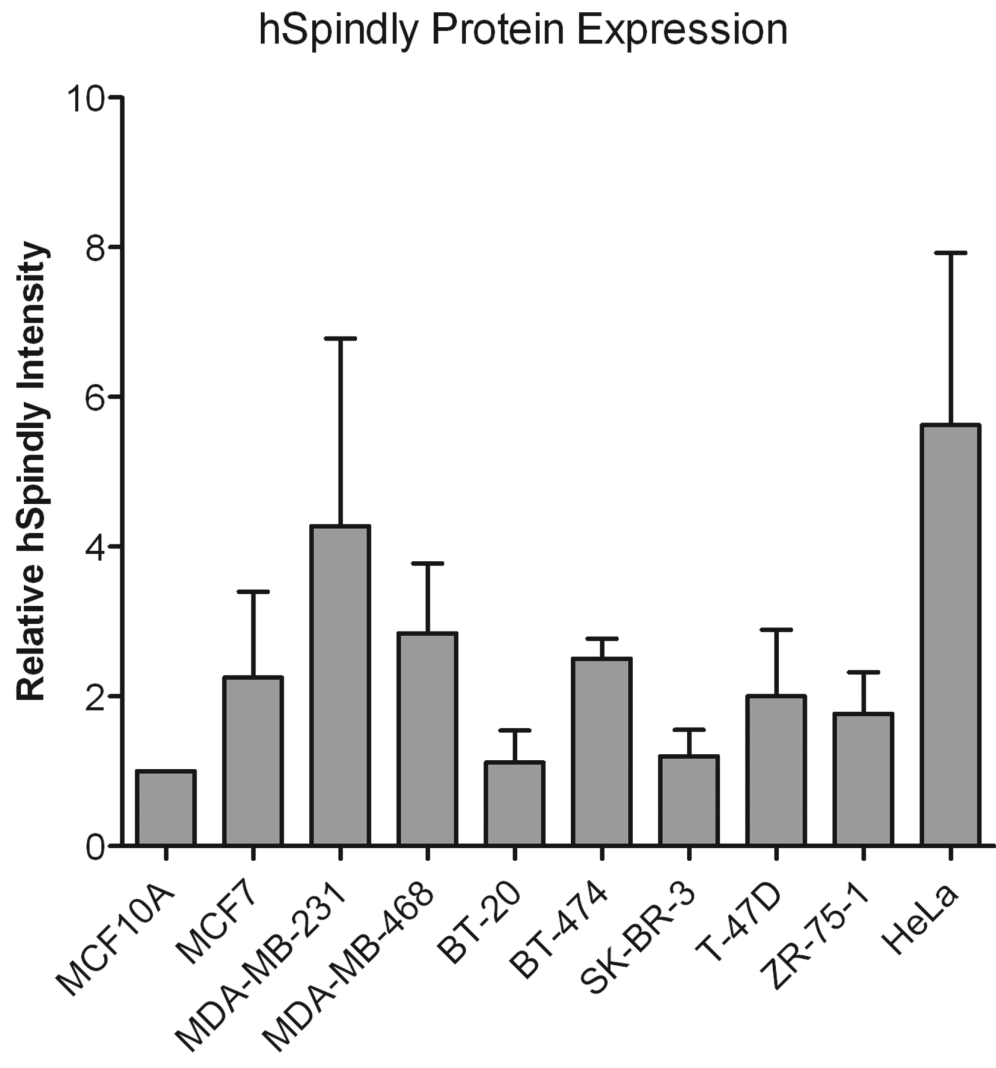
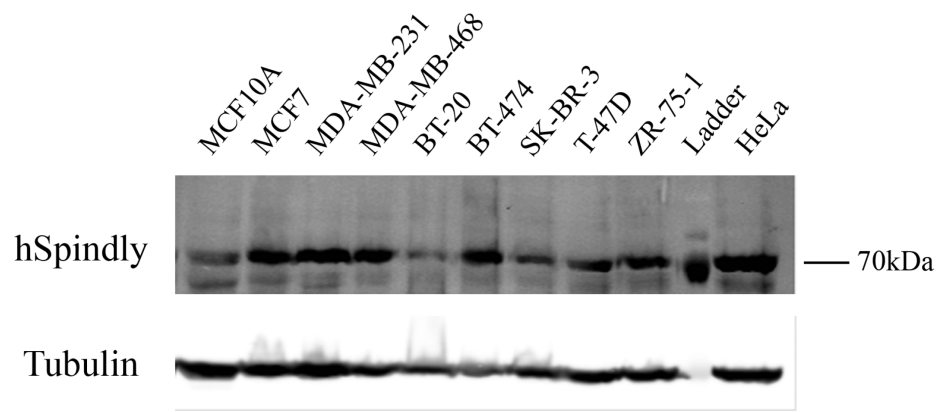


Figure A.3: hSpindly protein expression is variable in breast cancer cell lines and does not correlate with their localization pattern.

Breast cancer cell lines and non-tumorigenic MCF10A cell lines have less hSpindly protein expression compared to HeLa. The intensity of hSpindly and tubulin were determined and background corrected with Odyssey software and the intensity of hSpindly was normalized to tubulin intensity and plotted with Excel. The relative intensity for MCF10A was set at 1. n=3

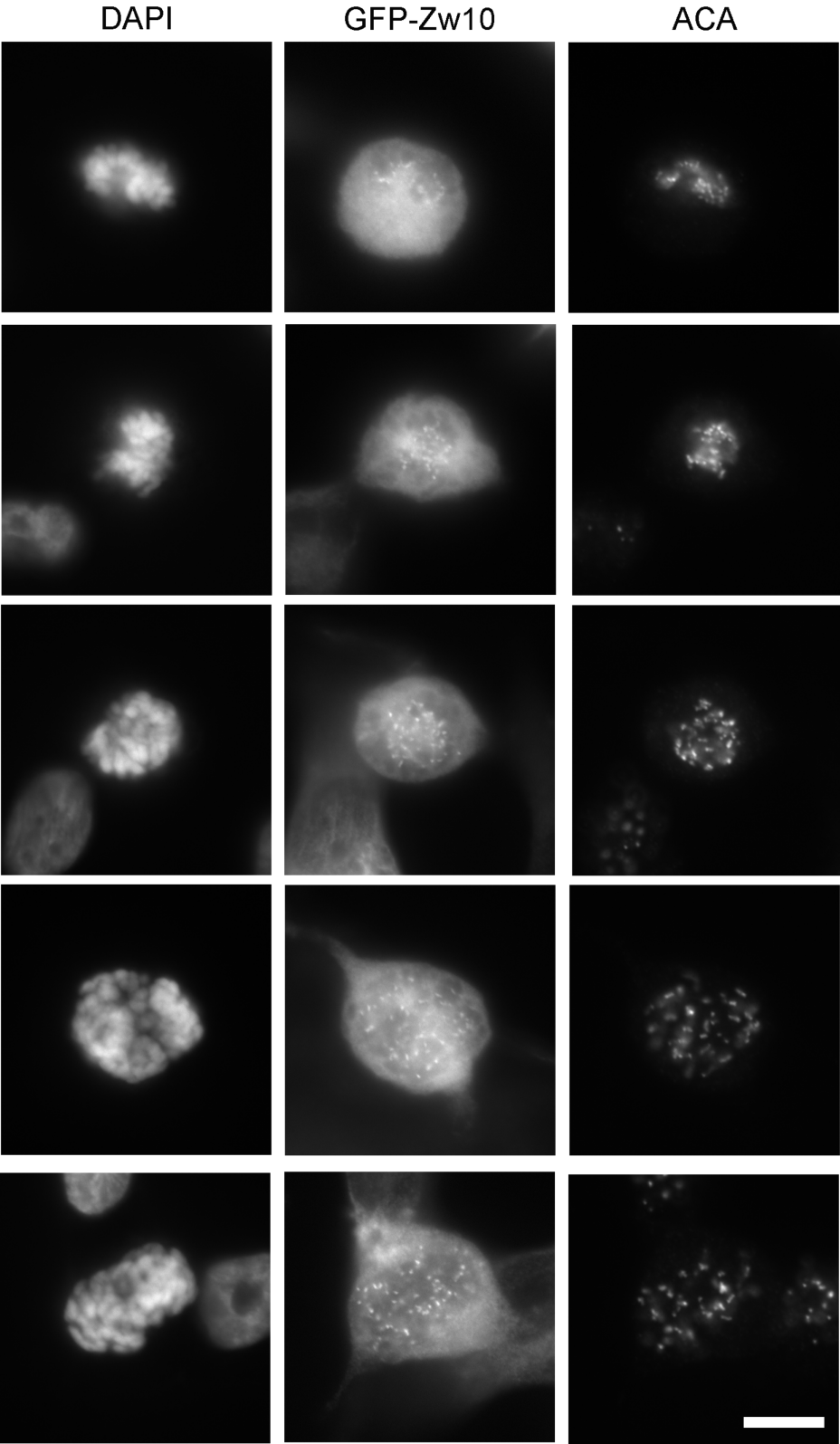


Figure A.4: WT-GFP-Zw10 expressing cells rescue normal Zw10 kinetochore localization in MDA-MB-231 cells.

MDA-MB-231 cells were infected with lentivirus containing WT-GFP-Zw10 and normal Zw10 kinetochore localization was observed. Chromosomes stained with DAPI. Scale bar = 10 μ m.

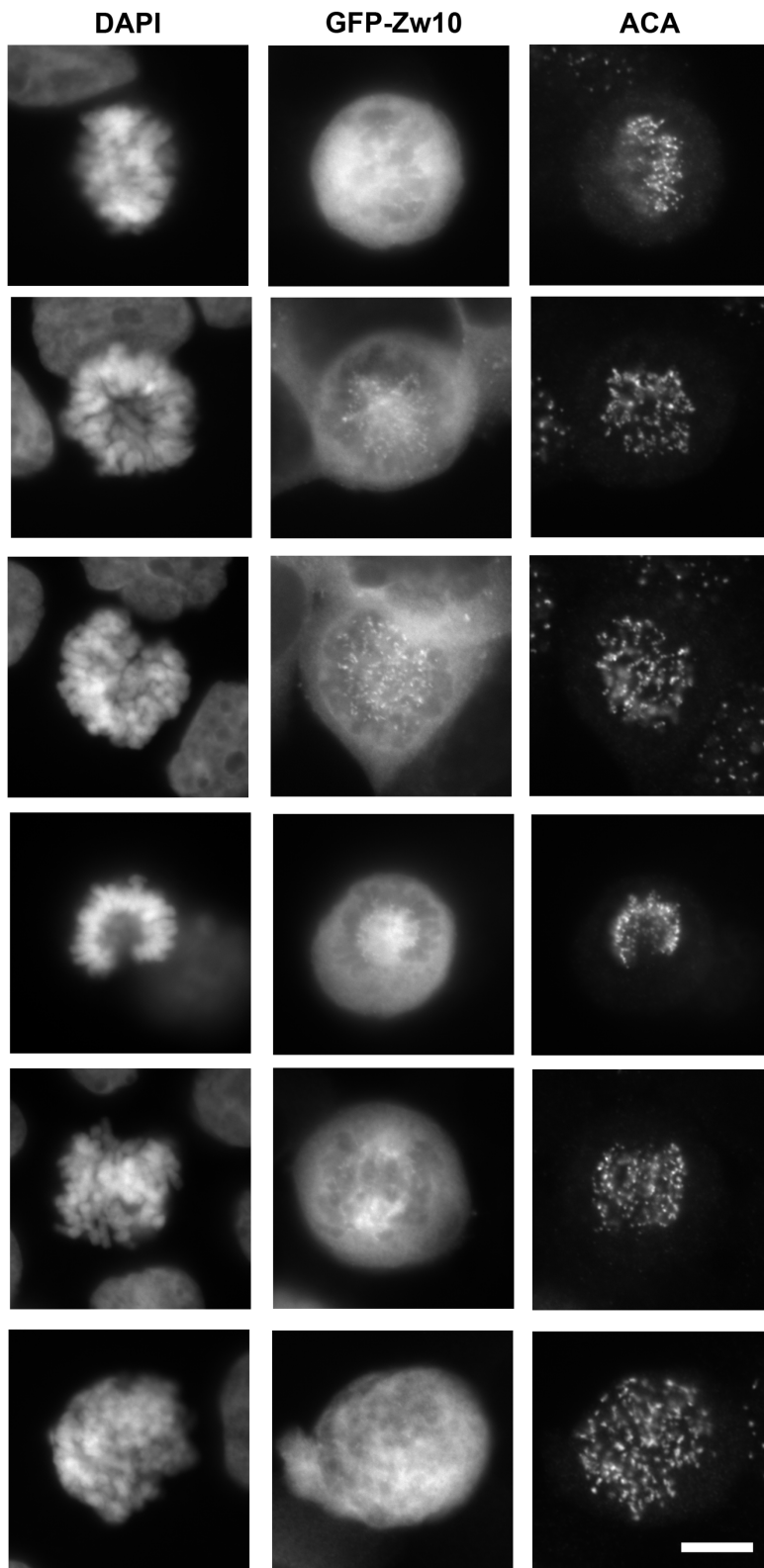


Figure A.5: WT-GFP-Zw10 expressing T47-D cells display a heterogeneous population with normal as well as absence of kinetochore localization of GFP-Zw10.

T47D cells were infected with lentivirus containing WT-GFP-Zw10 exhibited normal and no GFP-Zw10 kinetochore localization. Chromosomes stained with DAPI. Scale bar = 10 μ m.